



DESIGN & NATURE III

Comparing Design in Nature with Science
and Engineering

Editor: C.A. Brebbia



WITPRESS

Design and Nature III

Comparing Design in Nature
with Science and Engineering

WIT*PRESS*

WIT Press publishes leading books in Science and Technology.
Visit our website for the current list of titles.
www.witpress.com

WIT*eLibrary*

Home of the Transactions of the Wessex Institute.
Papers presented at Design & Nature III are archived in the
WIT eLibrary in volume 87 of WIT Transactions on
Ecology and the Environment (ISSN 1743-3541).

The WIT eLibrary provides the international scientific community with immediate and
permanent access to individual papers presented at WIT conferences.
<http://library.witpress.com>

This page intentionally left blank

THIRD INTERNATIONAL CONFERENCE ON
COMPARING DESIGN IN NATURE WITH SCIENCE AND ENGINEERING

Design and Nature III

CONFERENCE CHAIRMEN

C.A. Brebbia

Wessex Institute of Technology, UK

INTERNATIONAL SCIENTIFIC ADVISORY COMMITTEE

A G Abbott	D Lewis
M Atherton	R Lieb
M A Baez	G Lorenzini
G Barozzi	R L Magin
A Bejan	A C McIntosh
S C Burgess	P Pascolo
A Carpi	M Platzer
C Dowlen	G Prance
J Fernandez	A D Rey
S Gorb	T Speck
H Hendrickx	E Stach
C Jenkins	E Tiezzi
D Kirkland	GA Walters

Organised by

Wessex Institute of Technology, UK

Sponsored by

The International Journal of Design and Nature

This page intentionally left blank

Transactions Editor

Carlos Brebbia
Wessex Institute of Technology
Ashurst Lodge, Ashurst
Southampton SO40 7AA, UK
Email: carlos@wessex.ac.uk

WIT Transactions on Ecology and the Environment

Editorial Board

Y N Aboulseiman
University of Oklahoma
USA

D Almorza Gomar
University of Cadiz
Spain

M Andretta
Montecatini
Italy

J G Bartzis
Institute of Nuclear
Technology
Greece

J Boarder
Cartref Consulting
Systems
UK

H Boileau
ESIGEC
France

A Aldama
IMTA
Mexico

A M Amer
Cairo University
Egypt

J M Baldasano
Universitat Politecnica de
Catalunya
Spain

A Bejan
Duke University
USA

B Bobee
Institut National de la
Recherche Scientifique
Canada

C A Borrego
University of Aveiro
Portugal

A H-D Cheng
University of Mississippi
USA

A Cieslak
Technical University of
Lodz
Poland

M da Conceicao Cunha
University of Coimbra
Portugal

A B de Almeida
Instituto Superior Tecnico
Portugal

C Dowlen
South Bank University
UK

J P du Plessis
University of Stellenbosch
South Africa

D Elms
University of Canterbury
New Zealand

D Emmanouloudis
Technological Educational
Institute of Kavala
Greece

R A Falconer
Cardiff University
UK

G Gambolati
Universita di Padova
Italy

C-L Chiu
University of Pittsburgh
USA

W Czyczula
Krakow University of
Technology
Poland

M Davis
Temple University
USA

K Dorow
Pacific Northwest National
Laboratory
USA

R Duffell
University of Hertfordshire
UK

A Ebel
University of Cologne
Germany

D M Elsom
Oxford Brookes University
UK

J W Everett
Rowan University
USA

D M Fraser
University of Cape Town
South Africa

N Georgantzis
Universitat Jaume I
Spain

F Gomez

Universidad Politecnica
de Valencia
Spain

W E Grant

Texas A & M University
USA

A H Hendrickx

Free University of
Brussels
Belgium

I Hideaki

Nagoya University
Japan

W Hutchinson

Edith Cowan University
Australia

K L Katsifarakis

Aristotle University of
Thessaloniki
Greece

B A Kazimee

Washington State
University
USA

D Koga

Saga University
Japan

B S Larsen

Technical University of
Denmark
Denmark

D Lewis

Mississippi State
University
USA

K G Goulias

Pennsylvania State
University
USA

C Hanke

Danish Technical University
Denmark

S Heslop

University of Bristol
UK

W F Huebner

Southwest Research Institute
USA

D Kaliampakos

National Technical
University of Athens
Greece

H Kawashima

The University of Tokyo
Japan

D Kirkland

Nicholas Grimshaw &
Partners Ltd
UK

J G Kretzschmar

VITO
Belgium

A Lebedev

Moscow State University
Russia

K-C Lin

University of New
Brunswick
Canada

J W S Longhurst
University of the West of
England
UK

U Mander
University of Tartu
Estonia

J D M Marsh
Griffith University
Australia

K McManis
University of New
Orleans
USA

M B Neace
Mercer University
USA

R O'Neill
Oak Ridge National
Laboratory
USA

J Park
Seoul National University
Korea

B C Patten
University of Georgia
USA

V Popov
Wessex Institute of
Technology
UK

M R I Purvis
University of Portsmouth
UK

T Lyons
Murdoch University
Australia

N Marchettini
University of Siena
Italy

J F Martin-Duque
Universidad Complutense
Spain

C A Mitchell
The University of Sydney
Australia

R Olsen
Camp Dresser & McKee Inc.
USA

K Onishi
Ibaraki University
Japan

G Passerini
Universita delle Marche
Italy

M F Platzer
Naval Postgraduate School
USA

H Power
University of Nottingham
UK

Y A Pykh
Russian Academy of
Sciences
Russia

A D Rey
McGill University
Canada

R Rosset
Laboratoire d'Aerologie
France

S G Saad
American University of
Cairo
Egypt

J J Sharp
Memorial University of
Newfoundland
Canada

I V Stangeeva
St Petersburg University
Russia

T Tirabassi
Institute FISBAT-CNR
Italy

J-L Uso
Universitat Jaume I
Spain

A Viguri
Universitat Jaume I
Spain

G Walters
University of Exeter
UK

A C Rodrigues
Universidade Nova de
Lisboa
Portugal

J L Rubio
Centro de Investigaciones
sobre Desertificacion
Spain

R San Jose
Technical University of
Madrid
Spain

H Sozer
Illinois Institute of
Technology
USA

E Tiezzi
University of Siena
Italy

S G Tushinski
Moscow State University
Russia

R van Duin
Delft University of
Technology
Netherlands

Y Villacampa Esteve
Universidad de Alicante
Spain

This page intentionally left blank

Design and Nature III

Comparing Design in Nature
with Science and Engineering

Editor:

C.A. Brebbia

Wessex Institute of Technology, UK

WITPRESS Southampton, Boston



C.A. Brebbia

Wessex Institute of Technology, UK

Published by

WIT Press

Ashurst Lodge, Ashurst, Southampton, SO40 7AA, UK

Tel: 44 (0) 238 029 3223; Fax: 44 (0) 238 029 2853

E-Mail: witpress@witpress.com

<http://www.witpress.com>

For USA, Canada and Mexico

Computational Mechanics Inc

25 Bridge Street, Billerica, MA 01821, USA

Tel: 978 667 5841; Fax: 978 667 7582

E-Mail: infousa@witpress.com

<http://www.witpress.com>

British Library Cataloguing-in-Publication Data

A Catalogue record for this book is available
from the British Library

ISBN: 1-84564-166-3

ISSN: 1746-448X (print)

ISSN: 1743-3541 (on-line)

*The texts of the papers in this volume were set
individually by the authors or under their supervision.
Only minor corrections to the text may have been carried
out by the publisher.*

No responsibility is assumed by the Publisher, the Editors and Authors for any injury and/or damage to persons or property as a matter of products liability, negligence or otherwise, or from any use or operation of any methods, products, instructions or ideas contained in the material herein.

© WIT Press 2006

Printed in Great Britain by Cambridge Printing.

All rights reserved. No part of this publication may be reproduced, stored in a retrieval system, or transmitted in any form or by any means, electronic, mechanical, photocopying, recording, or otherwise, without the prior written permission of the Publisher.

Preface

This volume contains papers presented at the 3rd International Conference on Design and Nature, held in the New Forest, England, in 2006, and is part of the Transactions of the Wessex Institute, permanently available on-line at www.witpress.com.

Launched in 2002, this conference acts as a forum for researchers from around the world working on a variety of studies involving nature and its significance to modern scientific thought and design. The Conference provides a channel of communication between all those working in this exciting new discipline, whether they are in academia, research institutions or industry.

Many leading discoveries have been prompted by parallels between nature and human design. Today, advances in scientific knowledge coupled with powerful computers and simulation models have made comprehensive studies of nature possible.

This book includes sections dealing with: Design in nature; Shape and form in engineering and nature; Nature and architectural design; Thermodynamics in nature; Biomimetics; Natural materials in engineering; Mechanics in nature; Bioengineering; Bionics; Solutions from nature; Evolutionary optimisation; Complexity and Sustainability studies.

The Editor is grateful to the members of the International Scientific Advisory Committee and other colleagues for helping to select the papers published in this book and to all contributors for the quality of their work.

The Editor
The New Forest, UK, 2006

This page intentionally left blank

Contents

Section 1: Shape and form in engineering and nature

Flapping-wing aerohydrodynamics in nature and engineering <i>K. D. Jones & M. F. Platzer</i>	3
A graphic way for notch shape optimization <i>C. Mattheck, J. Sørensen & K. Bethge</i>	13
An inquiry into the morphology of Ciliate Protozoa using an engineering design approach <i>E. L. Benjamin, M. W. Collins & D. McL. Roberts</i>	23
The optimized shape of a leaf petiole <i>D. Pasini & V. Mirjalili</i>	35

Section 2: Nature and architectural design

Sculpture house in Belgium by Jacques Gillet <i>S. Van de Voorde, R. De Meyer, E. De Kooning, L. Taerwe & R. Van De Walle</i>	49
Analysis of the ‘Cappadocian cave house’ in Turkey as the historical aspect of the usage of nature as a basis of design <i>P. Yıldız</i>	61
Build trees <i>M. Despang</i>	71
Thermal performance of a dome-covered house <i>Y. Lin & R. Zmeureanu</i>	81
Biodegradable building <i>P. Sassi</i>	91

Section 3: Biomimetics

Self-healing processes in nature and engineering: self-repairing biomimetic membranes for pneumatic structures <i>T. Speck, R. Luchsinger, S. Busch, M. Rüggeberg & O. Speck</i>	105
Functional information and entropy in living systems <i>A. C. McIntosh</i>	115
Biomimetics of spider silk spinning process <i>G. De Luca & A. D. Rey</i>	127
The preparation of biomimetic nano-Al ₂ O ₃ surface modification materials on gray cast iron surface <i>Y. Liu, L. Q. Ren, Z. W. Han & S. R. Yu</i>	137
Biomimetics: extending nature's design of thin-wall shells with cellular cores <i>M. A. Dawson & L. J. Gibson</i>	145
Designing new lubricant additives using biomimetics <i>A. Morina, T. Liskiewicz & A. Neville</i>	157
Preparation, microstructure and properties of biomimetic nanocomposite coating <i>L. Q. Ren, Y. Liu, S. R. Yu, Z. W. Han & H. X. Hu</i>	167
Vision assistant: a human-computer interface based on adaptive eye-tracking <i>V. Hardzeyeu, F. Klefenz & P. Schikowski</i>	175

Section 4: Natural materials engineering

Structural and torsional properties of the <i>Trachycarpus fortunei</i> palm petiole <i>A. G. Windsor-Collins, M. A. Atherton, M. W. Collins & D. F. Cutler</i>	185
A model for adaptive design <i>T. Willey</i>	195
Reinforcement ropes against shear in leaves <i>C. Mattheck, A. Sauer & R. Kappel</i>	205

Experimental investigation of moist-air transport through natural materials porous media <i>I. Conte & X. Peng</i>	211
---	-----

Simulation of perspiration in sweating fabric manikin-Walter <i>J. Fan</i>	221
---	-----

Section 5: Bioengineering

State of the art of solid freeform fabrication for soft and hard tissue engineering <i>P. J. S. Bártolo</i>	233
--	-----

Using Murray's law to design artificial vascular microfluidic networks <i>R. W. Barber, K. Cieřlicki & D. R. Emerson</i>	245
---	-----

Biomimetic robots for robust operation in unstructured environments <i>S. R. Gajjar</i>	255
--	-----

Section 6: Solutions from nature

Animal analogies for developing design thinking <i>C. Dowlan</i>	267
---	-----

Development of a novel flapping mechanism with adjustable wing kinematics for micro air vehicles <i>A. T. Conn, S. C. Burgess & R. A. Hyde</i>	277
---	-----

Section 7: Sustainability studies

Bionics vs. biomimicry: from control <i>of</i> nature to sustainable participation <i>in</i> nature <i>D. C. Wahl</i>	289
--	-----

Active and adaptive sustainable environments for children's outdoor space <i>M. Winkler & S. Macaulay</i>	299
--	-----

The creation of an eco-tourism site: a case study of Pulau Singa Besar <i>A. Abdullah, A. M. Abdul Rahman, A. Bahauddin & B. Mohamed</i>	309
---	-----

Section 8: Education and training

Development and experience with a technical elective course
“fluid flows in nature”

J. A. Schetz319

New educational tools and curriculum enhancements for motivating
engineering students to design and realize bio-inspired products

*H. A. Bruck, A. L. Gershon, I. Golden, S. K. Gupta, L. S. Gyger Jr.,
E. B. Magrab & B. W. Spranklin*.....325

Author Index335

Section 1
Shape and form in engineering
and nature

This page intentionally left blank

Flapping-wing aerohydromechanics in nature and engineering

K. D. Jones & M. F. Platzer

AeroHydro Research and Technology Associates, Pebble Beach, California, USA

Abstract

Flapping wings have been the propulsion system used by birds, insects and fish for millions of years. Yet, the preferred system for aircraft and ship propulsion is the propeller or jet engine. It is the objective of this paper to show that recent interest in the development of micro air vehicles may lead to the adoption of flapping-wing propulsors as the superior system. Also, it is shown that flapping hydrofoils may have potential as effective water energy conversion devices. The knowledge gained in the aerohydromechanics of birds, insects and fish therefore may soon be applied to the design of air vehicles and power generators.

Keywords: air vehicle design, hydropower generation, flapping-wing aerohydro-mechanics.

1 Introduction

Birds, insects, fish and cetaceans use flapping wings as thrust and lift generators. Therefore, it is not surprising that the idea of adopting flapping wings for the propulsion of man-made objects was examined as early as 1490 by Leonardo da Vinci. At the end of the 19th century and the beginning of the 20th century, numerous attempts were made to develop flight vehicles using flapping wings. One of these early flight pioneers was Otto Lilienthal in Berlin, who remarked about his fascination in observing the flight performance of storks [1]. Indeed, anyone looking at fig. 1 will marvel at the pelican's flight abilities. An examination of the scientific literature on the aerohydromechanics of flapping wings, as conducted recently by Rozhdestvensky and Ryzhov [2], reveals many studies of the physics of flapping-wing propulsion with the goal of exploring



their potential as efficient propulsors and lift generators as well as wind and water energy conversion devices.



Figure 1: A brown pelican takes advantage of ground effect on Monterey Bay.

As stated by Rozhdestvensky and Ryzhov, interest in flapping-wing devices is justified because propulsive systems with flapping wings can be viewed as “ecologically” pure, are relatively low-frequency systems, possess sufficiently high efficiency, are multi-functional in the sense of being capable of operating in different regimes of motion, can combine the function of propulsor, control device, and stabilizer, can provide static thrust, can provide high maneuverability, possess more acceptable cavitation characteristics than conventional propellers, have relatively low aerodynamic drag in the “switched-off” position, and allow the use of modern controls, MEMS, piezo-electric, reciprocating chemical muscles, and other technologies.

Furthermore, the phenomenon of wing flutter is well known to aeronautical engineers causing an aircraft wing to absorb energy from the air flow due to the self-excited wing vibration. Flapping wings therefore have the potential of serving as efficient wind or hydropower generators.

Yet, it is a fact that flapping wings have found few applications as airplane or ship propulsors and as power generators. This raises the question whether systems which have been favored by nature for millions of years are inherently less suitable for man-made applications or whether this situation is likely to change in the near future because of the need for new vehicles and energy conversion devices. It is the objective of this paper to address this question.

2 Fundamentals of thrust generation by wing flapping

Airplanes are being propelled by ejecting high-velocity air from the propeller or the jet engine. It may not be obvious that the same principle holds for flapping wings. This can be understood from fig. 2. In a). we show a visualization of the



flow generated downstream of a NACA 0012 airfoil in a low-speed water flow. The foil is held steady at zero angle of attack. It is seen that a so-called vortex street is shed from the trailing edge consisting of two rows of vortices. The upper-row of vortices are turning clockwise, the lower-row of vortices are turning counter-clockwise. This type of vortex street is usually referred to as a Kármán vortex street, named after Theodore von Kármán who first explained its structure. The following three visualizations show the vortex streets which are being generated when the airfoil starts to flap in the vertical direction (pure plunge mode) with increasing frequency. It is seen that the vortex street eventually becomes the exact reverse of the Kármán vortex street shed from the stationary airfoil. It is therefore often referred to as the reverse Kármán vortex street. A closer inspection of the velocities induced by this vortex street reveals that counter-rotating upper-row vortices together with the clockwise lower-row vortices induce a time-averaged flow between the two rows which has the shape of a jet. Hence wing flapping achieves the same effect as man-made propellers or jet engines.

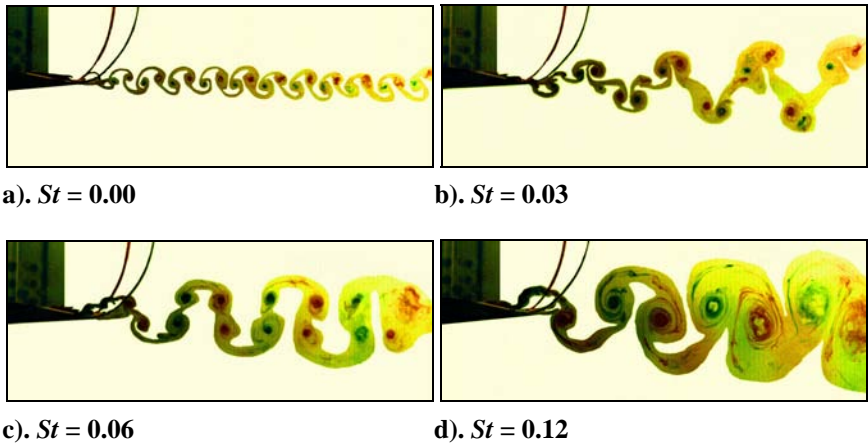


Figure 2: Vortex street formation with increasing Strouhal number.

A still closer inspection leads to the recognition that there are three parameters which affect this process, namely the amplitude and frequency of oscillation and the flying speed of the bird, insect, fish or cetacean. The flow features remain similar when the product of frequency, f , and amplitude, A , divided by the flying speed, U , remains constant. This quantity is usually denoted as the Strouhal number given by

$$St = fA/U. \quad (1)$$

The frequency and amplitude must be sufficiently large in order to generate a reverse Kármán vortex street and therefore a significant amount of thrust, as



shown in fig. 2. Most importantly, the flying speed must be small in order to obtain a sufficiently large Strouhal number which will lead to thrust generation.

This insight leads to the conclusion that flapping wing propulsion is inherently limited to relatively low-speed flight or low-speed motion in water. Hence, flapping-wing powered man-made vehicles are likely to be low-speed vehicles. It is therefore not surprising that flapping-wing systems received relatively little attention in the last century because speed was always a major objective.

3 Flapping-wing powered micro air vehicles

However, it now appears that a new class of vehicles is becoming of interest for a number of applications. It is the class of micro air vehicles (MAV) or nano air vehicles (NAV). MAVs are defined as vehicles whose length, span or height does not exceed 15 cm. NAVs have dimensions not exceeding 7.5 cm. Clearly, such vehicles have sizes comparable to those of birds, fish and, ultimately, of insects. The aeronautical and hydronautical engineer therefore is faced with the question of whether propulsion and lifting systems developed by nature are better suited for typical MAV and NAV missions than the conventional rotary systems developed over the past century.

It is too early to give a definitive answer to this question and we merely refer to our recent review paper [3] on this subject and the additional references quoted therein. Instead, we draw attention to two flapping-wing powered unmanned air vehicles which have been developed in recent years.

Basically, two approaches might be used for the development of flapping-wing powered vehicles. One may want to imitate existing living creatures to the maximum possible extent. This approach is usually referred to as the biomimetic design approach. The second method is based on the adoption of only a few features found in nature while retaining other features from conventional man-made vehicles. This is the biomorphic design approach.

The AeroVironment Company in California chose to pursue the biomimetic approach by imitating conventional bird flight. This vehicle called the *Microbat* is shown in fig. 3. It evolved from the well known rubberband powered designs by substituting an electric motor drive-train for the rubberband and adding a radio for control. The energy for the motor is supplied by a Lithium-polymer (LI-poly) battery. The span is 23 cm and the total vehicle weight is 14 g. It has made flights of 25 minutes duration.

In contrast, we have chosen the biomorphic design approach for our vehicle shown in fig. 4. It has a fixed wing for lift generation and two wings mounted behind the fixed wing which flap in counterphase, i.e., when the upper wing moves up the lower one moves down and vice versa. In this way the joint center of gravity of the two flapping wings remains stationary and therefore the flapping oscillation does not cause undesirable oscillation of the complete vehicle.



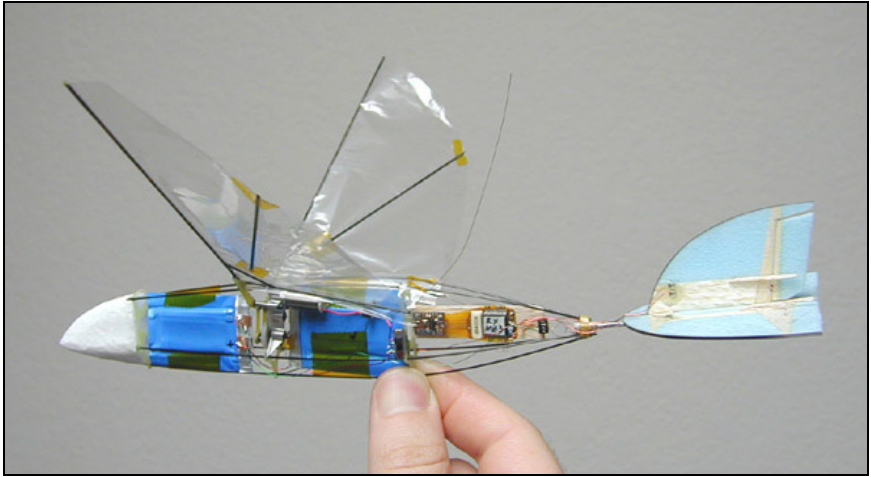


Figure 3: AeroVironment Microbat.

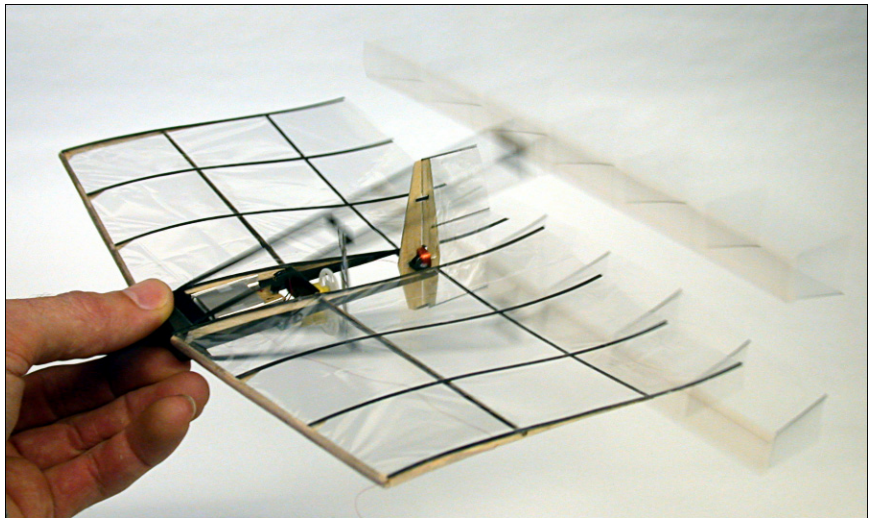


Figure 4: Authors' biomorphic flapping-wing propelled MAV.

Furthermore, the two flapping wings flap with constant amplitude along the span. This has the advantage that thrust is generated along the whole span in contrast to the bird wing where the flapping amplitude and hence the thrust decrease to zero at the wing root. Clearly, the bird has no choice whereas we were free to adopt only those features from nature which were most useful for our purpose. In this case we adopted from nature only the flapping wing concept, but retained the conventional airplane design feature of separating the thrust and lift generators. Actually, our arrangement is somewhat more sophisticated than



that because the flapping wings are mounted very close to the trailing edge of the stationary wing and therefore the three wings influence each other. It turns out that this mutual interaction is quite beneficial because the flapping wings cause an upstream entrainment effect which keeps the flow over the upper surface of the fixed wing attached to much larger incidence angles than would otherwise be the case. Our MAV therefore is remarkably insensitive to wind gusts.

Another interesting question is raised by our use of flapping wings in a biplane arrangement. We adopted this concept because our computational and experimental studies showed that flapping biplane wings generate more thrust and have higher propulsive efficiency than single wings. The effect is equivalent to flight of a single wing near a planar surface, such as the ocean surface. It is referred to as the ground effect. The pelican shown in fig. 1 flies in ground effect. One may therefore wonder whether flapping biplane wings evolved in nature. Although there are no current insects or birds using the biplane concept the answer, surprisingly, is that there is evidence of insects using this concept many millions of years ago. As discussed by Wootton and Kukalova-Peck [4], homiopteridae are an ancient group of large, sometimes gigantic insects, found in Carboniferous insect beds. Most had unusually large wings. The hind wings were usually broader-based than the fore-wings, but they overlapped extensively. This extensive overlapping appears to have been the case also for some members of the family Lycocercidae. In fact, in one case the wings appear to have overlapped almost completely. It remains an interesting question why biplane insects became extinct. Birds, on the other hand, evolved from 4-limbed ancestors, and since other requirements for survival required two to remain as legs, it was essentially impossible for birds to evolve into the biplane arrangement that we use, and yet, the Pelican in fig. 1 is most of the way there. He gets all the benefits of ground effect, but still misses out on the benefits of mechanical balance.

More details about this design, development and flight performance can be found in references [5] and [6].

4 Flapping-wing power extraction

The possibility of energy extraction from an air stream due to wing vibrations is a well known phenomenon in aeronautical engineering. Wing flutter can be so dangerous that it may break a wing in just a few seconds. The fundamental underlying mechanism can be understood by looking at fig. 5 which shows an airfoil that can oscillate in a combined pitch and plunge motion. It is readily seen from the upper figure that the lift acts in the same direction as the airfoil's motion if the pitch motion leads the plunge motion by 90 degrees. This implies that a net amount of work is done by the air on the airfoil, i.e., a certain amount of energy is absorbed from the air by the airfoil. As a result the amplitude of the airfoil oscillation will increase until the wing breaks. On the other hand, in the lower figure, the phase angle between the motions is zero and the lift opposes the motion during parts of the airfoil oscillation cycle. Hence in this case no net work is done by the air on the airfoil and no energy is transferred to the airfoil.



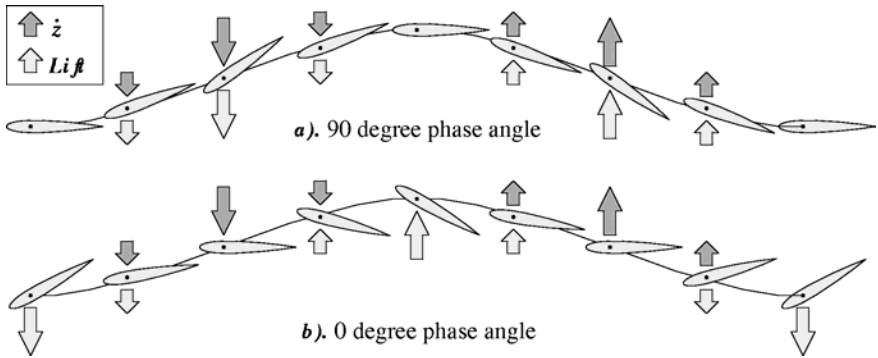


Figure 5: Combined pitch/plunge airfoil oscillation with a) 90 degree phase angle b) 0 degree phase angle.

It is evident that this phenomenon can be used for power generation if the airfoil motion is linked to an electric generator. McKinney and DeLaurier [7] built such an oscillating-wing power generator already a quarter of a century ago and showed the feasibility of extracting energy from a wind stream. However, little work was done since then to explore the competitiveness of such a system with the conventional wind turbines using rotating blades.

However, in recent years this possibility of power generation attracted interest in Great Britain, Germany and the United States for the extraction of the kinetic energy available in rivers and tidal streams. For example, according to J. Blumenfeld, director of San Francisco's Environment Department, nearly 400 billion gallons of water rush each day through the San Francisco Golden Gate at a speed of about 4 knots. If harnessed, the energy from this water could be an answer to the city's power needs [8].

Similar considerations motivated the British company *Engineering Business Limited* [9] to propose a tidal stream generator based on the flapping wing concept. Serious development of the technology started in late summer 2001 with the support of the British Department of Trade and Industry under its New and Renewable Energy Program. This generator consists of a large hydroplane which has a chord length of 3 m and a span of 15.5 m. Its angle of attack is varied to produce lift and drag, which forces a support arm to oscillate up and down. The arm is restrained by hydraulic cylinders and the resulting high pressure oil is used to drive a hydraulic motor, close-coupled to an electric generator. The design power output was 150 kW during operation in a 4 knot current. During the following three years this generator was built and mounted on the seabed of Yell Sound in the Shetland Islands. The company was able to demonstrate satisfactory operation, but the further development of the system was halted due to lack of follow-on funding.

In Germany a small company *Aniprop GmbH* [10] developed a small flapping-wing hydropower generator which was installed in summer 2003 in a channel located in the city of Augsburg. The generator consists of a single

hydrofoil with a chord length of 0.4 m and a span of 1.9 m. The power output was approximately 3 kW in a water flow of 2 m/s. Testing and further development of this generator is still continuing.

In the United States we started in 1996 with development of a micro hydropower generator which had a single hydrofoil of 62 mm chord length and a span of 350 mm. We then improved this generator by employing two wings in the tandem arrangement shown in fig. 6. The two hydrofoils were forced to flap with a 90 degree phase difference, such that the null spot of one coincided with the power stroke of the other. The hydrofoils could be forced to plunge with amplitudes up to $1.4c$ and pitch amplitudes up to 90 degrees. This generator was tested in a water tunnel at water velocities up to 0.4 m/s. Further details can be found in reference [11]. Encouraged by this experience, we have developed a new generator with an expected power output of several kW. Tests of this new generator are currently underway.

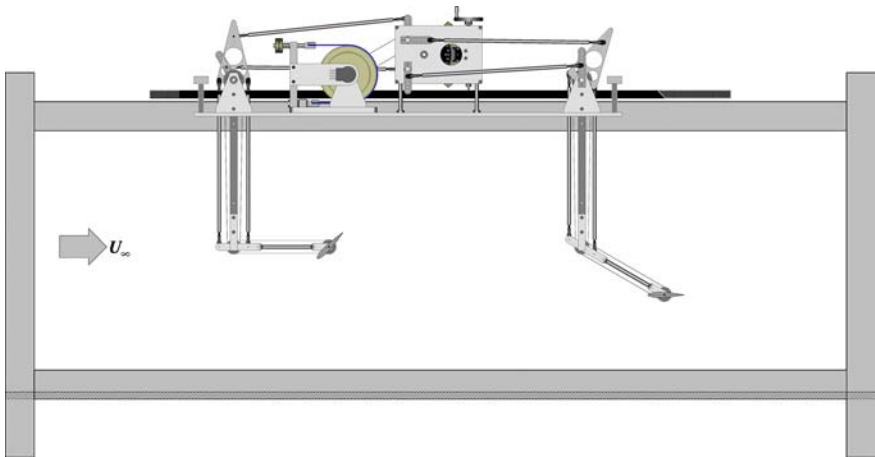


Figure 6: Authors' twin-wing hydropower generator in the water tunnel.

5 Summary and outlook

Aeronautical and power engineering are typically associated with systems not found in Nature, i.e., with propellers, jet engines, turbines etc. In this paper we tried to show that the design of new air vehicles, especially micro air vehicles, can benefit from propulsion and lift generation systems evolved by Nature over millions of years. Rubber powered birds could be purchased in many toy stores and such “micro air vehicles” were indeed regarded as toys of no practical value. Yet, it is now becoming clear that the coalescence of three technologies, namely flapping wing technology combined with enormous progress in battery and miniature electronics technologies, is soon making it possible to develop air



vehicles with great potential utility for a number of flight missions. Similarly, flapping hydrofoils are likely to open up new possibilities for renewable energy generation. Hence, it appears that there is much to be learned from Nature to stimulate new developments in aeronautical and power engineering.

References

- [1] Lilienthal, O., *Der Vogelflug als Grundlage der Fliegekunst*. Harenberg Edition, Dortmund, Germany, 3rd edition, 1992
- [2] Rozhdestvensky, K.V. and Ryzhov, V.A., Aerohydrodynamics of Flapping-Wing Propulsors. *Progress in Aerospace Sciences*, Vol. 38, No. 8, pp. 585-633, 2003
- [3] Platzer, M.F. and Jones, K.D., Flapping-Wing Aerodynamics – Progress and Challenges. AIAA Paper No. 2006-0500, 9-12 January 2006-01-2006
- [4] Wootton, R.J. and Kulakova-Peck, J., Flight Adaptations in Palaeozoic Palaeoptera. *Biol. Rev.*, Vol. 75, pp. 129-167, 2000
- [5] Jones, K.D. and Platzer, M.F., On the Design of Efficient Micro Air Vehicles. *Design and Nature*, edited by C.A. Brebbia, L.J. Sucharov, P. Pascolo, WIT Press, pp. 67-76, 2002
- [6] Jones, K.D., Bradshaw, C.J., Papadopoulos, J., Platzer, M.F., Bio-Inspired Design of Flapping-Wing Micro Air Vehicles. *The Aeronautical Journal of the Royal Aeronautical Society*, Vol. 109, No. 1098, pp. 385-393, August 2005
- [7] McKinney, W. and DeLaurier, J., The Wingmill: An Oscillating-Wing Windmill. *Journal of Energy*, Vol. 5, No. 2, pp. 109-115, 1981
- [8] Blumenfeld, J., Ebb and Flow Energy. *San Francisco Chronicle*, 2 August 2002
- [9] www.engb.com
- [10] www.aniprop.de
- [11] Jones, K.D., Lindsey, K., Platzer, M.F., An Investigation of the Fluid-Structure Interaction in an Oscillating-Wing Micro-Hydropower Generator. *Fluid-Structure Interaction II*, WIT Press, pp. 73-82, 2003



This page intentionally left blank

A graphic way for notch shape optimization

C. Mattheck, J. Sörensen & K. Bethge

Institute for Materials Research II,

Forschungszentrum Karlsruhe GmbH, Germany

Abstract

Many components have notches and notches are in the majority of cases the reason for failure. There are many options to reach a longer lifetime and a better utilisation of material. One method for the shape optimization of components, developed in Forschungszentrum Karlsruhe, uses the design rules of nature. During the last 15 years it has spread very well and proven itself in industry, especially in automotive engineering. The limits for using the CAO-method (Computer Aided Optimization) are more or less of an economic nature. So we need a method that allows optimization by everybody.

Now a new pure graphical method has been found, which works without any FEM or optimization software. It is called the “Method of Tensile Triangles” and requires only a set square and a piece of paper to optimize the notch shape in an effective and simple way.

Keywords: optimization of components, design rules, fatigue, graphical methods.

1 Introduction

It is of constantly increasing significance for industry to save time and money in order to produce more efficiently. The time to construct or modify components becomes shorter and shorter at the end of a development phase. Consequently, it is not always possible to apply complex, FE-based optimization methods. Such methods are mainly and justifiably used in special problem cases or highly loaded areas. The CAO method (computer-aided optimization) [1] eases problematic points, but often requires several iterations. In case of complex components, use of the CAO method together with FEM analyses is associated with the need for computing capacity and time.



In many cases, the “method of tensile triangles” would rapidly produce good results, and this only with a set square or with simple construction rules in CAD.

2 Procedure of the “Method of Tensile Triangles”

When studying the shoulder fillet under tensile loading (Fig. 1), potential slip planes and shear stresses due to an obvious longitudinal shear result in equivalent tensile stresses. This results in principle tensile stresses that are tilted by about 45° to the beam axis near the notch.

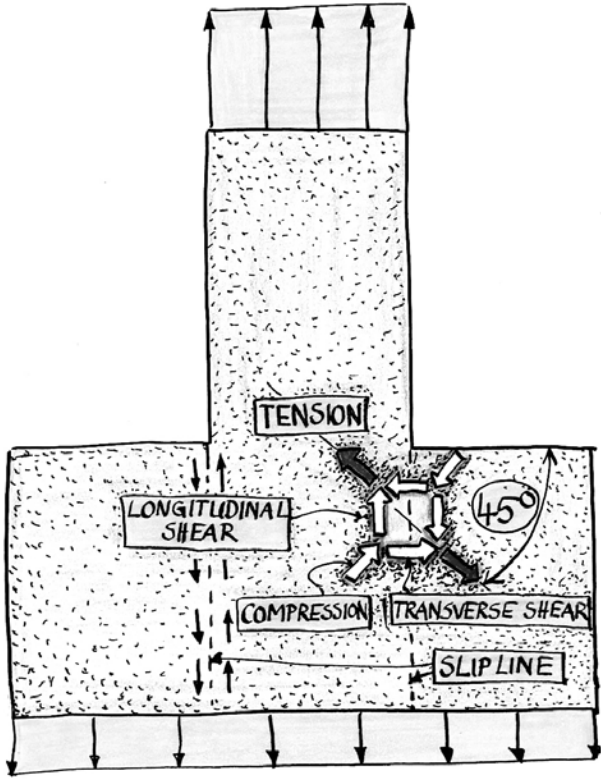


Figure 1: Stresses near a notch under tensile loading.

The “method of tensile triangles” starts with this knowledge. When looking at the foot of a tree’s trunk, see Fig. 2, a 45° tension rope is found to extend along the upper side of the root. When applied to technical components, an existing notch is bridged by a tensile triangle, as shown in Fig. 3. The repetition of this procedure is the method of tensile triangles. Figure 3 illustrates the method proposed by Mattheck and verified for a shoulder fillet in [2]. In a last step, the segments have to be rounded to obtain an optimized notch shape.



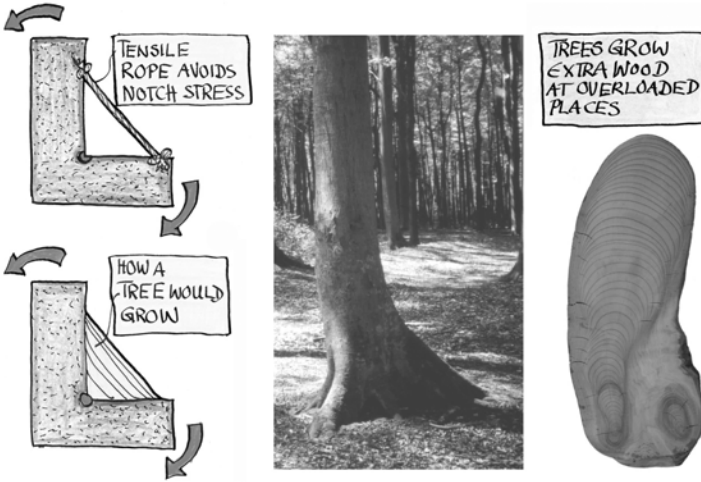


Figure 2: The buttress root bridges the sharp edge at the foot of the trunk like a rope.

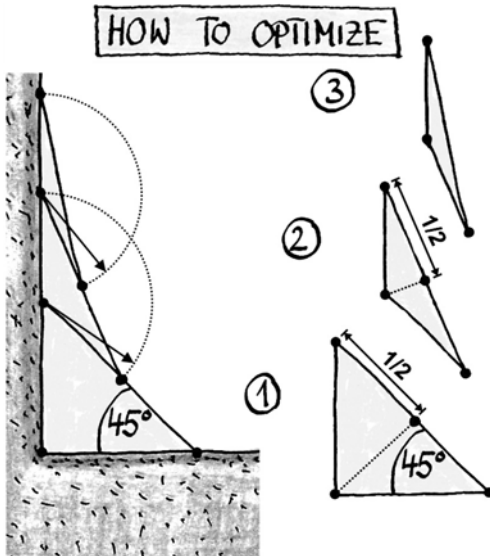


Figure 3: Principle of the method of tensile triangles for uniaxial tension.

3 Examples of application

3.1 Shoulder fillet

The optimization method is aimed at reducing notch stresses of components. These notch stresses are locally highly loaded areas which often represent the



starting points of cracks in the component and, hence, the start of failure. By optimizing the geometry of such notches, it is possible to reduce the notch stresses so that component lifetime is increased significantly.

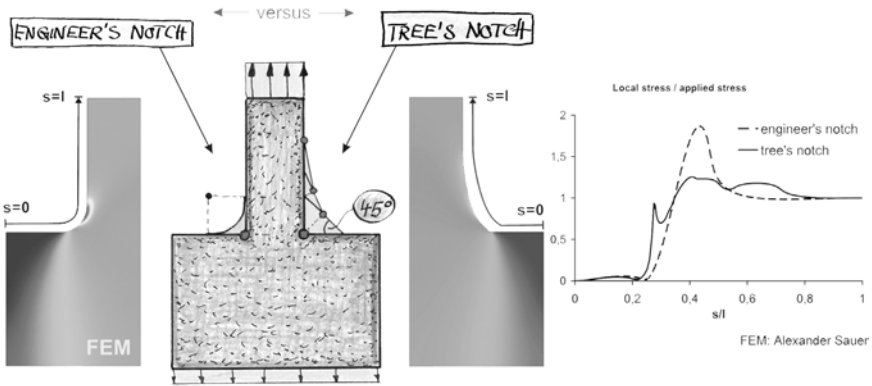


Figure 4: Stresses at the shoulder fillet. Rounding with a quadrant notch (left) and method of tensile tri-angles (right).

It is obvious from Fig. 4 that the shoulder fillet on the left that is rounded with a quadrant notch causes a locally high stress maximum. In contrast to this, the shoulder optimized by means of the method of tensile triangles is characterized by a very homogeneous stress along the contour.

3.2 Fork

Biaxial loads of forks e.g. may also be optimized by means of the method of tensile triangles (Figs. 5 and 6) [2]. At the same load ratios, a point of intersection of the bisecting line with the perpendiculars to the legs is obtained. From this point of intersection, the first tensile triangle is generated at an angle of 45° to the perpendicular. The following tensile triangles bridge the newly generated notches with increasingly obtuse angles and, thus, increasingly ease the notches.

Each leg with the corresponding perpendicular forms a shoulder and is optimized in analogy to the shoulder fillet.

At unbalanced load ratios, the bisecting line from Fig. 5 varies depending on the ratios. At a load ratio of 3 to 1, for instance, it changes to a ratio of 45° to 15° , as shown in Fig. 6. Variation of this ratio also changes the design space for the corresponding tensile triangles. The way of designing does not change. As described above, the individual straight lines are smoothed by radii.

As is obvious from the stress plot (Fig. 6), maximum stress of the stress curve is significantly reduced.

A common question in the optimization of a notch shape is “how large shall the design spaces be chosen?”. To answer this question, it can be stated that



irrespective of the other parameters, always the largest possible design space should be chosen in principle. In most cases, this “largest possible” design space is limited by the component function or accessory parts.

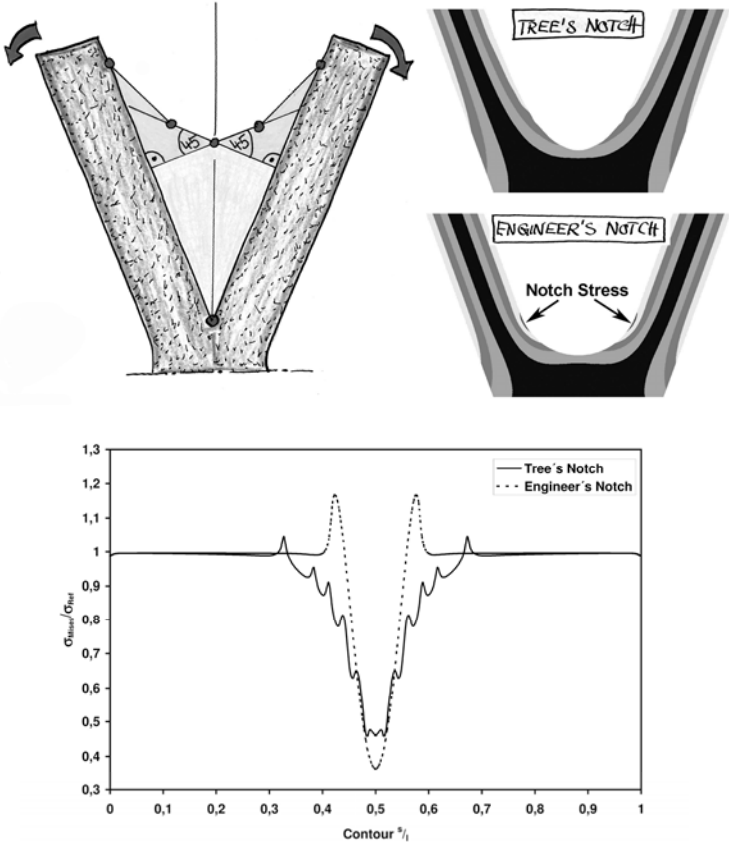


Figure 5: Fork under symmetric bending load.

To determine the design space required for a stress concentration factor of about 1, a FE model of the beam shoulder was studied using various radial design spaces. The geometry for all models studied is a beam shoulder under tensile loading with a width ratio of 3 to 1. Figure 7 shows the results of this study compared to the optimization by CAO. For the beam shoulder selected here, models with a radial design space of more than 45% of the largest possible design space, i.e. the width of the shoulder, exhibit a maximum stress similar to CAO optimization shown in Fig. 7. Furthermore, it can be noticed that an increase of the design space by more than 45% results in a small reduction of the stress only, whereas the same increase of the design space at lower levels causes high stress reductions.



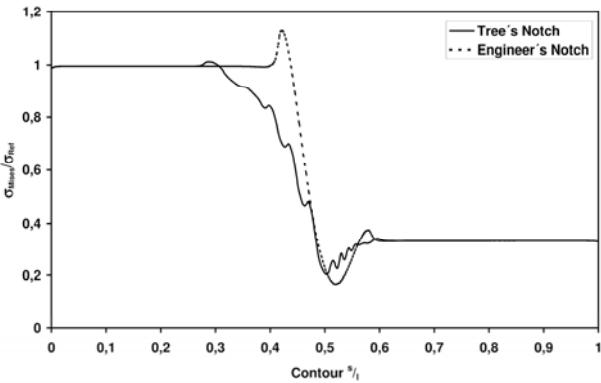
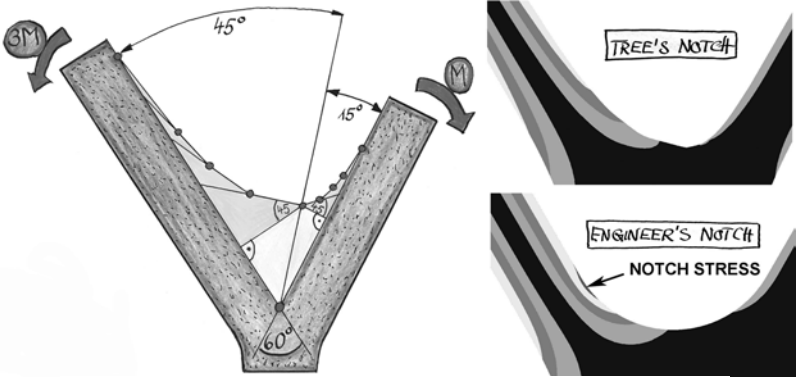


Figure 6: Fork under unsymmetrical bending load (3 to 1).

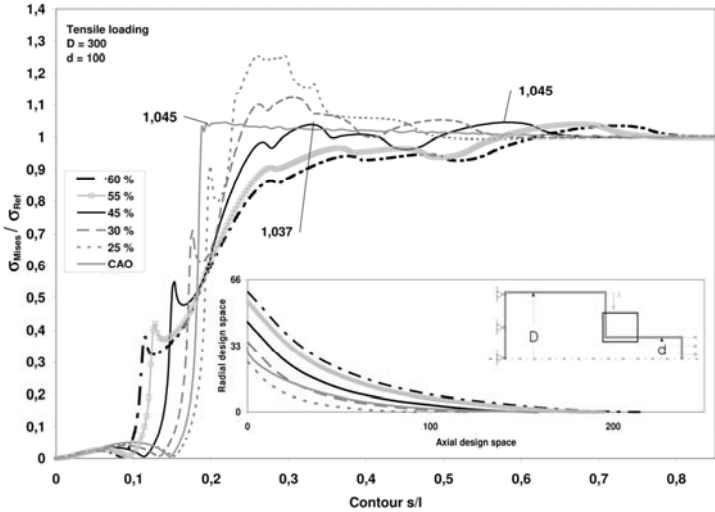


Figure 7: Studies related to the radial design space.



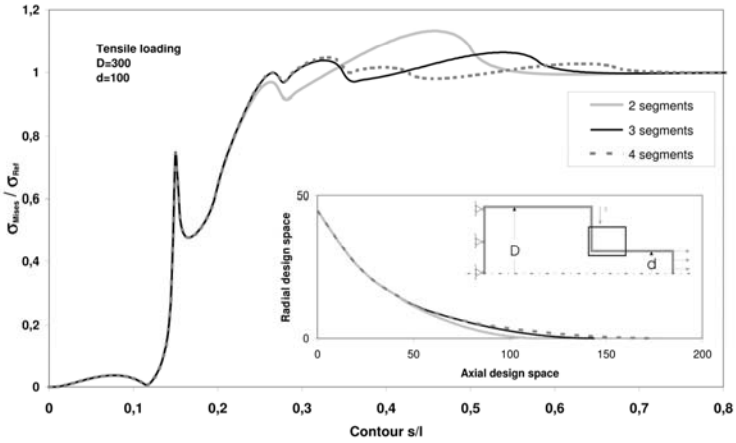


Figure 8: Studies related to the axial design space.

When looking at the number of tensile triangles used to determine the axial design space needed (see Fig. 8), it becomes obvious that the use of more than three tensile triangles does not reduce the stresses any further, but increases the required axial design space. Hence, not less than two, but, if possible, three tensile triangles should be used.



Figure 9: Non-optimized specimen (front) and two specimen with different degree of optimization.

4 Experiments

To verify the method of tensile triangles, beam shoulders were subjected to fatigue tests using a variable number of tensile triangles [3]. Figure 9 shows the specimen types and Fig. 10 the results of the fatigue tests. It is obvious that the notch located on the right side in the figure is always the most endangered one and that the initiation path of the crack is located vertically to the “tension rope” of the following tensile triangle. This makes the method of tensile triangles plausible. At the position of the potential crack, most material is applied and the tensile rope bridges the potential crack symmetrically.

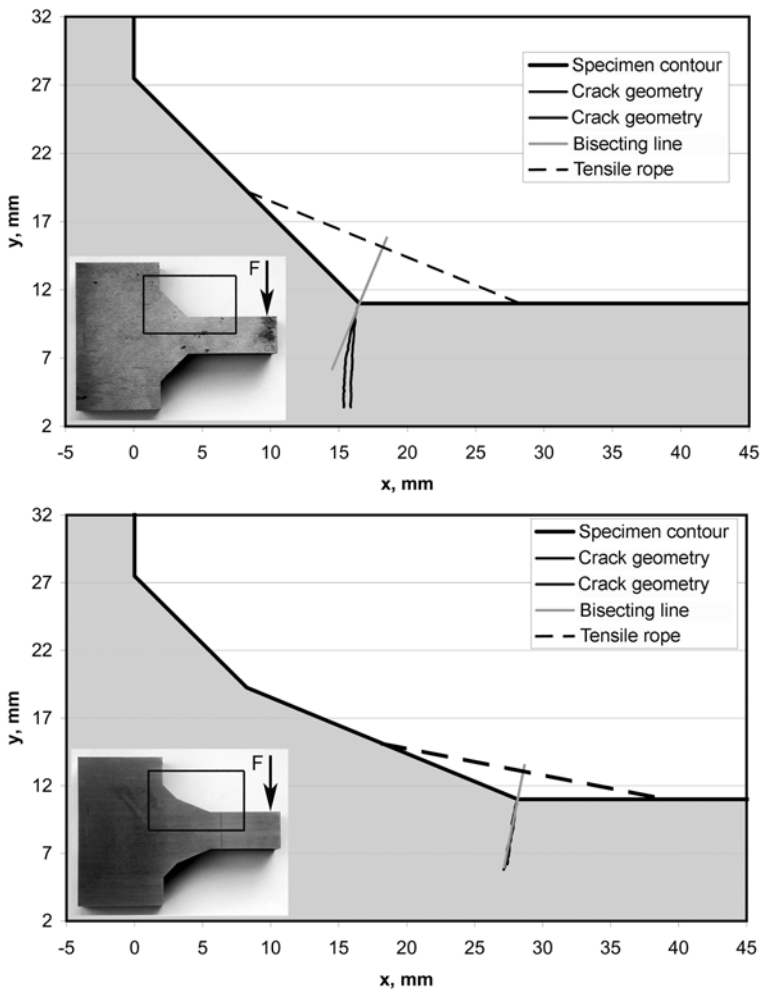


Figure 10: Results of fatigue tests with front- and backside crack path.



References

- [1] C. Mattheck, *Engineering structures grow like trees*, Materialwissenschaften und Werkstofftechnik, 1990, 143.
- [2] C. Mattheck, J. Sörensen, A. Sauer, I. Tesari, *Eine graphische Methode zur Kerbformoptimierung*, Konstruktionspraxis 2005, 10, 12.
- [3] C. Mattheck, K. Bethge, *On the Plausibility of the Method of Tensile Triangles (MTT)*, Materialwissenschaften und Werkstofftechnik, 2005, 36.



This page intentionally left blank

An inquiry into the morphology of Ciliate Protozoa using an engineering design approach

E. L. Benjamin¹, M. W. Collins² & D. McL. Roberts³

¹*Faculty of Business, Computing & Information Management, London South Bank University, London, UK*

²*School of Engineering and Design, Brunel University, London, UK*

³*Department of Zoology, The Natural History Museum, London, UK*

Abstract

Although cellular morphogenesis is an area of microbiology that is widely studied, very little is understood about the manner in which cells shape themselves or how they optimise their form to their environment. There exists an extensive literature on body shape, anatomy and life cycle of numerous single-celled micro-organisms including both prokaryotes and eukaryotes. However, with regards to morphology itself, there is a shortage of general empirical relationships to enable the interknitting of specific features that could lead to a biologically justifiable generic form. This paper comprises a concise review of the subject together with an assessment of the experimental approach which could be used, within an intended overall context of Engineering Design.

Keywords: morphology, morphogenesis, prokaryotes, eukaryotes, confocal microscope, microtubule, kinties, buccal cavity, oral apparatus, cytoskeleton, protozoa, ciliates, flagellates, protists.

1 Introduction

The cell shape is itself a characteristic property of a species. It would be most advantageous if the parameters of the surface could be used directly as characters themselves, particularly if their values could be used as a vector to define a location in some (morpho-) space, and with a distance between such locations being a measure of the difference between individuals. Sets of such vectors could then be subjected to cluster analysis and other grouping techniques to



uncover or establish relationships. The fitting of the extracted surface to a generic model is an application of several established techniques [21–26].

1.1 Biology

A fundamental objective of classical morphology in microbiology is the identification and classification of the basic shapes that cells can assume; to display morphological regularities corresponding to familiar categories, and, if possible to express mathematically the harmony of forms. This approach was proposed by Harold [1] but because it was not attractive to microbiologists, he did not pursue it. Instead however, he attempted to formulate ‘casual’ principles to explain how biological forms arise and how they are transmitted from parent to offspring. This approach has problems, as Harold appreciated, because microbial forms are so diverse that there is no obvious unitary principle of morphogenesis, in the sense that unitary principles do account for heredity, protein synthesis, or oxidative phosphorylation. On the other hand, it seemed implausible to him that each organism is altogether unique. Harold therefore suggested that the greater likelihood is that the multitudinous forms represent variations on a much smaller number of generative themes, whose discovery is the proper goal of research in cellular topobiology.

While Harold’s review is relatively recent – 1990, he harks back to the classic approach of D’Arcy Thompson, *On Growth and form*, first published in 1917. In Bonner’s Editorial Introduction to the Canto abridged reprint [2], he focuses on D’Arcy Thompson’s “... most conspicuous attitude [was] the analysis of biological processes from their mathematical and physical aspects” (pp. xiv). Specifically, his analyses related biological forms, and their changes “apparent in ... movements and ... growth ... as due to the action of force”, namely “a diagram of forces” ([2], pp. 11).

This approach has an enduring appeal, not least in Ball’s rather beautiful *The Self-Made Tapestry* [3]. D’Arcy Thompson features throughout ([3] pp. 1 and pp. 251-253, for example) and Ball concludes that whereas D’Arcy Thompson “was unable to persuade most of his peers of the importance of form and pattern”, now “pattern formation” (at least) is an “identifiable field of study in its own right.”

For protozoa, the most significant current expression of D’Arcy Thompson’s ‘mathematical aspects’ is that of Goodwin [4]. Applying various forms of Laplace’s field equation to *Tetrahymena* (See figure 4) in particular, he was able to generate convincing mathematical models of the buccal cavity asymmetry and the ciliature ([4], pp. 338). A brief description of the buccal cavity is given in section 3.1.

It is worthy to note Thompson’s recognition that, “Many a beautiful protozoan form has lent itself to easy physico-mathematical explanation; others, no less simple and no more beautiful, prove harder to explain.” ([2], pp. 171)].



1.2 Rationale

Even in the context of a single *Tetrahymena*, Goodwin noted that the “overall shape varies greatly, from pear to egg to cucumber” ([4], pp. 381). Figure 1 shows how the shape of protozoa varies from species to species.

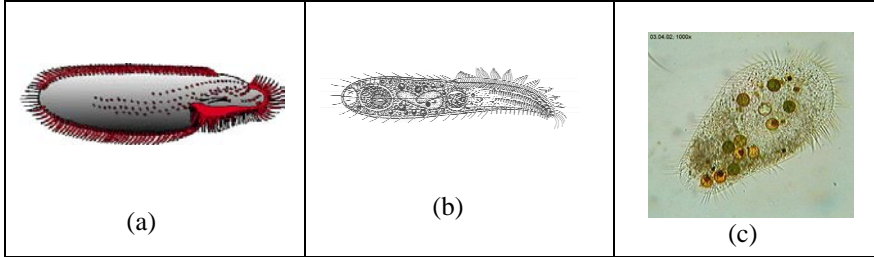


Figure 1: Some typical protozoa. (a) *Hypotrichida* (diagram from P. Eigner). (b) Type species: *Cultellothrix velhoi* sp. n. (diagram from Wilhelm Foissner). (c) *Stichotrich*. (from GNU Free Documentation License: <http://en.wikipedia.org/wiki/Ciliate>).

Bonner points out that D’Arcy Thompson “was in no way an experimenter,” ([2], pp. xv), and it is very clear that actual experimental data would not be helpful in testing the approach described briefly before.

Our hypothesis is that ciliate cell surfaces can be described with a few rules and a few parameters. To test the hypothesis, we are seeking to assemble a dataset of confocal images of stained single cells, which will then be analysed, from an engineering and design perspective. In more detail 3-D CAD (Computer Aided Design) models will be used to describe a surface onto which the morphology of a ciliate cell can be mapped. If the results of this study are positive, it will mean that a small set of invariants will suffice to describe the cells and become an aid to automating the identification of the species themselves and of quantifying the effects of variation due to environmental influences.

2 Mathematical modelling

2.1 D’Arcy Thompson’s legacy

To an intriguing extent, the foundation of D’Arcy Thompson’s explanations is that of engineering, as so aptly reiterated by Harold [1].

“The objects that surround us in daily life, most of them man-made, were produced by shaping a natural or artificial material to suit some function or purpose. They owe their form to the application of physical forces, most commonly mechanical ones. The idea that biological forms likewise reflect the action of physical forces on formless protoplasm is a venerable one, although somewhat unfashionable today.” ([1], pp. 393).



The first section of D’Arcy Thompson’s Chapter II ‘The principle of similitude’ ([2], pp. 15) corresponds to sections relating to convective heat transfer in a typical UK Undergraduate text on Thermodynamics – ‘The principles of dynamic similarity and dimensional analysis applied to forced convection’ ([5], pp. 571), for example.

2.1.1 Cartesian transformations

The above correspondence with engineering goes further. D’Arcy Thompson described “a net of rectangular equidistant co-ordinates (about the axes of x and y),” and showed that by altering or deforming the “network in various ways,” an organism’s appearance can be modified to resemble different species. This is predicated on the assumption that the organisms display a reasonable number of homologous (directly equivalent) landmark features and some smooth function exists to determine their spatial relationship.

Thompson stated “It follows that any figure which we may have inscribed in the original net, and which we transfer to the new, will thereby be deformed in strict proportion to the deformation of the entire configuration, being still defined by corresponding points in the network and being throughout in conformity with the original figure. For instance, a circle inscribed in the original ‘Cartesian’ net will now, after extension of the y-direction, be found elongated into an ellipse.” ([2], pp. 276).

Figure 2 illustrates Thompson’s approach.

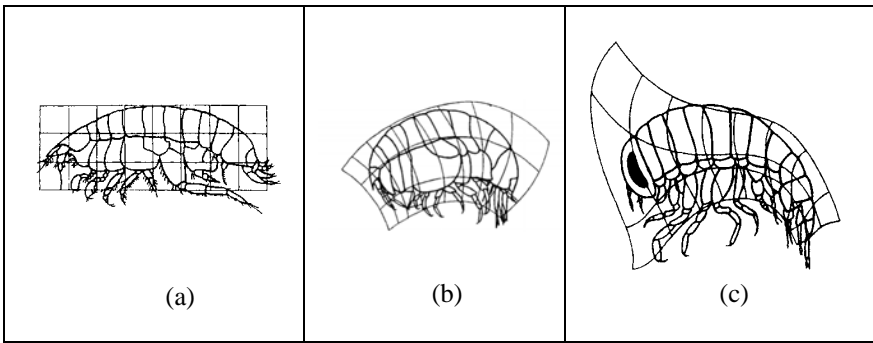


Figure 2: (a) *Harpinia plumose* Kr. a little amphipod of the family Phoxocephalidae (*Harpinia* sp.) (b) By deforming the co-ordinates of *Harpinia* into the curved orthogonal system, we at once obtain a very fair representation of the allied genus, belonging to a different family of amphipods, namely *Stegocephalus* (c) Greater deformation of *Harpinia* or *Stegocephalus* results in a tolerable representation of the aberrant genus *Hyperia*, with its narrow abdomen, its reduced pleural lappets, its great eyes, and its inflated head. (From D’Arcy Thompson, with his explanation, [2], pp. 295).

Now D’Arcy Thompson’s ‘similitude’ and ‘method of coordinates’ may be regarded as subsumed within the relatively recent engineering developments of



Computational Fluid Dynamics (CFD) and heat transfer – that is a modelling of the basic non-linear partial differential equations in preference to the prior ‘dimensional analysis.’

At one stage, the CFD gridding techniques involved co-ordinate transformation, of, if needed, only a *part* of the field, so in a CFD simulation of flying or swimming an overall Cartesian grid, could include local co-ordinate systems as in Figure 2. For ‘solid’ locomotion, outside CFD, the same principles could be applied.

What it means is that efficient alternative ‘locomotive’ shapes are possible, where simple coordinate transformation rules apply.

2.2 Preston’s legacy

In 1953, F. W. Preston [6] undertook studies on the shape of birds’ eggs. “This investigation was not undertaken primarily as a mathematical amusement. It seems likely that it may throw some light on several biological and ecological problems, but the present paper concerns itself namely with the broad question of what is the shape of a bird’s egg. The mathematics may conceivably show something of the physiology and mechanics of egg-laying, since the shape of the egg is a response to the forces exerted by the oviduct during shell-formation (Mallock, 1925; D’Arcy Thompson, 1943).” ([7], pp. 160). Figure 3 shows Preston’s circles of derivation.

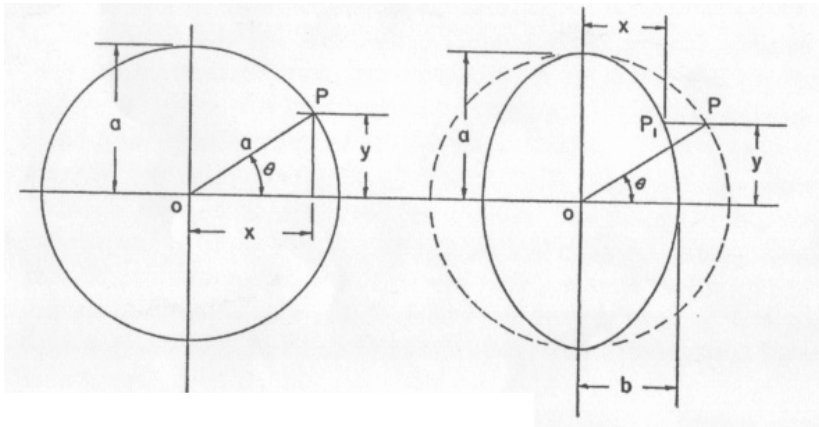


Figure 3: (left) Parametric equation of a circle in terms of eccentric angle. (right) Parametric equation of an ellipse. (From Preston with this explanation [6], pp. 161).

Starting with the parametric equation of a circle, Preston described the representation of birds’ eggs in terms of ‘circles of derivation’, which then describes the various shapes.

$$y = a \sin \theta ; \quad x = b \cos \theta (1 + c_1 \sin \theta + c_2 \sin^2 \theta + c_3 \sin^2 \theta)$$



which, except in the case of the Alcids, reduces to:

$$y = \text{Sin } \theta; \quad x = b \text{ Cos } \theta (1 + c_1 \text{ Sin } \theta + c_2 \text{ Sin}^2 \theta)$$

where c is a dimensionless parameter that may vary from egg to egg but is constant for any particular specimen.

for a few eggs: $y = \text{Sin } \theta; \quad x = b \text{ Cos } \theta (1 + c_1 \text{ Sin } \theta)$

and for a few others, whose ends are virtually alike, we may have:

$$y = \text{Sin } \theta; \quad x = b \text{ Cos } \theta (1 + c_2 \text{ Sin}^2 \theta).$$

Preston's work was supported by Okabe ("On the Form of Hens' eggs" Reports of Research Institute for Applied Mechanics, Kyushu University, Vol. 1, 1952). Okabe expressed the view that Preston's treatment of the shape of eggs, "as a problem in the forces that mould that shape," and then using the shape to interpret the interacting forces, is in tune with the desires of D'Arcy Thompson [6, pp. 161].

However, it should be appreciated that the model is an arbitrary geometric simulation, so should not be used predictively outside its range.

Very recently, Narushin [7, 8] developed further the following mathematical equation for bird's eggs profile.

$$Y = \pm \sqrt{(L^{2/(n+1)} x^{2n/(n+1)} - x^2)} \quad \text{in which} \quad n = 1.057 (L/B)^{2.372}$$

where L the length of the egg, B the maximum breadth of the egg, X the coordinate along the longitudinal axis and y is the traverse distance to the profile. Narushin has proposed "Indices of ellipticity and conicity for the calculation of the deviation of an egg from its theoretical profile, defined by the above equation..." On the same basis, "...formulae for the calculation of an egg's volume, surface area, longitudinal circumference length and normal projected area..." have also been proposed [8]. However, these derivations have been omitted here in the interest of space.

2.3 Goodwin's proposition

Goodwin's approach has already been mentioned. Space does not allow a full description of this but figure 4 shows the outcome of progressive developments in the Laplace equation.

Goodwin described the morphological features of *Tetrahymena* (figure 4(a)) by using the spherical shape of the organism as the basic shape, and using the basic polar organisation of its cortical field, to determine the global spatial ordering of the cilia. Figure 4(b) shows the anterior and posterior as north (N) and south (S) poles respectively. Goodwin further described this polarising field with the following general equation:

$$U(\theta, \varphi) = \alpha \text{ In Cot } (\theta/2) + \beta \varphi - b \text{ Cot } (\theta/2) \text{ Cos } \varphi \quad (1)$$



in which θ and ϕ determine the two locations, latitude and longitude respectively, α a parameter that determines the strength of the field, and U_0 a function which defines the poles. It varies from $\theta = \pi (-\infty)$ at the posterior pole to $\theta = 0 (+\infty)$ at the anterior pole. β is a parameter which determines the spiral orientation of the cilia. A negative value of β indicates a clockwise spiral and a positive value indicates an anticlockwise spiral. $\beta = 0$ is indicative of the rare case of a non-spiral polarity.

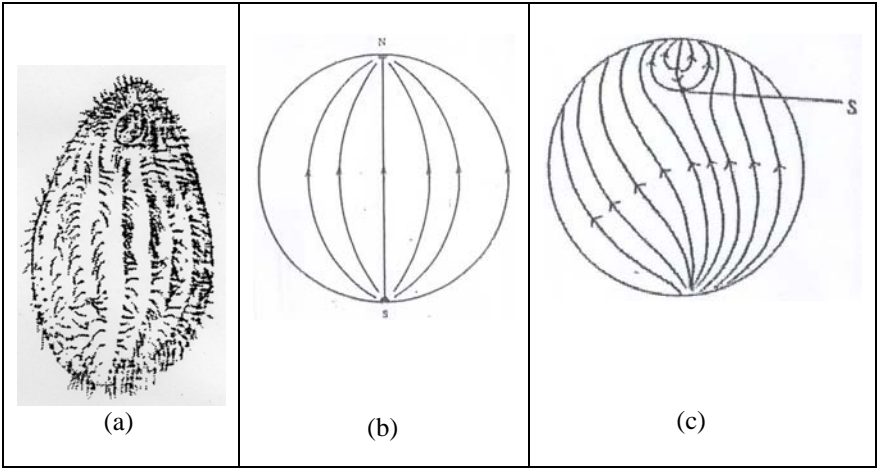


Figure 4: (a) *Tetrahymena pyriformis*, showing ciliary meridians and buccal cavity with its cilture (See section 3.1 below). (b) polarised meridians on the sphere defined by the basic polar field. (c) Members of the two families of curves on the sphere of equation (1) and (2). The arrows define the direction of increasing $U(\theta, \phi) S$, which established posterior-anterior polarity saddle points. (From Goodwin, with his explanation, [4], pp. 381, 383 and 388).

The parameter b takes into account the presence of the buccal cavity, a ‘saddle point’ depicting loss of polarity with respect to a Laplacean field. It is the measure or strength of asymmetry about the polar axis. For organisms lacking the asymmetry such as that of the ciliature spiral pattern found in *Tetrahymena pyriformis*, for example, $b = 0$. Further analysis gives rise to the equation:

$$V(\theta, \phi) = +\beta \ln \cot(\theta/2) - \alpha\phi + b \cot(\theta/2) \sin \phi \tag{2}$$

in which $V(\theta, \phi)$ is a harmonic conjugate function of $U(\theta, \phi)$ and describes the longitudinal direction which is orthogonal to the cilia meridians. Figure 4(c) shows curves corresponding to the kineties (ciliary meridians) in *T. pyriformis*, defined by $V(\theta, \phi) = \text{constant}$. As iterated by Goodwin, each curve corresponds

to a different value of the constant. Note that “The field geometry ... implies that the oral apparatus and the ciliary meridians are spatially organised by the same global field.” [4]. This is reiterated by Webster and Goodwin in their writing on *Morphometric fields and cortical inheritance* [28]. Another narrative worthy of note, is that of Goodwin’s on *A Generative Biology: Morphometric fields* [27].

3 Protists

We now review the evolutionary history of the protists.

Single eukaryotic cells, the Protista, evolved at some distant time in the evolutionary past, probably more than 2,000 Myr ago. Prokaryotic life almost certainly evolved very soon after there was liquid water available, more than 4,000 Myr ago. Eukaryotes differ from prokaryotes in many fundamental ways relating to cell structure and organisation. Probably most importantly, they possess a cytoskeleton which acts both as a frame against which forces generated by flagella can act (see section 3.2) and which permits the capture of particulate food.

By contrast, the earliest evidence for multicellular life does not appear until around 800 Myr ago, so the major chemical cycles evolved in an unicellular context. Multicellular organisms evolved in the presence of a fully-functional ecosystem.

3.1 Ciliated protists

Ciliated protozoa are one of the very few traditional groups of protists which are believed to be a good group in the context of modern evolutionary understanding. They are the best-studied of the non-pathogenic protists and have an established place in the laboratory where they are fairly easily manipulated [13]. They are large enough to image easily with light microscopy and are amenable to routine cytological staining [13, 18, 19, 20]. Staining of surface features for confocal microscopy is a known art, and a functional method was published by Ann Fleury [14, 15], Fleury and Laurent [6] and Fleury et al. [17].

Ciliates are supported by a microtubular cytoskeleton which runs from anterior to posterior pole. See figure 4(a). Somatic (body) cilia, responsible for locomotion, are arranged in rows (meridians) called kineties which also run from pole to pole [11, 12, 29 pp. 6-7]. The cell's mouth can be at the anterior pole or, more commonly, on the ventral surface. In transverse section they can be round or somewhat compressed (oblate). The shapes can be readily approximated by an asymmetric spheroid. The asymmetry required means that the widest point on the major axis is not necessarily located in the middle of the cell, for instance a pear-shape. Such shapes can be easily constructed by empirical equations with minimal parameterization (for example, see section 2.2 above), but there is no known theoretical reason yet established to choose one equation form over another.



The body characters, such as the kineties, are organised in a variety of ways. It is not known whether changes to the body shape affect the organisation beyond certain dramatic changes, such as the increase in the density of kineties in response to starvation condition to produce swarmer cells, adapted to swim faster and believed to be a dispersal mechanism.

The organisation of the oral (mouth) cilia is a central feature of ciliate taxonomy. In general the mouth is located at the bottom of a depression in the body called a vestibulum or buccal cavity. The oral cilia are organised into arrays called membranelles, which are designed to funnel water towards the mouth where particulate food is trapped by the final membranelle. The fluid dynamics of this process have been briefly studied by Tom Frenkel [9].

3.2 Flagellated protists

Flagellated protists are generally smaller than ciliates and most commonly carry two flagella (singular, *flagellum*) of unequal length. Flagella and cilia have an identical structure, although flagella tend to be longer and cells bear fewer of them, the different terms are maintained in the community for historical consistency. Cilia beat with an oar-like stroke [10] while the longer flagella have a sinusoidal stroke and, with a whip-like action ([29], pp. 11-13), normally move water from tip to base, so pulling the cell through the water. Some flagellates (the Stramenopiles) possess tripartite hair-like projections called retronemes along the length of the flagellum. As their name suggests, the effect of the retronemes is to reverse the flow of water as it travels from base to tip, so pushing the cell through the water.

Morphologically, flagellates are far more diverse than ciliates and it is believed that the ancestral eukaryotes carried a flagellum. They can also be phagotrophic, although osmotrophic and phototrophic lifestyles are also widespread. There are correspondingly many ways that cells capture particulate prey, including a gullet, tentacles which *may* act as a filter and a variety of adhesive mechanisms.

4 Conclusions

This research has three main themes of interest. It is strongly interdisciplinary, being a combination of the latest biological research interest allied with an engineering design approach. Secondly, it has a strong computational science focus and it is possible that subject to successful demonstration, the methods could apply more widely in morphogenesis. Finally, in combination with addressing the fluid dynamics of the nutrient dependent ciliate shape, it is intended to explore the water cleansing effectiveness of protists, leading to improved biological treatment of sewage systems. The research programme is therefore anticipated as contributing to three principle areas.

First, the academic question of evolutionary relationships and the problem of grouping organisms into informative assemblages. Unicellular eukaryotes are now understood to be an exceedingly diverse collection of taxa which have



traditionally, but erroneously, been classified by their morphological and functional similarity (e.g. the algae or the amoebae). We now recognise that these groups are intimately mixed in evolutionary descent based largely on discoveries made through molecular biology. Unfortunately, few taxa have been studied with molecular techniques or by detailed electron microscopy. Those that have are not well distributed amongst the recognized diversity of the group. Increased knowledge of body-plan and cellular organisation, based on a functional understanding, will contribute to efforts to integrate the classification of described taxa, particularly those that might be well described as legacy data.

Second, the organisation of characters on the body is known to change in response to environmental condition. Current methods can only detect gross changes in morphology. An improved method of assessing body conformation, specifically separating size and shape from component organisation, may well prove to be a powerful tool for monitoring environmental change. Such an approach is applicable in two domains: first, academically in ecology, to assign an individual or population to an ecological role. Second, practically, to provide a rapid-response method of assessing water quality.

Third, there is the practical question of how protists manage to remove bacteria from water so efficiently. The removal of very small particles (of the order of unit microns) from water is dominated by viscous forces. Such removal is industrially very important both in public health (the removal of pathogens from water) and in industry, for clean technologies. A better understanding of how protists achieve their filtration, which can even be selective, could lead to novel engineering solutions to this problem.

References

- [1] Harold, F. M., To shape a cell: an inquiry into the causes of morphogenesis of microorganisms. *Microbiological Reviews*, 54(4), pp. 381-431, 1990.
- [2] Thompson, D. W., *On growth and form*. Abridged, J. T. Bonner (ed). Cambridge University Press, London, 1961.
- [3] Ball, P., *The self-made tapestry: Pattern formation in nature*. Oxford University Press, 1999.
- [4] Goodwin, B. C., Pattern formation and its regeneration in the protozoa. *Sym. Soc. Gen. Microbiology*, 30, pp. 377-404, 1980.
- [5] Rogers, G. F. C. & Mayhew, Y., *Engineering Thermodynamics, Work and heat Transfer*, 4th ed., Prentice Hall, Harlow, UK.
- [6] Preston, F. W., The shape of bird's eggs. *The Auk*, 70, pp. 160-182, 1953.
- [7] Narushin, V. G., The avian egg: geometrical description and calculation of parameters. *J. Agric. Engng. Res.*, 68, pp. 201-205, 1997.
- [8] Narushin, V. G., Shape geometry of the avian egg. *J. Agric. Engng. Res.*, 79, pp. 441-448, 2001.
- [9] Fenchel, T., Protozoan filter feeding. *Progress in Protistology*, 1, pp. 65-113, 1986.
- [10] Sleight, M. A., *The Biology of Protozoa*, London: Edward Arnold, 1973.



- [11] Grell G. G., *Protozoology*. Springer-Verlag: Berlin, Heidelberg and New York, 1973.
- [12] Corliss, J. O., *The ciliated Protozoa: Characterization, classification, and guide to the literature*. Pergamon Press: Oxford, London, New York and Paris, 1961.
- [13] Roberts, D. McL. & Causton, H., Silver nitrate impregnation of ciliated protozoa. *Arch. Protistenkd.* 135, pp. 299-318, 1998.
- [14] Fleury, A., Dynamics of the cytoskeleton during morphogenesis in the ciliate Euplotes. 1. Basal bodies related microtubular system. *Europ. J. Protistol.*, 27(2), pp. 99-114, 1991.
- [15] Fleury, A., Dynamics of the cytoskeleton during morphogenesis in the ciliate Euplotes. 2. Cortex and continuous micro tubular systems. *Europ. J. Protistol.*, 27(3), pp. 220-237, 1991.
- [16] Fleury, A., & Laurent, M., Transmission of surface pattern through a dedifferentiated stage in the ciliate Paraurostyla. Evidence from the analysis of the microtubule and Basal body development. *J. Euk. Microbiol.*, 41(3), pp. 276-291, 1994.
- [17] Fleury, A., Le Guyader, H., Iftode, F., Laurent, M. & Bornens, M., A scaffold for basal body patterning revealed by a mono-clonal antibody in the Hypotrich Ciliate Paraurostyla weissei. *Dev. Biol.*, 157, pp. 285-302.
- [18] Garreau de Loubresse, N., Keryer G., Miguez, B. & Beisson, J., A contractile cytoskeleton network of Paramecium: the infracilliary lattice. *J. Cell Sci.*, 90, pp. 351-364.
- [19] Silva-Neto, I. D. da, Improvement of silver impregnation technique (protargol) to obtain Morphological features of protists ciliates, flagellates and opalينات. *Rev. Brasil. Biol.*, 60(3), pp. 451-459, 2000.
- [20] Nicolina, D., Renato, A., Mortara, N. L., Morphological and physiological changes in Tetrahymena pyriformis for the in Vitro cytotoxicity assessment of Triton X-100. *Toxicology in Vitro*, 17, pp. 357-366, 2003.
- [21] Alt, W., Statistics and Dynamics of cellular shape changes (Chapter 15). *On Growth and Form: Spatio-temporal pattern formation in Biology*, ed. M. A. J. Chaplain, G. D. Singh & J. C. McLachlan, Wiley, UK, pp. 288-307, 1999.
- [22] Auffray, J., Debat, V. & Alibert, P., Shape asymmetry and developmental stability (Chapter 16). *On Growth and Form: Spatio-temporal pattern formation in Biology*, ed. M. A. J. Chaplain, G. D. Singh & J. C. McLachlan, Wiley, UK, pp. 309-324, 1999.
- [23] Lele, S., Invariance and Morphometrics: A critical appraisal of statistical techniques for landmark data (Chapter 17). *On Growth and Form: Spatio-temporal pattern formation in Biology*, ed. M. A. J. Chaplain, G. D. Singh & J. C. McLachlan, Wiley, UK, pp. 325-336, 1999.
- [24] Mardia, V., Statistical shape analysis and its applications (Chapter 18). *On Growth and Form: Spatio-temporal pattern formation in Biology*, ed. M. A. J. Chaplain, G. D. Singh & J. C. McLachlan, Wiley, UK, pp. 337-355, 1999.



- [25] Lozanoff, S., Sphenoethmoidal Growth, malgrowth and midfacial profile (Chapter 19). *On Growth and Form: Spatio-temporal pattern formation in Biology*, ed. M. A. J. Chaplain, G. D. Singh & J. C. McLachlan, Wiley, UK, pp. 357-372, 1999.
- [26] O'Higgins, P., Ontogeny and Phylogeny: Some morphometric approaches to skeletal growth and evolution (Chapter 20). *On Growth and Form: Spatio-temporal pattern formation in Biology*, ed. M. A. J. Chaplain, G. D. Singh & J. C. McLachlan, Wiley, UK, pp. 373-393, 1999.
- [27] Goodwin, B. C., D'Arcy Thompson and the problem of biological form (Chapter 21). *On Growth and Form: Spatio-temporal pattern formation in Biology*, ed. M. A. J. Chaplain, G. D. Singh & J. C. McLachlan, Wiley, UK, pp. 395-402, 1999.
- [28] Webster, G., & Goodwin, B. C., *Unitary morphogenetic field. Form and transformation*, Cambridge university press, USA, pp. 221-229, 1996.
- [29] Goodwin, B., C., *How the leopard changed its spots*, Princeton University Press, Princeton, New Jersey.



The optimized shape of a leaf petiole

D. Pasini & V. Mirjalili

*Department of Mechanical Engineering, McGill University,
Montreal, Canada*

Abstract

A plant leaf is generally composed of a petiole and a leaf blade. The petiole connects the leaf blade to the plant stem and, from a structural viewpoint, it resembles a cantilever beam. Petiole design is driven by the minimum use of material to withstand a combined torsion and bending load. The cross-section has a transverse size decreasing lengthwise and has a grooved shape. This paper examines the structural efficiency of the petiole shape. Ten petiole specimens of dicotyledonous plants have been investigated. Continuum mechanics and dimensionless factors are used to model the stiffness properties of the petioles. The results of the characterization are visualized on maps that contrast petiole efficiency to that of reference cross-sections. Nature shapes the petiole material to secure the best trade off between torsional compliance and flexural stiffness.

Keywords: leaf petiole, structural efficiency, optimized shape, torsional compliance, bending stiffness.

1 Introduction

Plants are complex systems that perform several vital functions. Their organs work in synergy to govern a variety of tasks, such as mineral absorption, water supply, photosynthesis, food storage, and structural support. During growth, the plant organs that interface with the environment receive different stimuli from light, gravity, touch, as well as from change of soil salinity and stress concentration. As a response to these factors, the plant adapts its morphology.

Plants have a large variety of colours, forms and size, which make them attractive. Appearance, though, is just one among the remarkable features. Plants are designed to multi-function as well as to support a variety of loading configurations by using the least amount of bio-material [1].



This paper focuses on one specific organ of plants, the leaf petiole. From a vital point of view, the leaf is one of the crucial parts of a plant. Through photosynthesis, a plant processes the sun's energy to produce its own sugar [2]. However, from an engineering point of view, the leaf has a noteworthy structure, in particular its petiole. The shape of this organ is remarkable, for it permits an efficient support of loading. For example, it allows the leaf to swing freely in the wind in order to reduce the aerodynamic forces; it supports the weight of the leaf blade, as well as any moisture, rain, snow, and insects; it also enables the leaf blade to twist towards the sunlight and catch the sun's rays. To function with the least amount of material, the petiole exploits the material anisotropy and tailors the shape properties of its body [3–7].

This paper examines the structural efficiency of the petiole to bear combined loading. The aim is to look into the performance of its cross-sectional shape. The first part of the paper describes organs and functions of plants in order to put the petiole into the biological context. Then, the factors that stimulate shape changes are reviewed. In the last sections, the analysis is narrowed to the stalk structural design. Ten petiole specimens of dicotyledonous plants have been examined, and their efficiency compared to that of reference shapes. The analysis hinges on dimensionless parameters that are used for modeling and developing performance charts. The maps help to gain insight into the biological design of the leaf petiole.

2 Plant body and organs

Angiosperms are flowering plants where reproductive organs are within flowers, and seeds are in the fruits. The number of seeds, or cotyledons, is used to sort angiosperms into two classes: the monocots, which have a single cotyledon, and the dicots with two seeds. Despite the differentiation, three elements are common to all angiosperms: roots, stems, and leaves. These are grouped into two systems: the root and the shoot, which consists of stem and leaves (Fig. 1).

Root System. The main vital functions of roots are the absorption of water and minerals, their conduction from the roots to the stem and vice versa, and lastly, the storage of food. The structural function of the roots is to provide anchor in the soil (Fig.1). An analogy in engineering is bolts that hook a column firmly in a foundation. Whereas monocots develop a fibrous roots system, in dicots a major root grows vertically and it is called taproot. This structural diversity is reported in Table 1 together with other differences between the classes.

Shoot System. The stem supporting the leaves is the shoot system. Attached at nodes through petioles, leaves form an angle with the stem (Fig.1). Here, there are also axillary buds that can develop, although most of them are dormant. At the terminal top, an apical bud is partly responsible for inhibiting the growth of axillary buds. The phenomenon, called apical dominance, occurs because the plant has to increase exposure to light, especially in a location with dense vegetation [2]. The other constituents of the shoot are the photosynthetic organs. Although their form, size, and even colour, can vary, a leaf is generally



structured as a flattened blade, connected to the stem by a petiole, or stalk. Some monocots, however, lack petioles, such as in grasses.

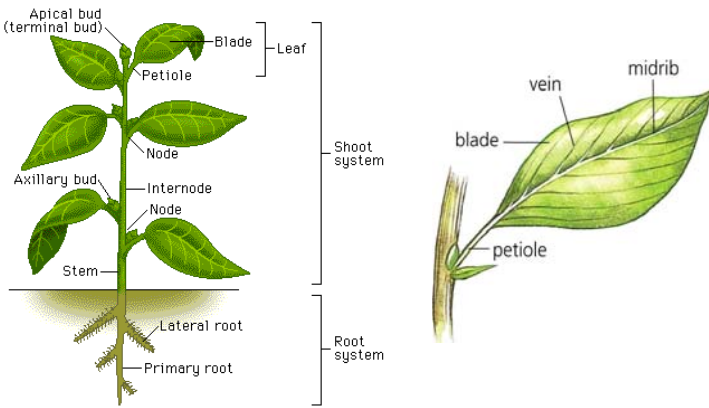


Figure 1: The structure of an angiosperm (right) and a zoom of its leaf (left) [2].

Table 1: A comparison of monocots and dicots [2].

	Monocots	Dicots
Embryos	One cotyledon	Two cotyledons
Leaf Venation	Veins usually parallel (e.g. palms)	Veins usually netlike (e.g. maples)
Roots	Fibrous root system	Taproot system
Stems	Vascular bundles usually complexly arranged	Vascular bundles usually arranged in a ring
Flowers	Floral parts usually in multiples of three	Floral parts usually in multiples of four or five
Growth	No secondary growth / annual ring formation	Secondary growth / annual ring formation

3 Plant tissue systems

The tissue is a cluster of similar cells into units. Three tissue systems grow continuously throughout a plant: dermal, vascular, and ground tissue. New tissues are formed at the meristems, the growing points on a plant.

Dermal System. The dermal tissue system is the epidermis. Analogous to our skin, the dermal tissue is a layer of tightly packed cells that protect plant organs. It is covered by a waxy coating, called cuticle, which reduces water loss through evaporation. This protection is imperative during dry summers. The pores, called stomata, control the exchange of gases between plant and surroundings. If a plant



undergoes secondary growth, the epidermis is replaced by dead waterproofed cells, the peridermis.

Vascular System. Xylem and phloem are two vascular systems. The former conveys water and minerals from roots into the shoots. The latter provides structural support and is in charge of transporting food from mature leaves to the roots, as well as to parts of the shoot system, e.g. developing leaves and fruits.

Ground System. Beyond photosynthesis, storage, and support, the ground tissue governs the metabolic processes. It is mainly made up of thin walled cells forming the parenchyma. This tissue fills the space between the dermal and vascular ones and makes up the plant bulk.

4 Plant movements

Plant movements change the body shape of an organ. Two types are the tropisms and the turgor. The former is a response of the plant curvature to stimuli. If toward the stimuli, the tropism is positive, whereas it is negative when the move is away from it. On the other hand, the turgor movements are rapid and reversible, often triggered by pressure changes in the state of the cells subject to stimuli.

4.1 Tropisms

Phototropism is the bending of a plant either towards or away from a light source. It ensures that photosynthesis will take place.

Gravitropism is the response of a plant to gravity. When it is positive, the roots grow deep into the soil to secure water and other nutrients. If negative, the shoots develop upwards to the sunlight for the photosynthesis.

Thigmotropism is a directional growth in reaction to touch. Unlike stems that grow straight, vines, for example, have tendrils that coil at touch with an object.

4.2 Turgor movements

Rapid leaf movements. Under strong winds, the leaves of the mimosa and other plants collapse and fold one upon another. It is speculated the rapid move helps plants retain water by reducing the surface area of the leaf.

Sleep movements are responses to changes of light during the course of the day. Legumes and bean plants, for example, raise their leaves horizontally in the morning, and then lower them vertically at the sunset.

5 Plant responses to environmental stresses

Besides morphological adaptation, plants modify their shape also in response to environment changes. For example, a **water deficit** stimulates the synthesis of a hormone, i.e. abscisic acid, which induces the pore closure and reduces evaporation. As a result, cells loose turgor and expose less surface to sun.



Oxygen deprivation is another cause that accelerates the growth of air tube cells in certain roots to ease oxygen supply.

Other triggers for shape changes are cold, heat, salt, and compressive stresses. **Cold temperature** makes the plant to increase its proportion of unsaturated fatty acids. **Heat stress**, above a certain temperature, stimulates the production of special proteins, called heat-shock proteins. **Excess of sodium**, also, threatens plant grow. Salt can cause root to loose water even though the soil is submerged in water. This occurs when the osmotic pressure of the surrounding water is more negative than that of the root tissue.

Lastly, the other important shape-adaptation is triggered by **compressive stresses**. In response to these, a plant modifies its size and shape. Cells grow in regions exposed to compressive stresses that make the thin-walls of the material micro-structure unstable. This sensitivity of shape to buckling stress is the reason why, for a plant, strength in compression is lower than strength in tension.

6 The leaf petiole

Previous sections have examined the vital functions of a plant, its organs and the triggers for morphological changes. This section zooms into one of its organ, the leaf petiole, and it examines its shape efficiency. This is not intended to suggest that only shape efficiency matters; all the other vital functions are essential, but they are not the focus here. The analysis is based on classic mechanics, although its limits when applied to the biological world. Before efficiency modelling, functions, morphology and bio-material of the petiole are described.

Loadings. The structural functions of a leaf resemble those of a cantilever beam. The petiole provides appropriate bending stiffness to support surface loads, such as the blade weight, as well as any other, whether it be rain, snow, moisture, or even the weight of an insect. But bending is not the only loading. The aerodynamic force of the wind causes the petiole to twist. In addition, the petiole coils to reach and to respond to sunlight. Hence, a combination of bending and torsion can be assumed as the overall loading.

Structural morphology. Fig. 1 illustrates the petiole connecting the leaf blade to the stem. In response to compressive stresses induced by the coupled load, the petiole results in being flexible, as opposed to conventional engineering cantilevers, which are designed to be stiff. The petiole is tapered lengthwise and it has often an asymmetric cross-section, grooved at its top. Such a shape lowers torsional stiffness without compromising the deflection resistance to gravity loading. The benefit of the groove is twofold. First, an increase of twist flexibility allows the leaves to bunch and reduce wind drag. Second, the leaf can orient itself towards downwind and even reduce the requirement for flexural stiffness.

Bio-material. Increasing torsion compliance without compromising resistance in bending is achieved by exploiting not only shape properties, but also material. Unlike most of engineering materials, petiole microstructure is inhomogeneous and anisotropic. It is made up of thick liquid cells supporting compression at the petiole bottom, and it has thin elongated cells at its top to



bear tension. Current biological models, however, find difficult to explain how anisotropy lowers torsion stiffness relative to bending stiffness [1].

The next section aims at obtaining insight into the macro-shape of the petiole. We are interested in how shape and size are tailored to better the petiole response to the combined load.

7 Case study: structural performance of dicotyledonous petioles

The petiole cantilever undergoes mainly the coupling of torsion and bending. Its structural response exploits flexibility, rather than stiffness. This section examines the cross-section efficiency at the stem node, where max load occurs. As performance index, we consider the ratio flexural to torsional stiffness.

10 specimens of dicots petioles (Table 2) have been analysed, and their shape performance has been examined. To compare their efficiency with those of elliptical and semi-elliptical cross-sections, we resort on dimensionless measures, called Shape Transformers [8]. A shape transformer, ψ_{gc} , is defined for a geometric quantity, gc , of a cross-section. It is obtained by normalizing gc to gc_D , which is the quantity of the rectangular Envelope described by the cross-section size. Shape transformers can govern the geometry metrics of a shape regardless of its size. For example, shape transformers for the area and second moment of area are $\psi_A=A/A_D$ and $\psi_I=I/I_D$. The normalization of the geometry enables to decouple the contribution of the shape to that of the Envelope.

The following examines the structural performance that the petiole cross-section exhibits to improve torsion flexibility without losing bending resistance. A way to describe this criterion of excellence is to consider the flexural to torsion stiffness ratio, such that efficiency is optimised by maximising the index:

$$P = \frac{EI}{GJ} = \frac{EI_D\psi_I}{GJ_D\psi_J} \quad (1)$$

where E and G are Young's and shear Modula, ψ_I and ψ_J are the transformers of second moment of area and the polar moment, and I_D and J_D are the quantities of the envelope. Table 2 reports ψ_I and ψ_J for the petiole specimen, and Table 3 lists those for solid and hollow ellipses and semi-ellipses.

Three design scenarios are now examined. First, we characterize the flexural stiffness of the cantilever; second, its torsional rigidity; and lastly, its efficiency described by the index (1). The results are displayed on efficiency maps that help gain insight into the biological design of the petiole.

7.1 Flexural stiffness

To characterize the flexural stiffness, ψ_I expressions from Table 3 have been plotted against ψ_A in Fig. 2. The coordinates of a point represent the bending stiffness of a cross-section shape for a given volume and regardless of material. Shapes that are stiff lie on the top left as opposed to those that have low ψ_I/ψ_A and lie on the bottom right. The chart illustrates two distinct domains of



properties. One encloses the ellipses classes and it is bordered by curves 1e and 2e. The other is for semi-ellipses and is bounded by curves 1s and 2s. Regardless of the envelope, each curve describes the flexural stiffness with respect to fraction and location of material within the envelope. For a given ψ_A , the ellipses' classes are not as stiff as the semi-ellipses, for the asymmetry permits the material to be placed far from the neutral axis. Specimen shape transformers from Table 3 have been plotted in Fig.2. The plot shows that petioles' shapes are quite efficient in providing flexural stiffness, considering their solid shape. Petioles n. 3,7,10 exhibit the highest resistance to bending deflection.

Table 2: Geometry of dicots petiole specimen.

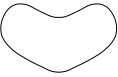



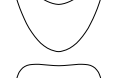





Petiole Cross-Section	Envelope size [mm]	Area [mm ²]	ψ_A	I [mm ⁴]	ψ_I	J [mm ⁴]	ψ_J
1 	B: 5.76 H: 3.41	13.64	0.69	8.56	0.45	39.04	0.53
2 	B: 4.56 H: 2.83	7.39	0.57	3.53	0.41	11.48	0.37
3 	B: 4.96 H: 3.60	12.34	0.69	10.50	0.54	27.23	0.49
4 	B: 8.941 H: 7.45	30.09	0.45	82.35	0.27	229.75	0.31
5 	B: 6.95 H: 5.62	21.40	0.55	35.25	0.34	103.05	0.40
6 	B: 4.37 H: 2.46	6.28	0.58	2.23	0.41	6.765	0.30
7 	B: 3.56 H: 2.29	6.58	0.80	2.22	0.62	7.765	0.63
8 	B: 1.88 H: 1.78	2.52	0.76	0.47	0.53	1.03	0.55
9 	B: 3.25 H: 2.38	6.24	0.81	2.25	0.62	6.75	0.65
10 	B: 2.99 H: 2.43	4.64	0.64	1.68	0.472	3.44	0.38



Table 3: Shape transformers and efficiency parameters.

Cross-section	ψ_I	ψ_J	ψ_I/ψ_A Range	ψ_J/ψ_A		ψ_I/ψ_J	
				Range for α 0	90	Range for α 0	90
	$\frac{3\pi}{16}$	$\frac{3\pi}{16}$	0.75	0.75	0.75	1	1
	$\frac{3}{2}\psi_A\left(1-\frac{2}{\pi}\psi_A\right)$	$\frac{3}{2}\psi_A\left(1-\frac{2}{\pi}\psi_A\right)$	0.75-1.5	0.75-1.5	0.75-1.5	1	1
	$\frac{1}{12}\frac{(9\pi^2-64)}{\pi}=0.66$	$0.66\sin^2(\alpha)+\frac{3\pi}{16}\cos^2(\alpha)$	0.84	0.75	0.84	1.12	1
	$0.66\left(1-\left(1-\frac{4}{\pi}\psi_A\right)^2\right)$	$\psi_I\left(\sin^2(\alpha)+\frac{\pi}{3.52}\cos^2(\alpha)\right)$	0.84-1.68	0.75-1.5	0.84-1.68	1.12	1
	$0.66\left(1-\left(1-\frac{4}{\pi}\psi_A\right)^3\right)$	$\psi_I\sin^2(\alpha)+\frac{3}{4}\psi_A\cos^2(\alpha)$	0.84-2.52	0.75	0.84-2.52	1.12-3.36	1

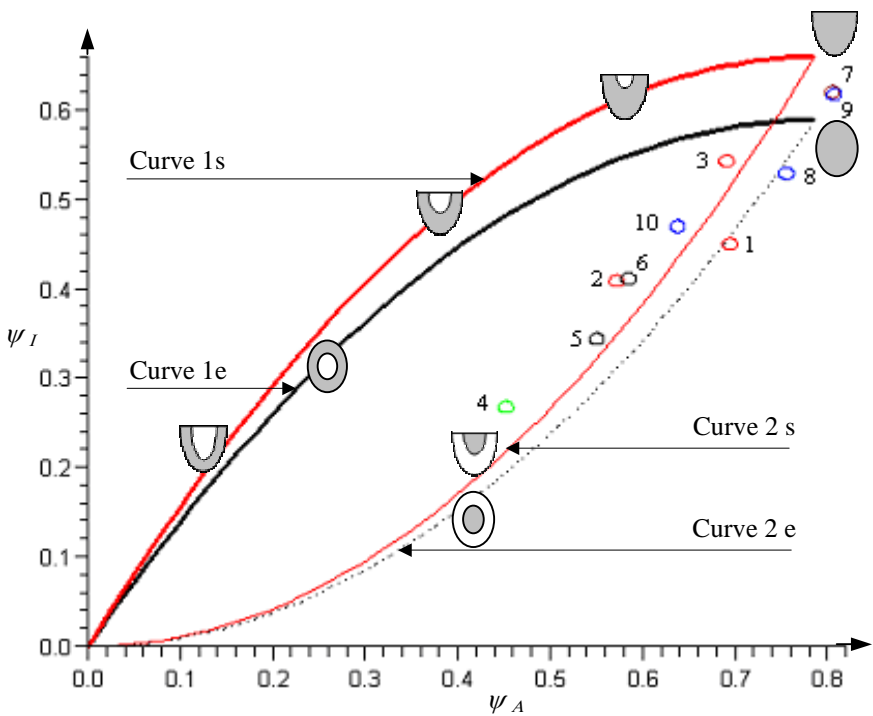


Figure 2: Flexural stiffness for specimen, ellipses and semi-ellipses classes.



7.2 Torsional stiffness

Unlike flexural shape transformers, ψ_I for asymmetric shapes depends on the ratio of the envelope size. Table 3 shows that for envelope stretched width-wise with $\alpha \rightarrow 0$, the semi-ellipses class is as stiff as that of the ellipses one. This is also illustrated in Fig. 3, where ψ_I is plotted versus ψ_A . The properties domain of the ellipses class is described by the same curves of the semi-ellipses class., i.e. curve 1e \equiv curve 1s ($\alpha \rightarrow 0$) and curve 2e \equiv curve 2s ($\alpha \rightarrow 0$). However, for $\alpha > 0$, there is a shift of the semi-ellipses domain upwards to the limit $\alpha \rightarrow 90$. This means that the ellipses' classes shown in Figure 3 are easier to twist. On the other hand, the semi-ellipses are stiffer for increasingly deeper envelopes.

We now contrast the domain properties with the Shape Transformers of the specimens. The petioles show low torsional stiffness although their shapes are asymmetric. Petioles n. 2,6,10 are even more compliant than the ellipses and semi-ellipses of the lower bound. As expected, petiole design is flexible; the leave can sway back and forth in order to reduce drag force and to reach sunlight.

7.3 Petiole scenario: torsion and bending coupling

Figure 4 illustrates the relation of ψ_I to ψ_J (Tables 2 and 3). The index 1, used for efficiency comparison, is the slope of the line a point forms with the origin. For a given flexural stiffness, the higher the slope, the easier it is to twist the shape.

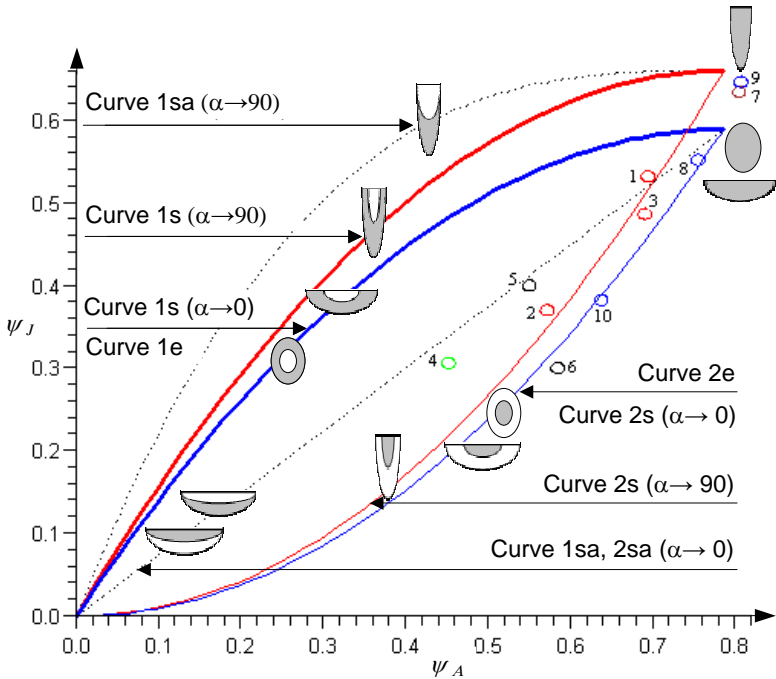


Figure 3: Torsional stiffness for specimen, ellipses and semi-ellipses classes.



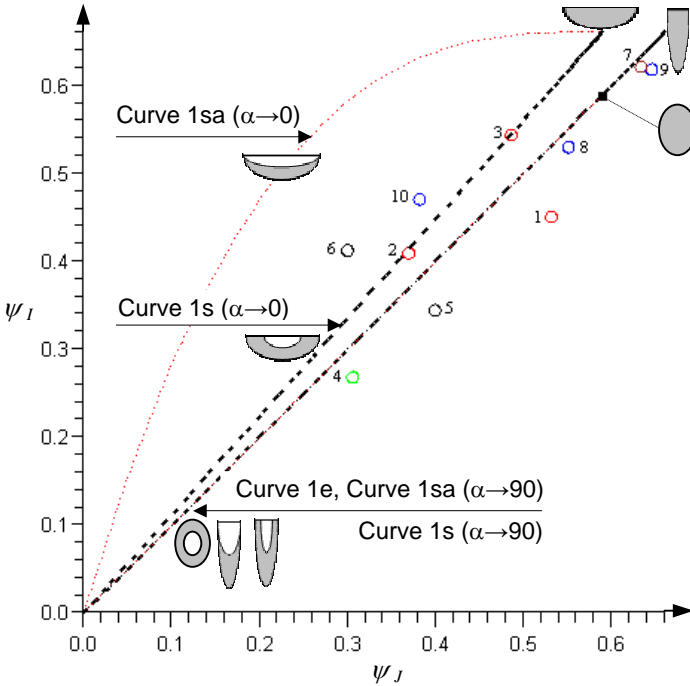


Figure 4: Flexural vs. Torsional stiffness for specimen, ellipses and semi-ellipses classes.

The map bisector describes shapes with same torsional and bending stiffness. These concepts are hollow ellipses as well as very deep semi-ellipses ($\alpha \rightarrow 90$). They are the best trade-off for both bending and torsion stiffness. However, stretching the semi-ellipse widthwise lowers the torsional stiffness. The curve 1s ($\alpha \rightarrow 90$) shifts left to curve 1s ($\alpha \rightarrow 0$) for proportionally scaled layers, whereas it moves further up to the curve 1sa ($\alpha \rightarrow 0$) for the other class of the semi-ellipses. Envelope changes, on the contrary, do not improve efficiency for symmetric shapes. The map highlights that lowering torsion stiffness by widening the envelope width has the impact of reducing the requirement for flexural stiffness.

The plot of specimens properties in Figure 4 illustrates petioles n. 2, 3, 6, 10 lie between curve 1s ($\alpha \rightarrow 0$) and curve 1sa ($\alpha \rightarrow 0$). Though solid, the shapes are better than the proportionally scaled semi-ellipses. They are stretched widthwise, and their shapes best resemble the semi-ellipses class shown at base of table 3.

Petiole design is optimized at different length scales. The maps presented in this section aim at gaining insight into the biological design of macro-shapes. However, the impact that material anisotropy has on petiole performance cannot be undervalued, even though current biological models strive to explain how Nature tailors G and E at the micro-scale.



8 Conclusions

The leaf petiole has a large number of functions. Its structure is optimized to bear mainly a combination of bending, due to gravity load, and torsion, induced by wind drag. This paper has examined the structural efficiency of petiole shapes. A case study of 10 dicotyledonous petioles has been carried out to gain insight into shape performance. Efficiency maps have been developed to contrast biological design to conventional engineering cross-sections. The charts show that size and shape of the petiole are exploited to ease the twist as well as to lower the requirement of flexural stiffness.

Acknowledgement

The authors thank Mrs. Stephanie Rinaldi, undergraduate of McGill University, for the collection of specimen data.

References

- [1] Vogel, Steven. *Comparative Biomechanics: Life's Physical World*. Princeton University Press, 2003.
- [2] Campbell, Neil A., Jane B. Reece, and Lawrence G. Mitchell. *Biology*. Fifth Edition. Don Mills: Benjamin Cummings, 1999.
- [3] Ennos, A.R., The mechanics of the flower stem of the sedge *Carex acutiformis*. *Annals of Botany*, 72(2), pp. 123-127, 1993.
- [4] Etnier, S. A. and Vogel, S., Reorientation of daffodil (*Narcissus*: Amaryllidaceae) flowers in wind: drag reduction and torsional flexibility. *American Journal of Botany*, 87, pp. 29-32, 2000.
- [5] Ennos, A.R., Spatz, H.C. and Speck, T., The functional morphology of the petioles of the banana, *Musa textilis*. *J. of Experimental Botany*, 51, pp. 2085-93, 2000.
- [6] Etnier, S. A., Flexural and torsional stiffness in multi-jointed biological beams. *Biological Bulletin*, 200, pp. 1-8, 2001.
- [7] Vogel, S., Twist-to-bend ratios of woody structures. *J. of Experimental Botany*, 46, 1995.
- [8] Pasini, D., Shape Transformers for Material and Shape Selection, ASME DETC-84894, 2005.



This page intentionally left blank

Section 2
Nature and architectural
design

This page intentionally left blank

Sculpture house in Belgium by Jacques Gillet

S. Van de Voorde, R. De Meyer, E. De Kooning, L. Taerwe
& R. Van De Walle
Ghent University, Belgium

Abstract

The Belgian architect Jacques Gillet designed the sculpture house in Liège (1967-1968) as a synthesis of structure and form, collaborating on this project with the sculptor Félix Roulin and the engineer René Greisch. This 'living-sculpture' was undertaken by the team as a reaction against the general pressure of that time towards standardisation of forms in architecture, in which an artistic poverty and deficiency needed to be counterbalanced through collaboration with sculptors and painters. The merit of the artistic collaboration is evident when looking at the scheme of the building yard. The materials and techniques used gave the team a creative liberty: steel bars were folded, and placed one by one, to enhance the contingency between nature, space, material and poetry. A metal mesh was affixed to the steel bars and the ultimate form was then secured by projecting a fast setting concrete onto it: direct, immediate and efficient. The exterior is just the mere envelope of the interior; no additional structure whatsoever was necessary. The structure was left bare on the outside, postulating a true unity between form and material.

Keywords: architecture, gun concrete, sculpture house, organic, Belgium, Jacques Gillet, Félix Roulin, René Greisch.

1 Introduction

Since the end of the Second World War, organic architecture has appeared as a search for beauty that concurs with the notion of ideal construction, as a synthesis of art and sciences. Protagonists of this tendency were, among others, Frederick Kiesler, Mathias Goeritz, Jacques Couëlle, André Bloc and Paul Virilio. Likely the best known example of this architecture, based on organic or sculptural forms is Le Corbusier's Chapel at Ronchamps. The term 'sculptural



architecture' or 'architectural sculpture' was used for the first time in 1963 by Michel Ragon, in his book 'Où vivrons-nous demain?' [1].

The origins of this movement go back as far as the end of the 19th century, with the work of Louis Sullivan and Frank Lloyd Wright in the USA, and Victor Horta and Antonio Gaudi in Europe. Gaudi achieved a synthesis of shape, structure and form, comparing wire skeletons and plaster models with the laws of nature. The sculpture house in Liège (1967-1968) was designed in a similar, experimental way by the Belgian architect Jacques Gillet, in collaboration with the sculptor Félix Roulin and the engineer René Greisch. However, in the scenery of 20th century Belgian architecture, it stands alone as an exception.

2 In search for a new architecture

2.1 Kindred spirits

Born in Liège in 1931, Jacques Gillet graduated from the Department of Architecture of the 'Académie des Beaux Arts' in Liège in 1956 [2]. One of his teachers was the Belgian architect Georges Dedoyard, an important exponent of the modern movement in Liège [3]. Gillet returned to the Académie as professor in 1964, which was later on renamed 'Institut Supérieur d'Architecture Lambert Lombard'. He conducted research on spontaneous architecture and the integration with nature [4]. He was also very interested in new building techniques and construction methods, which gave a certain creative liberty to the design process. Always being very eager to collaborate with artists and engineers, he looked upon architecture as a synthesis of art and science, a true unity between form and material.

In 1962, the Belgian engineer Jean-Mary Huberty (1932) asked Gillet to act as aesthetic advisor on the facades of his private house in La Hulpe, near Brussels. As a result, Gillet came in contact with two experts on concrete technology and was introduced to the possibilities of concrete [5]. The house was designed by Huberty himself in collaboration with André Paduart (1914-1985), both civil engineers, the former conducting research on concrete technology for the Belgian Federation of the Cement Industry, the latter being particularly specialised in the technology of thin concrete shells. The house stands out as a revolutionary and intellectual tour de force, in which these two young masters in concrete technology exploited the characteristics of the material to the utmost limit. Two parabolic hyperboloids, or hypars, were combined, thus defining the overall layout of the plan. The hypars were constructed as a concrete shell on a framework of wooden boards and thermal insulation. The shell of the concrete vault is only 5 centimeters thick. The collaboration led to a design in which both architectural and technological qualities stand out, but also demonstrates that it was not simple to go off the beaten track [5].

During the early sixties, Gillet came into contact with kindred spirits. In 1962 he became acquainted with the sculptor Félix Roulin (°1931) and the painter Gabriël Belgeonne (°1935), when their project for an auditorium for chamber music was granted the first prize in a competition on 'The synthesis of plastic



arts', organized by the Belgian Ministry of Cultural Affairs in 1961 [6, 7]. During the same year, Gillet met the Liège engineer René Greisch (1929-2000). Greisch was notable for his spirit of research and innovation. Greisch always tried to improve available techniques or simplify their implementation, qualities that were highly valued and shared by Gillet [8]. Gillet and Greisch were soon commissioned by the Liège University to design the Laboratory of Radiobiological Research. The building was completed in 1964 [9]. Later the same year, together with Félix Roulin, they were commissioned with the design of an observatory station for the Astrophysical Department of the Liège University [4, 10]. The design was undertaken in the same architectural language, which was later applied in the sculpture house in Liège. Although the observatory station was never realized, its design marks a first important phase in the collaboration of these three artists towards a synthesis of arts; a congenial group was formed.

In 1966, Gillet and Roulin collaborated with Belgeonne in the design of his private house and studio. The design, based on the same organic, architectural language, was constructed in wood and metal, as opposed to the auditorium for chamber music and the observatory station, which were designed to be constructed in concrete [10]. Around that time, several projects were undertaken, mostly by the twosome Gillet/Roulin, such as the private house and studio for a painter and a private house for a doctor [4]. Eventually, in 1967, Gillet's brother was willing to participate fully in the realization of the architect's dream and asked the team to design a private house for his family of six in the surroundings of Liège.

2.2 'Living-sculpture'

The experimental attitude of the physical-chemistry research scientist owner served as the basis for the entire approach to the project: "What is a house, for us as individuals, for our family, for this very place and this point in time?" was the first question [11]. After expressing his deepest concerns, the owner gave the team the chance to not only put their ideas into effect, but to do this at their own pace. For almost three years, Gillet, Greisch and Roulin sought, studied, tested, discussed and eventually built this 'living-sculpture', made to measure [4, 9].

Inspired by nature and organic forms, the design was undertaken as a synthesis of arts. According to their own words, they didn't want to start a revolution, but simply wanted to create something new, opposed to the standardisation of forms in architecture and the conditions of mankind's accommodation of those times, out of touch with nature [9]. It is not coincidental that all the comparisons the realization of this sculpture house have brought about, call forth associations with nature: a cave dwelling, a big mushroom in the middle of a forest or even a tortoise protected by his carapace [12]. The architectural language can best be described using the architect's own words: "We constantly tried to render these curves responsive and firm, which otherwise would flag and sag, becoming flabby and without vigour. But we did not want to geometrize these lines or standardize them. Spontaneity, tightness inspired by nature: purity, true simplicity—which is not of form but of soul—freshness that



so many are longing for and that cannot be commercialized without dying forthwith. To let others taste and share the plenitude of a curve, the boldness of a shape, the élan, the right place of a stroke or a volume, the play of light, is the most important role of this ‘thing’, ‘open to friends, ideas, emotion’ according to the inhabitants’ saying.” [11].



Figure 1: Sculpture house after completion in 1968 [13].

Describing the project outlines is far from simple. The ground plan is composed of four discrete wings: the living room facing south; the study, cloakroom, master bedroom and bathroom facing east; the dining room and kitchen facing west; and finally the children’s bedrooms and bathroom towards the north, sunlit by windows facing both east and west. A distinction is also made in elevation: the garage is located at the lowest level of the site; the floor level of the common rooms is situated half a floor level higher, thereby fully exploiting the natural differences in the height of the terrain. The floor level of the parents’ private wing is situated between the floor levels of the common rooms and the children’s private wing; the latter being raised again half a floor level according to the common rooms. The children’s bedrooms are superimposed on the garage. By creating a split-level, the architect obtained the two meters of height necessary for the garage without elevating the whole building.

These outlines are to be seen as a blueprint or diagram, put on paper so the team did not set to work without a set plan. The architect made a schematic drawing of his intentions, passed it on to the sculptor, who placed his own interpretation upon it, and the whole process started all over again. The facts and figures of the plan were touched upon, but not at all fixed. The design process was far from analytical or rational and the house was certainly not intended to be described that way. To understand the true meaning of the sculpture house, one has to visit the house and investigate the intentions of the designers. “Why this sculpture house? Explaining it would appear to be justifying it or making the design become ‘logical’. Explaining it means that one has to assume the ‘rational’ to understand. Here, there is nothing to understand. Here, you can feel everything, subjectively.” [4].



The inhabitants, answering many questions about how they could possibly live within those forms, simply replied with “And you, in yours?” [14]. Although many people had to be persuaded or convinced of the qualities of this new architecture, there were no great difficulties in obtaining the necessary permits. The local Department of Urban Planning and the municipal authorities truly believed in the possibilities of this project and displayed a certain audacity in authorizing this experiment [9, 15].

When construction was finished, the project began to lead a life on its own. Acquiring autonomy and independency towards the designers, the house immediately took on a dialogue not only with the visitors but especially the inhabitants. The moment they entered their new house, they really felt at home and became one with the project [12].

Creating such harmony and intimate peace was most important to the sculptor Roulin: he saw the sculpture house as a sculpture where the ‘inner void’, in contrast to the mass, was to be inhabited. He describes his own metier as manipulating and handling the forms and sensibility of raw materials, while architecture deals with the material of space, which is not at all less expressive but different, dealing with the area which has to be inhabited. Crossing the threshold between these two professions, led to a sculpture in which one penetrates, constantly revealing an entity of volumes and forms in perpetual movement to the inhabitant [14].

3 Work in progress

The project is not to be seen as a reaction against the building industry in general, since the team explored and experimented with new building techniques and materials throughout the entire design. It is a reply to the development of standardized forms and products, and at the same time a passionate plea in favour of an industrial policy which gets to the core of the matter: the molecule, the atom, the electron. “I believe in the miraculous industry of the tool made to measure the hand, material made to measure the human body, space made to measure the heart, Architecture made to measure the Inhabitant. I believe in the possibilities of this industry to provide for close contacts and let us delight in something: the delight in taking a venture, the pleasure of participating and the joy of constructing together. Never again the industry of the imposed or ready-made.” [4]. Partaking in this process was at least as important to the team as the achieved results. The mode of operation, the way in which the design was attended to, became a purpose on its own. Refusing to be driven back on traditional means, the team resorted to an uncommon construction method of projecting concrete onto a metal grid, which served as a projecting form itself.

3.1 Marking the outlines

During the design process, very few detail drawings were made. The scale models, first in modelling clay and later in an aluminium wire mesh, were the most important instruments by which to translate ideas [10]. When construction



started in April 1967, the overall structure was outlined, based on the aluminium wire mesh scale model, in reference to a few fixed elements. As these fixed elements, namely the concrete floor levels and chimney, are best served by horizontal and vertical planes, it was unnecessary to construct them in a non-traditional, sculptural way [16]. Crenellated steel bars, extending the floor levels and chimney, served as reinforcements. Measuring 8 millimeters in diameter, these bars were interspaced at 20 centimeters in two directions, thus creating a two-dimensional grid [2].



Figure 2: Steel lattice attached to the chimney.

Temporarily supported with thin wooden trunks, the lattice work was given shape by combining three distinct basic forms: the arch, catenary curve and parabolic hyperboloid. Given that the course of the lattice was not meticulously defined in advance, the shape was determined by experiment, by touch. Design and construction were dealt with together, according to four parameters: the inner space and the incidence of light, the future down course of the water, the stability and the sculptural characteristics. Therefore the architect, sculptor, engineer and client were constantly finalizing the generic form, very accurately, without there being a strict division of tasks. It appeared that the engineer, paradoxically, was most concerned with the sought-after sculptural or spatial effects [17].

Regarding stability, only a small part of the construction was meticulously calculated by the engineer. Full size rupture tests were conducted by the building contractor before starting construction, to determine possible difficulties and to define the most economical shapes and curves. With the result of these tests in mind, the actual construction was based on experience, intuition and experiments with life loads. When the ultimate form was outlined, the strength of the construction was once more tested on the spot by exerting concentrated pressure. Temporary supports were removed; workman and visitors of the construction site climbed the roof, moving up and down with a certain cadence. Wherever the

deformation exceeded 25 centimeters, the engineer reinforced the construction. This eurhythmics was right up the alley of the numerous students working on placement at the site, under the expert guidance of the architect [2].

The window frames, U-shaped profiles, were bent and cut at the spot by the team. Much attention was paid to the rigidity of their form and their exact verticality, so they would contrast to the sculptural concrete mass. Neither the steel profiles nor any other part of the structure were preventively treated or galvanized. The window profiles did however receive a thin coat of a transparent, dark paint. Economical use was made of the available materials, which were chosen for their easy implementation, organic qualities or even their availability and beneficial prices [2].

3.2 Guniting

Once the construction was sufficiently sturdy and solid, the next step was undertaken. An expanded iron mesh was fixed onto the steel bars, serving as projecting form. The casco was given its mass by the process of guniting a fast-setting concrete onto it: direct, immediate and efficient. A very dry and compact concrete was gunited on the mesh, setting in less than 15 minutes. This technique, mainly used for constructing blast-furnaces and grottos, was at this time very uncommon in Belgium. As it had never before then been used to construct a private home, a specialised team was asked to implement it.

The Czech-Belgian firm Pasek, established in 1960, was one of the only firms experimenting with sandblasting and the projecting of dry mortar. They had even designed their own projecting machine, Refra-Gun [18]. The team working on the Liège construction site consisted of 4 men, working in pairs. The first team handled the spraying hose, attached at the rear end to a large barrel, which contained the dry concrete. The barrel was divided into two compartments, so that the barrel could be continually refilled by one team, while the other team was guniting. Water was not added until the very last moment, at the spray-gun nozzle, which resulted in a very dry concrete. The final surface was, when properly applied, very compact and impermeable to water [2].

As guniting is not a tidy construction technique, precautions had to be taken. The window profiles were covered and small, temporary strips were placed at the edges of the shell structure to create a clear boundary between the house and its surroundings. Almost 15 percent of the concrete is lost during the process, as it shoots away from the mesh. This did not go to waste, as the architect used this to pave the access road to the house [2].

Concrete was sprayed at an angle of 45°. If concrete had been sprayed perpendicularly to the surface, considerably more than 15 percent of the concrete would be lost. Another advantage of this 'inclined technique', personally developed by Stephan Pasek [9], is that any water trying to penetrate the concrete shell, is drained immediately due to the inclined layers of concrete. Workmen were thus also enabled to estimate the thickness of the concrete shell. They had to carefully notice very small details, such as changes in the consistency of the concrete, and take immediate action to ensure a consistent product. The



responsibility shouldered by these workmen while participating in this experimental and revolutionary project, should not be underestimated [9].

The overall thickness was set at 5 centimeters and was only increased where implied by the construction. At some places, such as corbellings and clear-cut edges, supplementary stiffening and strengthening were necessary at a distance of 50 centimeters parallel to the edge. Girders were formed at the edge by aligning 4 steel bars, all measuring no more than 8 millimeters in diameter. To ensure a strong and rigid connection between girder and lattice, additional steel braces, measuring 5 millimeters in diameter, were folded by students into a triangular shape, wrapped around the girder and welded to the lattice. The cross section of the girders measures 7 centimeters, so the entire thickness of the construction locally amounted to around 12 centimeters [2].



Figure 3: Steel 'girders' at the edge.

3.3 Completion of the building process

Thermal insulation was provided by a rigid polyurethane foam projected with a spray-gun from the inside. Over the years, it has matured in the natural light and acquired a warm and nuanced colour [11]. Since this insulation was not universally applied, an additional, very thin layer of sprayed concrete was sometimes necessary to cover the iron mesh on the interior.

Beside this thermal insulation, no corrective measures or provisions were taken. The concrete was deemed waterproof and the roof thereby did not receive an extra coat. Construction was finished in September 1968, a total building time of 14 months (construction was interrupted during winter) [2]. When asked to compare to traditional building methods regarding construction time and building costs, the architect replied that he did not intend to be competitive. He was however quite certain that the building costs would not exceed those of a traditional house for a family of six [19].



Despite the fact that the house was in no need of supplementary measures during the following decades, some renovation became inevitable during the late eighties. The impermeability to water had been affected and needed to be repaired. The exterior was restored by impregnating it with a highly fluid, water-repellent, silicate based resin. Additionally, a special coating of semi-rigid epoxy resin was applied to those surfaces which had suffered the most from the down course of the water [2, 9].

4 Continues

While designing this sculpture house in Liège, the team was granted a second commission for a similar house to be erected on a hill close to a former World War I fortification. It was designed by the same team, but as the terrain and the personality of the clients was different, the ultimate form was also different. At the very last moment however, right before going on to the construction phase, the clients decided that this new architecture was too revolutionary after all [9, 20].



Figure 4: The sculpture-house, 2006.

It wasn't until the late seventies that another example of sculpture architecture appeared in Belgium. The architect Philippe Mousset, who had paid numerous visits to the building yard in Liège, erected a sculpture house in Fleurus [9]. The same uncommon genesis and architectural language was utilized, the applied technique was however a bit different: a glass fibre reinforced plaster was sprayed on an elastic tissue in stead of an iron mesh [21].

During the following years, a few architects followed in Gillet's footsteps, as he began to hold a course on organic architecture at the Institut Supérieur

d'Architecture Lambert Lombard in 1978. Henry Chaumont, Bernard Herbecq, Eric Furnémont, Yves Delhez and Vitor Forte are, among others, some of Gillet's former students still engaged on organic architecture [9].

The work of Jacques Gillet, first and foremost the sculpture house in Liège, still finds itself the subject of great public interest. This active interest is demonstrated by recent articles on the sculpture house published in international magazines, such as the German *Deutsche Bauzeitung*, the Swiss *TEC 21* and the Austrian *GAM*, and also exhibitions where the sculptor house occupies a prominent place [22–25].

Recent examples of modern architecture, such as the Educatorium by Koolhaas (OMA) and the Minnaertbuilding by Neutelings Riedijk Architects, both in Utrecht, demonstrate that this construction technique of projected concrete is still topical, bringing forth intellectual and architectural fireworks.

References

- [1] Ragon, M., *Où vivrons-nous demain?*, Paris, Laffont, 213 p., 1963.
- [2] Gillet, J., Personal communication, 4 January 2006, architect and professor on organic architecture, Institut Supérieur d'Architecture Lambert Lombard, Liège, Belgium (retired).
- [3] Van Loo, A., *Repertorium van de architectuur in België*, Antwerpen, Mercatorfonds, pp. 240-241, 2003.
- [4] Bekaert, G., *Bouwen in België 1945-1970*, Brussel, Nationale confederatie van het bouwbedrijf, pp. 317-318, 1971.
- [5] Huberty, J.-M., Personal communication, 12 January 2006, civil engineer and architect (retired).
- [6] Belgeonne, G., Personal communication, 21 December 2005, painter, engraver, former head of 'L'Ecole Supérieure des Arts Plastiques et Visuel de l'Etat', Mons, Belgium and 'L'Ecole Nationale Supérieure des Arts Visuel – La Cambre', Brussels, Belgium.
- [7] Joly, P., *Architectures de Sculpteurs, L'Architecture d'aujourd'hui*, 115, pp. 85, 1964.
- [8] Greisch, R., *Bureau d'études Greisch*, Antwerpen, de Singel, 207 p., 1996.
- [9] Gillet, J., Personal communication, 17 January 2006.
- [10] Roulin, F., Personal communication, 17 January 2006, sculptor.
- [11] Gillet, J., *The Sculpture House*, (unedited paper), 1978.
- [12] Gillet, J., *Habitat selon la nature, Neuf*, 18, pp. 12-15, 1969.
- [13] Pictures 1,2 and 3 were taken by Gillet, J. Picture 4 was taken by the author.
- [14] Gillet, J. & Roulin, F., *Habitation-sculpture près de Liège, Environnement*, 3, pp. 115-120, 1971.
- [15] X, *La maison sur mesure, Moustique*, 5 November 1967.
- [16] Henrion, P., *La maison-sculpture d'Angleur, Art & Fact*, 12, pp. 185-190, 1993.
- [17] Roulin, F., Personal communication, 15 December 2005.



- [18] Stouffs, S., *Spuutbeton, een techniek met toekomst*, (unedited essay), pp. 13-14, 1985.
- [19] A.S., Une maison-grotte à Angleur, *La Libre Belgique*, 16 April 1968.
- [20] X, Habitable pour une famille sur un promontoire bien dégagé, *La Maison*, 2, pp. 59-60, 1967.
- [21] Mousset, P., Personal communication, 17 January 2006, architect.
- [22] Holl C. & Merx, L., in die Jahre gekomen. Einfamilienhaus in Lüttich 1967-1968, *Deutsche Bauzeitung*, 10, pp. 74-80, 2004.
- [23] Holl, C. & Merx, L., Naturnähe und Naturdistanz, *Graz Architecture Magazine*, 2, pp. 42-61, 2005.
- [24] Holl, C. & Merx, L., Die Höhle als Bild und Vorstellung, *Tec 21*, 18, pp. 10-15, 2005.
- [25] Exposition on 'Architecture organique', Musée d'art moderne et d'art contemporain, Liège, 23 December 2005 – 5 February 2006.



This page intentionally left blank

Analysis of the ‘Cappadocian cave house’ in Turkey as the historical aspect of the usage of nature as a basis of design

P. Yıldız

*Department of Interior Architecture and Environmental Design,
Hacettepe University, Turkey*

Abstract

The Cappadocia region is located in the Anatolian part of Turkey surrounded by ancient civilisations where nature and history came together in good sequence. While geographic events had formed ‘Fairy Chimneys’ (Peribacaları), during the historical period, the signs of old civilisations of thousands of years can be seen with carved houses and churches within these earth pillars. Traditional Cappadocian houses carved into stone show the uniqueness of the region. These houses are constructed on the feet of the mountain via rocks or cut stones. Rocks, which are the only construction materials of the region, as they are very soft after quarrying due to the structure of the region can be easily processed but after contact with air it may harden and turn into a very strong constructional material. Cappadocia is also known for its rock hewn churches, monasteries and underground cities.

The cave houses are old residences carved centuries ago. They overlook a vast area surrounded by mountains. Restoration sometimes makes it possible to clean the rock oxidised or blackened by smoke and to clear certain parts, filled with soil over the centuries. The structure was also consolidated and certain vaults were rebuilt by original stones. The restoration continues, attempting to respect the original construction. The **purpose** of this study is to analyse the historical aspect of design with the basis of nature among cave house formation, with the usage in today’s conditions. The **results** of this study show the advantages and the disadvantages of the architectural space formed by cave structures while the **conclusion** is the criteria reached by the character of the residences based on natural formation.

Keywords: cave house, stone, fairy chimneys, underground cities, architectural rock construction.



1 Introduction

The purpose of this study is to understand the interaction of design with the basis of nature. According to architectural designing principles and relations, the aesthetical reflection in nature is so dynamic that all parts combining the whole is the ring to form the whole structure. A structure is sometimes poetic, sometimes dramatic but one thing is for sure that the most important thing for living things is the aim to supply the adaptation criteria in all changing and flexible surroundings, environments. Then the designing with the basis of nature concerns a great deal with the term adaptation. From an architectural perspective, living things from the very beginnings of earthly liveable conditions, always tried to adapt themselves to nature or adapt the natural meanings to themselves by a dynamic integration. One of the reflections of this happening is the need of shelter to prevent themselves from any harm and also from other living things like animals. In the most ancient times when there was no civilisation human beings used caves as shelter.

The caves are first sights of accommodation and space of ever in natural based interiors. The harmony between design and nature could be explained among these in historical aspect. Here, design indicates to form the internal living conditions concerning ecological ground. Some of these cave houses around some places in the world still survive and the usage of interiors are still going on. In my case study I would like to concentrate on the cave houses located in Turkey which are still being used today. These houses show the sustainability of the cave house formation as the long term usage of their spaces and with different functions.

2 The Anatolian region of Turkey and the location of Capadoccia

The city of Capadoccia is located in the Anatolian region of Turkey. The creation and formation of the Capadoccian landscapes began when 'Mount Argaeus' erupted millions of years ago, smoothening the entire surroundings with a torrent of lava that covered hundreds of kilometres.

High on the central Anatolian plain, close to the country's geographic centre, is a landscape with fairy chimneys capped with basalt to resemble giant mushroom shaped rocks. Others formations have been carved by wind, sand and rain into the shape of mythological beasts. Nearby stand cones hundreds of feet high. Volcanic eruptions 30 m years ago coated the land with ash, which over millennia compacted into the soft tufa rock. This the Hittites, who occupied the country in the third millennium BC, found easy to excavate into caves for storage at a constant cool temperature. As the Anatolian Region was fought over by successive empires, the inhabitants found it political to disappear, digging out secret cities in which to survive for months at a time. By the first century AD early Christians were using them to hide from Roman persecution. Some of the Capadoccian cave villages remained in occupation until recent times. Fairy chimneys, strange cone shaped rocks, formed due to centuries of erosion.





Figure 1: The geographical statement of Capadoccia in Turkey.

The most commonly held view is that the cities were excavated during Roman and Byzantine times [6]. Certainly during these years the region was often beset by internal strife in the form of persecutions of local Christian communities and external attacks by the Arabs. After the region was incorporated into the Ottoman Empire, in the 14th Century, the external threat abated, the Byzantines were forced to leave the area and with the outbreak of peace, the abandonment of the underground cities began.

2.1 The ecological and geographical statement of Capadoccia

It took millions of years for the ash from the volcanoes to form a layer of tuff, covered in places by a further layer of basalt lava. The basalt ultimately cracked and split under attack from the weather and rainwater seeped down through the cracks and splits to slowly erode the tuff itself.

The natural effects of alternating very hot and very cold weather and the rain and the wind breaking down the rock's resistance caused the emergence of the tall cones of tuff capped by hard basalt, which is called 'Fairy Chimneys'. Where there is no basalt layer to protect the tuff lovely valleys have been formed connected to the plateau by steep canyons of andesite and basalt. The canyons of Soğanlı and Ihlara are particularly stunning examples, Ihlara canyon being 650 feet in depth in some parts.

Geographically located in the centre of the country, Capadoccia is a mountain area that was created from a series of volcanic eruptions. Capadoccia is famous for its fairy chimneys, sort of strange shaped rocks (tuff rocks) sculpted by the erosion work. Thereby this natural property allowed Capadoccia to be a member of the UNESCO World patrimony.

There are caves, cave houses, churches and also whole underground villages in this region which still survive and which are being used at present. This landscape was created many millions of years ago at the time when the two volcanic mountains covered a vast area with lava and dust. Capadoccia is known today for its underground settlements as well as its painted Byzantine cave churches [1]. Roughly 50 to 150 million years ago, repeated volcanic eruptions



and subsequent erosion in central Turkey created a series of interconnected valleys, surrounded by limestone plateaus.



Figure 2: The sight of cave houses in Capadoccia.

The site recently surveyed under the auspices of the German Archaeological Institute, preserves the remains of hundreds of small rubble houses and several churches. The evidence for rock-cut architecture and fresco painting is more limited in the early Christian period.

The valleys are sheltered and fertile with an almost temperate climate. The tuff is easily worked and for millennia has provided dwellings and store rooms, both above and below ground, for smallholders.

This subterranean way of life resulted from several different factors. The dramatic landscape of Cappadocia is formed from tuffaceous rock which is easy to work but which dries to a hard surface resistant enough to allow the excavation of wide rooms with horizontal ceilings. Trees producing wood suitable for building use are scarce in Cappadocia so even the surface dwellings are barrel vaulted using squared tuffaceous stone.

Because of the nature of the land, many churches, monasteries and dwellings were cut from the rock rather than built. Typically a living unit was cut into the slope of a hill with carved chambers organized around three sides of a courtyard. The Cappadocian carvers began by burrowing out the centre of a space, perhaps following a natural fissure, next they roughed out the whole and carved the details.

This building culture, making use of existing formations rather than creating specialist building materials, can be found throughout the world but is particularly strong in the Mediterranean region. Cappadocia's underground cities are, however, unique in their range, their complexity, their variety and possibly in the time periods in which they were developed. Subsequently the dried lava were sawed away through generations of rain, wind and floods, thereby creating deep valleys, while the slopes were carved into the astonishing cones and columns we see today. Generations of local people have carved innumerable doorways and rooms in the rocks over an area of several hundred square kilometres. Some were homes for farmers, others were stables and chapels. Quite early on the inhabitants of this area discovered that the dust was very fertile and

also that it was possible to carve this stone material. They, therefore, over generations, made carves and store rooms in these rock formations.

2.2 The material analysis

The terrain consists almost exclusively of a fine-grained, compressed ash, creating Capadoccia's characteristic cone formations. In some instances, a layer of nonvolcanic rock remains balanced picturesquely on an eroded cone, producing fairy chimneys. In some areas the rock has a pinkish hue from the underlying sand bed. In the less-explored area of western Capadoccia, the volcanic landscape offers equally intriguing formations [7].

3 The sustainable meaning of cave house formation

In the region the aspect of functionality is a sustainable matter of fact. The interiors and environments of cave houses that have been used for hundreds of years are still being used in today and they also serve the functions and needs of present life. The energy conservative property of the interiors and functions suitable to climate factor are the reasons of sustainability. Also the functions that let these houses survive are another factor to be recognized.

There are still some semi-subterranean rooms in use. The underground storage of produce is common practice particularly around Ortahisar, where large quantities of locally grown potatoes and citrus fruits brought from the South coast are stored. The climate of Capadoccia is continental. Summers are hot and sunny but the altitude provides cool nights. At winter time, the climate is cold and the fairy chimneys are totally metamorphosed when covered with snow [10].

The underground sites are particularly useful for storage as the outdoor temperature can vary from minus 20°C to nearly 40°C. The internal temperature of the sites remains constant throughout the year at 7°C to 15 °C depending on the proximity of the air shafts.

4 The underground cities found in Capadoccia region

The underground cities were long stay settlements and they were built to withstand attack and to support long numbers of people and their domestic animals for long periods of time. More than 40 multi-storeyed underground settlements have been identified. In times of peace the people of this area could live and farm above; however, when they were being invaded by enemies they would retreat into these underground safe places where they could survive for up to 6 months. Some of these underground cities are still used today [10].

The urban organization was very complex and extensive networks of passages, tunnels, stepped pits and inclined corridors link family rooms and communal spaces where people would meet work and worship. The cities were complete with wells, chimneys for air circulation, niches for oil lamps, stores, water tanks, stables and areas where the dead could be placed until such time as conditions on the surface would allow their proper disposal. Most importantly,



carefully balanced moving stone doors, resembling mill stones, were devised to quickly block corridors in the event of an attack [7].

One of these cities is called 'Derinkuyu', which is a huge complex having 8 underground floors and reaching a depth of 55 meters (180 ft.). This underground city was built in 1300 BC. The city had excellent ventilation made possible by ventilation shafts, the deepest reaching depths of 85 metres. There could be as much as 20 levels underground.



Figure 3: The underground cities in Capadocia.

5 The architectural formation and space planning in Capadocia houses

The architectural elements of the rock-cut buildings were carved in imitation of Byzantine architecture. But there is an important difference. Most architectural features in rock-cut buildings are mere adornments with no structural purpose. Interior columns, for example, do not support roofs; they exist simply as decoration [5].

With the malleable volcanic rock, work would have proceeded quickly. A room 25 feet long, 14 feet wide and 10 feet high probably took a single man about a month to complete. Theirs is primarily architecture of interiors, though the Capadoccians sometimes gave their rock-cut buildings detailed facades, with gables and horseshoe-shaped arches.

The cave room has a smallish window; it is cooler than outside. The people who used to stay in this valley lived in such caves because they kept them cool in summers and provided warm waters in winters even though temperatures would take a dive after the sun set.

In figures 4 and 5 we can see houses of stone around the Capadocia region [2]. All these houses have similar characteristics. These characteristics are:

- Approximately all houses are formed by the basis of nature and ecological statement.
- The usage of interiors is sustainable as the air quality of the interior is suitable to the climate and the long term usage between cultures and societies is recognized.



- The functions of the structures are residences, houses, churches and storerooms.
- The most common material is stone added with wood so as to be suitable to climate and geography.
- The practical usage and interaction with environment are also characteristics in common.
- The interior organization of spaces is non-flexible and stable.

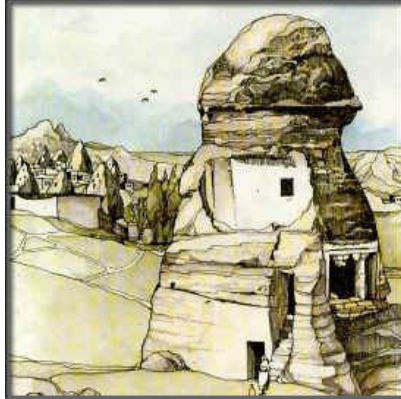


Figure 4: A house in Capadocia Uchisar.

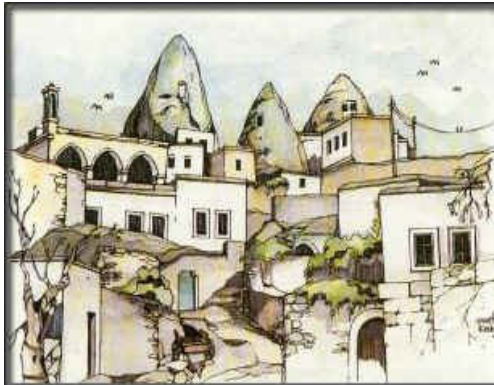


Figure 5: A house in Capadocia Avclar.

In figures 6 to 8 we can see the naturally based stone houses in harmony with Capadocian ecological formation. These are not cave houses but built by sequence with the cave formation and parallel with the architectural symbol of cave.





Figure 6: The typical view of a house in Güzelyurt.



Figure 7: The plan view.



Figure 8: The side view.

5.1 The analysis of atypical cave house in Capadocia

The cave houses that are still being used in today's conditions have functions as residences [11]. The cave house complex is the restored stone village houses, each different in architecture and character. These houses are a combination of six cave houses with a total of 17 private cave rooms dating back to 5th and 6th centuries and crowned with a 19th century Greek Mansion. But several are fifth, seventh century cave houses burrowed deep into the cliff that embraces the small market town. The experience of inhabiting one is surprisingly serene and dry although erosion and reconstruction have supplied windows and doors where originally there was a blank rock face with a concealed underground entrance. Now there are bathrooms with modern plumbing and sanitation. This is because enough of the surrounding Cliffside has eroded to reveal the pattern of troglodyte house, from stables at the lowest level to living rooms above and at the highest



level kitchens, from which smoke filtered up through the porous rock to escape invisibly from the hilltop. These exceptional cave houses are renovated and decorated with care and in their own distinct style while strictly respecting the local character. The décor is elegant and personalized with hand-crafted furnishings and antiques. There are 17 rooms in this cave. These are the balance between modern comfort and tradition [11].



Figure 9: The Cave house (Yunak House) in Cappadocia.

6 Results

6.1 The advantages of cave house formation

The main advantages of interior space planning in cave houses that this study reveals are:

- The virtual and mystic atmosphere of the cave interior,
- The air quality of houses regarding the climate,
- The sustainability factor of cave house among cultural, ecological, aesthetical etc. approaches.
- The adequate formation of ecology based architecture.
- The historical feature of space with a language of many cultures and religions.

6.2 The disadvantages of cave house formation

Because of the limited properties of space planning of cave interiors some disadvantages can be listed as follows:

- The impossibility of the flexible interior organisation,
- The improper sizes of interior dimensions as their naturally characteristic constructions,
- The impossibility of the multidisciplinary and optimal space formation,
- The lack of acoustical criteria as the usage of stone which is not proper for noise absorption and has the characteristic to reflect it.



7 Conclusions

Cave houses are important archetypes of space as they indicate the cultures, religions and tradition of centuries. As they are still being used today great concern must be shown and more adequate functions should be added so as to reach a more sustainable meaning to increase the concept of the *language of space survived from centuries* in order to let them be useful for more and more years by great recognition.

The most important thing in this study is to understand the importance of the historical aspect of design with the basis of nature and to create contemporary solutions in today's design problems with the solutions found in these types of natural architectural spaces. These spaces should be a sample for contemporary designers to create new sustainable spaces. Knowing the historical background of design and nature with the samples in which they are in good sequences designers could reach more and more liveable interiors with contemporary means and without energy loss. These criteria should be carried at the first levels of education in design training and be adapted beginning from graduate study.

Nature is a gift to all designers as it potentially carries important values like aesthetics, energy, dynamical circulation of life, materials, daylight, air, transformation etc. As designers use the present values of nature without giving any harm and instead by energy conservation then more optimal solutions could be reached.

References

- [1] Fırat, K., *Kapadokya*, Literatür Yayınları, Sanat Yaşam Kültür Dizisi, 1996.
- [2] Küçükerman, Ö., *Turkish House, Kendi Mekanının Arayışı İçinde Türk Evi*, T.T.O.K Yayını, 3. Basım, 1988.
- [3] Sözen, M., *Anadolu Türk Mimarisi*, Anadolu Uygarıkları, Cilt 5.
- [4] Ünver S. E., *Amucazade Hüseyin Paşa Yalısı*, T.T.O.K. Yayını, 1970.
- [5] Rodley, L. *Cave Monasteries of Byzantine Capadocia*, Cambridge University Press, 1986.
- [6] Rodley L., *Byzantine Art and Architecture. An Introduction*, Cambridge University Press, 1996
- [7] Capadocia Tourism Promotion Foundation. A complete Guide to Capadocia, ISBN 975 7672 106.
- [8] Liew, J. Capadocia, <http://www.jehpin.com/travel/turkey/cappadocia.php>
- [9] http://www.turkeytravelplanner.com/photo_galleries/cappadocia/
- [10] <http://www.wsu.edu/~wldciv/tours/turkey/cap01.html>
- [11] http://www.yunakevleri.com/useful_tips.html



Build trees

M. Despang

College of Architecture, University of Nebraska, Lincoln, USA
Despang Architekten Hannover, Germany

Abstract

This conference was held in a lodge in the “New Forest”. This is an ideal environment to make the conference participants aware of the topic, addressing wood as nature’s most direct and oldest building product, which has the greatest potential for helping the world into a postfossil future. Although wood is the most organic material, when it comes to public appreciation as a building material, it is not ranked highly. The author will question and answer how architecture technologically and aesthetically can treat wood as an “up-to-date” and “state of the art (and architecture)” building material truly belonging to today’s world. The author will show by means of students’, colleagues’ and personal work, how wood can create a sustainable architectural space and form evoking respect and appreciation from all human senses. Both practicing in Hannover, Germany and teaching in Lincoln, Nebraska, USA, the author will introduce in his paper the intercultural approach to wood research in natural building design. Work in progress and widely published built projects will illustrate the strategies for improving the environment with wood. The author’s recent experience with the new TMT (Thermal Modification Technology) and the results of his participation in the 4 European Thermowood conference in February 2006 in Leipzig, Germany will be shared with the conference participants. The paper presentation will point out the challenges and potential of rethinking and reinventing wood as the building material for a future related to postfossil nature.

Keywords: postfossil Midwestern architecture, progressive monolithic wood structures, Thermo Modification Technology, “Passivhaus” technology.

1 Introduction

Compared to the hard sciences architecture tends to have a lesser grade of innovation. Compared to the progression in natural, medical and computer-aided



science in the last century, building technology has nearly stagnated at a medieval level. The mainstream of architectural application is little influenced by the cutting-edge architectural research. On the other hand sheltering dramatically impacts the human environment. Architects should utilize innovative research such as eco-friendly building concepts tremendously helping to preserve the global environment. For example, due to a forestry mandate by the German government in 1999 Germany saw an increase of wood buildings from today 9% to 35%. This would compensate in 8.5 million tons of coal oxidant per year. Since building with wood obviously makes common sense, a conclusion could be to strategize and seek innovation from tradition creating buildings out of nature’s purest renewable material which is the oldest building tradition in the world. Wood, as compared to stone, has always been more appealing. The material’s advantages are easiness to work with simpler tools and machinery and being lively like human beings. One might think by this observation, that wood is the ideal material to build with and which is the favorite in modern building application. Reality however, looks different. In the following presentation, reasons for contemporary human problems with wood will be investigated and possible strategies on how to improve.

2 Analysis

Both academic and professional locations of Despang Architekten in Lincoln, Nebraska, USA and Hannover, Germany serve as case studies revealing both regions beginning from shared roots have emerged quite differently. What they have in common are the skeptics about wood as a primary building material, although both regions on different continents have intensively been growing trees. The traditional northern German half-timbered structure restricts use of wood already to a necessary minimum, could not survive with the dominantly pioneers from Germany in Nebraska, who were coming to settle on a treeless prairie. Since then, Nebraska systematically improved and initiated the “Tree City” initiative by the Arbor Day Foundation [1]. The foundation oversees the Morton’s family enthusiasm for regional and worldwide greening.



20



5



5

Figure 1.



However wood still almost exclusively appears in the predominant wooden platform, the former balloon frame structure system. This might be seen as in the tradition of the German ancestors and their half-timbered system when comes to the efficiency in using wood as little as possible and minimize the structure to tiny studs. The lack of thermal building mass in the USA leads to the introduction of air-conditioning as the standard, as the ultima of unsustainability. And the outside of the wooden home appears like the common shared ideal of a solid home, symbolized by brick or stone veneer and more and more plaster cladding or vinyl siding as a fake reference to the wooden heritage.

In northern Germany due to energy building codes, what was formerly structural part of the wooden posts is made by concrete masonry units. They are surrounded by insulation, but yet on the outside they are sheathed with a replication of the half-timbered structure, neglecting the originating authentic tectonical notion to degrading as a wallpapering illusion.

Almost like the new world's "woody cars" with their wood revealing plastic foil glued to the sides of the automobiles, sentimentally recalls the former structural making of cars out of wood for the body. This raises the question, why wood as a material is so positively responding to nature and is so little appreciated in natural condition? Finding the answer needs surprisingly more than architectural investigation, because the reason might be more sociologically/psychologically related than architecturally. Discussing the issue with specialists in this field, the advantage of wood being organic and similar to the human being turns out to be at the same time and to the same extent its disadvantage. As expressed by the media in western culture only the forever young and virgin appealing human beings are accepted. In opposition, any natural aging process is rated down. In the media this phenomenon is drastically expressed by beauty surgery series and the equivalent in the building world in terms of wooden facades. These are periodically coated with a white paint, which refers back to brightening toothpaste.

This fakeness in using more the imagery of a wooden building rather than as the concrete physical appearance has a long tradition since European romanticism. For instance, the King of Prussia, Friedrich Wilhelm IV, in 1847 tried to cure the homesickness of his Bavarian born wife, Elisabeth, by building her a Bavarian log cabin in the center of the Wilderness Park in Potsdam [2]. Following World War II the leader of the socialistic East "German Democratic Republic" Erich Honecker, although praising and practicing a strict modernistic architectural approach for the people, chose for himself this so called "Bavarian house" as a cozy background for private and official representations. In an almost exclusively historical pattern former East Germany is rebuilding the cultural heritage after the reunification of November 1989, specifically in picturesque areas with a rich wooden architectural history like the "Baederarchitektur" [3] on the island of Ruegen. This compared to the new urbanism in the USA seeking the solution of healing the contemporary human being with the realm of old-fashioned craftsmanship and details. The desire for the wooden vernacular has recently been in the process of being professionally touristically engineered and being promoted by the leisure industry. Referring to



the aura in the turn of the 20th century, lodges in the USA, like Robert Reamer's groundbreaking Old Faithful Inn in the Yellowstone National Park or the 1936 Oregon Timberland Lodge, today's clever hotel managements are trying to build upon the sentimentalities of people regarding these eras as opposed to contemporary, unpredictable and hectic times. Rarely do these enterprises make use of the historical predecessors as a spatial and tectonical starting point, to then find an own state of the art and architectural interpretation. In this new trend known as "parkitecture", most are rather literal replicas of the architecture of the "old times" representing only the "good ones". A positive exception to the rule is the Amangani Resort hotel in Wyoming [4], where the hotel chain's corporate office and Paris architect, Ed Tuttle, who grew up in the Pacific Northwest, was melting the cosmopolitan and the vernacular by basically focusing on the potential of space and views with natural preaged materials in a modern manner.

However showing aging both in human and building extend is generally disliked by the majority of people. A different attitude is to be found in the regions more exposed to nature's forces, as along the coasts or in the mountains on both the European and the American continent, where the tradition of wood construction and cladding transcends into a widely appreciated new wood architecture. The exposure to nature's power in the form of steady gusty winds helps in regulating the humidity and allowing the wood surfaces to get a more equal patina. This creates a natural look such as the face of the farmer in the plains or mountain women in the mountains, with an own beauty of the skin structurally carved by the wind and the sun. Taking a closer look and tracing a comparison from nature and the structure of the bark on the trunk of a tree to architecture, we see a potential of striking similarities in approaching a sustainable notion: the ultraviolet light darkens the wooden building skin as a protection for the surface below and carvings drain the humidity.

3 Development/results

The architectural work of Despang Architekten made use of this research when investigating the potential of sustainable wooden building concepts on a natural, yet truly modern and contemporary basis. In the case of the design for the school for mentally disabled children in Garbsen, Germany [5] this goal was achieved by seeking a materiality responding to the extremely strong demand of addressing all the five senses of these special children. On a small lot in an existing school complex, blending the urban edge into the surrounding landscape, a pavilion courtyard type organization was applied to integrate natural conditions in the form of bringing open space, light and air into the building. The tectonical concept was derived from an idea regarding of the substance of a section of a tree itself: inside a notion of stimulating bright wood, on the outside sheathed by a 'crusted' protecting bark. To achieve a thermal mass equivalent to the favored monolithic stone and brick house and unlike the common wooden lightweight structures, the mass of the trunk was taken literally by applying the wood in a massive way. The board staple-structure [6] insulates already rather well, so an average amount of insulation applied on it, achieves a much better u-



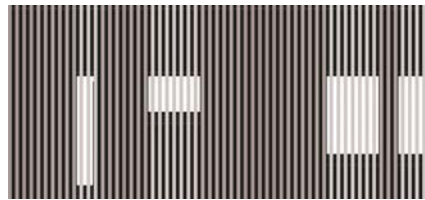
value. This system of nailing the boards to each other in a structurally engineered way, so that a slab results, was chosen for the application for the entire structure of load bearing walls and ceilings. Julius Natterer, Professor at the Ecole Polytechnique Fédérale de Lausanne, Switzerland and main mentor of the system, calls a social structure, where the weakness of one member (board) is compensated by the other ones [7]. This structural/tectonical principle nicely describes and stands as well for the pedagogical concept of solidarity being the primary strategy in the education of mentally disabled children. In nailing the boards, instead of laminating them to each other the system is emission free.

The goal of a consistent appearance outside matching the vertically louvered surface of the inside, the same pine boards could be used, by applying the emerging and innovative TMT, intensively researched and promoted by the “ihd / Institut fuer Holztechnologie Dresden gGmbH”, Germany [8]. Whereas untreated pine wood does not provide the affordable resistance against biological and insect attack, this improvement upgrades the resistance of the wood remarkably.

The public in general appreciates darkened, tanned and evenly textured wood characteristic for trees in seasonless regions which are mainly tropical areas. The massive and vast diminishing of the tropical rain forest is scientifically proven to have a hazardous impact on the global climate. However the TMT has been mainly invented to enhance the resistance against biological and insect attack, occurring based upon high humidity. The main environmental advantage of TMT is based upon another phenomenon. The exposure to heat and pressure let the wood turn dark and by this makes it attractive as an alternative for tropical hardwood. This way TM-wood helps to preserve the tropical rainforests and the global climate. In addition, the untreated wood is serving the local environment by having been regional softwood trees prior to becoming a TMT product and in this previous function, intensively helps to convert coal oxidant into oxygen. Even the energy for the modification process can be recruited from the natural resource circle itself, by firing the heat chambers with the same fast growing regional wood which is modified.



20



9

Figure 2.

While technologically convincing, on an emotional level the material yet still has to find an own identity, a soul, as a requirement for being accepted, which again is the basic requirement for sustainability. The material therefore has to overcome the substitutional character. The potential for an own realm is yet



obvious, but has to be explored furthermore on a broader architectural level. For example tropical hardwood, due to the lack of seasons, is often missing grain. The variety of these natural textures of local softwood can be strategically used, as the tectonics of the school in Garbsen demonstrates. Throughout the fine rhythm of the boards and the battens system, the texture of the pine wood works almost as a natural ornamentation.

The heat treated pine wood, made by diminishing the crystal water in the wood, already reacts like the tanned human skin, protecting the cells underneath and ages equally.

As part of the vertical tectonical sheathing elements like windows, gutters and down sprays are integrated flush into the surface. Equally exposed to sun and air, like the human skin of the mountain women, the façade of the building in this way has the chance to age in honor. This result is a higher grade of appreciation and acceptance for the architecture, because the architecture makes use of the tectonical principles and makes people collectively agree like they do on the natural beauty of a tree trunk.

Despang Architekten's project, which is building upon the previous experience but yet pushing the envelope to an even further extent, is a kindergarten building project in Hannover, Germany [9]. For another public client with a limited budget, the goal was to create a building with high comfort, while assuring a natural environment for the children. In addition to ending fossil resources, the building is mostly independent from this kind of energy. The building is situated in a consistent 1960's neighborhood, with a high urban quality and replaces an existing structure from 1970. The neighboring structure is a sustainable neighborhood grocery store center designed by Despang Architekten in 2004 [10] which received the Lower Saxony States Award of Architecture [11] that year.

The chair of the jury, Professor Carsten Roth, both of Hamburg and Braunschweig, Germany and Denver, Colorado honored the concept for the both rigid and poetic structure of a concrete frame. In terms of a neighborhood kindergarten building, the existing site with a yard of mature trees was carefully adapted to redesign the kindergarten building type. As a research result of the Garbsen school, the north side is treated in a similar manner, hosting the serving rooms, sheathed by a screen of heat modified wood battens which change from opaque to opal running over the solids and voids of the surface.

The approach of the application of the heat modified wood though goes beyond the achievements of the former one, by expressing the TMT process in the building design and using this as a creative exploration. In the areas of the windows, the brightest HM wood is applied, which is the one been processed the shortest time. In the closed wall areas the darkest one is used. In between, the transition from bright to dark will generate a notion of motion.

The application will enhance the character of TM wood and be of major contribution to the "no emission" building concept, which will be an opportunity to promote the material being rather unique than substitutional.

To keep the heat out in the summer and the cold in winter, highest insulation and thermal mass are incorporated. The search for the appropriate structural



system lead linearly back from the contemporary most commonly executed American platform type, to it's ecological precedent, a 1973 case study home in Lungby, Denmark [12]. Surprisingly enough research sources trace knowledge about this as far back as the last major global awareness of ending fossil resources in 1970.

Similar, in the kindergarten project, TJI studs are used with a foot deep insulation out of cellulose as another aggregate condition and use of trees. The necessary thermal mass is provided by massive wooden ceilings, once again in the board-staple structure and a PCM (Phase Changing Material) enriched concrete floor slab, again disconnected from the earth by a foot deep insulation.

The curvilinear southern façade is entirely glazed and maximizes the solar gain and transition of space from the inside to the outside. The existing trees, in addition to custom made umbrellas, keep the building from overheating in the summer. Although neither a romantic log cabin nor the beloved stone building, this project will convince the client in the way of its environmental friendliness, as the building material instead of polluting, cleans the environment.

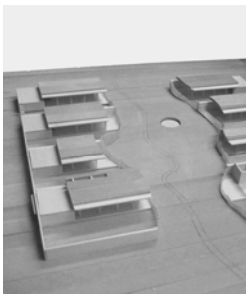
The project points out another important aspect by obeying all the parameters and applying all the tools of "passive house planning", but this alone does not yet generate a result which is satisfying from an architectural point of view. In other words green vocabulary does not automatically enable planners to speak a sustainable language, because architectural quality in a balanced relation of form, space and tectonics needs to be integrated to make the building pleasing to the occupants and endure or be able to be adapted, which is one of the most important integral aspects of sustainability. As much as the lack of environmental building sensitivity has been a concern in the past, the lack of innovative architectural character of "passive houses" might be a problem in the future. The questionable charm of glued together styrofoam boxes can already be seen as a problematic issue, keeping green building design away from becoming influential on a broader, widespread level. The kindergarten design by Despang Architekten demonstrates that passive house technology is not an aim but a tool to create ecological architectural space. To deal with these physically generated parameters is not the final destination but the starting point in greening design. The architectural exploration has to give these somehow restricted, nature-given parameters spatial character. And the design has to donate to the building a distinct, unpredictable character responding to the individual inspirations of exteriorities and interiorities as is always and ever the case with good architectural design, no matter if green or not. Wood as nature's oldest and regarding the future most emerging building material is ideal because it is inheriting both pragmatically and poetic quality.

However in regard of a global potential, wood has yet to be introduced to a wider audience by applying to a broader range of architectural building types, like the train stations designed for the Expo 2000 in Hannover by Despang Architekten [13]. However most important is to promote wood in terms of the organic human attitude in the domestic building typologies. The rental "treetop condominiums" by Despang Architekten in Hannover is an example of using wood in a building type commonly and traditionally in a particular

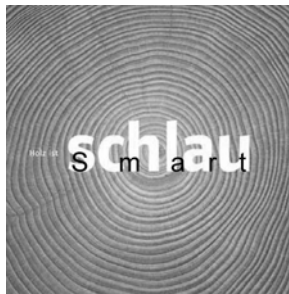


geographically area not familiar with wood. In this case the sentimental notion of wood as the structural material of a tiny half-timbered house which was previously occupying the lot is used to code and accentuate the areas of most intense human occupation, blending the space between the private and the public. Wood is by this transformed from a structural literal level to an abstract enveloping one.

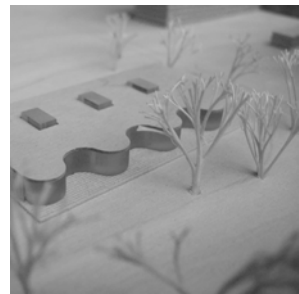
Using wood is from the matter of a wide public appreciation most important in small scale domestic building types, like in the case of the “house K.” [14] and the “wooden feathery extension” project by Despang Architekten [15], again in Hannover. Adding a one room extension and a canopy to an existing old house creates a new sense of place and a transition of space from the inside to the outside. In this case the physical capabilities of camballa wood enabled a concept of structure and architecture to blend into each other as integrative parts and work primarily with light and shade as major architectural components, like bamboo does in the natural world. Worth examining is once again the calculated notion of a comfy and warm environment, created by the material’s unique physical quality. The decades of the 1950s and 1960s, being influenced by the design of northern European countries, can be strategically seen as predominantly taking advantage of this. Instead of staying a local phenomenon, sensual architecture emerged to a global extent and excitingly down to the ordinary average single family house. The 1950s domestic case studies almost automatically resulted in relating to natural conditions, as blurring the boundaries from the inside to the outside, sun gaining floor to ceiling windows to the south and ventilating courtyards as “low technology” natural cooling devices. This notion is represented by the tropical hardwood resembling covers of the recent books about the west coast phenomenon of the “Eichler homes” [16] or about the more vernacular “ranch homes” [17]. The rising appreciation in this legacy is as well an indication of a potential of wood being strongly associated with progressive housing for a wide range of the population in the USA.



19



20



9

Figure 3.



4 Execution/conclusion

Researchers at the College of Architecture at the University of Nebraska-Lincoln will investigate the future potentials of the progressive Midwestern mid-century homes legacy. Starting from the analytic precedents from the past, the further goals and objectives are to trace the spatial, tectonical, environmental and social potential of wooden buildings into the future. The experience of professional practice of the instructors will help and encourage the students. In particular the Nebraskan Assistant Professors Jeffrey L. Day [18] with offices in San Francisco, California and Omaha, Nebraska and Martin Despang in Hannover, Germany will share their knowledge of investigation in the creative potential of wooden prefabrication production with the students for the benefit of the teaching and research exploration. Whereas Martin Despang's School in Garbsen, Germany was experimenting with automated prefabricated massive elements, creating efficient, ready made and thermal, acoustical and sensual qualified components, Jeff Day's "Wood Island House", deals with the challenging issue of defining an organic domestic space by using cutting-edge computer technology both in design and fabrication.

Leading in building energy consumption, the USA has to use the architectural academic freedom to address the potential of ecology in building design more aggressively, especially in the Midwest, with perfectly given natural resources of sun and wind. Rising energy costs might even give them the chance to receive a wider public audience and interest, making a virtue out of the dilemma and introduce progressive architectural dimension once more to the citizens of cities, communities, neighborhoods or just the single middle income family. In collaboration with involved faculty at the College of Architecture at the University of Nebraska-Lincoln, this issue will be addressed more intensively in architectural education.

Projects to be resolved are by intention small, giving students a chance to study the issue in more depth, rather than creating huge corporate architectural visions lacking sensitivity for the detail. Masters student Daniel Siedhoff is currently preparing for his master thesis, re-designing a house on a lake, being design/builder with hands on activity. Colleague Alissa Piere uses her childhood experience of having grown up close to the Winnebago Indian Reservation north of Omaha, Nebraska to re-think the domestic reality of contemporary Indian life [19].

For both students the investigation is a process getting back to their roots. Their ancestors instinctively knew how to survive in the harshness of the prairie plains by physically protecting themselves from the north wind and opening to the south sun, in this case literally "building" trees. When it comes to the point of creating truly contemporary ways of living environments in the beginning 21st century, this generation will be looking forward, in a highly advanced modern global world, seeing the tree as a metaphor for creating self sustainable and re-rooted architectural organisms.



References

- [1] www.arborday.org.
- [2] www.bayerisches-haus.de.
- [3] Reno Stutz, Thomas Grundner, Baederarchitektur, Hinstorff Verlag GmbH 2004.
- [4] Lauren Bernstein, Lodges de Luxe, United Hemisphere 01 2006.
- [5] Baumeister B4 2003, l'architecture d'aujourd'Hui 374: 2003, Holzbauatlas 2003, DETAIL 1/2 2004, tec 21 10 2004.
- [6] Herzog, Natterer, ..., Holzbauatlas Birkhaeuser 2003.
- [7] www.iez-natterer.de.
- [8] www.tmt.ihd-dresden.com.
- [9] Passive house kindergarten, Hannover, Germany scheduled for Fall 06.
- [10] db 09 2004.
- [11] www.aknds.de.
- [12] A travel report from a journey to Denmark and south Sweden by students and faculty from the of the University of Munich in 1976 /1978, Arbeitskreis Excursion Daenemark und Schweden, Munich.
- [13] DETAIL 04 2000, Wallpaper UK 05 2000, XS Thames & Hudson UK 2001, C3 Korea 01 2005, Material for Design Princeton Architectural Press USA 2006.
- [14] Cristina Del Valle, „compact houses“, Bookslab 2006.
- [15] DBZ 06 2000, C3 Korea 2003.
- [16] Jerry Ditto, Lanning Stern, “Eichler homes“, Chronicle books 1995.
- [17] Alan Hess, „Ranch House“, Harry N. Abrams, Inc. Pub 2004.
- [18] www.minday.com.
- [19] Alissa Piere, master thesis: “REZidential Housing, a prototype for the Winnebago reservation, UNL Spring 2006.
- [20] Infodienst Holz 2006 campaign: “sexy”, “Holz ist ewig jung- wood is forever young” + “Holz ist schlau - wood is smart”.



Thermal performance of a dome-covered house

Y. Lin & R. Zmeureanu

*Centre for Building Studies,
Department of Building, Civil and Environmental Engineering,
Faculty of Engineering and Computer Science, Concordia University,
Montreal, Canada*

Abstract

A dome-covered house is an example of designing sustainable buildings by learning from the optimized biological forms from nature. This paper presents the mathematical model for estimating the energy performance of the ensemble dome-house. The heat balance equations are written at the dome surface, for the air inside the dome, at the outside surfaces of the house, at the inside surfaces of the house, at the ground surfaces, and for the air inside the house. The annual energy performance of the dome-covered house is presented and compared with that of an isolated house located in Yellowknife (Canada) at 61°N latitude.

Keywords: energy performance, dome-covered house, optimized biological form, mathematical model.

1 Introduction

Dome structure is based on self-generating forms in nature, bubble clusters being typical examples. It is based on the natural form-optimizing process in biological structures and can be translated into the architectural world in the form of pneumatic structure [1, 2]. The dome configuration applies nature's principles of forming a highly efficient system. The advantages of designing a dome-covered house in Canada are [3]: it can provide a shelter to withstand high winds and extreme temperatures in northern part of Canada; it can store large amounts of solar radiation and thus reduce the heating load of the covered house in the winter; and it can provide pleasant view without sense of enclosure if the dome is transparent or translucent.

Examples of dome structures in nature are the sunflower, the shell of sea urchin, and the rose bubble shell. The dome-like shape of the sunflower enables



it to receive maximum solar radiation during daytime. The dome-like shapes of the sea urchin and the rose bubble shell enable them to overcome the water pressure.

More attention has been given to the structural configurations than on the thermal performance of dome-like buildings. According to the Buckminster Fuller Institute [4], some of the largest geodesic-dome structures (listed in descending order from largest diameter) are presented in Table 1:

Table 1: The largest geodesic-dome structures.

No.	Name	Location	Diameter (m)
1	Fantasy Entertainment Complex	Kyosho Isle, Japan	216
2	Multi-Purpose Arena	Nagoya, Japan	187
3	Tacoma Dome	Tacoma, WA, USA	161
4	Superior Dome	Northern Michigan Univ Marquette, MI, USA	160
5	Walkup Skydome	Northern Arizona Univ. Flagstaff, AZ, USA	153

According to Monolithic Dome Institute [5], a monolithic dome home has approximately 333 m² of living space, walls and ceiling with thermal resistances of 10.5 m²·K/W, low emissive windows and low flow water fixtures. The owner obtained energy savings of over \$2000 per year compared to a conventional masonry house of the same size. Croome [3] presented his concept of building a covered township in the northern part of Canada. In his studies, the dome structure was composed of double layer membrane material. The simulation results predicted a 15.7% reduction of the annual heating energy consumption for houses built under that cover, compared with houses without cover.

Transparent and translucent domes have been used as skylights for daylighting and energy saving purposes. Some models [6-9] have been developed to predict the optical and thermal properties of the dome skylight. Those models replaced single-glazed hemispherical dome skylights by optically and thermally equivalent single-glazed planar skylights. Smith [10] developed a mathematical model to predict the impact of thermal exchange within pyranometers, simulated as a small glass dome, considering only convection and conduction. Electrochromic glazing may be used to prevent the overheating inside such structure in the summer. For instance, Porta-Gándara & Gómez-Muñoz [11] modeled a Fuller type geodesic dome to estimate the solar energy that passes through the dome, when it is covered with electrochromic glazing, compared with the case of a common glass.

2 Mathematical model

2.1 Heat balance of the dome glazing

The dome surface is divided into 84 rows and 26 columns that give 2184 cells (Figure 1). The heat balance equation at the center of each cell (i,j) is written as:



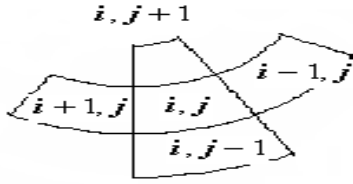


Figure 1: Adjacent cells.

$$\begin{aligned}
 &kdl_{i+1,j}(T_{i+1,j} - T_{i,j}) + kdl_{i-1,j}(T_{i-1,j} - T_{i,j}) \\
 &+ kdl_{i,j-1}(T_{i,j-1} - T_{i,j}) + kdl_{i,j+1}(T_{i,j+1} - T_{i,j}) \\
 &+ (q_{sol,ij} + q_{conv,ij} + q_{LWR,ij} + q_{surf,ij})A_{ij} = m_{ij}c_p \frac{dT}{dt}
 \end{aligned} \tag{1}$$

where $q_{sol,ij}$ = the absorbed incident solar radiation, in W/m^2 ; $q_{conv,ij}$ = the convective heat flux over the inside and outside cell surfaces, in W/m^2 ; $q_{LWR,ij}$ = the long wave radiation with the outdoor environment (ground and sky), in W/m^2 ; $q_{surf,ij}$ = the net long-wave surface-to-surface radiation between the cell and other surfaces inside the dome, in W/m^2 ; m_{ij} = the mass of cell (i,j), in kg; c_p = specific heat of the dome glazing, in $J/kg \cdot ^\circ C$; T = temperature, in $^\circ C$; t = time, in sec, k = conductivity of the glazing, in $W/m \cdot K$; d = thickness of the glazing, in m, l = length of the interface between two adjacent cells, in m.

2.2 Heat balance of the air inside the dome

The indoor air is assumed well mixed and therefore it is represented by one node. The heat balance equation for the air inside the dome is written as:

$$Q_{conv,in} + Q_{inf} + Q_{exf} = m_{in}c_p \frac{dT}{dt} \tag{2}$$

where $Q_{conv,in}$ = the convective heat flux over all inside surfaces, in W; Q_{inf} = the infiltration heat gain/loss due to the outside air, in W; Q_{exf} = the exfiltration heat gain/loss from the air inside the house, in W; m_{in} = the mass of air inside the dome, in kg; c_p = specific heat of air inside the dome, in $J/kg \cdot ^\circ C$.

2.3 Heat transfer through walls

Each exterior wall of the house inside the dome is assumed to have four layers. Nine nodes are used to discretize each wall/roof. The governing equation for the one dimensional heat transfer process in each layer is written as follows:

$$\frac{\partial T}{\partial t} = \alpha \frac{\partial^2 T}{\partial x^2} \tag{3}$$

where α = the thermal diffusivity of each layer of the wall, in m^2/s ; x = thickness of the layer, in m.



The outside boundary conditions can be written as follows:

$$-k_1 \frac{\partial T}{\partial x} \Big|_{x=0} + q_{sol,l,out} + q_{conv,l,out} + q_{surf,l,out} = \rho_1 * \frac{1}{2} dx_1 * c_{p1} * \frac{dT}{dt} \quad (4)$$

where k_1 = thermal conductivity of the first layer of the wall/roof, W/m-K; $q_{sol,out}$ = the absorbed solar radiation that is received at the outside wall surface, W/m²; $q_{conv,out}$ = the convective heat transfer over the outside wall surface, W/m²; $q_{surf,out}$ = the net surface-to-surface radiation leaving the outside wall surface, W/m²; ρ_1 = density of the first layer of the wall, kg/m³; dx_1 = thickness of the first layer of the wall, m; c_{p1} = specific heat of the first layer of the wall, J/kg·°C.

The inside boundary conditions can be written as follows:

$$-k_4 \frac{\partial T}{\partial x} \Big|_{x=th} + q_{conv,l,in} + q_{surf,l,in} + q_{rad,ihg} = \rho_4 * \frac{1}{2} dx_4 * c_{p4} * \frac{dT}{dt} \quad (5)$$

where k = thermal conductivity of the last layer, W/m-K; $q_{conv,l,in}$ = the convective heat transfer over the inside wall surface, W/m²; $q_{surf,l,in}$ = the net surface-to-surface radiation leaving the inside wall surface, W/m²; $q_{rad,ihg,l}$ = the radiation heat flux due to internal heat gain, W/m²; dx_4 = thickness of the last layer, in m.

2.4 Heat transfer through the ground inside the dome

The one-dimensional heat transfer equation (3) is applied. The outside boundary conditions can be written in similar way as equation (4). The temperature of undisturbed ground at 3.0 m is assumed to be equal to the soil temperature obtained from Energyplus [12]. A number of nine layers are used to discretize the ground on the vertical direction.

2.5 Heat balance of the house indoor air

The air inside the house is assumed well mixed and therefore it is represented by one node. The indoor air temperature T_a is held at the set-point value by a heating, ventilation and air-conditioning (HVAC) system. The heat balance for the indoor air is written as:

$$Q_{HVAC} + \sum_{j=1}^6 A_j h_a (T_{j,in} - T_a) + Q_{inf} + Q_{internal,conv} = 0 \quad (6)$$

where $T_{j,in}$ = the inside surface temperature of the j th wall, window, roof or floor, in °C; Q_{HVAC} = the heat extraction/addition rate by the HVAC system, in W; Q_{inf} = the infiltration heat gain/loss due to the air inside the dome, in W; $Q_{internal,conv}$ = the convective part of internal heat gain, in W; T_a = room air temperature (e.g., $T = 20^\circ\text{C}$).

2.6 Inside convection coefficient

The inside convection coefficient for each dome cell is calculated by assuming natural convection [13]:



$$h_n = 9.482 \cdot \frac{\sqrt[3]{|\Delta T|}}{7.238 - |\cos \Sigma|} \quad (\text{for upward heat flow}) \quad (7)$$

$$h_n = 1.810 \cdot \frac{\sqrt[3]{|\Delta T|}}{1.382 + |\cos \Sigma|} \quad (\text{for downward flow}) \quad (8)$$

where ΔT = the temperature difference between surface and air, °C; Σ = the tilted angle of surface, degree.

2.7 Outside convection coefficient

The outside convection coefficient is calculated as follows [14]:

$$h_o = \sqrt{h_n^2 + [aV_{az}^b]^2} \quad (9)$$

where h_o = the outside convection coefficient, in $W/m^2 \cdot ^\circ C$; h_n = the natural component of convection coefficient, in $W/m^2 \cdot ^\circ C$; V_{az} = the wind speed over the surface, in m/s.

2.8 Radiation coefficient

The net radiation exchange of a surface is equal to the difference between the surface radiosity and irradiation. The total long-wave incident radiation of surface A_j is:

$$A_j \frac{J_j - \epsilon_j E_j}{\rho_j} = \sum_{i=1}^{N_{surfaces}} J_i F_{ij} A_i \quad (10)$$

where ϵ =the emmissivity of each surface, J = the radiosity of each surface, W/m^2 , E_j = the blackbody emissivity power, W/m^2 , F_{ij} = the view factor between two surface i and j .

Hotel and Sarofim [15] simplified the calculation of the radiant exchange calculation by pre-calculating all geometry and surface-related properties using a total gray interchange area, S_{ij} . By applying this concept, the net radiation exchange at one surface becomes a simple summation of all the incident radiations from other surfaces to the destination surface. With this method, the network equations can be solved once and used throughout the rest of the simulation period. In this paper, a new view factor based on the total interchange area is defined and used to calculate the long-wave radiation between inside surfaces. The total interchange view factors can be obtained by solving the systems of equations. With the total interchange view factor, the radiation coefficient between two surfaces i and j can then be written as:

$$h_{r,ij} = \sigma \cdot F_{ij} (T_i^2 + T_j^2)(T_i + T_j) \quad (11)$$

where σ = Stephan-Boltzmann constant, $5.67 \times 10^{-8} W/m_2 \cdot K^4$; F_{ij} = the total interchange view factor between surfaces i and j .



3 Comparison with analytical model/experimental data

3.1 Comparison with a simplified analytical model

A simplified case was used for preliminary verification of the computer model where the ground, wall and roof are assumed to be well insulated. No wind, sky radiation, longwave radiation between the dome and outdoor ground, and solar radiation is considered. A simplified mathematical model composed of three nodes, one for the air inside the dome, one for the ground inside the dome, and one for the glazing, is developed:

$$h_{in} A_{dome} (T_s - T_{in}) + h_{in} A_g (T_g - T_{in}) = m_{in} c_{p,in} \frac{dT_{in}}{dt} \quad (12)$$

$$h_r (T_s - T_g) + h_{in} (T_{in} - T_g) = \frac{1}{2} \rho_g dx c_{p,g} \frac{dT_g}{dt} \quad (13)$$

$$h_o (T_o - T_s) + h_{in} (T_{in} - T_s) + h_r (T_g - T_s) = \rho_s d_s \frac{dT_s}{dt} \quad (14)$$

where h_{in} is the convection coefficient over the inside surface of dome; A_{dome} is the area of the dome surface; T_s is the glazing temperature; T_{in} is the air temperature inside the dome; A_g is the area of the ground; T_g is the temperature of the ground surface; m_{in} is the mass of the air inside the dome; $c_{p,in}$ is the specific heat of air; h_r is the radiation coefficient; ρ_g is the density of soil; dx is the thickness of ground layer; $c_{p,g}$ is the specific heat of soil; h_o is the convection coefficient over the outside surface of dome; ρ_s is the density of the glazing; and d_s is the thickness of glazing.

The solution of equations (12-14) is obtained in the MATLAB environment. Initially, all temperatures are assumed to be equal to (-10°C). Then, the outdoor air temperature rises suddenly to 0°C. The variation of air temperature inside the dome under this step change of outdoor air temperature, as estimated by the detailed computer model and by the simplified model, is presented in Figure 2. The results indicate a good agreement between the two models, as the maximum difference is less than 0.7°C. The three temperatures converge to the outdoor air temperature of 0°C after about 17 hours.

3.2 Comparison with experimental data

The simulation results are compared with the experimental data of two cases as presented by Smith [10] (Figure 3 and Figure 4). In the first case, the temperature of dome and of air inside the dome is assumed to be equal to 0°C initially. Then, the outdoor air temperature rises suddenly to 19.25°C. In the second case, the initial temperature is (-4.65°C) and the final temperature is 22.85°C. The simulation results agree well with experimental data.



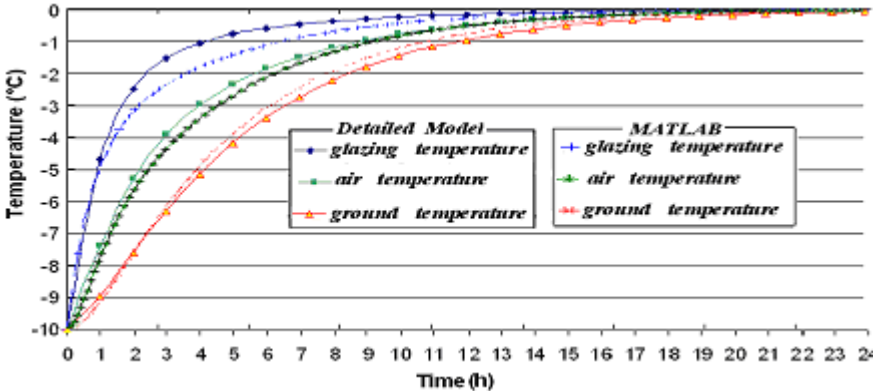


Figure 2: Variation of air temperature inside the dome following a step change of outdoor air temperature from (-10°C) to 0°C. Comparison between the detailed computer model and MATLAB solution to equations (12-14).

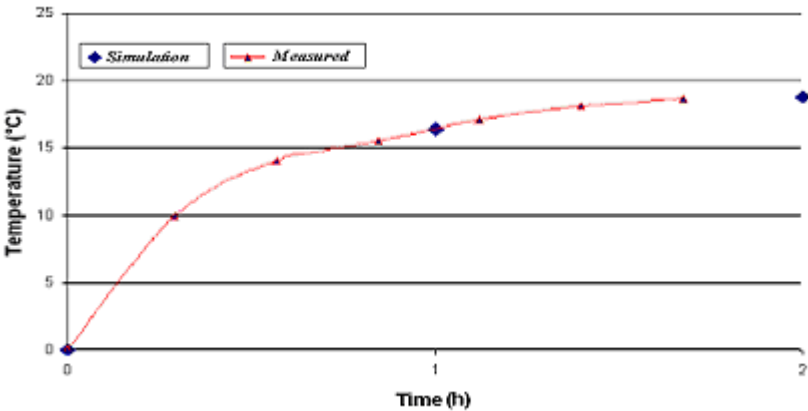


Figure 3: Variation of the glazing temperature following a step change of outdoor air temperature from (0°C) to 19.25°C. Simulated vs. measured [10].

4 Case study

A dome with radius of 20m, built around one house with the following dimensions L = 10m, W = 10m, H = 4m is selected as a case study. The results are compared with a house unprotected by a dome.

The ground surface temperature and air temperature inside the dome, and the heating load of the house on February 21st, are shown in Figures 5 and 6 for the dome-covered house located in Yellowknife (Canada). This city is located at 61°N latitude, has the outdoor design temperature for heating of -38°C and the annual number of heating degree days equal to 8256°C.



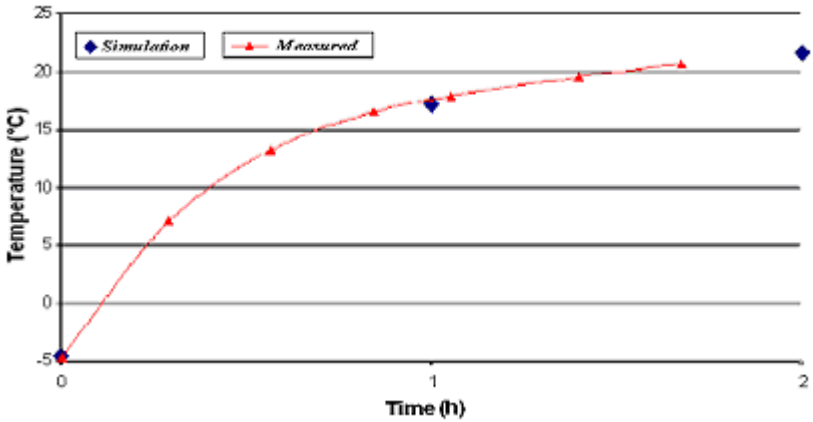


Figure 4: Variation of the glazing temperature following a step change of outdoor air temperature from (-4.65°C) to 22.85°C. Simulated vs. measured [10].

Simulation results show that the air temperature inside the dome can be lower than the outdoor air temperature at night (Figure 5), however, at 14:00 hours the air temperature inside the dome can be 12.4°C higher than the outdoor air temperature. Figure 6 shows a reduction of 34.9% in heating load on February 21st. Table 2 compares the daily heating load of one house without and with a dome cover. It can be seen that during winter season, the dome helps to reduce the daily heating load of the house between 1.1% and 80.1%. The annual average reduction of heating load is 19.1%.

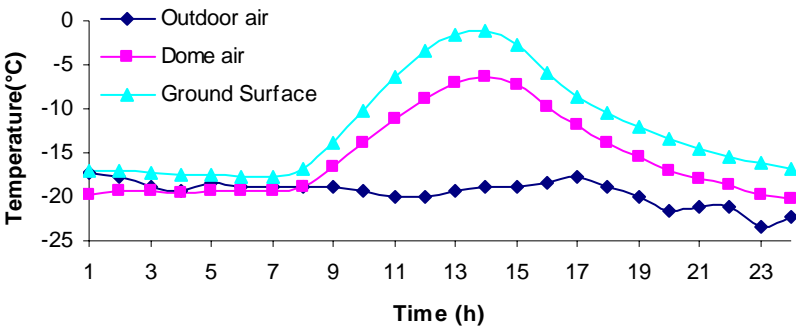


Figure 5: Air and ground temperatures inside the dome on February 21 versus the outdoor air temperature (Yellowknife).

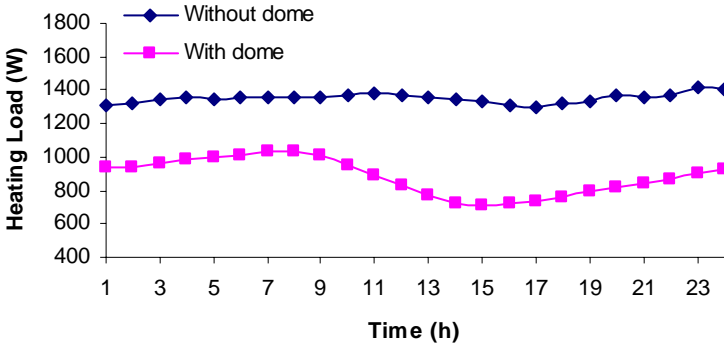


Figure 6: Hourly heating load on February 21 (Yellowknife).

Table 2: Daily heating load of the house, in kWh.

Day	Without dome	With dome	Reduction (%)
Jan. 21	69.9	69.1	1.1
Feb. 21	32.4	21.1	34.9
Mar. 21	29.1	5.8	80.1
Apr. 21	0	0	-
May 21	0	0	-
June 21	0	0	-
July 21	0	0	-
Aug. 21	0	0	-
Sep. 21	0	0	-
Oct. 21	0.14	0	-
Nov. 21	50.2	45.4	9.6
Dec. 21	49.4	45.5	7.9

5 Conclusion

The simulation results predicted a reduction of about 19.1% of the annual heating load of a house when a dome is used compared with the case of an unprotected house. The development of zonal models to simulate the air temperature inside the dome is currently under way.

Acknowledgement

The authors acknowledge the financial support from Natural Sciences and Engineering Research Council of Canada.



References

- [1] Stach E. Form-optimizing processes in biological structures-self-generating structures in nature based on pneumatics. *Design and Nature II*, M.W. Collins & C.A. Brebia (Editors). WIT Press, pp. 3-14, 2004.
- [2] Arslan S. and Sorguc A. G. Similarities between “structures in nature” and “man-made structures”: biomimesis in architecture. *Design and Nature II*, Collins M.W. & Brebia C.A. (Editors). WIT Press, pp. 45-54, 2004.
- [3] Croome, D.J. Covered Northern Township. *International Journal of Ambient Energy*, 6(4): 171-186, 1985.
- [4] <http://www.bfi.org/domes/>.
- [5] <http://www.monolithicdome.com/>.
- [6] IESNA. *Lighting Handbook, Reference and Application Volume*. New York: Illuminating Engineering Society of North America, 2000.
- [7] Wilkinson M. A. Natural Lighting under Translucent Domes. *Lighting Research Technology*, 24 (3), pp. 117-126, 1992.
- [8] Laouadi A. & Atif M.R. Transparent domed Skylights: Optical Model for Predicting Transmittance, Absorptance and Reflectance. *Lighting Research and Technology*, 30(3), pp. 111-118, 1998.
- [9] Laouadi A. & Atif M.R. Predicting optical and thermal characteristics of transparent single-glazed domed Skylights. *ASHRAE Transactions*, 105(2), pp. 325-333, 1999.
- [10] Smith A. M. *Prediction and Measurement of Thermal Exchanges within Pyranometers*. MS Thesis. Virginia Polytechnic Institute, 1999.
- [11] Porta-Gándara M.A. & Gómez-Muñoz V. Solar performance of an electrochromic geodesic dome roof. *Energy*, 30(13), pp. 2474-2486, 2005.
- [12] http://www.eere.energy.gov/buildings/energyplus/cfm/weather_data3.cfm/
- [13] ASHRAE. *ASHRAE Handbook Fundamentals*, Chapter 3, *Heat Transfer*. Atlanta, 1993.
- [14] Yazdanian, M. and Klems, J. Measurement of the Exterior Convective Film Coefficient for Windows in Low-Rise Buildings. *ASHRAE Transactions*, 100(1), pp. 1087-1096, 1994.
- [15] Hottel H.C. and Sarofim A. F. *Radiative Transfer*. McGraw-Hill Book Company, 1967.



Biodegradable building

P. Sassi

Welsh School of Architecture, Cardiff University, Wales, UK

Abstract

Waste minimisation is increasingly being considered as part of a comprehensive approach to sustainable design. Good site practice and procurement systems can realise some reductions in construction and demolition waste, but to significantly reduce waste and create a virtually zero waste building changes in the building design are necessary. To achieve zero waste buildings, inspiration can be drawn and lessons can be learnt from nature. The cyclical characteristic of natural processes, where plants grow, die and biodegrade becoming a resource for new growth, can be applied to building construction. The concept of biodegradable buildings relates to nature at a theoretical level and its implementation in practice can contribute to a comprehensive agenda for sustainable design.

This paper reports on a study of the potential for reducing end of life waste associated with buildings by constructing buildings to be biodegradable, and considers the options for integrating biodegradable materials in mainstream construction. The study compares the end of life waste produced by three building designs including a traditional construction, a mainstream advanced design and a maximum biodegradable design. The results identify possible waste reductions of 85% of non-biodegradable waste measured by weight and 93% measured by volume for the advanced design and 99.6% (weight) and 99.9% (volume) for the maximum biodegradable design compared with the traditional construction. Both designs also achieved overall waste reductions of approximately 70% by weight and 20% by volume. The study concludes that feasible and worthwhile waste reductions can be achieved in mainstream housing construction by designing biodegradable buildings.

Keywords: waste minimisation, biodegradable materials, recycling, natural materials ecological building.



1 Introduction

Designing sustainable buildings involves addressing a broad spectrum of issues. A comprehensive approach to sustainable building design addresses large scale and urban design issues affecting community stability, social well-being and the environment, as well as building-related issues affecting resource use and human and environmental health. Certain sustainable design approaches, such as energy efficiency, are well understood and extensively implemented; others are still at an experimental stage and seldom put in practice. Among the less widely implemented sustainable design approaches is that of minimising construction and demolition (C&D) waste. However, with increasing environmental concerns also this area is now being addressed.

Waste from construction and demolition work constitutes a significant percentage of the total 400 million tonnes of waste produced in England and Wales, which include industry, commerce, household, agricultural and mining wastes, plus sewage sludge and dredged spoils [1]. An estimated 90-120million tonnes of C&D waste per annum are produced in the UK, of which 15-20 million tonnes are thought to be construction waste, the rest is demolition waste [2]. Most of the demolition waste measured by weight is concrete (making up 40%) and masonry (24%). The remaining demolition waste is made up of paper, cardboard, plastic (17%), asphalt (15%), wood based (3%) and other materials (0.6%). Approximately half of the inert waste is used as fill materials in landscaping and road building, as little as 3 million tonnes of the total C&D waste is reclaimed for reuse in the building industry and most of the rest currently goes to landfill [3]. An estimated 16 million tonnes of C&D waste designated for landfill is classified as special waste requiring treatment before being landfilled. Biodegradable waste makes up less than 20% of the total demolition waste and some of it, such as treated timber, is sometimes classified as special waste [4].

Waste is associated with a number of environmental problems. The transport of waste is associated with pollution to air and resource consumption. Waste disposal through landfill is associated with the use of land, which in many densely populated countries is becoming a scarce resource [5], and with pollution to land, water and air [6]. Incineration also generates pollution and contaminated ash, which is generally landfilled.

To reduce the environmental impacts associated with waste both the amount and the pollution potential associated with the waste should be minimised. The Waste hierarchy determined by the EC Framework Directive on Waste (Council Directive 75/442/EEC) sets out waste options in descending order of environmental benefit. Prevention or minimisation of waste is identified as the most preferred waste minimisation solution. This is followed by reuse; recovery, which includes recycling and composting; energy recovery from waste through incineration; and finally disposal through landfill [7].

In respect of building design, prevention or minimisation of waste begins at design stage and can be addressed by making efficient use of building materials through value engineering, but also by only building what is really necessary. In



terms of material selection to minimise waste, inspiration can be drawn and lessons can be learnt from nature. The cyclical characteristic of natural processes, where plants grow, die and biodegrade becoming a resource for new growth, can be applied to building construction. Such a cyclical, or closed loop, system for buildings and their materials could be created through the use of both biodegradable and recyclable materials. In both cases the existence of a closed loop systems is subject to the segregation of waste when it occurs i.e. during the demolition or dismantling of the building, as well as during maintenance work. Biodegradable materials are part of a naturally occurring closed loop cycle. Recyclable materials are part of a closed loop 'man-made' cycle. While the waste hierarchy puts reuse above recycling and composting in respect of reducing the environmental impacts associated with waste, only if a reusable element or material is also biodegradable or recyclable can it form part of closed loop cycle. The reuse of components or materials that are not recyclable or biodegradable may extend their useful life, but they will nonetheless constitute part of a linear system, typically associated with high levels of waste, rather than a cyclical system. To maximise the waste minimisation efforts materials should be both reusable and part of a closed loop cycle [8].

From an environmental point of view closed loop cycles of biodegradable materials are preferable to those of recyclable materials as they generally require fewer reprocessing resources and are associated with less pollution. For example: the embodied energy of imported timber is 3 MJ/kg, a third of that of recycled aluminium estimated at 9.2 MJ/kg (5% of 184 MJ/kg for virgin aluminium) [9]. The 'reprocessing' of timber through natural cycles involves the timber biodegrading. This can produce carbon dioxide through aerobic decomposition or methane through anaerobic decomposition. The resulting compost can replace peat and artificial fertilisers and methane can be used as a fuel. Trees absorb carbon dioxide through their growing period and also provide other benefits such as natural habitats for flora and fauna, soil erosion prevention, environmental cooling and much more. The reprocessing of aluminium, on the other hand, is an industrial process associated with pollution to air albeit reduced compared to the production of new aluminium.

2 Research aims

Reducing waste associated with buildings throughout their lifetime by designing closed loop material system composed of biodegradable materials is not part of mainstream practice. As could be seen from the composition of demolition waste, only a small percentage is biodegradable. Timber, an extensively used biodegradable material, only makes up 3.1% of the total materials used. To increase the use of biodegradable materials in buildings, a broader range of products is required. Furthermore a clear case has to be made for the use of biodegradable materials as an effective approach to waste minimisation.

This study considered the potential for constructing buildings, and in particular mainstream housing, with biodegradable materials as a means of reducing end of life waste associated with buildings demolition and



deconstruction. Currently available biodegradable building materials were identified, including those in common and less common use, and assessed for their appropriateness for use in mainstream housing construction, by comparing their cost, technical performance and aesthetic equivalence to that of standard materials. To quantify the potential for reducing waste through the use of biodegradable materials the construction specification of three different house types was compared to assess the volume of biodegradable and non-biodegradable waste that would be produced at the end of the buildings' life. The designs discussed in section 4 ranged from conventional to highly biodegradable.

3 Biodegradable building materials

Biodegradable - Property of a substance that enables it to be decomposed by microorganisms. The end result of decay is stable, simple compounds (such as water and carbon dioxide). This property has been designed into materials such as plastics to aid refuse disposal and reduce pollution [10].

While biodegradability is often associated with natural materials, as the above definition suggests, man-made materials can also be made to biodegrade. Natural biodegradable building materials have a very long history, but with the advent of synthetic and contemporary materials, biodegradable materials have progressively lost their share of the building industry market. However, increasing environmental concerns have again brought natural materials to the fore as well as pushed the plastics industry to develop biodegradable plastics.

Biodegradable materials can be grouped in four categories: natural materials that can be used following minimal processing (e.g. timber, bamboo); natural materials bonded with a resin or mesh (e.g. sisal carpet, soy boards); natural compounds used in manufacturing products including adhesives and other polymers (e.g. natural protein to manufacture biodegradable plastics); and biodegradable synthetic materials (biodegradable plastics).

3.1 Minimal processing natural biodegradable materials

In contemporary construction, natural biodegradable materials that need minimal processing include timber, straw and bamboo used for structural purposes; straw, cork, flax, hemp and sheep's wool insulation; cork floor and wall finishing; bamboo and timber rigid floor finishes; timber and thatch timber roofing finishes; and timber fixtures and fittings, including bathtubs and sinks.

3.2 Bonded biodegradable materials

Examples of bonded biodegradable materials include mixtures of hemp or straw and clay used to infill external wall frames; straw bonded between two layers of kraft paper to form non-loadbearing internal partitions; timber, straw and soy finishing or structural boards; jute carpet backing and wall coverings; seagrass, sisal, coir, cotton, paper and wool carpeting; cork mixed with wood flour, powdered limestone, linseed oil and natural resin to make linoleum. Natural fibres have been shown to have equivalent performance characteristic to



synthetic fibres, [11] and their use in concrete and cement products has generated great interest in the research community [12]. However, bonding a biodegradable material with a non-biodegradable material, such as concrete or cement will compromise overall biodegradability. Similarly effects may occur when including additives to improve the performance of building products. For example some insulation products made with natural and polyester fibre mixed are unsuitable for composting, but equally inappropriate for landfilling due to the large percentage of organic matter [13]. Some bonding mediums, such as the kraft paper in straw walls or the natural resins in hardboards are themselves biodegradable, others are not. To maximising the biodegradability of building products natural fibres should be bonded with the biodegradable naturally derived high performance plastic resins, as discussed in the next paragraph.

3.3 Natural biodegradable plastics

Biodegradable plastics, which include adhesives and resins, can be made from naturally occurring polymers such as cellulose, starch, protein, and sugar molasses extracted from plants. Historically natural adhesives, such as potato and rye flour starch, soya protein and natural rubber have been used very successfully, and while still in use are now largely superseded by higher performance synthetic glues [14]. Research is now focussing on manufacturing natural and biodegradable plastics with performance characteristics equivalent to synthetic options. Corn zein, wheat gluten, soy protein, and peanut protein have been investigated for potential uses. New building products made in this way are not yet available, but industries such as the paper and colouring industry are beginning to replace synthetic polymers with natural ones [15]. The packaging industry is also making use of natural plastics for food packaging and protective mouldings. The use of expanded starch packaging is already relatively widespread and could be introduced to building industry [16].

3.4 Synthetic biodegradable plastics

Petroleum-based plastics, mainly polyolefins such as LDPE in, LLDPE, can now be modified with additives to be made biodegradable and able to be converted through digestive activity of microorganisms into water and carbon dioxide [17]. Current uses include biodegradable waste bags. Building products made with synthetic biodegradable plastics are unlikely to be developed for the time being, due to the higher manufacturing costs, but could be developed in future.

3.5 Technical aspects of ensuring biodegradability

To ensure that material integrated into a building can be biodegraded at the end of the building's useful life, the building elements' installations in the building as well as their material characteristics have to be considered.



3.5.1 Building element installation and deconstruction

As with any form of closed loop material cycle, being able to recover different materials separately is essential to enable their composting or recycling. Demolition is therefore an unsatisfactory end of life disposal approach as it results in a mixture of different waste types, which are time-consuming and costly, if not impossible, to separate. Deconstruction, on the other hand, enables the segregation of waste types. For buildings that are 100% biodegradable separating waste would not be necessary, but as becomes evident later, in mainstream construction 100% biodegradability is unrealistic at the moment.

To facilitate the deconstruction, building elements should be mechanically fixed, preferably with few fixings; easily accessible; easily handled with minimal associated health hazards; and able to be deconstructed using simple tools and with minimal additional information [18, 19].

3.5.2 Building element components

To be suitable for composting, a material recovered from the dismantling of a building must also be as pure as possible. As discussed in section 3.2 a careful analysis of the constituent parts of a predominantly biodegradable material is necessary to establish whether it is in fact biodegradable. Treatments, as well as additives, can hamper the biodegrading process by slowing down the process and creating a non-biodegradable residue, which, as with some timber treatments, may also be toxic. Treatment may, however, be essential in improving the product durability and further development of safe treatments could contribute to creating more biodegradable buildings.

To maximise biodegradability in practice materials may also need to be identified as being biodegradable. Awareness of the biodegradability of materials such as timber is widespread, but knowledge of new plant-based boards and biodegradable plastics is limited. Furthermore some biodegradable materials cannot be visually distinguished from their non-biodegradable counterparts. In this respect, a tagging system, as used in the plastics recycling industry, and a comprehensive account of the materials installed may prove essential.

4 The use of biodegradable materials in practice

Mainstream construction makes little use of biodegradable materials. The main mainstream biodegradable material used is timber and even this material may be rendered non-biodegradable by the way it is installed. The increase in use of synthetic adhesives to fix skirting or bond floor finishes to a substrate can make the building element and the substrate non-biodegradable. Yet, there is currently a good selection of materials that are biodegradable and can be installed in a way to retain this characteristic.

To assess the waste reduction potential of biodegradable buildings, this study compared the amount of biodegradable and non-biodegradable waste that would be produced at the end of the life of three different specifications for a typical three bedroom detached two storey house. The three house plans and their thermal performance are identical. The structure, in view of the government drive for prefabrication, is timber in all three cases, but other elements vary. The



material specifications for House 1 and 2 are based on completed projects studied by the author [20]. House 1 comprised materials typically used by UK housing developers and is based on the 21st Century homes in Aylesbury by Briffa Phillips Architects for Hightown Preatorian Housing Association. House 2 is a mainstream advanced design and comprised commercially available biodegradable materials keeping in line with current aesthetic expectations and is based on the Toll House Gardens in the Fairfield estate, Perth, Scotland, by Gaia Architects for Fairfield Housing Co-operative. House 3 maximises the use of biodegradable materials choosing where possible but not limiting the choice to the most commercially realistic materials. All three house structures were detailed and the volume and weight of the materials included in the buildings were measured. Services and fixtures and fittings were not included in the assessment. The materials compared and used in the model specification are identified in Table 2. When assessing the biodegradability of the materials specified the following three issues were considered.

1. Constituent materials of building elements.
2. Finishes and treatments that may compromise biodegradability.
3. Fixing methods that would compromise biodegradability.

The main differences in the house types include:

1. House 1 has a concrete ground floor bearing slab, while House 2 and 3 have suspended floors and House 3 includes timber piles.
2. The external cladding material in House 3 is timber, while House also has brick and House 2 render elements.
3. The internal finishes in House 1 and 2 are applied (skim finish to plasterboard), while in House 3 mechanically fixed self-finished products are used.

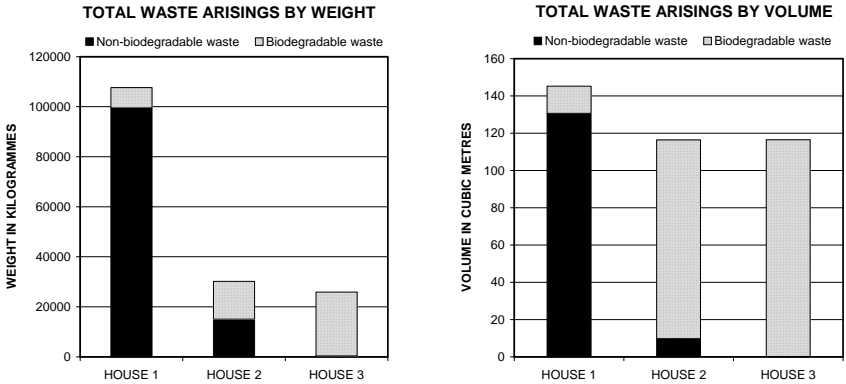
Table 1.

WASTE ARISING	measured by weight (kg)			measured by volume (m ³)		
	House 1	House 2	House 3	House 1	House 2	House 3
non-biodegradable	99501	15076	355	131	10	0.2
	92.5%	50.0%	1.4%	90.0%	8.4%	0.1%
biodegradable	8111	15090	25522	15	107	116
	7.5%	50.0%	98.6%	10.0%	91.6%	99.9%
TOTAL WASTE	107612	30166	25877	145	116	117

4.1 Waste reductions achieved

House 1 design resulted in 99.5 tonnes of non-biodegradable waste and 8 tonnes of biodegradable waste. House 2 design resulted in 85% reduction of non-biodegradable waste measured by weight and 93% reduction by volume compared with House 1. The biodegradable waste increased, but the overall waste was reduced by 72% by weight and 20% by volume. House 3 design resulted in 99.6% reduction of non-biodegradable waste by weight and 99.9% reduction by volume compared with House 1. Total waste was reduced by 76% by weight and 20% by volume. Table 1 and Figures 1 and 2 show the amount and percentage of biodegradable and non-biodegradable waste for each option.





Figures 1 and 2: Waste arisings by weight and by volume.

Table 2.

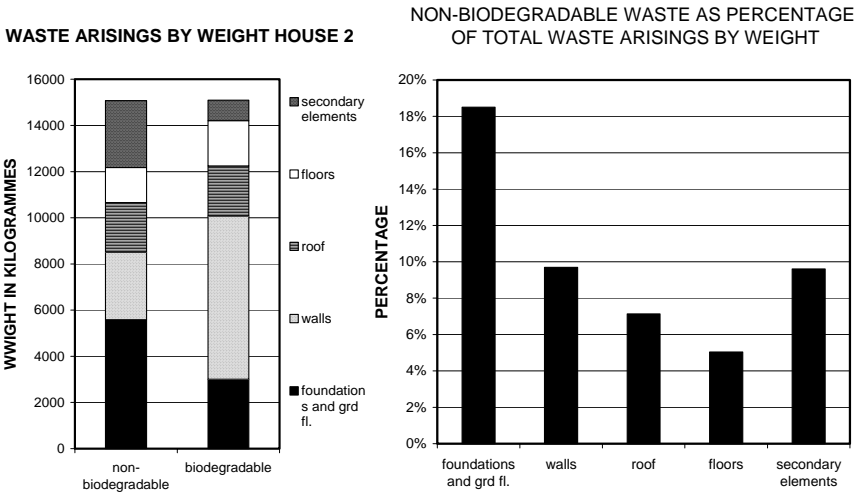
Specification comparison for house types 1, 2 and 3 and assessment of biodegradable option			Cost equivalence	Technical performance	Aesthetic conformity	Mainstream acceptance
Building elements	Non-biodegradable material	Biodegradable building material options				
Foundations	Concrete ①②	timber③	◐	○	◐	○
Frame		timber①②③	●	●	●	●
Insulation below ground	Expanded polystyrene①					
Insulation between studs	Rockwool①	Recycled cellulose fibre (Warmcell) ②③	◐	●	●	●
External insulation	polyurethane①	Wood fibre insulation (Diffutherm) ②	◐	◐	●	●
Wall panel lining	OSB ①	Hardboard (Paneline /Panelvent)②③	◐	●	●	●
Vapour control	PE① / ②					
External cladding	Brick① Render②	Timber①②③	●	●	●	●
Roof finishes	Concrete Tiles① Slates②	Timber③	◐	◐	●	◐
Rainwater goods	PVC① Metal②	Timber ③	○	○	◐	○
Windows doors		Timber①	●	●	●	●
Floor panel lining	Chipboard ①	Timber ②③	◐	●	●	●
Internal wall & ceiling finishes	Plasterboard①②	Ply with natural glues ③	○	●	◐	◐
Floor finishes	Carpet① Vinyl①	Timber③②	●	●	●	●
	Ceramic tiles ②	Cork③	◐	◐	●	●



4.2 Barriers and opportunities to maximising biodegradable materials

The main sources of non-biodegradable waste can be identified by analysing the amount of non-biodegradable waste resulting from House 2 option, designed to maximise biodegradable waste with a design suitable for mainstream construction. As shown in Figure 4, non-biodegradable waste from foundations and the ground floor makes up 19% of the total waste. This can be accounted for by the use of concrete in the foundations and represents the biggest barrier to creating mainstream biodegradable houses. House 3 makes use of timber foundations, but this approach, due to the limited durability of timber foundations, is inappropriate for mainstream construction. A potential environmental improvement would be to use prefabricated concrete foundations that can be reused and recycled.

A second significant source of non-biodegradable waste is plasterboard, accounted for in the construction of the walls and roof. House 3 replaces plasterboard with ply bonded with natural glue, other biodegradable finishes would include timber boarding or cork, but none of these at the moment are acceptable by the general public, who expects smooth plastered walls. The performance of all the alternatives is equivalent to that of plasterboard and it is a perception barrier that prevents any deviation from the use of plastered finishes.



Figures 3 and 4: House 2 waste analysis.

In House 1 the potential for biodegrading the timber structure, which is generally very easily dismantled and can be biodegraded, was reduced in comparison to House 2 by the use of adhesive fixings for floor finishes and skirting.

Two small but difficult to overcome sources of non-biodegradable waste identified are glass and metal fixings. In House 3 this represented a very small amount of waste: 1.4% by weight and less than 1% by volume. Both materials are

however recyclable. Other similarly difficult products not covered by this study include electrical wiring, second fix electrical goods (e.g. socket outlets, switches), water supply and disposal, which are now generally made of non-biodegradable plastics. Here too metal alternatives exist. It is perhaps to replace these types of products that research into biodegradable plastics would be worthwhile.

5 Disposal of biodegradable materials

To realise the waste minimisation advantages of using biodegradable materials a number of issues have to be addressed. These include technical aspects of building design and materials specification, as discussed in section 3.5; the facilities for and infrastructure associated with waste composting; and the economic barriers and incentives for environmentally friendly waste disposal options.

5.1 Facilities and infrastructure for waste composting

Currently composting at a municipal level treats mainly plant waste. Even the composting of domestic waste can be seen as problematic due to potential contaminants. A 1992 review of waste management options identified the potential for composting but also a distinct lack of facilities [21]. A 2003 review highlighted a lack of progress in this field [22] and for composting to be applied on a large scale to be able to deal with building waste a fundamental change in the government's approach to waste disposal would be necessary.

5.2 Economic barriers and incentives for environmentally friendly waste disposal options.

In addition to adequate facilities the economics of composting needs to be convincing. In their 2001 report on the Landfill Tax, *Resource productivity, waste minimisation and the landfill tax*, the ACBE concludes that while the Landfill Tax has had some success at increasing the amount of inert waste recycled on site, it has had little success at reducing waste taxed at standard rates and increasing recycling. The report recommends an increase of the tax in line with other European countries, which benefit from far higher recycling rates [23].

While in the UK waste minimisation within the construction industry can prove cost-effective. A comprehensive approach to waste minimisation that includes reduced disposal costs of segregated waste as well as reduced costs associated with new material purchase, delivery and handling can save the house building industry as much as £1400 per house unit [24]. But when it comes to selecting a disposal method, composting is the most expensive, with the combined collection & gate cost per tonne of £42-£103 comparing poorly with landfill (£19-£29), incineration (£30-£40), paper and board recycling (£19-£25), plastics recycling (£2 £5), not to mention recycling of aluminium where a tonne of waste is worth £411- £338 [25].



6 Conclusion

Numerous barriers exist to creating a building industry that makes use of biodegradable materials and composting as a means of reducing the end of life building waste. Nonetheless, the study identified potential for significant reductions in non-biodegradable waste through the use of biodegradable materials. It also concludes that constructing a virtually 100% biodegradable building is technically possible and implementing such technologies into mainstream construction is to some extent feasible.

To bring biodegradable buildings into mainstream construction more research is required in material sciences to bring down costs and reassure buyers of the materials' performance. Also an attitude change is needed. Currently there is a perception barrier: natural materials are sometimes associated with old fashion and backwards. But as the culture that views humans as stewards of the environment spreads and is reinforced by the trends of downshifting, back to nature and even slow food, people's perception will change in favour of natural materials making biodegradable mainstream building possible.

It is worth noting that natural biodegradable materials are also associated with other benefits such as creating healthy living environment and providing a low embodied energy structure with a low overall ecological footprint. Biodegradable plant-based materials can also prove cost-effective and particularly in developing countries have the potential to make a significant contribution towards providing low cost housing.

Perhaps a realistic approach to achieve the overall aim to bring closed material cycle building into mainstream construction is to use a combination of both recyclable and biodegradable materials.

References

- [1] Department of the Environment, Transport and the Regions, *Waste Strategy 2000: England and Wales (Part 1)*, DETR: London, pp9, May 2000.
- [2] Building Research Establishment, *Construction and Demolition waste Report GBG 57 Part I and II*, BRE: Watford, pp1, 2003.
- [3] McGrath et al., *UK Deconstruction Report, Overview of Deconstruction in Selected Countries. CIB Publication 252, Proceedings of CIB Task Group 39*, Construction Industry Board: Florida, pp159-160, 2000.
- [4] Department of the Environment, Transport and the Regions, *Waste Strategy 2000: England and Wales (Part 2)*, DETR: London, pp117, May 2000.
- [5] Advisory Committee on Business & the Environment (ACBE), *Resource productivity, waste minimisation and the landfill tax*, pp1, August 2001
- [6] Implementation of Council Directive 1999/31/EC on The Landfill of Waste: Second Consultation Paper p53
- [7] Department of the Environment, Transport and the Regions, *Waste Strategy 2000: England and Wales (Part 2)*, DETR: London, May 2000.



- [8] Sassi, P. 'Designing buildings to close the material resource loop', *Proceedings of the Institution of Civil Engineers, Engineering Sustainability* 157, Issue ES3, pp163-171, 2004
- [9] Berge, J., *The Ecology of Building Materials*, Oxford: Architectural Press, pp20-24, 2000
- [10] *World Encyclopedia. Philip's, 2005. Oxford Reference Online.* Oxford University Press. Cardiff University. 20 January 2006 <http://www.oxfordreference.com/views/ENTRY.html?subview=Main&entry=t105.e1302>
- [11] Wambua et al, 2003. "Natural Fibres: can they replace glass in fibre reinforced plastics?", *Composites Science and Technology*, vol 63, pp 1259-1264
- [12] Sorbal, H.S. ed., 'Vegetable Plants and their Fibres as Building Materials', *Proceedings of the second International RILEM and CIB Symposium*, Brazil September 1990, London: Chapman Hall, 1990
- [13] Cripps et al. *Crops in construction handbook CIRIA C614* London: CIRIA pp34 Nov 2004].
- [14] Berge B, *The Ecology of building materials*, Architectural Press: Oxford, pp391-399, 2000.
- [15] Swain et al., 'Biodegradable Soy-Based Plastics: Opportunities and Challenges', *Journal of Polymers and the Environment*, Vol. 12, No. 1, pp35-42 January 2004
- [16] Cripps et al. *Crops in construction handbook CIRIA C614* London: CIRIA pp102 Nov 2004].
- [17] Swain et al., 'Biodegradable Soy-Based Plastics: Opportunities and Challenges', *Journal of Polymers and the Environment*, Vol. 12, No. 1, pp35-42 January 2004
- [18] Addis, W., Schouten J. *Principles of design for deconstruction to facilitate reuse and recycling CIRIA 608* CIRIA: London pp19-29, 2004
- [19] Sassi P, Summary of study on the suitability for designing for recycling and designing for durability, *Proceedings of SB200, International Conference Sustainable Building 2000*, Maastricht, Oct 2000
- [20] Sassi P *Strategies for Sustainable Architecture*, London: Taylor Francis, 2006
- [21] Department of Trade and Industry, Waste Management Paper No1 A review of Options, London: DETR pp30-34 1992
- [22] Environment, Food and Rural Affairs Committee, The Future of Waste Management, London: EFRA, pp24-25 2003
- [23] Advisory Committee on Business & the Environment (ACBE), *Resource productivity, waste minimisation and the landfill tax*, ACBE, pp4, 2001
- [24] Construction and demolition waste BRE2003 GBG57-1, Building Research Establishment, pp2, 2003
- [25] Advisory Committee on Business & the Environment, *Resource productivity, waste minimisation and the landfill tax*, ACBE, pp20, 2001



Section 3

Biomimetics

This page intentionally left blank

Self-healing processes in nature and engineering: self-repairing biomimetic membranes for pneumatic structures

T. Speck^{1,2}, R. Luchsinger³, S. Busch¹, M. Rüggeberg¹
& O. Speck^{1,2}

¹*Botanic Garden, University of Freiburg, Freiburg, Germany*

²*Competence Networks Biomimetics and BIOKON*

³*Prospective Concepts ag, Glattbrugg, Switzerland*

Abstract

Self-repairing processes in plants sealing fissures caused by natural growth processes (e.g. in the vine *Aristolochia macrophylla*) or by artificial injuries (e.g. in the common bean *Phaseolus vulgaris*) serve as concept generators for the development of a biomimetic coating for membranes of pneumatic structures based on the Tensairity[®] concept. First results with foam-based biomimetic self-repairing coatings for technical membranes are very promising. For lesions with nails of up to 5mm diameter, reductions of the air-leakage of two to three orders of magnitude could be achieved.

Keywords: self-healing, vines, biomimetics, self-repairing membranes, pneumatic structures, Tensairity[®].

1 Introduction

Over the last two decades, plants have proved to be a real treasure trove as models for the construction of biomimetic technical structures and materials [1, 2]. One example are self-healing processes which are very common in nature. Self-repair is still uncommon in technical products but especially over the last few years some interesting solutions for special applications have been presented [3–7]. Plants have evolved an amazing capacity to seal and mend internal fissures caused by growth processes and wounds effected by artificial external injuries. For analytically describing the (fast) self-repair characteristics of the



parenchyma, vine (e.g. *Aristolochia*) and herbaceous plants (e.g. *Phaseolus*, *Ricinus*) are used as model organisms. These plants react to fissures and ruptures in their peripheral tissues by a rapid repair mechanism, which seals the lesion very effectively and secures the functional integrity of the plant stem.

2 Biological templates

Vines of the genus *Aristolochia* proved to be especially suitable models for quantitatively studying self-repair processes caused by internal secondary growth as they exhibit very efficient rapid repair mechanisms in their stems. The Dutchman's Pipe (*Aristolochia macroplylla*) was chosen as model species as stem mechanics and functional anatomy of this species were extensively examined during the last years [8]. In young, one year old stem parts, this plant possesses a closed ring of sclerenchyma fibres in the stem periphery, fig. 1A.

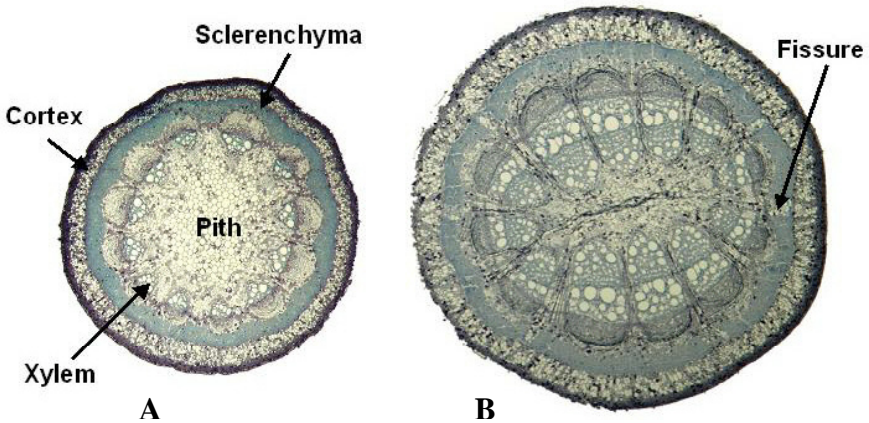


Figure 1: Cross-sections of stems of the vine *Aristolochia macroplylla*. (A) Tissue distribution in a one year old stem with closed peripheral ring of lignified strengthening tissue (sclerenchyma fibres). (B) As a consequence of secondary growth a two year old stem shows an increase in the amount of vascular tissues (especially of xylem) and a segmentation of the peripheral sclerenchymatous ring.

This tissue causes the high bending stiffness found in young *Aristolochia* stems. When the stems become older, secondary growth processes occur, and the vascular tissues - phloem and especially xylem (wood) both located inside of the sclerenchymatous ring - significantly increase in size. Secondary growth of the vascular tissues causes radial stresses and strains in the soft parenchymatous tissues located between the vascular tissues and the sclerenchymatous ring and tangential stresses and strains in the sclerenchymatous ring. When the stresses

and strain more and more increase due to continuous secondary growth, the sclerenchymatous ring finally ruptures and splits into segments, fig. 1B. The fissures typically run through the middle lamellas of neighbouring sclerenchyma cells [9]. *A. macrophylla* seals these lesions very effectively by a rapid repair mechanism and secures the functional integrity of the plant structure.

The repair process can be subdivided in at least four phases. The first phase (on which we concentrate in our biomimetic approach) is based on fast strain-triggered deformation processes of pressurized parenchyma cells that swell into the fissure and seal it, fig. 2A. We hypothesize, that this first phase of fissure repair is mainly caused by viscoelastic-plastic deformation of the internally pressurised (turgescient) parenchyma cells. In how far cell wall mechanics in a second phase of fissure repair are changed due to a process of hydroxyl-radical induced cell wall loosening ('plastification'), recently described for growing cells [10, 11], is subject of ongoing projects. In the third phase of repair when the fissure extends deeply into the sclerenchymatous ring, the repairing cells start to divide mainly tangentially. Later in this phase the fissure runs through the sclerenchyma ring, and the repairing cells show significant radial and tangential cell division, fig. 2B. In some fissures the repairing cells may remain entirely parenchymatous. In other fissures a fourth phase can be discerned in which the walls of the most peripheral sealing cells increase in thickness and start to lignify, fig. 2C. Through this the mechanical function of the sclerenchyma ring can be – at least – temporarily restored.

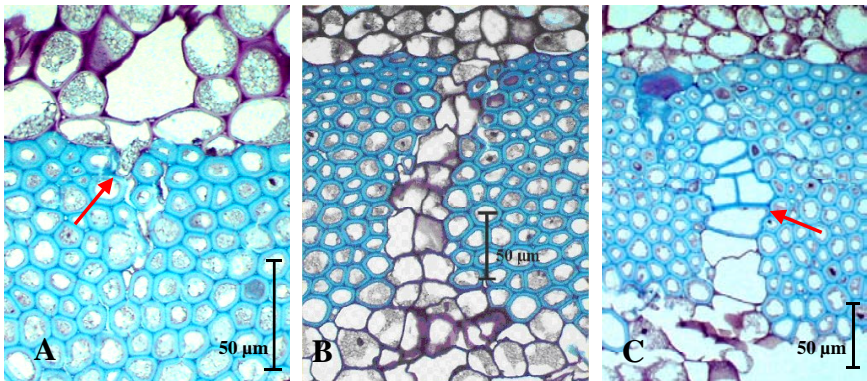


Figure 2: Fissure repair in the vine *Aristolochia macrophylla*. (A) An adjacent parenchyma cell expands into a small fissure in the sclerenchymatous ring (phase I), see arrow. (B) A broad fissure in the sclerenchyma ring is sealed by parenchymatous repairing cells having the typical irregular shape (phase III). (C) The walls of peripheral repair cells are thickened and lignified (phase IV).

Cell shape and cell wall thickness differ remarkably between 'normal' parenchyma cells of the cortex and parenchymatous repairing cells sealing fissures in the sclerenchyma ring. 'Normal' parenchyma cells are round/elliptical



in cross-section, whereas repairing cells typically possess an irregularly shaped cross-section, allowing a tight sealing of the fissure. Additionally, during the initial phases of fissure repair the cell walls of sealing parenchyma cells become significantly thinner, fig. 2A-B. As a measure of cell shape the ratio of perimeter to cross-sectional area (P/A) was used. For the initial phases of fissure repair preliminary analyses indicate an increase of P/A by a factor of 1.4 from $161 \pm 39 \text{ mm}^{-1}$ for 'normal' parenchyma cells to $229 \pm 130 \text{ mm}^{-1}$ for fissure-sealing cells. At the same time cell wall thickness decreases by a factor of 1.4 from $1.18 \pm 0.22 \text{ }\mu\text{m}$ for 'normal' parenchyma cells to $0.87 \pm 0.37 \text{ }\mu\text{m}$ for fissure sealing cells. The most parsimonious explanation is that the cross-sectional area (and the volume) of individual cells remains constant (i.e. no cell wall biosynthesis takes place) when the cells change in shape in the first phase of fissure repair. In this case both factors are expected to be nearly identical, since the existing cell wall material is merely rearranged. For a more detailed discussion of this phenomenon we refer to Speck et al. [9]. We suggest that the initial phases of fissure repair take place without cell division and (significant) cell wall biosynthesis, but involve mainly physical-chemical reactions of the parenchyma cells to a perturbation of the local stress-strain-field caused by the lesion. This result is encouraging for a transfer of this fast repair mechanism into biomimetic solutions for technical applications.

Similar processes as described in *Aristolochia macrophylla* for fissures caused by growth processes are found in the hypocotyls of herbaceous plants (e.g. *Phaseolus*, *Ricinus*, *Helianthus*) during the (fast) self-repair taking place as a reaction to wounds effected by artificial external injuries, fig. 3.

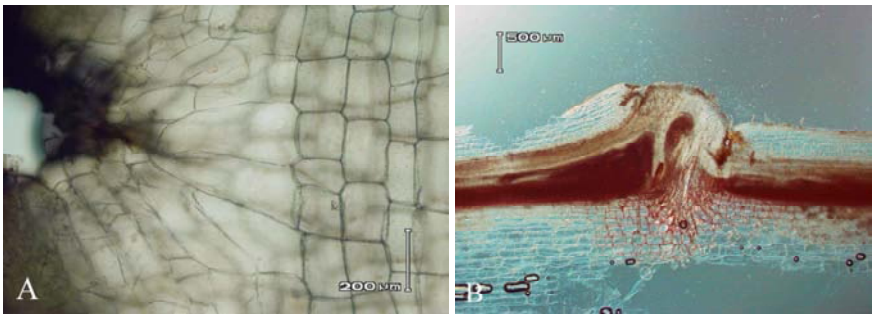


Figure 3: Fissure repair after an artificial external injury in Common Bean (*Phaseolus vulgaris*). (A) Early phase of self-repair, parenchyma cells expand into the artificial injury. (B) Late phase of self-repair, the lesion is entirely sealed by a callus of newly formed thickened (often lignified) repair tissue.

3 Technical applications

In cooperation with the Swiss company prospective concepts ag, biomimetically inspired self-repair functions are transferred into technical membranes of ultra-



light pressurized beams based on the Tensairity® concept. This technology represents a combination of cylindrical membranes filled with compressed air under moderate overpressure and supporting struts and cables, fig. 4. This technology yields ultra-light deployable structures as strong as steel [12–15].

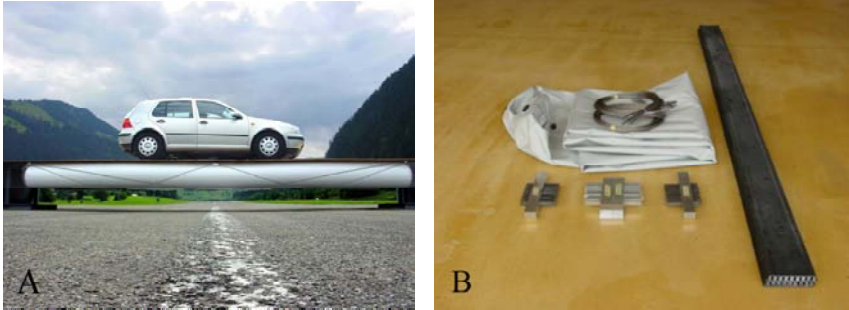


Figure 4: (A) Tensairity® demonstration bridge with 8 m span and 3.5 tons maximal load. (B) Components of the Tensairity® demonstration bridge showing the non-inflated cylindrical membrane

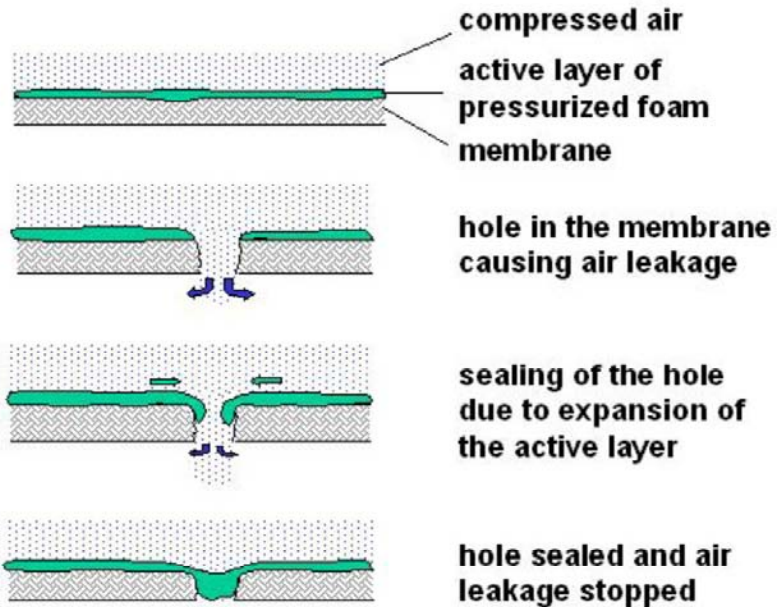


Figure 5: Functional model for a self-repairing technical membrane.

One shortcoming of all pneumatic structures is the vulnerability of the membrane to tearing and puncturing which cause a drop in the internal pressure



and a subsequent reduction of the load-carrying capacity of the beams. Tensairity® technology is much less jeopardised by holes than other (high pressure) pneumatic structures as the air beam mainly acts as distance piece to prevent the buckling of compression elements. The main load bearing elements are the cables and compression struts. Tensairity® technology works with moderate overpressure in the range of 50 to 500 mbar and compressors or fans are used to adjust the internal pressure to variable environmental conditions. Because of the moderate overpressure, the compressors or fans can also cope with air leakage due to small holes. Nevertheless a self-repairing function will significantly improve the market prospects of this new technology.

In order to transfer ideas based on the first phase of fast self-repair in plants into a biomimetic ‘self-healing’ membrane for Tensairity® beams a functional model was developed, fig. 5. The basic idea is to develop a ‘foamy’ layer made of a pressurized cellular technical material that biomimicks the self-repair mechanism in plants. This biomimetic material is used as an inner coating of the membrane and if the membrane is punctured, the foamy repair layer seals the hole as the foam cells – like the parenchyma cells in the biological template – expand into the hole due to their internal pressure and to surface tension effects occurring in the prestrained foam. In a first approach polyurethane-foam was used for the biomimetic coating of the self-repairing membrane.

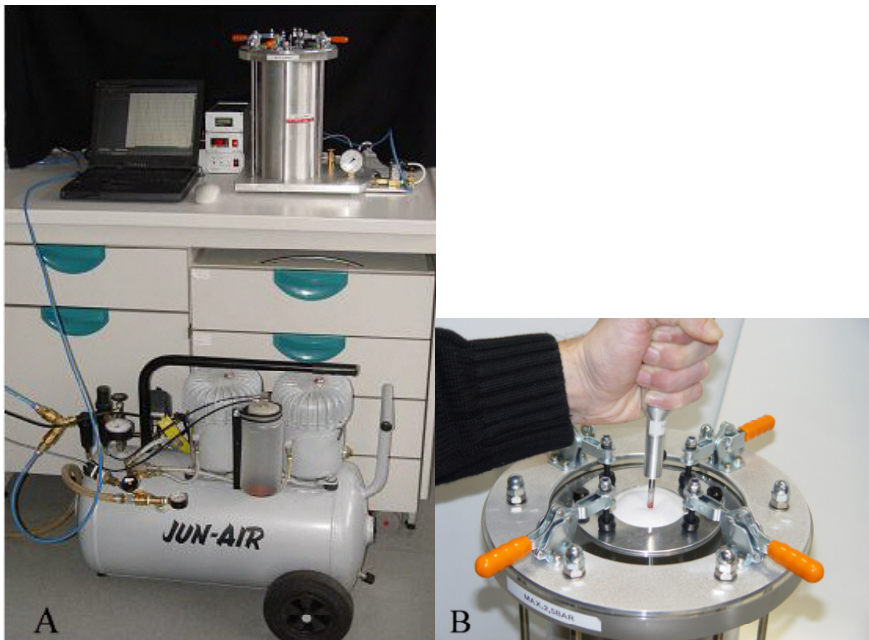


Figure 6: (A) Experimental set-up for testing the self-repair quality of coated membranes. (B) Puncturing of a coated membrane with a nail of 5 mm diameter.

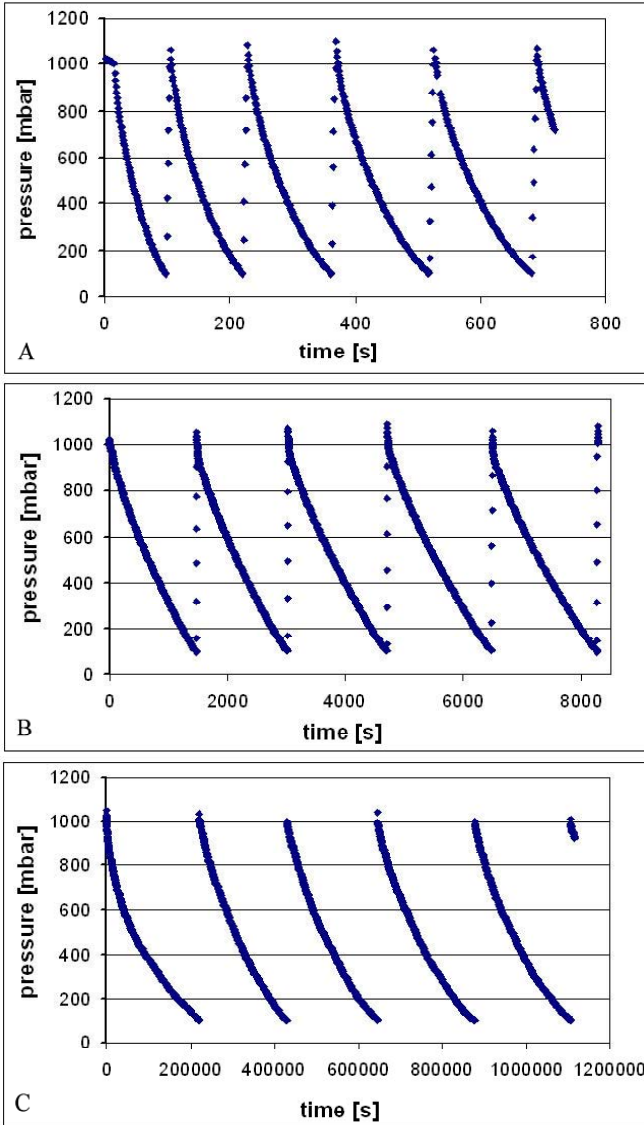


Figure 7: Graphs showing the duration of pressure drop from 1000 mbar to 100 mbar for membranes punctured with a nail of 2.6 mm diameter. (A) Uncoated membrane; mean duration of pressure drop: 130 seconds. (B) Membrane coated with a biomimetic foam polymerised under ambient pressure; air-leakage reduced by about one order of magnitude. (C) Membrane coated with a biomimetic foam polymerised under overpressure; air-leakage reduced by three orders of magnitude.



In order to test the self-repair quality of different biomimetic coatings an experimental set-up was developed that allows to measuring how long a defined pressure drop takes for specific types of lesions in uncoated and coated membranes. The ratio of duration in a coated membrane over duration in an uncoated membrane was defined as repair factor. As higher the repair factor is as better the self-repair function of a given coating is. The experimental set-up consists of a pressure cylinder in which membranes with and without coating can be clamped, fig. 6.

The overpressure is maintained by means of a supercharger. The set-up is computer controlled as well as to the execution of the tests as to data storage. We have chosen a test protocol in which the cylinder is pressurized up to 1000 mbar and the time is measured until the pressure is dropped down to 100 mbar. When the upper pressure limit is reached the control programme automatically switches off the supercharger, when the lower limit is reached the supercharger is switched on. This allows consecutive measurements of the duration of the predefined pressure drop for a given type of lesion and membrane coating.

Pilot studies with self-repairing foam-based biomimetic membrane coatings have produced highly promising results. These biomimetic coatings are able to reduce significantly the air-leakage of the pneumatic structure after puncturing of the membrane by nails of up to 5 mm diameter. With biomimetic coatings based on polyurethane foam polymerised under ambient pressure air-leakage can be reduced by about one order of magnitude, i.e. repair factors of 10 are found. With biomimetic foam based coatings polymerised under overpressure air-leakage can be reduced by two to three orders of magnitude, fig. 7.

Technical applications of self-repairing processes inspired by biological templates are obviously not limited to the application to Tensairity® structures or other pneumatic structures but can be realised with other types of biomimetic self-repairing materials for many applications in industry, clothing and medical technology.

Acknowledgements

The project was supported by the Ministerium für Wissenschaft, Forschung und Kunst des Landes Baden-Württemberg within the framework of the Kompetenznetz, Pflanzen als Ideengeber für die Entwicklung biomimetischer Materialien und Technologien' and by the INTERREG III Programm (BioValley).

References

- [1] Speck, T. & Spatz, H-Ch., Transkription oder Translation: Pflanzen als Ideengeber für neue Materialien und technische Leichtbaustrukturen. *BIONIK - Ökologische Technik nach dem Vorbild der Natur*, ed. A. von Gleich, Teubner-Verlag: Stuttgart, 2. ed., pp. 229–245, 2001.



- [2] Speck, T. & Neinhuis, C., Bionik, Biomimetik – ein interdisziplinäres Forschungsgebiet mit Zukunftspotential. *Naturwissenschaftliche Rundschau*, **57(4)**, pp. 177–191, 2004.
- [3] Gerl, B. & Sterbak, R., Eine tragende Rolle: Ein ausgeklügelter Materialmix hält Fahrzeuge sicher in der Spur. *Spektrum der Wissenschaft*, **1**, pp. 42–43, 2005.
- [4] White, S.R., Sottos, N.R., Geubelle, P.H., Moore, J.S., Kessler, M.R., Sriram, S.R., Brown, E.N. & Viswanathan, S., Autonomic healing of polymer composites. *Nature*, **409**, pp. 794–797, 2001.
- [5] Kessler, M.K., Sottos, N.R. & White, S.R., Self-healing structural composite material. *Composites Part A: Applied Science and Manufacturing*, **34**, pp. 743–753, 2003.
- [6] Pang I.W.C. & Bond I.P., ‘Bleeding composites’ – Damage detection and self-repair using a biomimetic approach. *Composites Part A: Applied Science and Manufacturing*, **36**, pp. 183–188, 2004.
- [7] Pang, J. & Bond, I.P., A hollow fibre reinforced polymer composite encompassing self-healing and enhanced damage visibility. *Composites Science and Technology*, **65**, 1791–1799, 2005.
- [8] Speck, T., Rowe, N.P., Civeyrel, L., Claßen-Bockhoff, R., Neinhuis, C. & Spatz, H.-Ch., The potential of plant biomechanics in functional biology and systematics. *Deep Morphology: Toward a Renaissance of Morphology in Plant Systematics*, eds. T. Stuessy F. Hörandl & V. Mayer V., Koeltz: Königstein, pp. 241–271, 2004.
- [9] Speck, T., Masselter, T., Prüm, B., Speck, O., Luchsinger, R. & Fink, S., Plants as concept generators for biomimetically technical light-weight structures with variable stiffness and self-repair mechanism. *Journal of Bionics Engineering*, **1(4)**, pp. 199–205, 2004.
- [10] Schopfer, P., Hydroxyl radical-induced cell-wall loosening in vitro and in vivo: implications for the control of elongation growth. *The Plant Journal*, **28**, pp. 679–688, 2001.
- [11] Liskay, A., van der Zalm, E. & Schopfer, P., Production of reactive oxygen intermediates (O_2^-), H_2O_2 , and OH) by maize roots and their role in wall loosening and elongation growth. *Plant physiology*, **136**, pp. 3114–3123, 2004.
- [12] Luchsinger, R.H., Pedretti, M. & Reinhard, A., Pressure induced stability: from pneumatic structures to Tensairity. *Journal of Bionics Engineering*, **1(3)**, pp. 141–148, 2004.
- [13] Luchsinger, R.H., Pedretti, A., Steingruber, P. & Pedretti, M., The new structural concept Tensairity: Basic Principles. *Progress in Structural Engineering, Mechanics and Computation*, ed. A. Zingoni, A.A. Balkema Publishers: London, 2004.
- [14] Luchsinger, R.H., Pedretti, A., Steingruber, P. & Pedretti, M., Light weight structures with Tensairity. *Shell and Spacial Structures from Models to Realization*, ed. R. Motro, Editions de l’Espéro: Montpellier, 2004.



- [15] Luchsinger, R.H., Crettol, R., Steingruber, P., Pedretti, A. & Pedretti, M., Going strong: from inflatable structures to Tensairity. *Textile composites and inflatable structures II*, eds. E. Onate & B. Kröplin, CIMNE: Barcelona, 2005.



Functional information and entropy in living systems

A. C. McIntosh

Energy and Resources Research Institute, University of Leeds, Leeds, UK

Abstract

In any living system one quickly becomes aware of the extraordinary complexity that so organises the chemical proteins at the biochemical level as to effectively build digital machinery which for many years, since the discovery by Crick and Watson of DNA, has been the goal of modern software engineers to emulate. The functional complexity of these systems is clearly heavily dependent on the material environment in which such a system is operating and indeed uses all the same chemical and physical laws that are used to such good effect by any man made machines. What though are the laws that such organisation must inherently obey for natural systems? Can one quantify the organisational structure that sits on top of the matter and energy in any real system?

In this paper, the author will consider the fundamental aspects of entropy and the second law of thermodynamics applied first of all in the traditional definitions used in heat and chemical systems. Then analogous representations of 'logical entropy' will be discussed where for a number of years many scientists (such as Prigogine) have been attempting to simulate in a rational way the idea of functional complexity. Prigogine's work has primarily been seeking to express self organisation in terms of non-equilibrium thermodynamics and the term 'Prigogine entropy' has thus been introduced. Allied closely to this is the concept of the definition of information which must go beyond the simple recipe of Shannon's Theory, that essentially only deals with the transmission of existing data. The main issue at stake in any discussions of functional complexity is arriving at a logical approach to describing the possible states of the system, and secondly to establishing a valid proportionality constant that is analogous to the Boltzmann constant of traditional thermodynamics. In this paper we discuss how the laws of thermodynamics can be understood in terms of the possible information content of molecules. We build on the concept of information transfer and the notion of 'logical entropy', to considering the application of the laws of thermodynamics to non-equilibrium chemistry. This then concerns the basic definition of how information is defined and connected to the fundamental laws of thermodynamics. Although the paper may raise more questions than answers, the aim will be to at least move further towards a rigorous scientific treatment of the whole concept of organisation and system structure by seeking parallel (logical) laws of complexity in system states to the well known laws of thermodynamics.



1 Introduction

The defining of information is a key issue in the origins debate, since terms such as ‘advance’ and ‘simple to complex’ have little direct meaning at the biochemical level. Intuitive reasoning presupposes the worldview of such statements, and the discussions on origins are fundamentally to do with worldviews. Consequently the biochemical arguments are always going to be a vital battleground because of the root issues at stake.

Claude Shannon in 1948 [3] introduced the basis for the definition of the unit of information content. He argued that any logical process can be reduced to a series of either/or decisions (called in mathematics Boolean Algebra). Each decision can be represented by a 1 or 0, represented in computer hardware terms by whether a microcircuit is ‘on’ or ‘off’ respectively. This unit is termed a ‘bit’ of information, and as complication increases it is more convenient to use the unit of a byte (8 bits). Thus any system and its information content can now be quantified in terms of this unit of information. Dawkins referring to the Shannon concepts in an essay entitled ‘The Information Challenge’ [4] made the following statement which is quoted in full, since it lies right at the heart of the thesis held by most evolutionary biologists that information increase is possible by natural selection operating on successive mutations :

“Let me turn, finally to another way of looking at whether the information content of genomes increases evolution. We now switch from the broad sweep of evolutionary history to the minutiae of natural selection. Natural selection itself, when you think about it, is a narrowing down from a wide initial field of possible alternatives, to the narrower field of the alternatives actually chosen. Random genetic error (mutation), sexual recombination and migratory mixing all provide a wide field of genetic variation: the available alternatives. Mutation is not an increase in true information content, rather the reverse, for mutation in the Shannon analogy, contributes to increasing the prior uncertainty. But now we come to natural selection, which reduces the ‘prior uncertainty’ and therefore, in Shannon’s sense, contributes information to the gene pool. In every generation, natural selection removes the less successful genes from the gene pool, so the remaining gene pool is a narrower subset. The narrowing is non-random, in the direction of improvement, where improvement is defined, in the Darwinian way, as improvement in fitness to survive and reproduce. Of course the total range of variation is topped up again in every generation by new mutation and other kinds of variation. But it still remains true that natural selection is a narrowing down from an initially wider field of possibilities, including unsuccessful ones, to a narrower field of successful ones. This is analogous to the definition of information with which we began: information is what enables the narrowing down from prior uncertainty (the initial range of possibilities) to later certainty (the ‘successful’ choice among prior probabilities). According to this analogy, natural selection is *by definition* a



process whereby information is fed into the gene pool of the next generation.”

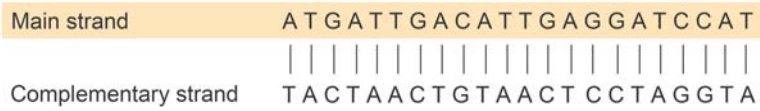


Figure 1: Sample genetic code with complementary strands.

This important paragraph shows the dilemma that faces an approach which only considers matter and energy without information (the ‘bottom up’ approach). There is an admission of the need for new information to counter the narrowing effect of natural selection as usually defined. This definition is simply that natural selection is the favourable advantage of random mutations in one generation making that alteration more likely to survive and be thus more prolific in the next generation. The narrowing effect is that the number of options to choose from is reduced since once the selection is made, the original gene pool is reduced. The answer suggested here is to alter the definition of natural selection (see last sentence of quote) and to further propose the topping up of the gene pool by the very mutations themselves. The formidable obstacles to this proposition lie on a macroscopic level in the very nature of DNA (see fig. 1) which has been shown to have the immense capability of in situ repair work. For example there are enzymes which are *specifically* assigned to nucleotide excision repair – they recognise wrongly paired bases in the DNA nucleotides (Adenine (A), Thymine (T), Cytosine (C) and Guanine (G)) connecting the two deoxyribose sugar-phosphate strands. This means that mutations are generally corrected (see for example the papers by Jackson [5] and de Laat et al [6]), so that even if speciation does occur due to slight modifications and adaptations of the phylogeny, any serious departures in the genetic information would be acted against by the DNA’s own repair factory. Mutations do not increase information content – rather the reverse is true. The flightless Galapagos Cormorant is a classic example. Evidently repair by the above techniques was not possible, and the genetic defect has persisted, such that information has certainly been lost, and the gene pool (in that case irrevocably) reduced. At the very least Dawkins’ assertion at the end is misleading, for it suggests there is a natural *source* of new information which experimental observation denies. Natural selection cannot be redefined and is not the handmaid of macro evolution.

However there is a more fundamental issue. At the molecular level, the laws of thermodynamics do not permit step changes in the biochemical machinery set up for a particular function performed by the cells of living organisms. That is any random mutations always have the effect of increasing the disorder (or what we will shortly define as logical entropy) of any particular system, and consequently decreasing the information content. What is evident is that the initial information content rather than being small must in fact be large, and is in fact vital for any process to work to begin with. The issue of functional complexity and information is considered exhaustively by Meyer [7] who argues that the neo-Darwinist model cannot explain all the appearances of design in

biology. Even within the neo-Darwinist camp the evidence of convergence (similarity) in the suggested evolutionary development of disparate phylogeny has caused some writers [8] to consider 'channelling' of evolution. Such thinking is a tacit admission of a teleological influence. That information does *not* increase by random changes (contrary to Dawkins' assertion) is evident when we consider in the following section, the logical entropy of a biochemical system.

2 The second law of thermodynamics

A succinct statement of the second law is "The amount of energy available for useful work in a given system is decreasing. The entropy (dissipated useful energy per degree Kelvin) is *always* increasing."

Examples of this principle abound. Heat always flows from hot to cold. In the process it can be made to do work but always some energy will be lost to the environment, and that energy cannot be retrieved. Water flows downhill and loses potential energy which is changed into kinetic energy. This can again be made to do work (as in a hydroelectric power plant). However some energy will be lost such that if one was to use all the energy generated to pump the same water back up to its source, it would not reach the same level. The difference of original potential energy to that corresponding to the new level, divided by the temperature (which in that case is virtually constant) is the entropy of the system. Such a measure will always give an entropy *gain*.

There is no known system where this law does not apply. The fact that the entropy of a given closed system increases, effectively brings with it an inevitable decline in usefulness of all systems. The phrase 'arrow of time' is often used to describe this since the second law brings in the concept of non-reversibility of all real systems.

2.1 The second law and open systems

In that the second law of inevitable entropy increase applies to a closed system, some have maintained that with an open system one could have entropy decreasing in one area while the overall entropy of the two systems together (closed) is increasing. An illustration would be of two ice boxes A and B (see fig. 2) where there is an allowance for small contact between them but with (perfect) insulation round the rest of the cube A and poor insulation round cube B. Systems A and B are both then open systems, as is the system A and B together (referred to as A+B), but system A and B with the surrounding region 1, (that is the complete system) is closed. The entropy of the overall complete system then must increase with time. That is there will eventually be equilibrium throughout every region. Suppose we start with Temperature T_1 appreciably hotter than T_A and T_B . Thus for instance we could have $T_1 = 100^\circ\text{C}$ and T_A and T_B both at -10°C . Initially as time progresses the original equal temperatures T_A and T_B become different. T_A will stay close to the original -10°C , but T_B will begin to move to a higher value (say $+5^\circ\text{C}$) due to there being good conduction of heat into ice box B (as against the insulated ice box A). Now consider system



A and B together (A+B). One now has an open system with decreasing entropy, in that useable energy transfer between the two ice boxes is possible, and work can be achieved where before in that system, treated in isolation, none was possible. However one notes two things. First that this is possible only for a finite time – eventually the temperature difference will reach a maximum (when T_B gets close to T_1) and at this point system A+B will have a minimum entropy condition. After this system A+B will then experience a rising entropy condition. Notice also that the initial conditions (different insulation levels) are important for it to be possible to achieve a low entropy condition local to system A+B. Effectively one has an elementary ‘machine’ which is making use of the non-homogeneous temperature across the complete system. This demonstrates the reality of how the second law applies in open systems, and that extra energy from outside is no use *unless there is a machine* (i.e. teleonomy / information) available.

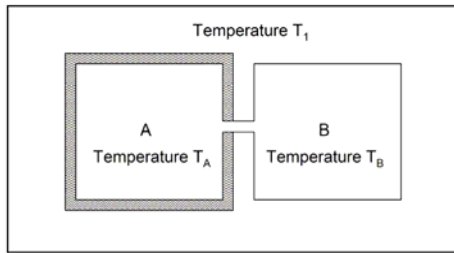


Figure 2: Open system A and B.

2.2 Thermodynamic entropy and logical entropy

A connection can also be made between entropy and disorganisation or disorder. The first to formalise this use of the concept of entropy was the Austrian physicist Ludwig Boltzmann.

Klyce [9] in a useful article, introduces the concept of logical entropy as follows. As the laws of thermodynamics were investigated in the latter part of the nineteenth century, it was evident that the second law implied there was a preferred direction in time even at the molecular level, which seemed to contradict the growing physical understanding of the laws of physics applied to molecular collisions, which indicated here there was no preferred direction in time — an elastic collision between molecules would look the same going forward or backward. In the 1880s and 1890s, Boltzmann used molecules of gas as a model, along with the laws of probability, to show that there was no real conflict. The model showed that heat, no matter how it was introduced, would soon become evenly diffused throughout the gas, as the second law required.

The cleverness of Boltzmann’s ideas however was that the model could also be used to show that two different kinds of gases would become thoroughly mixed even though the temperature of each gas may in fact be the same. Thus an analogy is really being made between the diffusion of heat and the diffusion of



two gases. The parallel between disorganisation and diffusion across basic distinct states was thus made. Quoting Klyce [9]

“The reasoning used for *mixing* is very similar to that for the diffusion of heat, but there is an important difference. In the diffusion of heat, the entropy increase can be measured with the ratio of physical units, joules per degree. In the mixing of two kinds of gases already at the same temperature, if no heat is exchanged, the ratio of joules per degree — thermodynamic entropy — is irrelevant. The mixing process is related to the diffusion of heat only by analogy. Nevertheless, Boltzmann used a factor, now called Boltzmann's constant, to attach physical units to the latter situation. Now the word entropy has come to be applied to the mechanical mixing process, too. (Of course, Boltzmann's constant has a legitimate use — it relates the average kinetic energy of a molecule to its temperature.)”

To gain understanding of this type of model of logical entropy we illustrate by following the example of the entropy of a gas using the Boltzmann approach.

2.3 Entropy of a gas – an example of ordered states

The entropy of a gas is given by

$$s = -\frac{k}{W} \sum_i f_i \ln f_i \quad , \quad (1)$$

where i : tabulates the state i This is usually a speed. Thus $i = 10$ could represent the state of molecules moving in the x - direction at say speed 10 m s^{-1} . There can be negative i 's as well. W is the molecular weight (kg mol^{-1}) and k is Boltzmann's constant ($k = 1.3805 \times 10^{-23} \text{ J mol}^{-1}\text{K}^{-1}$), so that the entropy is in specific terms (energy per unit mass per degree, $\text{J kg}^{-1} \text{K}^{-1}$)

f_i is the fraction of the parts (i.e. of the molecules) which are in state i - i.e. moving at a certain speed. The sum \sum will add the terms $f_i \ln f_i$ for all the parts (speeds). The f_i 's are fractions between 0 and 1, so that the log function ($\ln \equiv \log_e$) will be negative and S will thus be positive.

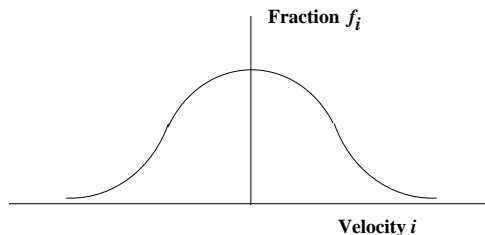


Figure 3: A particular non-equilibrium state (normally distributed).

Suppose all the molecules are moving at 10 m s^{-1} , then all of the parts of the system would be in state $i = 10$, so f_{10} would be 1 with the rest of the f_i 's at zero. Now for $f_i = 0$ or 1, then $f_i \ln f_i = 0$. For a particular state of non-equilibrium, there is roughly a normal distribution of possible states with a mode near one state (see fig. 3) so that with the maximum f_i being less than unity, the \log_e of all the f_i 's is



negative, and therefore $\sum f_i \ln f_i$ is negative, so that s is positive. The more narrow the mode of fig. 3 (i.e. the more ordered the state), the smaller s becomes, so that in the limit of a zero thickness to the curve (meaning all the molecules are at a single speed i) the limiting value of s is zero. This shows that entropy is small in ordered states which are near equilibrium.

3 Combined entropy changes?

Prigogine [10] and others have proposed the addition of other entropies which could feed negative entropy into a given (open system). Consequently the total entropy is considered to be

$$ds = ds_T + ds_{\text{logical}} \quad (2)$$

where ds is the total change in entropy, ds_T is the change in thermodynamic entropy and ds_{logical} is the change in entropy due to complexity — that is Prigogine or logical entropy. The thermodynamic entropy ds_T for a gas would be described by the Boltzmann law of eqn. (1), and for other types of energy exchange there will be an appropriate way of describing the internal energy, whether it be for electromagnetic, thermal, kinetic etc. While ds_T tends to increase, the term ds_{logical} can increase or decrease or remain zero (it is considered positive if entropy enters the system and negative if entropy leaves the system). The important implication of the additional logical entropy term is that then the total entropy change of any open system, ds , can be considered positive, negative, or zero. Systems for which $ds < 0$ (that is where entropy is decreasing) are said to be self-organizing (Cambel [11]), though this term needs care since the organising is only reflecting an ordering principle *already present*.

A good example of ds_{logical} would be the order inherent in crystals due to the atomic structure of a particular chemical compound. When such a compound is cooled to produce crystals, it is not the cooling itself which causes the crystals to occur, but the response to the precise molecular bonding within the material itself, and which is a definite function of the state variables. Often this is falsely used as an argument for increase in order (and thus an argument for increase in order) when in fact the ordering principle is latently already in the elements involved.

The all important question that many have addressed is how to quantify ds_{logical} for real systems, particularly in the life sciences. It has been suggested with some cogency that, on the basis of Shannon's theory of information transmission³, one can express ds_{logical} as an equivalent to the Boltzmann law of eqn. (1). This follows since Shannon's theory is based simply on parcelling any information into a series of irreducible packets such that at the fundamental level, a digital switch is either 'on' or 'off'. Each of these represents a state (rather like the discussion of molecule states in Boltzmann's theory in section 2.3) and adding up all the probabilities of whether each state is present, gives

$$ds_{\text{logical}} = -L \sum_{i=1}^N p_i \ln p_i \quad (3)$$



where L is a constant whose value is of course one of the major difficulties, since the number of possible states of any open system is not known (particularly as quantum states may also need to be invoked). Setting this at unity is often the assumption in recent studies [12, 13], but when dealing with *arrangements* of biological systems (such as the arrangement of DNA and the nucleotides, enzymes, ATP etc) the definition of what to include as a system state is moot. Thus Peter Coveney and Roger Highfield were being brutally honest when they stated in their classic book “The Arrow of Time” that [14]

“There is, however, nothing to tell us how fine the [parcelling] should be. Entropies calculated in this way depend on the size-scale decided upon, in direct contradiction with thermodynamics in which entropy changes are fully objective”

There is another major difficulty which concerns the definition of information. Gitt [15] has shown that the Shannon information concept is not really the main contributor, since this carries no concept of function [7] and purpose (termed ‘apobetics’ in Gitt’s work) which is essential to any real information exchange in any working system. Consequently to define complexity as a gradual seepage in of ‘negative entropy’ is predicated on the notion that information can gradually increase from a random state. However in reality information is not defined in the coded sequence itself (such as the DNA nucleotide sequence of fig. 1) but rather (Gitt has shown) as five levels of signal statistics: (the Shannon level), code (syntax), expression (i.e. message at the semantic level), expected action (pragmatics) and intended result (apobetics). To summarise just two of these levels succinctly, the code used is not defined by the material it orders, and the expression (message) is not defined by the code it uses. Gitt argues that information has to be thought of as a third fundamental quantity which cannot be defined in terms of matter and energy.

4 A new approach: entropy constrained by functional information

We propose a different treatment which quantifies the effect of functional information in a system. This approach recognises Gitt’s important deductions concerning real information systems being impossible to define in terms of matter and energy alone. However one can recognise the effect of machines / information systems (that is teleonomy) being present in exactly the same way as a digitally controlled machine (i.e. a computer) is operated by software. The high level program controls a set of electronic switches on a micro chip which are set in a certain predefined pattern. Thus the logical entropy ds_{logical} (the switching of the micro chip in the analogy) rather than being the *source* of the information should be thought of as the *effect* of information carrying systems. For a pure materialist there may be a natural reticence to adopting such an approach, but the evidence of the thermodynamics of living systems supports this.



4.1 Gibbs free energy

An illustration of how an information bearing system relates to thermodynamic entropy is demonstrated by the code carrying DNA polymer (see fig. 1). As is well known, DNA is a double helix. The outer edges are formed of alternating ribose sugar molecules and phosphate groups. The two strands go in opposite directions either side of the nitrogenous bases which are like the inside rungs of a ladder. Adenine (A) on one side pairs with thymine (T), and on the other by hydrogen bonding, and cytosine (C) pairs with guanine (G). It has been noted that the C-G pair has three hydrogen bonds while the A-T pair has only two, which keeps them from pairing incorrectly. But this only dictates side-to-side pairing, but says nothing about the order *along* the molecule which is of course the all important digital information. There is no physical / chemical law which *of itself* stops other bonds forming which are not recognised in the DNA code, such as A-G or T-C though in terms of efficient use of space, the base pair A-T is identical in size to G-C which makes stacking very regular and precise. The point here is that it is the information contained in the DNA itself which causes particular bonds to be made, not the chemistry itself. Furthermore if one takes a solution of adenosine monophosphate (AMP) and a solution of thymidine monophosphate (TMP), and mix them together, they will not form base pairs A-T in solution because the bases will H-bond with water molecules. So this illustrates that for the information to exist at all in the system, there needs to be the correct thermodynamic energy relationships existing at the fundamental level, constrained by low levels of logical entropy (from high level information).

This is best discussed in the context of the Gibbs free energy g which effectively takes away the unusable lost energy (associated with entropy) from the enthalpy h (which can be regarded as the total thermodynamic energy available). Thus

$$g = h - Ts \quad , \quad (4)$$

It can be shown that for a chemical reaction, the change between the initial reactants to products is related to the change in the Gibbs free energy through

$$\Delta g = -\frac{RT}{W} \ln K \quad , \quad \text{i.e. } K = -\exp(-W\Delta g/RT) \quad (5a,b)$$

where K is the reaction rate constant. Assuming that the reaction itself proceeds at constant temperature, then from equation (4) one can also state that

$$\Delta g = \Delta h - T\Delta s \quad , \quad (6)$$

and referring to base states (superscript 0) we have from equations (5a) and (6)

$$\ln K = \frac{-W\Delta h^0}{RT} + \frac{W\Delta s^0}{R} \quad . \quad (7)$$

From eqn. (5b), for a reactant F going to product P , the probability p of any one state is given by

$$p = \frac{K}{1+K} = \frac{\exp(-W\Delta g/RT)}{1+\exp(-W\Delta g/RT)} \quad (8)$$

The equilibrium constant K governs the progress of the chemical reaction to completion. The K will be large where reactions have a maximum value of Δs^0



and a minimum value of Δh^0 . Natural systems will tend to configurations where the entropy Δs^0 is greatest and the heat content Δh^0 is lowest. And we note that the lowest heat content configurations are generally associated with molecular configurations in which the atoms are bound most securely to one another. All chemical reactions without external influences will minimize g . Furthermore any natural process occurs spontaneously if and only if the associated change in Gibbs free energy g for the system is negative ($\Delta g < 0$). Likewise, a system reaches equilibrium when the associated change in g for the system is zero ($\Delta g = 0$ — and note that the probability p is then $\frac{1}{2}$), and no spontaneous process will occur if the change in g is positive ($\Delta g > 0$). It is the information within the structure which enables a non-equilibrium chemistry to be maintained, such that low logical entropy ($\Delta s_{\text{logical}}$) is added to the fundamental molecular structure. Another very clear example is the famous Urey-Miller experiment which produced left handed and right handed chirality amino acids by firing sparks across a reducing mixture of methane, ammonia, water and hydrogen. The mixture was racemic in left handed and right handed chirality whereas in life systems one requires only left handed amino acids. The probability of any one state is in fact $\frac{1}{2}$ since there is equilibrium between the two possible end states. Only by driving the net Gibbs free energy between the two end states to an impossible infinite value (that is impossible without an information-rich machine) could one get an entirely left handed system which is what life systems actually do have. However if we consider the information in the system as being the *source* and the logical entropy as being the *effect*, then there is a logical coherency in the argument. (In this case from eqn. (6), Δg is large and positive precisely because $\Delta s_{\text{logical}}$ is large and negative).

Consequently to suggest that reactions on their own can be moved against the free energy principle is not true, since they could not be sustained. The DNA molecule along with all the nucleotides and other polymers could not change radically such that a low entropy situation would emerge. To alter the DNA constituents from one stable state say to another representative state with a distinct improvement cannot be done by natural means alone without additional *information*. The thermodynamic laws are against such a procedure.

Dickerson hoped for a different physics when he stated [16]

“Through some gradual means, about which we can only speculate, an association of nucleic acids as the archival material with protein as the working catalyst evolved into the complex genetic transcription and translation machinery that all forms of life exhibit today”

5 Conclusions

In this paper we have considered the concept of logical entropy as a parallel to the Boltzmann probability formula for system states. We have then considered the role of information in reducing at a fundamental level the logical entropy and concluded that rather than regarding negative entropy as being a *source* of information at the fundamental level, it is far more self-consistent to regard the



information defined in terms of a source from which negative logical entropy is *derived* at the molecular level, and which can be quantified using Shannon principles.

It has often been asserted that the logical entropy of an open system could reduce through chance exchanges of that system with its environment. By considering the Gibbs free energy connecting two possible states, it is evident that this involves thermodynamic hurdles which demand effectively a different physics. Self-organisation (so called) only takes place when existing information is already inherent in the system and not vice versa. In an open system, energy (such as from the sun) may increase the local temperature difference (and thus increase the *potential* for useful work that can be done locally), but without a *machine* (that is, a device which is made or programmed to use the available energy), there is still no possibility of the self-organisation of matter. There has to be previously written information or order (often termed “teleonomy”) for passive, non-living chemicals to respond and become active. Thus the following summary statement applies to all known systems:

Energy + Information → Locally reduced entropy (Increase of order)
(or teleonomy)

with the corollary:

Matter and Energy alone \nRightarrow Decrease in Entropy

Another way of saying this is that for an open system, energy must be *directed* to be of any use.

In this paper we have argued that for living systems, rather than regarding negative entropy as a quantity generated within, one should regard the information as being the *cause* and the logical entropy reduction being the *result*. That which is dead (such as a stick or leaf from a tree) has no information or teleonomy within it to convert the sun’s energy to useful work. Indeed it will simply heat up and entropy will increase. However, a living plant has information within it, such that the energy from the sun is absorbed (along with carbon dioxide and water) by its leaves, through photosynthesis. The chlorophyll of the leaf enables such a biochemical reaction to take place. To quote Wilder-Smith [17, p.59],

“..raw matter within a *closed* system, plus a teleonomic machine, might yield auto-organisation derived from endogenous [that which comes from within] energy. Raw matter within an *open* system, plus a teleonomic machine may yield auto-organisation derived from endogenous and/or exogenous [that which comes from without] energy. *Within both open and closed systems, however, a mechanism (machine, teleonomy, know-how) is essential if any auto-organisation is to result.*”



References

- [1] Watson, J. D. and Crick, F. H. C. "Molecular structure of Nucleic Acids", *Nature* 171, 737-738 (1953).
- [2] See for example Nicolis, G. and I. Prigogine. *Exploring Complexity: An Introduction*, Freeman, New York, (1989) and the useful web site where these matters of non-equilibrium thermodynamics are discussed: http://www.schuelers.com/ChaosPsyche/part_1_9.htm (accessed 2006).
- [3] Shannon, C.E., "The Mathematical Theory of Communication", *The Bell System Technical Journal*, Vol. 27, pp. 379-423, 623-656, July, October, (1948).
- [4] Dawkins, R. "The Information Challenge", pp. 107-122 (quote is from pp. 120-121), Chapter 2.3 of *A Devil's Chaplain; Selected Essays by Richard Dawkins*, Ed. Latha Menon, Phoenix, 2003.
- [5] Jackson, S.P., "Sensing and repairing DNA double strand breaks", *Carcinogenesis*, Vol. 23, No. 5, 687-696, OUP, May 2002.
- [6] de Laat W. L., Jaspers, N.G.J., and Hoeijmakers, J.H.J., "Molecular mechanism of nucleotide excision repair", *Genes and Development*, Vol. 13, No. 7, pp. 768-785, April, 1999.
- [7] Meyer, S.C., "The origin of biological information and the higher taxonomic categories", *Proceedings of the Biological Society of Washington*, 117(2), 213-239, 2004.
- [8] Conway Morris, S., "Evolution : bringing molecules into the fold", *Cell* 100, 1-11, 2000.
- [9] Klyce, B. "The second law of thermodynamics", essay at <http://www.panspermia.org/seconlaw.htm> (accessed 2006).
- [10] Nicolis G. and Prigogine, I., *Exploring complexity: An introduction*, W.H. Freeman, New York, 1989.
- [11] Çambel, A. B., *Applied chaos theory: A paradigm for complexity*, Academic Press, Boston: 1993.
- [12] Wicken, J.S., *Evolution, Thermodynamics and Information: Extending the Darwinian Program*, Oxford University Press, 1987.
- [13] Penrose, R., *The Emperor's New Mind*, Oxford University Press, 1989.
- [14] Coveney, P. and Highfield, R., *The Arrow of Time*, Ballentine Books, 1990. p 176-177.
- [15] Gitt, W., "Information: the third fundamental quantity", *Siemens Review*, Vol 56, Part 6, pp.36-41, 1989.
- [16] Dickerson, R.E. "Chemical Evolution and the origin of life", *Scientific American* 239(9), 73, 1978.
- [17] Wilder-Smith, A.E., "The Natural Sciences know nothing of evolution", *Master Books*, San Diego, California 1981. See particularly chapter 4 "The Genesis of Biological Information". Bracketed material added.



Biomimetics of spider silk spinning process

G. De Luca & A. D. Rey

Department of Chemical Engineering, McGill University, Canada

Abstract

Spiders, with their ultra-optimized spinning process, are able to produce super-fibers with remarkable mechanical properties. The precursor material is a lyotropic nematic liquid crystalline anisotropic fluid. The mechanical properties and processability of the silk fiber are intimately connected to the structural transition undergone by this ordered fluid through the spinning pathway. In this work we study a complex mesoscopic structure present in the extrusion duct of spiders' spinning glands, whose stability depends on the interaction between point defects located on the axis of the cavity. The phenomenon described is important in understanding the process-induced structuring of silk fibers and to defect physics in a more general context.

Keywords: spider's silk, liquid crystalline spinning, nematic point defects.

1 Introduction

Spiders ecologically produce fibers with mechanical properties comparable or superior to the best man-made superfibers [1, 2]. There is therefore a considerable interest in understanding the design and processing details of the silk-precursor materials. *Green* spinning processes as well as various exiting applications are envisaged upon the successful mimetic of spider extrusion system and fibers [3, 4, 5].

Spider silk fibers are spun from a highly concentrated water-based solution of elongated rod-like molecules or aggregates forming a lyotropic nematic liquid crystal phase [6, 7, 8]. This silk precursor can flow as a liquid while maintaining at the same time some degree of orientational order as a crystal. This orientational order is characterized by the tendency that have neighboring rod-like entities to align their long axis in parallel along a common direction [9, 10]. This preferred molecular orientation usually varies from subregion to subregion in the mesophase (*i.e.*, intermediate phase) due to elastic effects coupled with geometrical and interfacial constraints [9]. The evolution of orientational order or molecular orientation



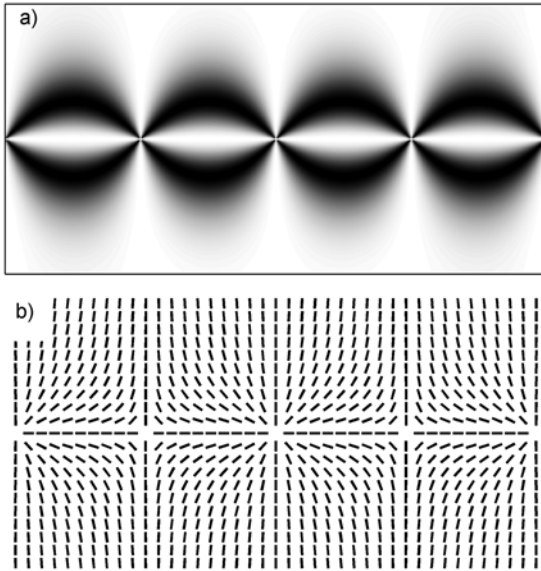


Figure 1: Typical polarized light pattern seen in the extrusion duct of spiders' spinning glands and its correspondence to the ERPD molecular orientation as represented by the director field $\mathbf{n}(\mathbf{r})$.

throughout the spinning pathway is extremely important as it affects the processability of the silk precursor mesophase and determines the microstructural details of the solidified fiber and hence its remarkable mechanical properties [6, 7, 8].

The spinning apparatus of spiders basically consist of three major regions: a tail where the silk precursor material is synthesized, a central bag where it is stocked in a concentrated solution, and a spinning extrusion duct from which the silk fiber is drawn [11].

Observations made by polarized light microscopy in the extrusion duct have revealed the presence of a complex orientation structure known as escaped radial with point defects (ERPD) [8, 12, 13, 14]. Figure 1 shows a typical polarized light pattern observed along the spinning duct and its corresponding ERPD molecular orientation using the director field representation. The director field $\mathbf{n}(\mathbf{r})$ is given by unit vectors defining local average preferred molecular orientations. Generally $\mathbf{n}(\mathbf{r}) = -\mathbf{n}(\mathbf{r})$ and therefore the unit vectors are arrowhead-free [9, 10]. The point defects, referred as hedgehogs, are located where the direction of bending distortions changes; at those particular locations, no unique director \mathbf{n} can be defined as the orientational order *melts*. As it can be seen from Fig. 1(b), two types of defects are found in an alternative manner. The point defect found at the center of this figure is of the radial type whereas its two neighbors belong to the hyperbolic type [15].

Whether this particular molecular configuration is an accident of Nature or a necessary ingredient of the spider biospinning process is unknown at this time. Nevertheless, it might be hypothesized that this structure may play a role in the control of material crystallization along with water pumping, ions exchanges and pH reduction phenomena [8]. A premature crystallization of the silk may indeed cause the permanent blockage of the extrusion system and lead to the death of the animal [8, 16].

In this work, we investigate the stability of the ERPD structure occurring in the extrusion duct of spiders spinning glands. The stability of the ERPD structure is known to be governed by the interaction between the nematic point defects found along the axis [15, 17]. This interaction, mediated by the elastic deformations of the material, can cause the defects to move along the axis of the cavity. When two defects of opposite type are sufficiently close to one another they usually annihilate. On the other hand when defects are well separated their interaction is screened [15].

2 Modeling

In order to study the stability of the ERPD structure in the extrusion duct of spider we consider two point defects of opposite types located on the axis of cylindrical cavity. Due to the rotational symmetry of the structure, we consider a simple two dimensional rectangular domain representing half of a cross section. Dimensionless quantities (denoted by overbars) and equations are used to reduce the number of parameters and facilitates analysis as well as comparisons. The dimensionless width and height of the computational domain correspond respectively to the dimensionless length \bar{Z} and radius \bar{R} of the cylindrical cavity. The dimensionless position vector is defined as $\bar{\mathbf{r}} = \mathbf{r}/R$ where R is the dimensional radius of the cavity .

The continuum nemato-dynamics equation describing the structure evolution of a nematic liquid crystal is typically derived from the minimization of a free energy functional depending on some order parameter [9]. In this work the nematic ordering is described in terms of a tensor field $\mathbf{Q}(\mathbf{r})$, called tensor order parameter [9]. This tensor order parameter is symmetric traceless (*i.e.*, $Q_{ij} = Q_{ji}$ and $Q_{ii} = 0$) and, according to a spectral decomposition, reads:

$$Q_{ij} = \mu_n n_i n_j + \mu_m m_i m_j + \mu_l l_i l_j \quad (1)$$

In this expression, \mathbf{n} , \mathbf{m} and \mathbf{l} are unit eigenvectors forming an orthogonal triad and μ_n , μ_m and μ_l are their corresponding eigenvalues. The director triad and the eigenvalues are characterizing the orientation and the strength of alignment of the phase respectively. The largest eigenvalue in magnitude or absolute value, μ_n , gives the strength of ordering along the uniaxial director \mathbf{n} previously defined. The second μ_m and third μ_l eigenvalues correspond respectively to the biaxial directors \mathbf{m} and \mathbf{l} ($\mathbf{l} = \mathbf{n} \times \mathbf{m}$). At equilibrium, an undistorted nematic phase is uniaxial; however, in distorted regions like in the vicinity of defects the phase may exhibit some biaxiality [9].



The eigenvalues μ_i ($i = 1, 2, 3$) of the tensor order parameter are restricted by: $-1/3 \leq \mu_i \leq 2/3$ and $\mu_n + \mu_m + \mu_l = 0$. The ordering states described by the tensor order parameter are: isotropic ($\mu_n = \mu_m = \mu_l = 0$; $\mathbf{Q} = 0$), uniaxial ($\mu_n > \mu_m = \mu_l$) and biaxial ($\mu_n \neq \mu_m \neq \mu_l$). Finally it is stressed that within this tensorial formalism, order is continuous and defined everywhere including at defect cores unlike in the simpler vectorial description in terms of the director field (See Fig. 1).

It is also often useful to represent the tensor order parameter \mathbf{Q} in the following alternative, but more compact format:

$$Q_{ij} = S(n_i n_j - \frac{\delta_{ij}}{3}) + \frac{P}{3}(m_i m_j - l_i l_j) \tag{2}$$

In this expression, S and P are uniaxial and biaxial scalar order parameters describing respectively the strength of alignment around the uniaxial and biaxial directors (*i.e.*, \mathbf{n} and \mathbf{m}). The Kronecker δ stands for the unit tensor. The scalar order parameters are defined as: $S = 3/2(n_i Q_{ij} n_j)$ and $P = 3/2(m_i Q_{ij} m_j - l_i Q_{ij} l_j)$. The correspondence between the scalar order parameters and the eigenvalues is as follows: $\mu_n = 2/3S$, $\mu_m = -1/3(S - P)$ and $\mu_l = -1/3(S + P)$. The scalar order parameters obey the following restrictions: $-1/2 \leq S \leq 1$ and $-3/2 \leq P \leq 3/2$.

The dimensionless total free energy of a nematic liquid crystal \bar{F} system under strong anchoring conditions (*i.e.*, the orientation of the molecules at the boundary is fixed) is generally written as [9]:

$$\bar{F} = \int_V (\bar{f}_h + \bar{f}_g) d\bar{r}^3 \tag{3}$$

In this expression, \bar{f}_h and \bar{f}_g represent respectively the homogeneous and gradient bulk free energies. We note that $\bar{f}_b = f_b/A$ where $\bar{f}_b = \bar{f}_h + \bar{f}_g$ and A is an energy density scale. Also, accordingly $\bar{F} = \frac{F}{AR^3}$. The homogeneous free energy describes the short-range ordering effects related to the amplitude of the tensor order parameter. This expression permits to describe the first order isotropic-nematic phase transition but also the variation of ordering in the vicinity of defects. This contribution is often referred as the Landau-de Gennes free energy. According to Doi's formalism [18], this expansion of the order parameter may be written, in dimensionless form, as:

$$\bar{f}_h = \frac{1}{2}(1 - \frac{U}{3})Q_{ij}Q_{ji} - \frac{U}{3}Q_{ij}Q_{jk}Q_{ki} + \frac{U}{4}(Q_{ij}Q_{ji})^2 \tag{4}$$

In this expression U is a dimensionless phenomenological parameter called nematic potential which controls the magnitude of the equilibrium tensor order parameter. In general the nematic potential U can be assigned a dependence on either temperature or concentration depending on the nature of the nematic liquid crystal (*i.e.*, thermotropic or lyotropic) [18]. Within this format, the first order phase isotropic-nematic phase transition occurs at nematic potential $U_{IN} = 2.7$. Also, the system is isotropic for $U < U_{IN}$ and nematic for $U > U_{IN}$. The limit



of metastability for the isotropic and nematic phase are $U^* = 3$ and $U^{**} = 8/3$, respectively.

The gradient bulk free energy \bar{f}_g represents the energy variations due to long-range ordering effects. This energy penalty associated with the elastic distortions of the phase can be expressed in dimensionless form as:

$$\bar{f}_g = \frac{\bar{\xi}^2}{2} \bar{\nabla}_k Q_{ij} \bar{\nabla}_k Q_{ij} \tag{5}$$

In this equation $\bar{\xi}$ represents the reduced nematic coherence length which gives a characteristic scale for the variation of the tensor order parameter and the size of defect cores or thickness of the nematic-isotropic interface. It is noticed that $\bar{\nabla} = R\nabla$, $\bar{\xi} = \xi/R$ and $\xi = \sqrt{L/A}$ where L a material-specific elastic constant.

The dynamic equation describing the relaxation of the tensor order parameter $\mathbf{Q}(\mathbf{r}, t)$ towards an equilibrium value that minimizes the total free energy \bar{F} follows from variational principles and is given in dimensionless format by [19]:

$$\frac{\partial Q_{\alpha\beta}}{\partial \bar{t}} = -\frac{\delta \bar{F}}{\delta Q_{\alpha\beta}} \tag{6}$$

The right-hand side of this expression corresponds to functional derivative of the of the total free energy. Here again we stress that $\bar{t} = \frac{A}{\gamma}t$ where γ a kinetic constant associated with rotational viscosity. From variational calculus it can be shown that:

$$\frac{\delta \bar{F}}{\delta Q_{\alpha\beta}} = \frac{\partial \bar{f}_b}{\partial Q_{\alpha\beta}} - \bar{\nabla}_\gamma \frac{\partial \bar{f}_b}{\partial \bar{\nabla}_\gamma Q_{\alpha\beta}} \tag{7}$$

Only the symmetric traceless part of this expression is retained in order to satisfy the constraints of the tensor order parameter.

The boundary conditions for the problem are as follows: at the wall of the cylindrical cavity (upper part of the rectangular domain), the tensor order parameter is assumed to be uniaxial and describe a strong radial anchoring condition so that $Q_{ij}(r = R) = S_e(e_i^r e_j^r - \frac{\delta_{ij}}{3})$, where e^r is the unit vector along the radial direction. The equilibrium scalar order parameter S_e is obtained analytically from Eq. 4 and is given by the relation [18]:

$$S_e = \frac{1}{4} + \frac{3}{4} \sqrt{1 - \frac{8}{3U}} \tag{8}$$

On the z -axis (lower part of the rectangular domain), rotational symmetry boundary condition is assumed. Finally, on the sides of the domain, Neumann conditions are enforced so as to emulate an infinitely long cavity.

Initially, the systems contains a hedgehog pair whose cores are separated by a distance $\bar{D} = 2.4$. The hyperbolic and radial hedgehogs are respectively located at $\bar{z} = -1.2$ and $\bar{z} = 1.2$. The corresponding initial tensor field $\mathbf{Q}(\mathbf{r}, t = 0)$ is obtained by taking a few time steps starting from a trial configuration satisfying



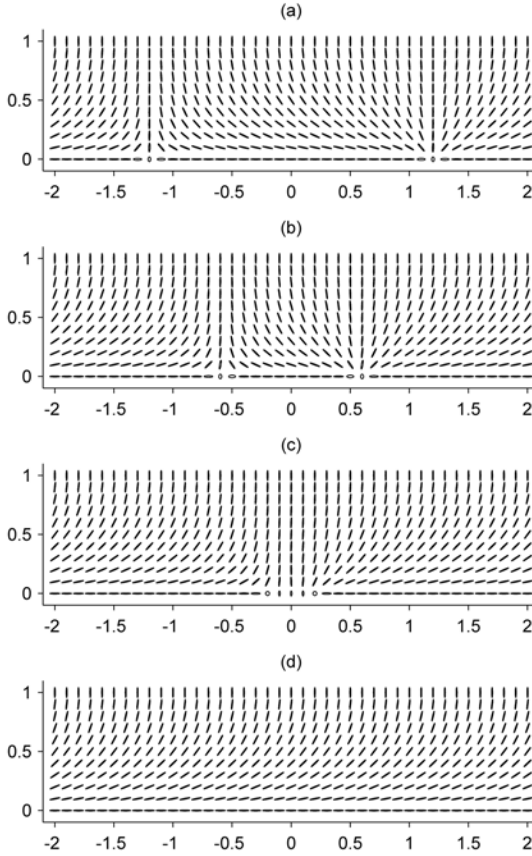


Figure 2: Evolution of orientational order during the annihilation of two nematic point defects confined in a cylindrical capillary. Each ellipse represents a tensor order parameter \mathbf{Q} . The orientation and amplitude of an ellipse is given by the eigenvectors and eigenvalues of \mathbf{Q} . (a) $\bar{t} = 0$, (b) $\bar{t} = 39740$, (c) $\bar{t} = 40600$ and (d) $\bar{t} = 40900$.

all the boundary conditions. Other initial defect configurations do not change the essential features of the results.

The model used in this work contains two parameters: the nematic potential U and the reduced nematic coherence length ξ . For all the simulation results presented in this paper, the nematic potential is set to $U = 6$ which corresponds to an equilibrium scalar order parameter of $S_e = 0.809$. Other values of U in the stable nematic range do not change the underlying process under study. The value of the reduced coherence length is fixed at $\xi = 1/30$.



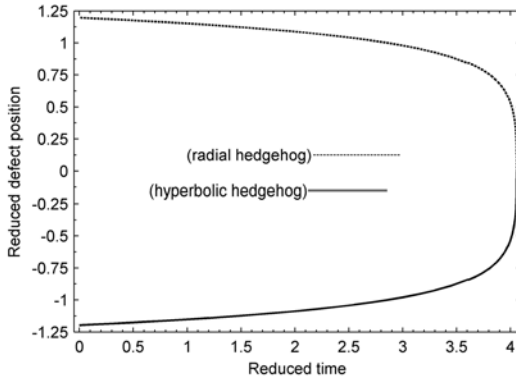


Figure 3: Position of the point defects along the cavity axis as a function of time.

The governing dynamic equation for the tensor order parameter $\mathbf{Q}(\bar{\mathbf{r}}, \bar{t})$ is solved using the standard numerical method of lines. The space discretization is achieved by the finite element method. The time integration of the resulting differential equations is obtained using an adaptive implicit scheme. The density of element is higher in the region describing the trajectories of the defects along the \bar{z} -axis. The independence of solutions on mesh density was verified using standard procedures. The size of the triangular elements is always smaller than the reduced coherence length $\bar{\xi}$ (smallest length in the problem) to accurately capture the amplitude variations of the tensor order parameter. The reduced width and height of the computational domain are respectively $\bar{Z} = 6$ and $\bar{R} = 1$.

3 Results

This section illustrates the dynamic interaction between two nematic hedgehogs confined in a capillary tube. A similar process is thought to occur in the extrusion duct of spider's spinning gland. Figure 2 shows the typical evolution of orientational order during the annihilation of the point defect pair. In this figure, the tensor order parameter $\mathbf{Q}(\mathbf{r}, t)$ is represented as an ellipse. The orientation and amplitude of each ellipse is given by the eigenvectors and eigenvalues of the order parameter. Within, this representation, an elongated ellipse corresponds to a well-ordered nematic region whereas a circle corresponds to a low orientational ordering. Three stages of the annihilation process are shown. In the pre-collision regime Fig. 2(a) and Fig. 2(b), the two point defects have distinct, well separated, cores. As they move closer one another, the distortion in the ellipses orientation increased. However, this process is not accompanied by any significant changes in the defect core structure and ordering. In the collision regime Fig. 2(c), the cores of the defects slowly overlap to finally become indistinguishable. In this regime, structural changes are mainly given by changes in alignment (*i.e.*, amplitude of the



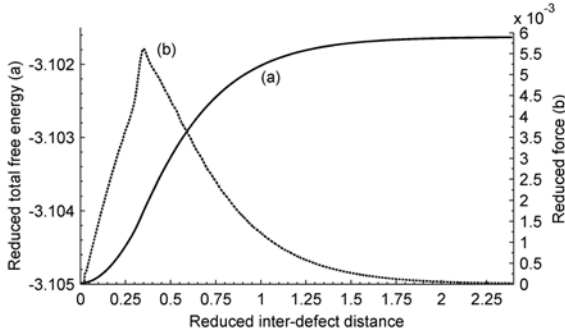


Figure 4: Total free energy and interaction force between the point defects as function of the inter-defect distance.

tensor) rather than orientation. It can be seen that the shape of the ellipses now changes in the inter-defects region in contrast to the pre-collision regime. Finally in the post-collision regime Fig. 2(d), the tensor order parameter field relaxes to its equilibrium value and the remaining axial gradients are smoothed-out. The resulting structure, known as escape radial (ER), is defect free and possesses a single bending direction.

Figure 3 illustrates the displacement of the two point defects during the annihilation process. The positions of the defects correspond to the minima of the uniaxial scalar order parameter S . The two trajectories show that the defects travel at identical speeds. The speed of each defect is however not constant and tend to dramatically increase as the defects approach each other. At large separating distance, the defects speed is essentially null.

Figure 4 shows the variation of the total free energy as a function of the defect separating distance and corresponding interaction force. The interaction force is computed by differentiating the total free energy with respect to the inter-defect distance. It can be seen from this figure that the interaction force tends to zero as defects are separated by more than a diameter. However as defects approach each other, this interaction force increases exponentially. In the late stage of the collision regime, governed by alignment and therefore the amplitude of the tensor order parameter, the interaction force is decreasing in a quasi-linear fashion. The value of the force at vanishing defect separating distance is small but finite to the level of discretization of our model.

4 Conclusions

Motivated by the reported experimental observation of ERPD structures in the extrusion duct of spiders spinning apparatus, we have investigated numerically the dynamic interaction between two nematic point defects of opposite topological charge confined in cylindrical cavity. In contrast to previous analytical [17]



and numerical [15] studies we employed the tensor order parameter formalism to describe the orientational order of the nematic phase, which allows for an unambiguous description of defects and reliable estimation of energies. Three distinct regimes leading to the annihilation of the antagonist point defect pair were described. The trend of the defect trajectories agree very well the one found in theoretical [17] and experimental [20] studies. The absence of asymmetry in the defect trajectories as reported in Ref. [21] is attributed to the absence of back-flow effects as well as to the isotropy of the elastic constant. These effects will be investigated in future work and will be reported. The reasons of the point defect annihilation were also investigated. In particular, the dependence of the total free energy and corresponding interaction force on the inter-defect distance was analyzed. It was shown that the interaction force between the defect, which set them into motion, is decreasing exponentially at large defect separating distance. As predicted theoretically in Ref. [22] and shown experimentally if the point defects are separated by a distance greater than a diameter, the interaction force is shielded and the defects pinned. In contrast to previous studies having reported explicitly the force of interaction, we have found that at short separating distance, the interaction force was decreasing very steeply in a linear way. We show that this distinctive behavior is due to the significant variation of the order parameter in the late stage of the collision regime. During the whole process the interaction force was found to be strictly attractive. Finally we would like to emphasize that despite that the context of our study is the process-induced structure in the biospinning of spider silk, the results obtained should be useful to the field of defect physics. The present work provides a theoretical framework to eventually extract engineering principles used in the biospinning process. Having established the stability properties of the structural unit (pair of point defects) in the spider duct, the next step will be to elucidate the emergence of this structural unit and its interaction with other neighboring point defects, as they arise in real spider ducts. This work is supported by the Natural Science and Engineering Research Council of Canada (NSERC). G.D. wishes to acknowledge financial support from NSERC through the CGS program.

References

- [1] Gosline, J., DeMont, M. & Denny, M., The structure and properties of spider silk. *Endeavour*, **10(1)**, pp. 37–43, 1986.
- [2] Ko, F. & Jovicic, J., Modeling of mechanical properties and structural design of spider web. *Biomacromolecules*, **5**, pp. 780–785, 2004.
- [3] Atkins, E., Silk's secrets. *Nature*, **424**, p. 1010, 2003.
- [4] Jin, H.J. & Kaplan, D., Mechanism of silk processing in insects and spiders. *Nature*, **424**, pp. 1057–1061, 2003.
- [5] Turner, J. & Karatzas, C., *Natural Fibers, Plastics and Composites*, Kluwer Academic Publishers, chapter 1, Advanced spider silk fibers by biomimicry, pp. 11–23, 2004.
- [6] Kerkam, K., Viney, C., Kaplan, D. & Lombardi, S., Liquid crystallinity of natural silk secretions. *Nature*, **349**, pp. 596–598, 1991.



- [7] Viney, C., Huber, A., Dunaway, D., Kerkam, K. & Case, S., *Silk Polymers: Materials Science and Biotechnology*, American Chemical Society, chapter 11, Optical Characterization of Silk Secretions and Fibers, pp. 120–136, 1993.
- [8] Vollrath, F. & Knight, D., Liquid crystalline spinning of spider silk. *Nature*, **410**, pp. 541–548, 2001.
- [9] de Gennes, P. & Prost, J., *The Physics of Liquid Crystals*. Oxford University Press, 1995.
- [10] Collings, P., *Liquid Crystals: Nature's Delicate Phase of Matter*. Princeton University Press, 2001.
- [11] Foelix, R., *Biology of spiders*. Oxford University Press, 1996.
- [12] Knight, D. & Vollrath, F., Liquid crystals and flow elongation in a spider's silk production line. *Proc R Soc Lond B*, **266**, pp. 519–523, 1999.
- [13] Vollrath, F., Strength and structure of spiders' silks. *Reviews in Molecular Biotechnology*, **74**, pp. 67–83, 2000.
- [14] Lydon, J., Silk: the original liquid crystalline polymer. *Liquid Crystals Today*, **13(3)**, pp. 1–13, 2004.
- [15] Vilfan, I., Vilfan, M. & Zumer, S., Defects structures of nematic liquid crystals in cylindrical cavities. *Physical Review A*, **43(12)**, pp. 6875–6880, 1991.
- [16] Wainwright, S., Biggs, W., Currey, J. & Gosline, J., *Mechanical Design in Organisms*. Princeton University Press, 1982.
- [17] Peroli, G. & Virga, E., Annihilation of point defects in nematic liquid crystals. *Physical Review E*, **54(5)**, pp. 5235–5241, 1996.
- [18] Doi, M., *The Theory of Polymer Dynamics*, 1998.
- [19] Beris, A. & Edwards, B., *Thermodynamics of Flowing Systems*. Oxford University Press, 1994.
- [20] Peroli, G., Hillig, G., Saupe, A. & Virga, E., Orientational capillary pressure on a nematic point defect. *Physical Review E*, **58(3)**, pp. 3259–3263, 1998.
- [21] Cladis, P. & Brand, H., Hedgehog-antihedgehog pair annihilation to a static soliton. *Physica A-Statistical Mechanics And Its Applications*, **326(3-4)**, pp. 322–332, 2003.
- [22] Semenov, A.N., Interaction of point defects in a nematic liquid. *Europhysics Letters*, **46(5)**, pp. 631–636, 1999.



The preparation of biomimetic nano- Al_2O_3 surface modification materials on gray cast iron surface

Y. Liu¹, L. Q. Ren¹, Z. W. Han¹ & S. R. Yu²

¹The Key Laboratory for Terrain-machine Bionics Engineering, The Ministry of Education, Jilin University, People's Republic of China

²College of Materials Science and Engineering, Jilin University, People's Republic of China

Abstract

Through evolution over hundreds of millions of years, the natural biomaterials generally have superior microstructure and function to normal material. The surface layer of teeth is enamel, which is the hardest structure in the human body. Enamel as a kind of nanoceramic biomaterial; most of its physical and chemical characteristics are similar to normal ceramics. It is of high hardness and is particularly wear resistance. However, the gray cast iron is one of widely used materials. In the process of casting, surface blowholes and micro-pores, which can't be seen by the naked eye, are formed in castings because of the solidification shrinkage of alloy and separation of gas dissolving in liquid alloy, which results in the poor property of materials. Therefore, the gray cast iron and nano- Al_2O_3 were chosen as the substrate and reinforcement in this paper, respectively. A laser cladding method was used to prepare biomimetic nanoceramic surface modification composite materials. The surface property of gray cast iron was largely improved. The process and the factors influencing laser cladding were analysed. The microstructure of the surface modification layer can be divided into a cladding layer, bonding layer and substrate layer, and the formation mechanism of each different layer was researched.

Keywords: nano- Al_2O_3 , biomimetic, surface modification, gray cast iron, microstructure.



1 Introduction

Tooth enamel is a kind of mineralized structure containing about 96% minerals, consisting mainly of calcium and phosphorus as calcium phosphate. As a kind of nanoceramic biomaterial, the surface of enamel has high hardness and wear resistance [1]. According to the special structure of teeth, a bio-inspired nano- Al_2O_3 surface modification material on gray cast iron was designed and prepared with a laser cladding method. Nano- Al_2O_3 was chosen as reinforcement in this paper. The process and the factors influencing laser cladding were analysed. The optimal technology parameters of laser cladding were obtained from this experiment. The solidification process and microstructure of the surface modification layer were researched.

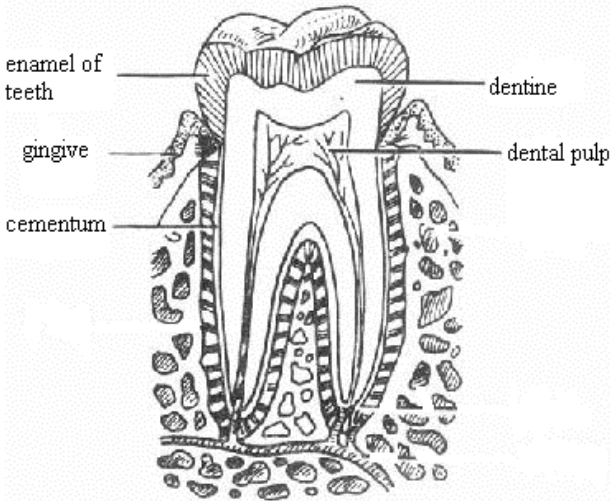


Figure 1: The microstructure of a tooth [2].

2 The preparation of biomimetic nano- Al_2O_3 surface modification layer

Laser cladding is a very quickly dynamic melting and solidifying course, whose cooling speed is quick (up to 10^6C/s). The microstructure was fine due to non-equilibrium solidification [3]. The reuniting of nanomaterials was effectively avoided. At the same time a small amount of nanomaterial formed a fine metallic bond between the cladding layer and the substrate, increases surface hardness and wear resistance.



2.1 The choice of modification materials

Nano- Al_2O_3 was chosen as modification material. The average granularity of nano- Al_2O_3 was 50nm ~ 180nm , with purity more than 99.99% and physics phase α - Al_2O_3 . α - Al_2O_3 grain is stable, has a high hardness and has uniform dimensions.

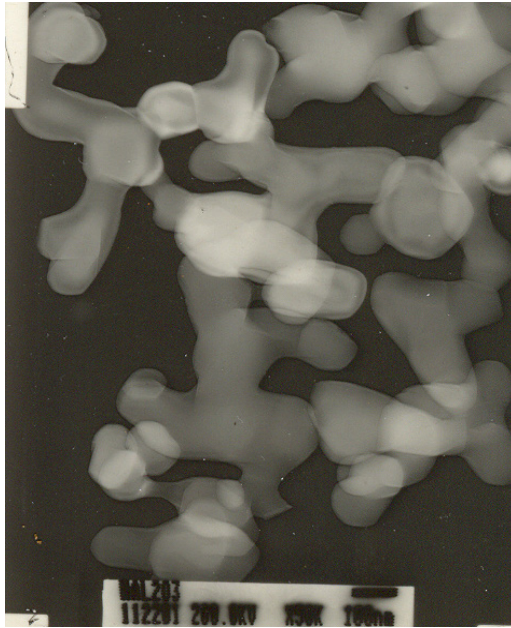


Figure 2: Nanoalumina microstructure (SEM).

2.2 Optimization of technology parameters

A 5 kW CGJ-93 type crosscurrent CO_2 laser machining equipment developed by Changchun University of Science and Technology was used. The colophony alcohol solution was chosen as a binder. The coating material was coated on gray cast iron surface and then scanned by laser.

The laser equipment usually has two kinds of facula including gauss facula and rectangle facula with broadband. The energy density of the broadband rectangle facula is uniform and fit for laser cladding. The dimension of the sample is $500 \times 50 \times 150 \text{mm}^3$, and the dimension of facula is $15 \times 2 \text{mm}^2$. The range of power is 2.0 ~ 3.0kw and the scanning speed is 90 ~ 120 mm/min. The power and scanning speed were chosen as technology parameters. The result of our experiment indicated that the optimal technology parameters were to use a 3.0 kW laser and scanning speed of 90mm/min.



3 Analyses on the course of laser cladding

Laser cladding is a dynamic melting and solidifying course, and non-equilibrium state. With the laser beam scanning continually the melting and solidifying of metal occurred in the melting pool at the same time. In the fore of the melting pool, alloy powder enters the melting pool and melts quickly, governed by self-diffusion, surface tension due to temperature gradient on surface and gravity, diffusing in very short time. In the back of the melting pool, as the laser beam moved away a great deal of heat was transferred quickly by substrate and liquid metal suddenly cooled and solidified. In the process of laser cladding, molten metal solidifies very quickly, and the nucleation rate increases greatly. Thus the microstructure of the cladding layer was fined [4,5], which was a key element improving cladding layer property.

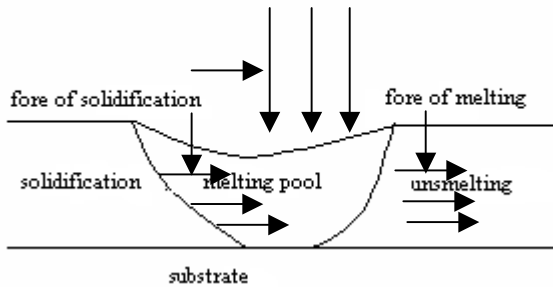


Figure 3: The course of laser cladding.

4 The microstructure of cladding layer

The gray cast iron used contained 3.4 wt%C was hypoeutectic. The sample of laser cladding had three different layers including a cladding layer, bonding layer and substrate layer. Fig.4.1-4.4 showed the three layers of the microstructure.

a) Fig.4.1 shows the microstructure of the cladding layer. The non-equilibrium solidifying microstructure was formed under the condition of fast solidification. In the solidification process, the nucleation rate increased greatly and the grain growth was prevented due to the large temperature gradient in melting pool. The microstructure was fine and dense and C didn't diffuse and existed as carbide in the cladding layer so that the gray cast iron transformed into white cast iron in which a ledeburite phase exists. The martensite phase was formed in the cladding layer due to the fast cooling speed.

b) Fig.4.2 shows the microstructure of the interface bonding layer that was affected by temperature gradient. The temperature near the cladding layer exceeded autenitic temperature due to the influence of surface laser energy. In the process of fast cooling, in addition to a small amount of residual autenitic,



most of the autenitic had transferred martensite. A good metallurgy bonding between the cladding layer and substrate was formed as shown in Fig.4.2.

c) The substrate was gray cast iron, whose microstructure was pearlite + ferrite + flaky graphite as shown in Fig 4.3. The microstructure didn't change and still kept a typical gray cast iron microstructure because the layer was far from the surface, only transferred heat and its temperature wasn't high.

It can be found that the microstructure of the cladding layer was dense and uniform (as shown in Fig.4.4), but the microstructure of the substrate was loose. The bonding layer between the cladding layer and the substrate produced a good metallic bonding.

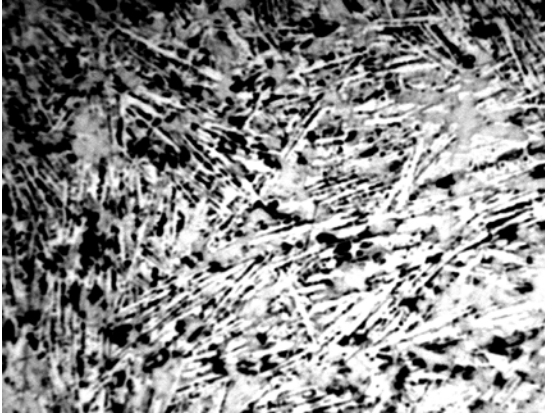


Figure 4.1: Cladding layer micro-metallographic structure $\times 250$.

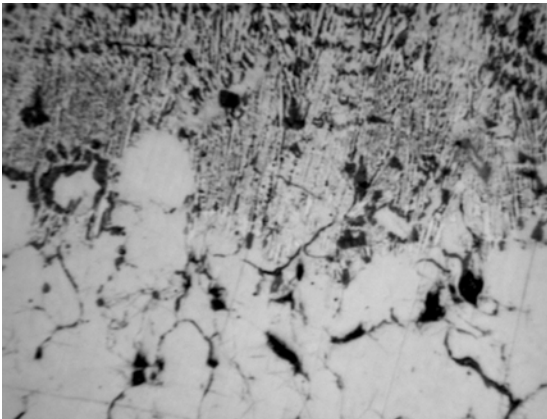


Figure 4.2: Bonding layer micro-metallographic structure $\times 250$.

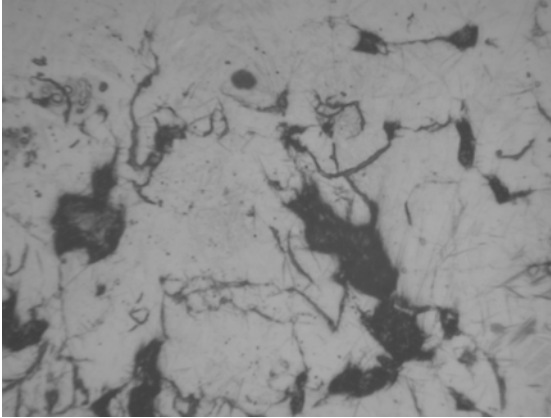


Figure 4.3: Substrate micro-metallographic structure $\times 250$.

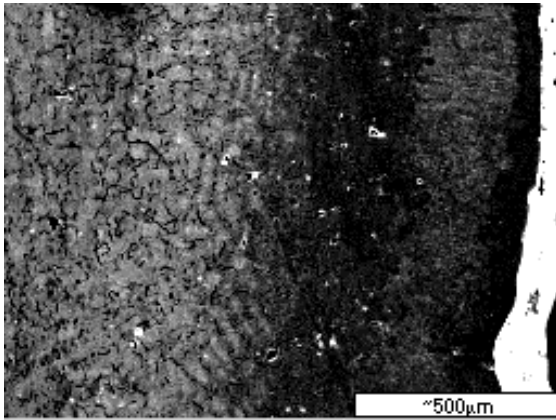


Figure 4.4: Interfacial microstructure (SEM).

Fig.5 showed the element component of cladding layer. The result proved that nano- Al_2O_3 diffused into the cladding layer under laser beam scanning. Fig.6 showed the element component of the substrate and the component of substrate is still gray cast iron.

The technology parameters in the process of laser cladding have important effects on the microstructure of the cladding layer. When the output wavelength of the laser was determined, the main parameters affected the process of laser cladding included laser power P , dimension of facula D and scanning speed v [7]. The facula was a fixed value in this experiment, so the main parameters were laser power P and scanning speed v . When P was too high and v was too low, the energy absorbed by the cladding layer was increased, and the temperature was high. The substrate was melted, the dilution ratio was increased, which resulted

in burning loss of the coating materials. On the other hand, when P was too low and v was increased, the energy absorbed by the cladding materials was reduced. Therefore, the temperature was lower, the substrate didn't melt, and the cladding layer was easy to break off. A good metallic bonding was not formed in the interface, and the surface was very rough. The influence of the scanning speed on the cooling speed was important. The cooling speed was increased if the scanning speed was increased. Therefore, the grains of the cladding layer were fine. Increasing the scanning speed was essential for producing a good metallic bond between the cladding layer and the substrate.

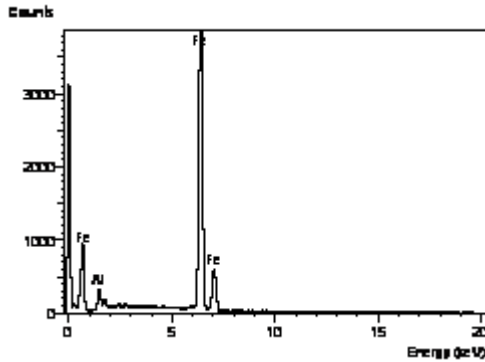


Figure 5: Energy spectrum curve of the cladding layer.

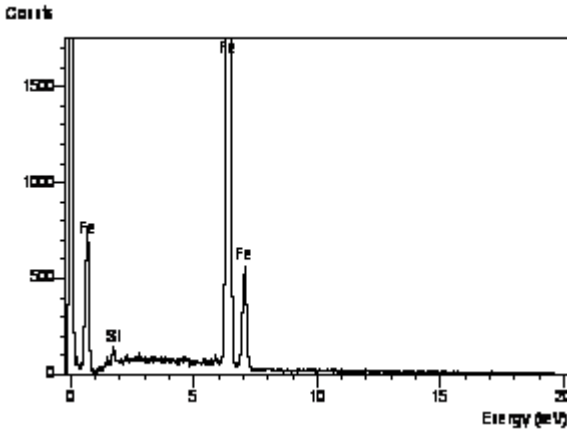


Figure 6: Energy spectrum curve of the substrate



5 Conclusion

1. The gray cast iron was used as a substrate, and nano- Al_2O_3 was chosen as reinforcement. A laser cladding method was used to prepare biomimetic nanoceramic surface modification composite materials.

2. The course of laser cladding was analysed. The microstructure can be divided into a cladding layer, a bonding layer and a substrate layer. The forming factors of different layers were researched.

3. The influence of technology parameters on the microstructure of the laser cladding layer was researched.

Acknowledgements

The authors are grateful for the financial support provided by Trans-Century Training Program Foundation for the Talents by Chinese Ministry of Education (2003) and the Foundation for Distinguished Young Scholars of Jilin Province (Grant No. 20040104)

References

- [1] Cui F.Z. Bionic materials, Beijing: The Chemistry industry press. 2004.
- [2] He Z.Y., Cheng L.Z., Histology and embryology. Beijing: The people sanitation publishing company. 1983.
- [3] E. Lugscheider, H. Bolender, and H. Krappitz, Laser cladding of paste bound hardfacing alloys. Surface Engineering, 1991, 7(1):341~344.
- [4] Zheng S., Zhang Y.M., Ma Y.Q., Huang J.L., Microstructure and Solidification Process of Laser Remelted Alloy Coatings. [J].Journal of Iron and Steel Research, 1996, 8(4):46~51.
- [5] Wang X.L., Shi S.H., Zheng Q.G., Study on Solidification Feature and the Solidification Microstructure of Laser Cladding Layer [J]. Applied Laser, 2001, 21(3):164~167.
- [6] Nicolas. G, Yanez. A, Ramil. A, Alvarez. J.C, Saavedra. E, Garcia-Beltran. A, Molpeceres. C, Autric. M, Ocana J L.UV. Laser Surface Processing of Metallic Alloys: Comparison of Experimental and Numerical Results. Applied surface science 1999, 138-139: 169-173.



Biomimetics: extending nature's design of thin-wall shells with cellular cores

M. A. Dawson¹ & L. J. Gibson²

¹*Department of Mechanical Engineering,
Massachusetts Institute of Technology, USA*

²*Department of Materials Science and Engineering,
Massachusetts Institute of Technology, USA*

Abstract

Thin-walled, cylindrical structures are found extensively in both engineering and nature. Minimum weight design of such structures is essential in a variety of engineering applications, including space shuttle fuel tanks, aircraft fuselages, and offshore oil platforms. In nature, thin-walled cylindrical structures are often supported by a honeycomb- or foam-like cellular core, as for example, in plant stems, porcupine quills, or hedgehog spines. Previous studies have suggested that a compliant core increases the elastic buckling resistance of a cylindrical shell over that of a hollow cylinder of the same weight. We extend the linear-elastic buckling theory by coupling basic plasticity theory to provide a more comprehensive analysis of isotropic, cylindrical shells with compliant cores. The minimum weight design of a thin-walled cylinder with a compliant core, of given radius and specified materials, subjected to a prescribed load in uniaxial compression or pure bending is examined. The analysis gives the values of the shell thickness, the core thickness, and the core density that minimize the weight of the structure for both loading scenarios. The weight optimization of the structure identifies the optimum ratio of the core modulus to the shell modulus. The design of natural, thin-walled structures with cellular cores is compared to the analytical optimal, and the deviation about the theoretical optimum is explored. The analysis also discusses the selection of materials in the design of the cylinders with compliant cores, identifying the most suitable material combinations. Finally, the challenges associated with achieving the optimal design in practice are discussed, and the potential for practical implementation is explored.

Keywords: biomimetic, buckling, cellular, core, compliant, cylinder, shell, thin, wall.



Nomenclature

a	Radius to mid-plane of thickness shell	t_{eq}	Thickness of equivalent hollow shell
E	Young's Modulus of the shell	λ_{cr}	Value of λ minimizing critical axial load
E_c	Young's modulus of the core	ν	Poisson's ratio of shell
E_s	Young's modulus of the solid core	ν_c	Poisson's ratio of core
M_{ib}	Buckling moment of shell & core	ρ	Density of the shell
M_{eq}	Buckling moment of hollow shell	ρ_c	Density of the core
P_C	Axial failure load of shell & core the core	ρ_s	Density of the solid comprising
P_H	Axial failure load of the hollow shell material	σ_f	Critical failure stress of material
t	Thickness of shell with core buckling	ζ	Degree of ovalization at local buckling

1 Introduction

Throughout history man has been intrigued by natural phenomena. Inventors have drawn inspiration from Nature to achieve some of the most influential developments in history, ranging from the utilization of composites in structures to the innovation of the airplane. Over the past few decades, interest in applying nature's model to engineering design has rapidly increased. This has been manifest in the creation of the field of biomimetics, which seeks to develop a better understanding of natural organisms and apply this understanding to improve engineering designs.

Thin-walled, cylindrical structures are found extensively in both natural organisms and engineering components. In nature, thin-walled structures are often subjected to a combination of an axial compressive load and a bending moment. Because of their innately efficient design, they are highly susceptible to buckling failure, so natural structures have been optimized to resist buckling failure. Plant stems, animal quills, and bird feather rachis all have a thin-walled, shell supported by a honeycomb- or foam-like cellular core, which increases their resistance to buckling (Fig. 1). A cellular core acts to reduce the weight of the structure without compromising the structural stability or load capacity. We examine the applicability of extending nature's model into engineering structures where minimizing the weight of the structure is an essential component of design, such as space shuttle fuel tanks, aircraft fuselages, and offshore oil platforms.

Previous studies of elastic buckling have suggested a thin-walled shell, supported by a compliant core, can achieve a higher buckling load than an equivalent hollow shell of the same weight and radius both for axial compression and pure bending. Karam and Gibson [2] analyzed the elastic buckling of a thin-walled, isotropic, cylindrical shell with a compliant elastic core to develop a



simplified analysis for axisymmetric buckling in uniaxial compression and local buckling in pure bending. They determined the addition of a compliant core significantly increases the resistance of a shell to buckling failure.

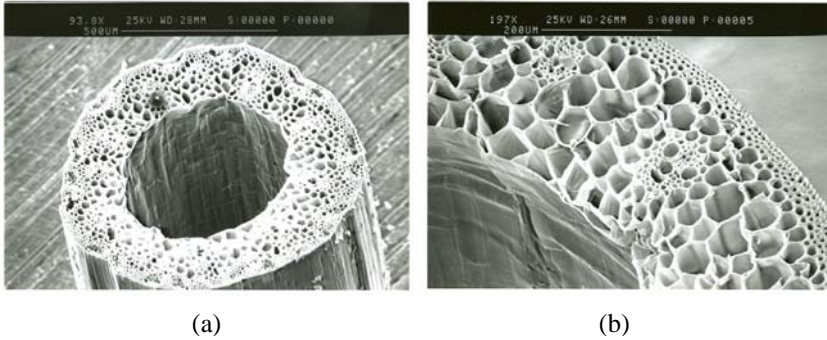


Figure 1: Micrographs of natural shell structure with compliant cores; Cross section of grass stem (*Elytrigia repens*) with a foam-like core.

In this paper, we extend the linear-elastic buckling theory from Karam and Gibson [2] by coupling basic plasticity theory to provide a more comprehensive analysis of isotropic, cylindrical shells with compliant cores. The goal is to examine the minimum weight design of thin-walled, cylindrical shells with compliant cores subjected to uniaxial compression and pure bending. For a given radius and length of the cylinder, required critical load, and shell and core materials, design equations for the shell thickness, the core thickness, and the core density that minimize the weight of the structure are presented. The improvement in the ratio of the critical load of the optimized shell with compliant core over an equivalent hollow shell of the same weight and radius is also examined for both uniaxial compression and pure bending, defined as $P_{[C]}/P_{[H]}$ and $M_{[C]}/M_{[H]}$, respectively. The optimized design for a shell with a compliant core presented here shows significant theoretical improvements over an equivalent hollow shell.

The design of natural, thin-walled structures with cellular cores is investigated and compared to this analysis. The functional utility, environmental stresses and material composition of natural structures is explored and contrasted with engineering designs.

This analysis further examines the feasibility of implementing compliant cores in thin-walled engineering structures where the weight to load bearing ratio is a critical element of design. The material and structural design constraints for this design in engineering structures are discussed, and the most advantageous engineering materials are presented. Based on the constraints, recommendations are developed and the potential for implementing compliant cores into thin-walled, engineering structures is discussed.



2 Optimal configuration

The optimization analysis describes the minimum weight design of a thin-walled cylindrical shell with compliant, cellular-solid core loaded in uniaxial compression or pure bending. The analysis assumes the radius and length of the cylinder, the required load capacity, and the materials of the shell and the core are given. The values of the shell thickness, the core thickness, and the core density that minimize the weight of the structure are determined.

A thin-walled shell with a compliant core has an overall radius a , length L , outer shell thickness t , inner core thickness t_c , and weight w . It is compared with an equivalent hollow cylinder of radius a , length L , wall thickness t_{eq} , and identical weight w in (Fig. 2). The outer shell of the cylinder with the compliant core and the hollow cylinder are made of the same isotropic material, with density ρ , Young's modulus E , material failure strength σ_f , and Poisson's ratio ν . Similarly, the core has density ρ_c , Young's modulus E_c , and Poisson's ratio ν_c .

2.1 Assumptions

We limit our analysis to thin-walled shells with large radius to thickness ratios, a/t . The materials under consideration are considered to behave linearly elastically up to the material failure, which we take to be deviation from linear elasticity. For simplification, Poisson's ratio has been evaluated for all of the figures and tables using $\nu = \nu_c = 0.3$.

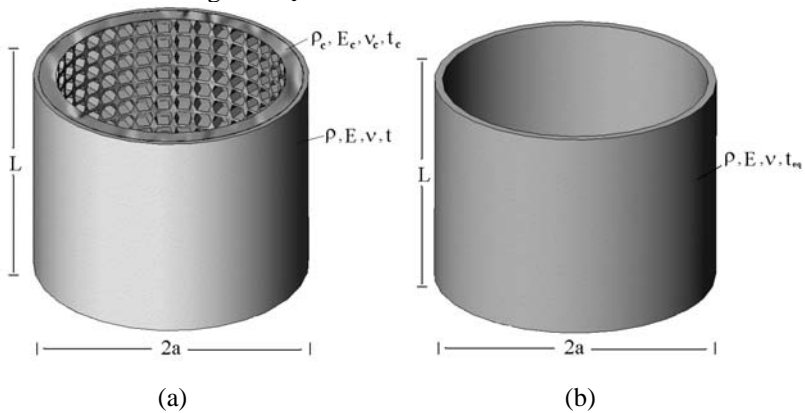


Figure 2: (a) A thin-walled cylindrical shell with a honeycomb core. (b) An equivalent thin-walled hollow cylindrical shell.

We also note that for the shell with a compliant core, the load is assumed to be entirely supported by the shell, and the compliant core behaves like an elastic foundation. This is justified by the fact that the core modulus in the plane of the load is negligible for both honeycomb and foam cores. According to Karam and Gibson [2], the stresses within the compliant core decay radially such that they become negligible at a depth into the core of 1.6 times the buckling half wavelength or $5\lambda_{cr}$. The thickness of the compliant core t_c is taken to be this



depth. The length of the shell L is also assumed to be at least several times the buckling half wavelength.

2.2 Transition regions

This analysis incorporates the possibility of material failure. If there is material failure of the hollow cylinder, then the axial load-carrying capacity of the cylinder with the compliant core will always be less than that of the hollow cylinder, since the shell thickness for the cylinder with the compliant core is always less than that of the corresponding hollow cylinder. A similar argument can be made for the case of pure bending where only negligible improvement is possible. Therefore, we only examine the two remaining failure scenarios where the hollow cylinder fails by elastic buckling and the corresponding shell with the compliant core fails by either material failure or elastic buckling. For the hollow shell to fail by elastic buckling eqn. (1) must be satisfied.

$$\frac{a}{t_{eq}} \geq \frac{E}{\sqrt{3(1-\nu^2)}\sigma_f} \quad \text{Uniaxial Compression} \quad (1a)$$

$$\frac{a}{t_{eq}} \geq \frac{.939E}{\pi\sqrt{1-\nu^2}\sigma_f} \quad \text{Pure Bending} \quad (1b)$$

At lower ratios of a/t_{eq} material failure occurs in the hollow shell, while at higher ratios failure is by elastic buckling. Evaluating Poisson’s ratio as 0.3 in eqn. (1b), shows the a/t transition for a hollow shell in pure bending is approximately one-half the value for axial compression. This lower transition allows for a larger variety of engineering materials to be used in the design of shells with compliant cores against failure in pure bending.

The transition of a shell with a compliant core, subjected to axial compression, between the buckling and material failure modes is found to depend only on the material properties of the shell and the core. Represented as a function of the core modulus to shell modulus ratio, it is given to be

$$\left(\frac{E_c}{E}\right)_{A-transition} = \frac{2(1+\nu_c)(3-\nu_c)(\sqrt{1-\nu^2})}{3} \left(\frac{\sigma_f}{E}\right)^{3/2} \quad (2)$$

As the ratio of the stiffness of the core to the stiffness of the shell is increased, the shell with the compliant core transitions to the material failure region. Assuming thin-walled structures with large a/t ratios, the transition for a shell with a compliant core, subjected to pure bending, between elastic buckling and material failure modes is given by

$$\left(\frac{E_c}{E}\right)_{B-transition} = \left(\frac{2}{3}\right)(1+\nu_c)(3-\nu_c)(\sqrt{1-\nu^2}) \left(\frac{\sigma_f}{(1-\frac{3}{2}\zeta)E}\right)^{3/2} \quad (3)$$

For large a/t ratios, the ovalization approaches zero, and the modulus transition ratios $E_c/E_{transition}$ for both axial compression and pure bending are identical.



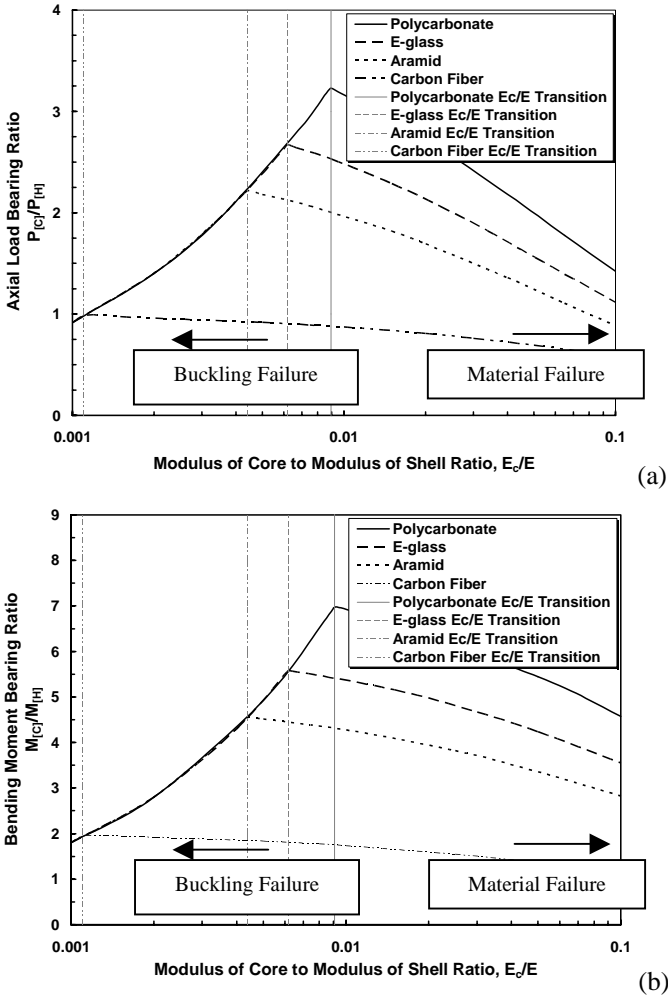


Figure 3: Load ratio plotted against the modulus ratio for a range of materials. For consistency, the shell and the honeycomb core are assumed to be made of the same material. All cylinders have equivalent radius to thickness ratios, $a/t=100$. (a) Uniaxial compression; (b) Pure bending.

2.3 Design configurations

The design problem presented contains non-linear equations with inequality constraints, requiring an analytical optimization for the minimum weight design to be a function of only one variable, which we selected to be the modulus ratio E_c/E . Assuming large radius to thickness ratios, maximizing the axial load ratio, $P_{[C]}/P_{[H]}$ and bending moment ratio, $M_{[C]}/M_{[H]}$ in both the material failure region and the buckling failure region reveals the optimal value of the modulus ratio is

always given by the transition modulus ratios in eqn. (2) and eqn. (3). The analysis assumes the shell and the core are made of the same material, but a parametric study reveals this analysis is valid for all engineering materials.

For large radius to thickness ratios, the optimal value for E_c/E , which maximizes the axial load ratio and moment ratio for both the material and buckling failure modes is given by

$$\left(\frac{E_c}{E}\right)_{optimum} = \frac{2(1+\nu_c)(3-\nu_c)\sqrt{1-\nu^2}}{3} \left(\frac{\sigma_f}{E}\right)^{3/2} \tag{4}$$

This analysis demonstrates that optimization of the improvement in the load ratio and moment ratio is independent of whether or not the core is a honeycomb structure or a foam structure. The improvement for a shell with a honeycomb core over an equivalent hollow shell is significantly greater than that for a shell with a foam core for any given a/t ratio and material combination; therefore, the focus of this analysis is on shells with honeycomb cores. The optimal modulus ratio is also independent of the radius to thickness ratio, a/t because it is incorporated into the analysis through the constraint given by eqn.(1). Furthermore, the optimization is valid for all isotropic structural material combinations. Fig. 3 demonstrates the material independence with four common engineering materials and their corresponding $(E_c/E)_{transition}$ values.

Table 1 provided for the convenience of the reader, shows the material properties used for this analysis. The optimization based on the maximum improvement for a given design implies minimization of the weight for a prescribed load.

Table 1: Material properties.

Engineering Material	Modulus, E (GPa)	Material Failure Stress, σ_f (MPa)	Density, ρ (g/cm3)
Polycarbonate	2.6	66	1.2
E-glass	38	750	1.8
Aramid	83	1300	1.4
Carbon Fiber	220	1400	1.7
Titanium	110	825	4.5
Aluminum	69	240	2.7

Sources: Data supplied by manufacturers and Shackelford [4].

Even though a shell with a compliant core may be optimally designed, it does not guarantee improvement over an equivalent hollow shell. A constraint for the minimum modulus ratio which results in improvement can be found. Assuming Poisson’s ratios are given as $\nu=\nu_c=0.3$ and t_{eq} is 15% larger than t (from typical experimental data), a conservative guideline is given to be:

$$\frac{E_c}{E} > \left[\frac{4}{3} \left(\frac{t}{a} \right) \right]^{3/2} \tag{5a}$$

Axial Compression



$$\frac{E_c}{E} > \left[\frac{2}{3} \left(\frac{t}{a} \right) \right]^{3/2} \quad \text{Pure Bending} \quad (5b)$$

For the cylinder with a compliant core to outperform an equivalent hollow cylinder the optimal modulus ratio given in eqn. (4) must satisfy eqn. (5). This equation is valid in both the buckling region and the material failure region. The minimum modulus ratio in pure bending is lower than the minimum modulus ratio in axial compression. This result is expected and supports the theory that a compliant core acts more to resist local buckling failure when subjected to pure bending than when subjected to axial compression. Therefore, we develop the optimal design of a cylinder with a compliant core against failure under axial compression.

Given that the optimal modulus ratio occurs when elastic buckling and material failure occur simultaneously, the optimal design for a shell with a compliant core can be determined. Equations (6-7) then give the core density, the shell thickness, and the core thickness that minimize the weight of a cylinder with compliant honeycomb or foam core for a prescribed axial load.

$$\rho_c = \rho_s \frac{2(1 + \nu_c)(3 - \nu_c)\sqrt{1 - \nu^2}}{3} \left(\frac{\sigma_f}{E_s} \right) \left(\frac{\sigma_f}{E} \right)^{1/2} \quad \text{Honeycomb} \quad (6a)$$

$$\rho_c = \rho_s \sqrt{\frac{2(1 + \nu_c)(3 - \nu_c)\sqrt{1 - \nu^2}}{3}} \left(\frac{\sigma_f}{E_s} \right)^{1/2} \left(\frac{\sigma_f}{E} \right)^{1/4} \quad \text{Foam} \quad (6b)$$

$$t = \frac{P}{2\pi a \sigma_f} \quad t_c = \frac{5P}{4\pi a \sigma_f} \left[\frac{E}{(1 - \nu^2)\sigma_f} \right]^{1/2} \quad (7)$$

3 Nature’s design

A study of thin-walled, natural structures with a cellular-solid core was conducted by Karam and Gibson (1994b). We examine the animal quills and spines, which most closely match the shell with compliant core designs discussed in this analysis.

3.1 Natural design vs. optimal configuration

The primary constituent of animal quills and spines is a family of proteins called keratin. While various types of keratin can co-exist in the same structure, quills and spines are taken to be composed of α -keratin. The mean failure stress and elastic modulus of compact alpha-keratin is taken to be 226 MPa and 2.52 GPa, respectively (Crenshaw, 1980). Based on these values, the optimal modulus ratio and the minimum modulus ratio in axial compression and bending can be determined. Table 2 demonstrates a comparison of the optimal modulus ratio to



the actual modulus ratio found experimentally (after Karam and Gibson [3]). The average experimental modulus ratio is 0.061 with a standard deviation of 0.036. The optimal modulus ratio of 0.060 demonstrates natural structures closely approach the analytical optimal design presented in this analysis. The apparently large standard deviation about the mean is expected. Natural structures are designed differently than engineering structures. In nature, porous structures are found to have extremely small cell-sizes on the order of 10-100 microns, which may be necessary for structural support during formation. Engineering structures are, practically, manufactured with much larger cell-sizes. In addition, natural structures often serve to provide greater utility than support alone supplying nutrients, providing the thermal regulation, and allowing for communication. Accounting for all of these functions surely will cause deviation from the structural optimization. Moreover, the material properties of keratin are highly dependent on temperature, humidity, and mechanical conditions, and keratin itself is a complex structure. Keratin is often modeled as a multiphase structure with a large range of elastic modulus; nearly all of the experimental data is within the range of corresponding optimal modulus ratios. Therefore, the functional utility of each structure, the environmental stresses acting on each structure, and the composition of the keratin in each species may account for the differences in core configuration, variations in the modulus ratio, and large standard deviation in the modulus ratio.

Table 2: Comparison of experimental, optimal, and minimum modulus ratios for animals.

Animal (genus/species)	Common Name	(a/t) ratio	Experim. (E _c /E)	Optimal (E _c /E) _{Op}	Axial (E _c /E) _{Mi}	Bending (E _c /E) _{Mi}
Coendou Prehensilis	Braz. Porc.	14.0	0.040	0.060	0.029	0.010
Erethizon	NA Porc.	18.0	0.016	0.060	0.020	0.007
Tachyglossus Aculeatus	Echidna	2.3	0.012	0.060	0.440	0.156
Hystrix Galeata	Echidna	17.6	0.047	0.060	0.022	0.008
Hystrix Idica-Cristata	Porcupine	9.5	0.052	0.060	0.052	0.018
Hystrix Subristatus	Porcupine	10.0	0.081	0.060	0.048	0.017
Erinaceus Europaeus	Hedgehog	13.7	0.100	0.060	0.030	0.011
Erinaceus Europaeus	Hedgehog	12.5	0.100	0.060	0.035	0.012
Hemichinus Spinus	Spiny Rat	12.7	0.100	0.060	0.033	0.012

*After Karam and Gibson [3].



4 Material design

The feasibility of this design has been examined for a wide variety of materials. The constraint given by eqn. (1) indicates materials with low E/σ_f ratios are ideal for the shell of the cylinder with the compliant core, such as polymers or select composites. Table 3 further demonstrates the importance of the ratio of the elastic modulus to the material failure strength in the shell material, referred to here as the intrinsic stability ratio. Shells made of materials with a low intrinsic stability ratio have the most substantial improvement in the axial load ratio and bending moment ratio from the addition of a compliant core.

Table 3: Load ratio and moment ratio for variable intrinsic stability ratios.

Engineering Material	$(E/\sigma_y)/(E/\sigma_y)_{\text{Polycarbonate}}$	$P_{[C]}/P_{[H]} (a/t=100)$	$M_{[C]}/M_{[H]} (a/t=100)$
Polycarbonate	1.0	3.2	7.0
E-glass composite	1.3	2.7	5.6
Aramid composite	1.6	2.1	4.5
Titanium	3.4	1.2	2.3
Carbon Fiber composite	4.0	1.0	2.0
Aluminum	7.3	1.0	1.0

The stability ratios, E/σ_y are normalized by that of polycarbonate. The shell and the core are assumed to be made of the same material.

5 Discussion

Analyzing natural phenomena has provided insight into engineering design throughout the millennia. This analysis discusses the applicability of extending nature’s model of thin-walled shells supported by a compliant, cellular core into engineering structures. The optimization of a shell with a compliant core displays promising results. We discovered the optimal configuration occurs when the shell with a compliant core is designed to fail in elastic buckling and material failure simultaneously. Tractable equations, which can be used to optimize the design of a cylinder with a compliant core based on a minimum weight design are provided. The constraints on the optimal modulus ratio reveal materials with the most potential for practical implementation have relatively low intrinsic stability ratios, such as polymers or select composites.

Natural, thin-walled structures provide support for much of the analysis. Furthermore, hedgehog spines, which exhibit a core structure resembling the honeycomb design, prove to have a greater resistance to buckling than porcupine quills, which exhibit a core structure resembling the foam design. Experiments have also shown that the average modulus ratio of animal quills and spines is nearly identical to the optimal modulus ratio discussed here and may only differ due to the need for functionality in addition to structural support. Moreover, natural structures also reveal shells with compliant cores are more effective at



increasing the resistance to buckling when subjected to a bending moment than when subjected to an axial load.

6 Conclusion

Theoretically, the optimized shell with a compliant core demonstrates substantial improvement in weight savings over a comparable hollow shell. However, this design is only practical for implementation in structures requiring large radius to thickness ratios, where the weight to load ratio is a critical element of design. Therefore, it is feasible to consider implementation of this design in relatively large scale engineering structures, such as space shuttle fuel tanks, aircraft fuselages, and offshore oil platforms. Natural structures support this optimization, indicating the optimized shells with compliant cores have enormous potential to be a competitive technology in select engineering structures.

Acknowledgements

Financial support for this project was provided by the National Science Foundation (Grant Number CMS-0408259), for which we are grateful. This research was performed while on appointment as a U.S. Department of Homeland Security (DHS) Fellow under the DHS Scholarship and Fellowship Program, a program administered by the Oak Ridge Institute for Science and Education (ORISE) for DHS through an interagency agreement with the U.S. Department of Energy (DOE). ORISE is managed by Oak Ridge Associated Universities under DOE contract number DE-AC05-00OR22750. All opinions expressed in this paper are the author's and do not necessarily reflect the policies and views of DHS, DOE, or ORISE.

References

- [1] Crenshaw, D.G. (1980). *The Mechanical Properties of Biological Materials*. Symposia Soc. Exp. Biology XXXIV. Cambridge University Press, Cambridge.
- [2] Karam, G. N. and Gibson, L. J. (1994). Elastic buckling of cylindrical shells with elastic cores—I. analysis. *Int. J. Solids Structures* **32**, 1259-1283.
- [3] Karam, G. N. and Gibson, L. J. (1994). Biomimicking of animal quills and plant stems: natural cylindrical shells with foam cores. *Material Sci. & Eng.* **C2**, 113-132.
- [4] Shackelford, J. (2000). *Material Science for Engineers*. Prentice Hall, New Jersey.



This page intentionally left blank

Designing new lubricant additives using biomimetics

A. Morina, T. Liskiewicz & A. Neville

*Corrosion and Surface Engineering Research Group,
School of Mechanical Engineering, University of Leeds, Leeds, UK*

Abstract

Nature produces some complex nanocomposite structures having the following properties, self-healing capability, functional gradation and smartness. These properties are all required of tribofilms in the field of lubrication technology where their structure, formation and removal rate and smartness are key to their ability to maintain fuel economy and durability. In this paper the potential for using biomimetic principles in the field of tribology and specifically as a means of improving tribological performance in the boundary lubrication regime is investigated. The paper initially describes the challenges associated with operating tribological contacts in the boundary lubrication regime, assesses the need for new approaches to lubrication and gives a preliminary appraisal of biomimetic principles applied to this engineering problem.

Keywords: biomimetics, tribology, tribofilm, TRIZ, bionanocomposites.

1 Introduction

1.1 Setting the scene – current situation in lubricant additive technology

It is perhaps surprising that a link can be made between claims from ecologists, (reported in the national press [1]) that 1,000,000 species could be extinct in the next decade and engine lubrication. However, passenger and commercial light vehicles have been estimated [2] to account for 20% of the total CO₂ delivered into the atmosphere from hydrocarbon sources in the US and other developed countries. When the population of vehicles in the western world is considered, it is perhaps easier to see how a realistic link between tribology and ecology can be made. According to recent UK government statistics [3], in 2000 in the UK alone



there were 29 million motor vehicles registered for use on the public highway. International numbers are even more impressive, with the total number of road vehicles in service in Europe, Japan and the USA in 1999 being of the order of 530 million. Bearing in mind that this total excludes all of Asia except Japan, former Soviet block countries, Australasia, Africa and South America then the staggering scale of the use of the reciprocating internal combustion engine becomes clear.

On a global scale there is a real urgency to achieve step changes in the level of CO₂ emission. Reduction of CO₂ emissions is achieved by increasing fuel economy and, as summarised by Okuno and Bessho [4] there are several means of achieving “good gas mileage” (Figure 1). Advances are being made in both areas 1 and 2 as defined in Figure 1. With respect to 2, weight reduction and reduced aerodynamic resistance [5] have been instrumental in achieving the 30% reduction in fuel consumption of the new Volkswagen Lupo 3L TDI. As material development continues at an alarming rate and evermore new alloys [6], composites and nano-engineered structures are developed and embraced by the automotive sector [7], it is expected that the trend will continue.

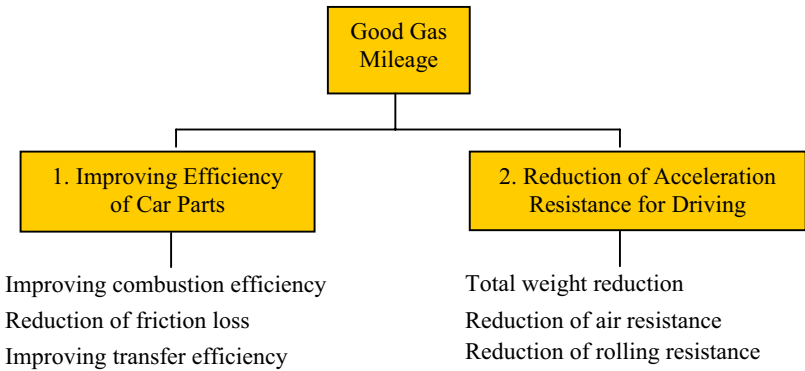


Figure 1: Techniques for improving fuel economy [4].

However, by far the greatest challenges for engineers in terms of maintaining engine performance are associated with area 1 and, in particular, with components operating in the **boundary lubrication regime**. It is in this regime that metal-to-metal asperity contact occurs and high friction and wear rates ensue if proper protection, in the form of lubricant additives, is not used.

Understanding the nature of the additives used in formulated engine oils to reduce wear, lower friction, maintain engine cleanliness and reduce soot formation has been the subject of much research since the advent of commercial lubricant additives in the early 1940s. Dominating in this respect has been the anti-wear additive Zinc DialkylDithioPhosphate (ZDDP).

It is critical to understand a few aspects of tribology in the boundary lubrication regime if the challenge of replacing boundary lubricant additives is fully appreciated. The performance of the contact in terms of friction and wear



are dependent on the formation of a **tribofilm**. The tribofilm is a very thin layer (in the order of tens of nanometres) which covers the asperities and prevents direct metal/metal contact. Work to characterise the tribofilm has been successful in terms of being able to understand its structure, chemical composition and mechanical properties. One example of a schematic representation of the tribofilm is presented in Figure 2.

Of key importance to this proposal are the following aspects of the tribofilm

- It **spontaneously forms** through intimate contact/interaction between the surface and the lubricant additives
- It has a **layered structure on a nanometric scale** comprising a base glassy structure and an upper organic-rich layer.
- It is **self-healing**
- It is **smart** – it reacts to changes in load, temperature, pressure, sliding speed

All in all the tribofilm is an example of the **ultimate smart, nanocomposite material**.

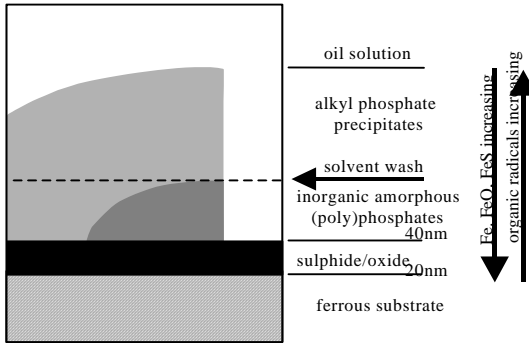


Figure 2: Schematic representation of tribofilm layered structure [8].

The fact that the film has all these amazing attributes is by accident rather than any so called molecular engineering when the lubricant additive was first derived. There is no literature to account for the development of the ZDDP anti-wear additives which have been the workhorse for lubricant technology for over 60 years.

Now that radical changes in lubricant additive technology are being forced on formulators, primarily through changes in legislation, there is a need for a more radical, innovative and risky approach to new additive design. Incremental steps are being made to get towards environmentally-acceptable solutions to achieve target CO₂ emissions, alongside retained engine performance but these are unlikely to deliver any more than an incremental move to keep in line with the shifting targets imposed by government. As examples:

- The level of P has progressively decreased from 0.12wt% in 1993 for ILSAC (International Lubricant Standardization and Approval




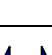

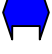


Committee) GF-1 oils, to 0.1wt% in 1996 and 2001 (GF-2 & 3) and it will be further reduced to 0.08wt% when GF-4 is introduced.

- The CHON concept (lubricating engines with only Carbon, Hydrogen, Oxygen and Nitrogen) has been introduced by formulators although no real progress in this respect has been made
- Alternative additives, some based on e.g B, are being introduced to replace some of the functionality of P. Future legislation on B-containing compounds is not yet clear

To use biomimicry to develop a new generation of lubricant additives challenges conventional thinking with respect to additive design.

Table 1: Rationale for choosing the biomimetic approach.

Natural Materials/Biological Systems		Tribology/Tribofilm Analogies
Nature provides us with infinite examples of where reactions spontaneously occur as a result of surface/environment interactions		Tribofilm formation is critically controlled by the nature of surface/environment interactions
Numerous organic/ceramic composites (or O-I hybrids) are seen in nature (e.g. proteins and polysaccharides with calcium carbonate produced at a cellular level; molluscs [12] ; coccolithophores [13])		Their structures can be viewed as potential tribofilm materials since the key component of a tribofilm is the blend of inorganic glass/organic material
Biocomposites often have complex layered structures with functional gradation (Figure 3). Their structure is controlled by constituents of the surrounding fluid (e.g proteins (silaffins) controlling silica structure growth)		The successful formation of tribofilms depends on the ability of layers with low shear strength and layers with high strength and toughness to co-exist in a complex arrangement. Their structure depends on the constituents in the lubricant and their surface reactivity.
In biomineralisation the biomolecules catalyse and direct the synthesis of organic networks to produce hybrid structures (often with stunning complexity)		In tribofilm formation one key aspect is the replenishment of reactants at the surface to continually re-form and repair the film
Natural structures (e.g plants) can adapt in real time to their environment. They sense the data, process the data and respond.		For tribofilms to be fully effective they must be able to react to their environment – they must sense for example cold start conditions, production of wear debris, changing lubrication regime
Nature presents renewable structures from inorganic and organic structures (e.g ormosils) [14]		Tribofilms must be renewable from sources within the lubricating fluid. Formation and replenishment rates are key to sustainability.



2 Synthesising natural bionanocomposites

2.1 Rationale for using nature as lead

There are many examples of the successful use of biomimicry for the derivation of new structural materials such as ceramics with improved toughness based on mother of pearl [9], underwater adhesives based on mussel adhesives [10] and adhesive tape based on the Gecko foot mechanism [11].

However, no applications in boundary lubrication tribology exist. A clear distinction between this approach and the vast work on biotribology must be made. In biotribology, the tribological performance of biological systems is evaluated. In this current paper the focus is entirely different; the aim being to assess the feasibility of using complex biocomposites as a basis for synthetic derivatives for **real** engineering tribological systems. These demand stability at high temperature, high pressures, high shear rates – not at all the same requirements for biotribology systems.

Biocomposites are proposed as the route towards achieving this step change in lubricant technology rather than nanocomposites *per se* due to their inherent potential for greenness – a feature of major importance for tomorrow’s lubricants.

So why is there even a glimmer of hope that new generation lubricant additives can be derived using this approach? In Table 1 the analogies between tribofilm characteristics (i.e. requirements) and natural biomaterials are given which provide an indication of some potential areas for progress to be made.

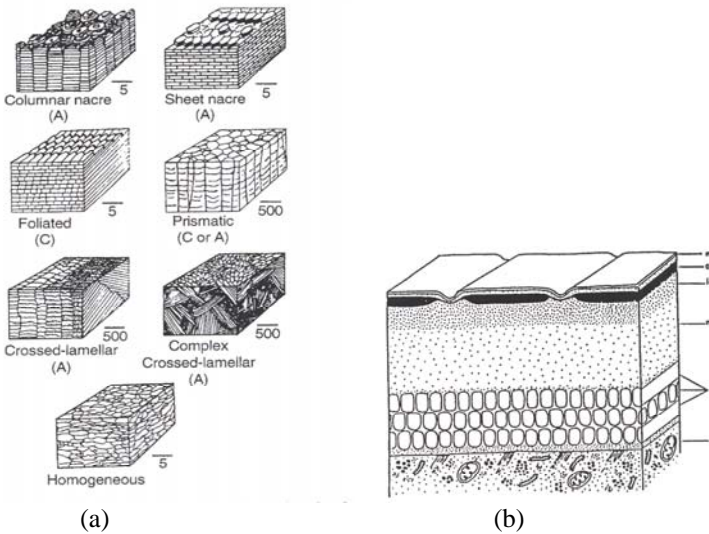


Figure 3: (a) Types of mollusc shell material [15]. Illustrating the complexity of the composite structures (b) Outer covering of roundworm skin – nanocomposite properties and functional gradation are evident [16].



2.2 Identifying bio-systems with potential for mimicry in lubrication systems

The strategy applied to accomplish the aim of this work, which can be summarised as, “to solve lubrication problems through synthesising natural-derived bionanocomposites”, involves work in two directions:

1. Identification of natural systems where there is a lubrication process and study the mechanism of lubrication. This involves conducting case-studies which will result in selecting natural material systems to be used as models for synthetic efforts.
2. Identification of the mechanisms used in nature for providing self-healing structures and “smart” materials and study the possibilities to mimic the mechanisms used to form them and not completely the structure. This involves the use of a molecular biomimetics concept [17] to bridge the materials-biology gap. Using this concept, hybrid materials that would replace current tribofilms could be potentially assembled from the molecular level.

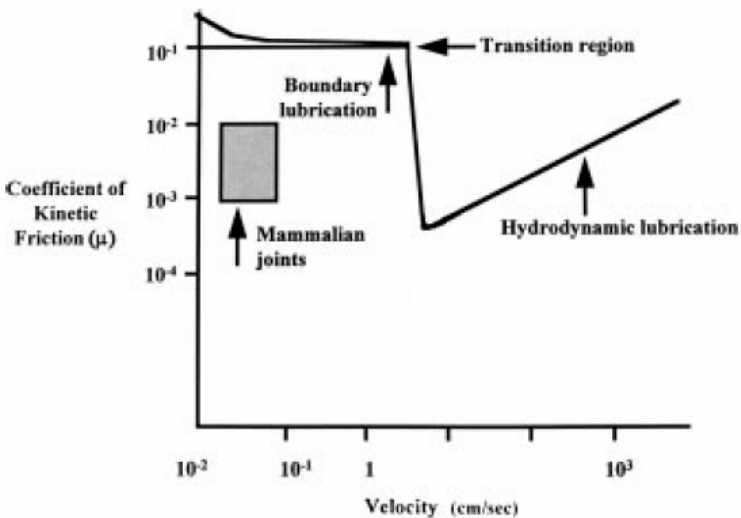


Figure 4: Mammalian joints friction in Stribeck curve.

These two directions are interconnected since most lubricated systems in nature use materials with unique properties.

The most obvious example is the lubrication in mammalian joints. Figure 4 shows the relation of the friction coefficient in these joints with the friction values obtained by existing technology in a Stribeck curve [18]. This demonstrates how either hydrodynamic lubrication needs to be extended to velocities two orders of magnitude lower or the natural boundary lubricants are superior to their synthetic counterparts by much the same margin [18]. The low

friction in these joints shows the remarkable solution provided by nature. Analysing the lubrication characteristics of this very effective lubricated system in nature, it can be seen that materials lubricated and the lubricant are considered as a single system (interaction of articular cartilage with synovial fluid).

There is still a great debate about the definite mechanism of lubrication in joints [19] but whichever mechanism is applied it can be of great importance to lubrication of engineered materials. Nature has solved the friction problem in mammalian joints by either maintaining a hydrodynamic lubrication through using a special material (articular cartilage) or/and producing a very effective boundary film on the surface of the articular cartilage. Industry has begun to appreciate that efficient lubrication of engine components cannot be achieved solely by improving the lubricants and their chemical composition but a “system solution”, involving both the surface to be lubricated and the lubricant should be applied [20], a concept which is applied in nature.

3 TRIZ – helping to solve the problem?

Designing new lubricant additives using biomimetics principles represents a challenging problem and progress towards solving this problem requires a structured way of thinking and transferring ideas between biology and engineering [21]. To support this the original problem solving methodology TRIZ (Teoriya Resheniya Izobreatatelskikh Zadach), which is a Soviet initiated Theory of Inventive Problem Solving [22] is being used. TRIZ is a mixture of philosophy, methodology and specific tools which all together make the research process significantly quicker, more effective but mainly much more innovative than traditional Western methods, like brain storming or lateral thinking. The power of TRIZ comes from a key finding that all of the world’s most outstanding solutions emerge from a repeatable, very small number of inventive principles. These have been identified using the knowledge and experience of former inventors through a study of more than 3 million successful patents to date.

3.1 Problem definition

TRIZ provides a number of tools not only to solve, but initially to properly define, a problem. The definition stage is crucial for successful output of each project and is usually harder and longer to complete than the second, solution stage. From the choice of different problem definition tools offered by TRIZ, such as Problem Explorer, Function/Attribute Analysis, S-Curves and Ideal Final Result, the S-Curves methodology has been adopted in this project in order to identify how mature the current lubrication technology system is (Figure 5(a)). The S-Curve depicts the level of ideality of a system as a function of time. Generally ideality is defined as the benefits divided by a sum of cost and harm. In our case the *benefits* are related to low friction and low wear, *cost factor* to lubrication expense and *harm factor* to environmental issues. TRIZ recommends that the S-Curve is analysed in order to determine how ideal the current system is and, as a result, to decide if there is potential for further development or whether a novel (and often radical) approach is required.



The analysis of current lubrication technology suggests that for a number of reasons the current system is in the *retirement* phase. The conception of lubrication can be dated back to Ancient Egypt civilisation when some olive oil was poured under the runners of great sledges dragged along by sleeves to reduce friction. Nevertheless, the birth of real lubrication technology coincides with the technical revolution at the beginning of the twentieth century. The sudden growth of main classes of lubricant additives took place in the 1930s and 1940s when the need for well-lubricated and reliable machines increased rapidly, partly due to wartime demands (Figure 5(b)). From the 1950s until now lubrication technology has constantly been developed. Significant progress towards optimising current additive technology has been made in parallel with chemical characterisation tools evolving. “Design” of additives was made possible once key functionality of additives was delivered. Molecular modelling introduced into this area in the last 10 years has added to the capabilities of synthetic chemists in being able to design and make functional additives. There is little doubt that the speed at which lubricant additive technology is evolving has slowed in the last decade – partly due to the ever-increasingly stringent legislative constraints imposed on additive manufacturers. Taking into account that official legislations force further reduction of phosphorus and sulphur, the ideality of a lubrication technology is likely to drop from the current level as the removal of those compounds will dramatically decrease the benefits unless effective replacements are found.

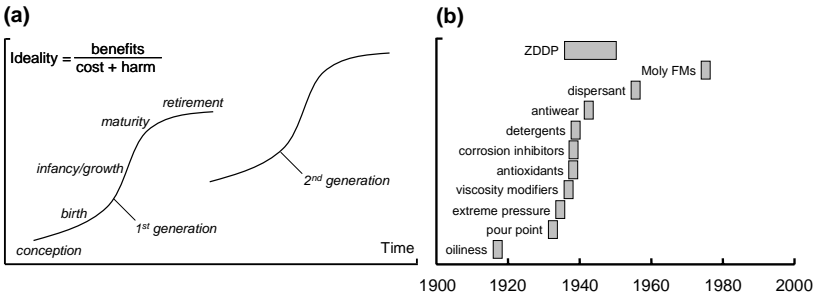


Figure 5: (a) S-Curve characteristics; (b) chronology of development of main classes of lubricant additive [23].

Summarising the S-Curve analysis for a current lubrication technology, there is little scope for the development of a present system and so the most likely way to improve the ideality is through introduction of a new approach. The next generation technology will be characterised by another S-Curve and the initial ideality is likely to be even lower than that for a current system. Nevertheless, it will be on the first - concept stage, from which the ideality will evolve with time according to the S-Curve shape to yield longer term benefits.

3.2 Problem solution methodology

Finding the problem solution using the TRIZ methodology is the next stage of the project. Generally to benefit from rich TRIZ opportunities, the specific



problem needs to be reformulated into an abstract domain (Figure 6), where all TRIZ problem solution tools can be applied: Technical and Physical Contradictions, S-Field Analysis, Laws of Technical Evolution, Resource Identification, Algorithm for Problem Solving, Trimming and Subversion Analysis. To define the desirable specific solution the general solution provided by TRIZ has to be interpreted in the light of an examined problem. The way between Problem and Solution through the TRIZ process in Figure 6 seems to be longer than the direct one, however in practice it has been found to be much quicker and efficient [22], it also generates novel ideas which have not previously been identified.

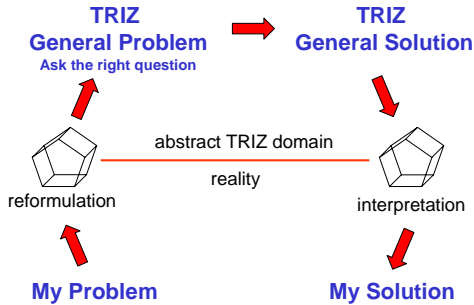


Figure 6: General problem solution path defined by TRIZ researchers.

4 Remaining challenges and future look

The application of biomimetic principles in tribology is new and poses some great challenges to engineers and scientists. This preliminary study has identified that there is potential to learn from nature in the area of bionanocomposites – thus opening the door to find solutions to lubrication in engineering from nature. There is however some way to go before current additive technology is replaced. To assist in the transfer of ideas between nature and technology, TRIZ has clearly enabled the problem to be defined. The next stage is to use TRIZ to help in the problem solution.

References

- [1] The Independent: Revealed: how global warming will cause extinction of a million species. January 8th 2004.
- [2] http://www.ems.org/energy_policy/cafe.html.
- [3] DTLR (Department of Transport LGatR, Transport Statistics Great Britain 2001, The Stationery Office, London, 2001.
- [4] Ukuno K, Bessho T: Need for environmentally friendly surface modification technology in the Japanese automotive industry. *Surface Modification Technologies XIV*, Ed T S Sudershan and M Jeandin, ASM International:135-140, 2001
- [5] Curro S: Economical and earth-friendly, the Lupo 3L TDI, AL Alluminio E Leghe.119-121, 2000



- [6] Powell R: The USAMP Magnesium powertrain cast components project. *JOM*:49-51, 2002
- [7] Presting H, Konig U: Future nanotechnology developments for automotive applications. *Materials Science and Engineering, C* 23:737-741, 2003
- [8] Bec S, Tonck A, Georges JM, Coy RC, Bell JC, Roper GW: Relationship between mechanical properties and structures of zinc dithiophosphate antiwear films. *Proc R Soc Lond A*, 455:4181-4203, 1999
- [9] Jackson AP, Vincent JFV, Turner RM: A physical model of nacre. *Composites Science and Technology*, 36:255-266, 1989
- [10] Holl SM, Hansen D, Waite JH, Schaefer J: Solid-state NMR analysis of cross-linking in mussel protein glue. *Arch Biochem Biophys*, 302:255-258, 1993
- [11] Geim AK, Dubonos SV, Grigorieva IV, Novoselov KS, Zhukov AA, Shapoval SY: Microfabricated adhesive mimicking gecko foot-hair. *Nature Materials*, 2:461-463, 2003
- [12] Aizenberg J, Lambert G, Addadi L, Weiner S: *Adv Materials*, 8:222, 1996
- [13] R. N. Pienaar in A Winter WGSC, Cambridge University Press, New York, p13, 1994
- [14] Castelvetro V, Vita CD: Nanostructured hybrid materials from aqueous polymer dispersions. *Advances in Colloid and Interface Science*, 108-109:167-185, 2004
- [15] J. F. V. Vincent, Ceramics from invertebrate animals, in Handbook of Elastic Properties of Solids, Liquids and Gases, edited by Levy, Bass and Stern, Volume III: Elastic Properties of Solids: Biological and Organic materials, Earth and Marine Sciences, 2001.
- [16] Vincent JFV, Jeronimidis G, Topping BHV, Khan AI: The mechanical design of skin - towards the development of new materials. 1991.
- [17] Sarikaya M, Tamerler C, Alex K -YJ, Schulten K, Baneyx F: Molecular biomimetics: nanotechnology through biology. *Nature Materials*, 2:577-585, 2003
- [18] Hills BA: Boundary lubrication *in vivo*. *Proc Instn Engrs Part H*, 214:83-94, 2000
- [19] Furey JM: Joint lubrication. In: *The biomedical engineering handbook*. Edited by Bronzino JD: CRC Press LLC; 2000.
- [20] Erdemir A: Review of engineered tribological interfaces for improved boundary lubrication. *Tribology International*, 38(3):249-256, 2005
- [21] Vincent JFV, Mann DL: Systematic technology transfer from biology to engineering. *Phil TransRSocLondA*, 360:159-173, 2002
- [22] Altshuller G: Creativity as an exact science. New York: Gordon & Breach; 1984.
- [23] Spikes H: The history and mechanisms of ZDDP. *Tribology Letters*, 17(3):469-489, 2004



Preparation, microstructure and properties of biomimetic nanocomposite coating

L. Q. Ren¹, Y. Liu¹, S. R. Yu², Z. W. Han¹ & H. X. Hu²

¹*The Key Laboratory for Terrain-machine Bionics Engineering, The Ministry of Education, Jilin University, People's Republic of China*

²*College of Materials Science and Engineering, Jilin University, People's Republic of China*

Abstract

Bamboo is a typical natural composite material, and its special structure and excellent properties provide important information for the biomimetic design of composites. To strengthen the fiber content of bamboo distributed in a gradient, a biomimetic nano- Al_2O_3 composite coating was designed and prepared on the surface of metal parts using a nanocomposite electrodeposition method. The optimal technology parameters were obtained, such as current density, PH value, nano- Al_2O_3 content in electrolyte, and style of stirring etc after the experiments. The microstructure of the biomimetic nanocomposite gradient coating was very dense, and the contents of nano- Al_2O_3 were distributed in the gradient. The microhardness of the composite coating changed from the surface to the inside in the gradient also. Moreover, the wetting angle between water and composite coating obviously increased and reached 97° at room temperature.

Keywords: nanocomposite coating, biomimetic, preparation, microstructure, properties.

1 Introduction

The bamboo is a typical example of a naturally occurring composite material. The structural character, mechanical properties, and wear resistance of bamboo and the biomimetic application of bamboo structures have been widely used in biomimetic material fields in recent years. The special structure and excellent properties of bamboo have yielded important information for the biomimetic



design of advanced composites, and an important progress in the research field was made.

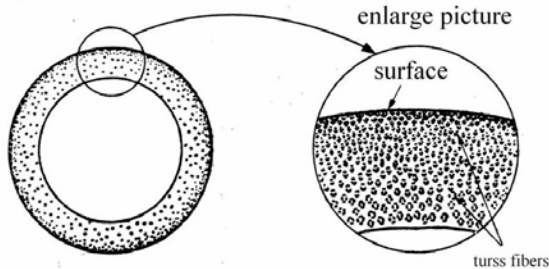


Figure 1: The structure of bamboo's cross-section [1].

The microstructure of bamboo mainly includes thick-walled cells and thin-walled cells. The thick-walled cells provide the strength of bamboo, referred to as truss fibers, and the thin-walled cells constitute the matrix of bamboo [2]. The hardness of truss fibers is higher than the matrix. The wear resistance of bamboo's surface is improved due to the content of truss fibers decreases gradually from the surface to interior. Corresponding to bamboo's microstructure character, the content of nano- Al_2O_3 in the biomimetic nanocomposite coating varies from the surface to the interior, and this structure avoids the bad interface bonding and illogical stress distribution induced by the sudden change of the structure and properties.

According to the structural character of nature biomaterials such as bamboo, where the strengthening phase is distributed in the matrix, a kind of new biomimetic gradient nanocomposite coating was designed and prepared by using a bionics viewpoint and a nanocomposite electrodeposition method. The composition in the coating distributes in gradient from the substrate to the surface of the coating. A good bonding between the coating and substrate was obtained. The coating surface is hydrophobic, and its hardness is high.

2 Preparation of biomimetic Nano- Al_2O_3 /Ni-cCo gradient composite coating

2.1 Choice of coating materials

The nanocomposite coating consisted of matrix metal and nano-grains. Ni was chosen as the matrix metal, and a small amount of Co was added. Nano- Al_2O_3 particles were chosen as the second phase nanograins. Compared with micro-grains, the nanograins have special properties due to dimension character. The surface effect is the dominant factor [3]. The average granularity of nano- Al_2O_3 is 60nm, with a purity greater than 99.99%, specific surface area $180 \pm 10 \text{ m}^2/\text{g}$, and physical phase γ - Al_2O_3 .





Figure 2: Morphology of nano γ - Al_2O_3 .

Watt electrolyte is widely used in plating Ni and consists of NiSO_4 , NiCl_2 and H_3BO_3 . To prevent pinholes, a small amount of wetting agent, such as $\text{Na}_2\text{SO}_4 \cdot 12\text{H}_2\text{O}$, is usually added. The advantages of the electrolyte are that it is cheap and easy to operate and safeguard. The brittleness and inner stress of the coating were small, and the speed of deposition was quicker.

2.2 Optimization of the preparing technology parameters of nanocomposite coating

In the course of composite electrodeposition, the optimal technology parameters were necessary to obtain a high quality coating. The optimal technology parameters, such as the current density, stir method, pH value and temperature of electrolyte, time and the content of nanoparticles etc, largely affected the quality of coating in the electrodeposit experiment after the electrolyte was determined. The optimal technology parameters were obtained by orthogonal testing, and they are the current density of $4\text{A}/\text{dm}^2$, pH value 3~4, electrolyte temperature 40°C ~ 50°C , the content of nano- Al_2O_3 in electrolyte 20g/l, and the stirring method used was a mechanical stir with ultrasonic vibration.

2.3 The preparation method of biomimetic Nano- Al_2O_3 /Ni-Co gradient composite coating

The biomimetic nano- Al_2O_3 /Ni-Co gradient composite coating was prepared on the surface of metal parts. Firstly, Ni-Co alloy without nano- Al_2O_3 was plated for

30min. Then nano- Al_2O_3 was slowly added to the plating solution in the amount of 10g/l and plated for 50min. The mechanical stir and ultrasonic vibration were employed together.

Finally more nano- Al_2O_3 was slowly added to the plating solution in the amount of 10g/l and the content of nano- Al_2O_3 in the plating solution was increased to 20 g/l, then the plating was carried out for 50min.

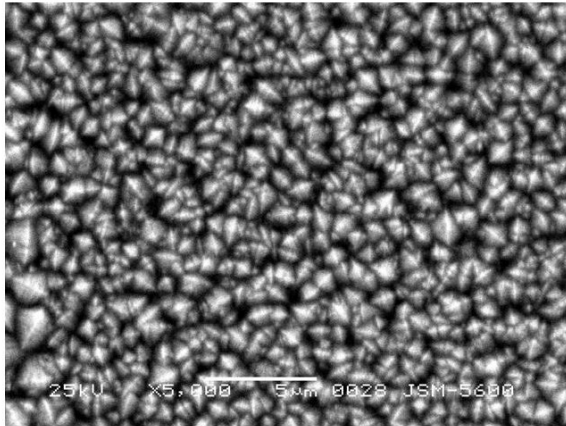


Figure 3: Morphology of Ni-Co coating surface without n- Al_2O_3 .

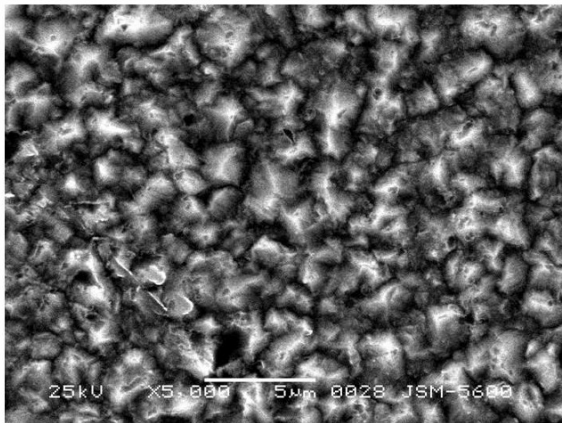


Figure 4: Morphology of n- Al_2O_3 /Ni-Co nanocomposite coating surface.

3 The microstructure and composition of biomimetic gradient n-Al₂O₃/Ni-Co nanocomposite coating

3.1 Morphology of Ni-Co coating and n-Al₂O₃/Ni-Co composite coating

The morphology of the biomimetic nanocomposite coating surface was observed by means of SEM (JSM-5500LV Japan electronic) (as shown in Fig. 3 and Fig. 4). Compared with a Ni-Co coating, the sizes of crystal grains in the n-Al₂O₃/Ni-Co nanocomposite coating largely decrease due to the dimension effect of nanoparticles. The highly active surface of nanoparticles provides an amount of nucleus for Ni atoms in the process of electrodeposition. The overpotential of the metal forming nucleus reaction decreases. A composite coating with a fine and dense microstructure was obtained because of the higher nucleation rate [5].



Figure 5: Cross section of the biomimetic gradient n-Al₂O₃/Ni-Co nanocomposite coating on the surface of metal metallurgy parts.

3.2 Analysis of the composition for biomimetic gradient n-Al₂O₃/Ni-Co nanocomposite coating

The cross section of a biomimetic gradient nanocomposite coating on the surface of metal parts was polished and then was eroded with a 4% HNO₃ alcohol solution. The microstructure of coating section was observed by means of SEM, and the content of the elements was measured by means of energy spectrum. The results show that the thickness of the coating is 82.8 μm, and the content of

elements at the different positions on the section changes in gradient (as shown in Fig. 5). Table 1 showed the element contents of different positions in coating. Al(wt%) was the most abundant element in the nano- Al_2O_3 in the coating. The result indicated that the content of Al element is the highest in the upper layer (a) of coating, the content of Al element in the middle layer (b) is less than the upper layer, and the bottom of coating only contains Ni-Co without Al. Therefore, the nano- Al_2O_3 content changes in gradient.

Table 1: Distribution of elements in the composite coating.

Element content Section parts	Al (wt%)	Co (wt%)	Ni (wt%)
A (upper layer)	1.35%	9.88%	88.77%
B (middle layer)	0.8%	11.88%	87.32%
C (bottom layer)	0	8.5%	91.5%

4 Properties of biomimetic gradient n- Al_2O_3 /Ni-Co nanocomposite coating

4.1 Microhardness

The microhardness of the composite coating was measured with microsclerometer (HXD-1000TM). Fig. 6 shows the distribution of microhardness of the biomimetic nanocomposite coating from the upper layer to the bottom layer. The result indicated that the upper layer, from the coating surface to a depth of $20\mu\text{m}$, contains the most nanoparticles, is the hardest and its microhardness was $400\sim 600\text{Hv}$. The content of nanoparticles decreases in the middle layer, from $20\mu\text{m}$ to $65\mu\text{m}$, and its microhardness was $300\sim 400\text{Hv}$ and lower than that of the upper layer. It forms a bottom layer (purity Ni-Co layer), from $65\mu\text{m}$ to $80\mu\text{m}$, the microhardness was $130\sim 300\text{Hv}$. It forms the substrate when the distance is more than $80\mu\text{m}$ away from the surface. Consequently, the microhardness of the composite coating changes in gradient from the coating surface to the substrate due to of the change in concentration of nano- Al_2O_3 .

4.2 Wettability

The wettability between water and the biomimetic gradient n- Al_2O_3 /Ni-Co nanocomposite coating on metal parts surface was determined by measuring the static contact angle of a water droplet (2-3mm diameter) on the nanocomposite coating surface using JC2000A Interface Tension/Contact Angle Measure Equipments (Powereach, China). The experiment was made at 20°C . The result shows that the wetting angle is up to 97° (as shown in Fig 7), whereas the metal



parts are usually hydrophilic after removing oil and other impurities from the surface. So the nanocomposite coating developed has improved water repellence.

There are two main reasons why the coating is hydrophobic. The one is that the surface morphology of the composite coating, which looks like particles or a cauliflower, is different from that of metal parts and belongs to the geometrical non-smooth surface; the another reason is that nano- Al_2O_3 grains in the coating are hydrophobic.

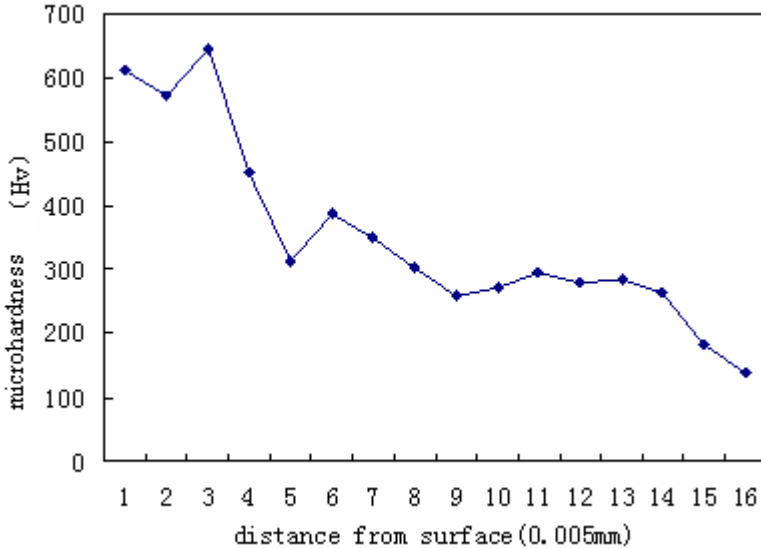


Figure 6: Distribution of microhardness in the biomimetic gradient nanocomposite coating.

5 Conclusions

(1) According to the characteristic gradient distribution of strengthening fibers in bamboo, biomimetic nano- Al_2O_3 composite coatings were designed and prepared on gray cast surface using a nanocomposite electrodeposition method. The optimal technology parameters were obtained from experiments.

(2) The microstructure in the biomimetic nanocomposite gradient coating is dense, the grains are fine, and the contents of nano- Al_2O_3 are distributed in gradient.

(3) The microhardness of the nanocomposite coating changes in gradient. Moreover, the wetting angle between water and the composite coating increases obviously and reaches to 97° at room temperature.



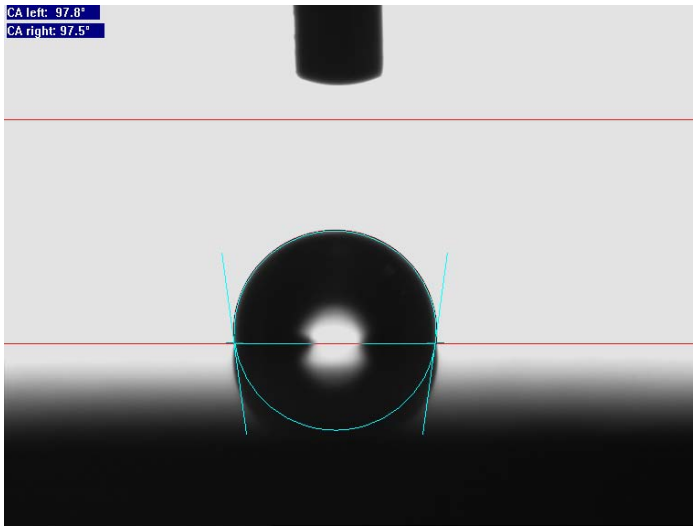


Figure 7: The wetting angle between water and the biomimetic gradient nanocomposite coating.

Acknowledgements

The authors are grateful for the financial support provided by Trans-Century Training Program Foundation for the Talents by Chinese Ministry of Education (2003) and the Foundation for Distinguished Young Scholars of Jilin Province (Grant No. 20040104)

References

- [1] Hiyoshi Yui. Structure and properties of macromolecule composite materials. *Plastic age*.1999, 45(4)152~158.
- [2] Zhou B L. Some progress in the biomimetic study of composites materials. *Mater. Chem. Phys.*, 1996, 45:114~119.
- [3] Zhang Lide, Mo Jimei. *Nanomaterials*. Shenyang: Liaoning Science and Technology Press, China, 1994.
- [4] Lei Shi, Chufeng Sun, Ping Gao. Mechanical properties and wear and corrosion resistance of electrodeposited Ni-Co nanocomposite coating. *Applied Surface Science*, 2005, (in press)
- [5] Lingzhong Du, Binshi Xu, Shiyun Dong. Study of tribological characteristics and wear mechanism of nano-particle strengthened nickel-based composite coatings under abrasive contaminant lubrication. *Wear*, 2004, 257: 1058-1063.



Vision assistant: a human–computer interface based on adaptive eye-tracking

V. Hardzeyeu, F. Klefenz & P. Schikowski

Fraunhofer Institute for Digital Media Technology, Ilmenau, Germany

Abstract

The Vision Assistant is designed as an intelligent tool to assist people with different disabilities. The goal of this project is to replace the mouse and keyboard by an adaptive eye-tracker system (so called mouseless cursor) which will help to establish a universal and easy-to-use human–computer interface. Using a camera, it works with a pattern recognition algorithm based on a Hough–transform core to process the streaming image sequences. This technique is known for its performance in locating given shapes. In particular, it is used to extract the shapes that relate to the human eye and analyze them in real–time with the purpose of getting the position of an eye in an incoming image and interpreting it as the reference position of a mouse cursor on the user’s monitor. The possibility of the Hough transform parallelization and its execution on the Hubel–Wiesel Neural Network for ultra fast eye-tracking is also discussed in this paper. The results of several experiments in this paper proved that the system performs quite well with different colours of the subjects’ eyes as well as under different lighting conditions. In the conclusion we paid attention to the problems of further improvement of the functional and algorithmic parts of the Vision Assistant.

Keywords: HCI, eye-tracking, gaze estimation, Hough transform, Hubel–Wiesel neural network.

1 Introduction

Real-time systems that use eye-tracking technology have been explored for many years (Duchowski [1]). In our research we wanted to build a non-invasive video-based real-time eye-tracking system to let disabled people take a more active part



in every day life, like writing messages, surfing the web, playing games, educating themselves and communicating to each other.

2 Proposed method

The Vision Assistant is based on the architecture shown in figure 1. It starts with an image acquisition step from the streaming video of a camera, which is connected to the computer. After that the image preprocessing takes place. At this stage we prepare the row image for processing in the Hough Core module. The Hough Core makes the transformation from the Cartesian coordinates to the Hough Space in which the shapes that are related to the human eye are located.

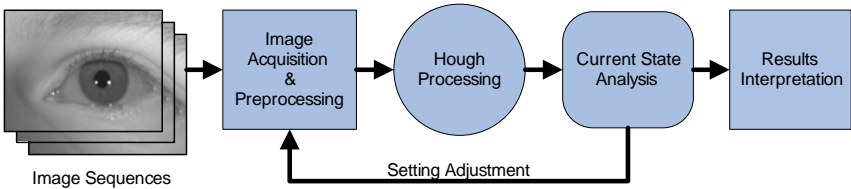


Figure 1: Vision Assistant’s architecture.

After the human’s eye shapes have been located, the Current State Analysis module inspects the features that were extracted from the image with the help of the Hough Transform and makes a setting adjustment for the next turn. The final block on this diagram is the block of the result interpretation, which interprets the calculated position of a human iris to the reference position of a mouse cursor on the user’s monitor.

2.1 Image acquisition and image preprocessing

On the image acquisition stage, Vision Assistant grabs the image from the video stream through Direct X services to internal memory and converts it from the colour RGB-schema into grey scale. After this step we perform the Edge detection [2]. Edges are areas with strong intensity contrasts – a jump in intensity from one pixel to the next. In addition, they characterize object’s boundaries on the image and therefore their detection makes further scene decomposition and feature extraction easier. Considering the procedure of edge detection applied to the image significantly reduces the amount of data and filters out useless information, while preserving the important structural properties in an image. In Vision Assistant for each pixel on the frame we apply a convolution algorithm, based on the Sobel 3x3 convolution matrices, which performs four operations:

- a) calculation of the gradient information for the vertical direction is presented by eqn. (1):

$$G_y = \sum_j \sum_i (P_k \bullet maskY_{ji}) \tag{1}$$



- b) calculation of the gradient information for the horizontal direction is presented by eqn. (2):

$$G_x = \sum_j \sum_i (P_k \bullet maskX_{ji}) \tag{2}$$

- c) gradient calculation for a given pixel is presented by eqn. (3):

$$|G_k| = \sqrt{G_y^2 + G_x^2} \tag{3}$$

- d) the mechanism of taking the decision upon current pixel is an edge or not is presented by eqn. (4):

$$P_{knew} = \begin{cases} yes, & \text{if } G_k > \tau \\ no, & \text{if } G_k \leq \tau \end{cases} \tag{4}$$

Here P_k is the current pixel of the image; P_{knew} is the pixel of edge; $maskX$ and $maskY$ are the convolution matrices for the Sobel operator and G_k is a computed value of gradient for the current pixel. The Threshold τ was chosen empirically through performing a number of tests for preprocessing.

2.2 Hough processing

After the incoming image has been prepared with the help of Sobelization for feature extraction, the Hough transformation takes place [3]. The Hough transformation is a pattern recognition technique which is known for its performance in locating given shapes on images. In particular, it is used to extract the shapes that relate to the human eye. In addition, the Hough transform is capable of identifying artefacts caused by shadowing, reflections and heavy light conditions, which is very important for eye-tracking. The final results of this transform represent the most reliable centers of both eyes.

Since the human’s iris and pupil in most situations looks like a circle, the use of the adapted Circle Hough Transform makes sense for this application. A General circle representation can be described by eqn. (5):

$$(x - a)^2 + (y - b)^2 = r^2 \tag{5}$$

Here, (a,b) is the coordinate of the centre of the circle that passes through the set of points (x,y) , and r is its radius. Since there are three free parameters $(a,b$ and $r)$ for this equation, it follows that the results of the Hough transform should be represented by three-dimensional array. Considering transformation from Euclid to Hough space can be performed with the eqn. (6):

$$b = y - \sqrt{r^2 - (x - a)^2} \tag{6}$$



This is computationally expensive and circles clearly require more calculations to find than, for instance, lines. To solve this problem and achieve faster processing, we applied two-steps matching process:

In the beginning, the 1st step – 3D Hough Transform for circles takes place in the Hough Space of a, b and r (assuming that the radius can change only in range of $[0 \dots 100]$ pixels and a, b are the dimensions of the current video frame). During the first iteration the system gathers all necessary information about the iris position (a, b) and its optimal radius r_{iris} . This process takes a lot of time, even for a 400×500 pixels image and, of course, can't be treated in real-time. However, these first iterations are approximately enough to gather the information about the optimal radius value and the offset position of the eye's centres. Besides, it's feasible that the eye position can't change dramatically from frame to frame if the operation performs at 25 frames per second, even if saccade movement (300 degree/s) takes place. Thus, we introduce the next step of the calculation process, the Reduced Hough Transform.

Since the optimal iris radius r_{iris} has been selected during previous phase, the system doesn't need to perform the Hough for all possible radiuses from 0 to 100 pixels. On this stage we assume that the radius can change from a small number of values and this gives the possibility to decrease the number of radiuses that should be taken into account during the calculation process. This process might be represented within the conditional eqn. (7):

$$r_{iris} - 3 < r_i < r_{iris} + 3 \tag{7}$$

where r_i is a radius on the certain frame.

In addition, a given estimation of the Iris positions on the image brings the possibility to decrease the region of interest for fine search of the Iris centres. These sub regions of interest will be bounded by rectangle with a height in the range of $[b_{i-1} - 2 \cdot r_i \dots b_{i-1} + 2 \cdot r_i]$ and a width of $[a_{i-1} - 5 \cdot r_i \dots a_{i-1} + 5 \cdot r_i]$, where a_{i-1} and b_{i-1} are consequently the horizontal and vertical positions of the iris centre on the previous frame. The windowing is shown in figure 2.

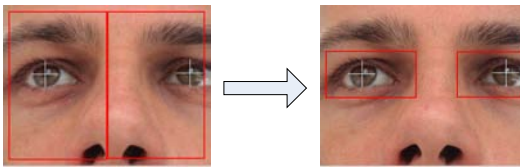


Figure 2: Presentation of the Full (left) and Reduced (right) Hough windows.

This approach has been organized with the help of a Current State Analysis block, which performs the parameter's recalculation for each step of the Hough Transform. In particular, it decreases the search window on the original image and as a consequence, decreases the complexity of the Hough Space as well. As a result, it brings an increase in the number of images processed in one second



and the performance of the whole system grows rapidly to the real-time operation mode.

3 Implementation

We implemented the Vision Assistant with Microsoft Visual Studio.NET 7.1.3088, Framework .NET Version 1.1.4322 SP1. For visualization part, which captures the image from a camera, we used Direct X 9 SDK (Summer 2003 Release) on a computer with Pentium 4 2GHz processor and Direct X 9 compatible graphic card. The SONY DCR-PC110E camera with zoom, nightvision and autofocus functions was attached to the computer through Firewire. This choice was made because this camera has all necessary functions for plug-and-play operation. Its nightvision function replicates the work of InfraRed (IR) filter which is good to use for object tracking applications. Since Vision Assistant is working only with the region of the eyes the camera should have the possibility to zoom directly to the face. If the camera has an Autofocus function, this would be easier to adapt the focus of the camera during on-tracking operation. Using high speed IEEE-1394 (Firewire) camera-to-computer connection instead of USB will improve the performance of the application. All in all, the current system was able to proceed up to 30 frames per second from the camera and show the relevant cursor position on the screen.

Besides, to give more freedom to the user, at his or her choice the system can track left, right or both eyes simultaneously. This approach gives a possibility to choose the best way for tracking when the light conditions are not the same from left and right sides of the face (e.g. when the side sun light beams into the face).



Figure 3: Examples of the subjects' faces.

4 Experiments

To test the Vision Assistant we performed several test sequences on people with different iris colours and different ethnic backgrounds. The subjects were asked to feel free with the computer and non-invasive camera and move their eyes as they do all the time. During the tests we found that ethnic background makes no effect on the software precision and performance. In figure 3 some images that were made during the tests with the Reduced Hough windows are presented.

After this we performed the test for the correct iris position recognition and coordinates interpretation in dependency of the eyes colour. The results of this test are presented in table 1:



Table 1: Correct iris position recognition in dependency of the eye colour.

Brown	Dark Brown	Light Blue	Green Brown	Dark Blue	Blue Grey
96.0%	95.5%	99.1%	97.2%	99.0%	98.6%

Additionally we have tested the algorithms for their performance in dependency of the software operational mode, because this feature is very important for any eye-tracking applications. Here Calibration mode means the work of the 1st processing step - Full 3D Hough Transform. Normal mode means the usage of the Reduced Hough windowing. The tests were performed on the P4-3.2 GHz with a Matrox Millennium G400 graphic card and a firewire camera. The results are presented in the table 2:

Table 2: Dependency between the calculation time and the working mode.

Running mode	Calculation time	Standard deviation	Average framerate
Calibration Mode			
Both Eyes	73ms	± 5ms	13.7 fps
One Eye	44ms	± 3ms	22.7 fps
Normal Mode			
Both Eyes	47ms	± 5ms	21.2 fps
One Eye	35ms	± 3ms	28.5 fps

As the reader can see from the table above the average performance has been reached the point of 22-28 frames per second.

5 Hough parallelization

This part of the development aims to create an Ultrafast Eyetracker which takes high-velocity pictures of the human eye and localizes the iris centres within few milliseconds. As it was mentioned above, the main algorithm for iris localization is based on the Hough transform which uses the “voting” technique for detecting the eyes shapes. However, as it is described in [4], this general method of the shapes localization can be well parallelized using the neural network approach. Being implemented on the FPGA (Field Programmable Gate Array) this will give an outstanding performance improvement of the eye-tracking system.

The parallelization approach uses the Hubel–Wiesel neural network. Neurobiologists David H. Hubel and Torsten N. Wiesel [5], who shared a Nobel Prize in medicine for discovering the VI region of the brain, proposed a wiring diagram of the visual cortex. Based on this knowledge the considered neural network has been investigated its digitalized model has been created. The natural



shape of the Hubel–Wiesel neural network and its digital representation is shown in figure 4:

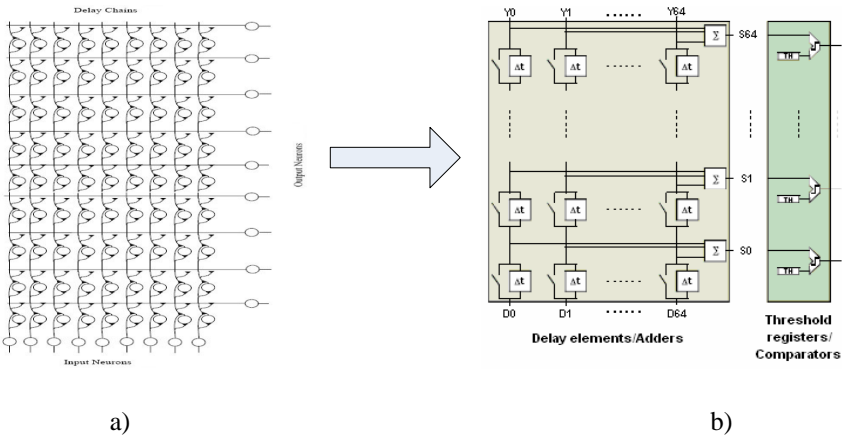


Figure 4: The natural (a) and digital (b) representation of the Hubel–Wiesel neural network.

This structure has proved to be a good basis for a highly dynamical computer vision system that is based on the cognitive principles like self-organization and self-modification. Furthermore, it is well suited for extracting the 2-D slopes and sinusoidal-like shapes from the image as well [6].

Using this technology, the Parallel FPGA Core is now under development and by the end it will be able to simulate the work of the Hubel–Wiesel neural network in order to execute the Hough eye center’s localization routine on it.

Current implementation uses Xilinx Virtex II 6000 platform. An estimated frame rate of the considered system varies from 300 fps for the images of 512 x 512 pixels to 1500 fps for the pictures of the lower resolution.

6 Conclusion

In this paper we present a robust eye-tracking system that was adapted for the needs of the handicapped people. The system uses the Hough transform for circles. It produces information about the centers and radius of the eyes in real time. The possibility of the system design for high speed eye-tracking based on the bio-inspired approach was also discussed here.

Future work will concentrate on improving the robustness of the centre localization as an accuracy of one – two pixels is not sufficient enough. In addition, we will investigate and implement a method of dynamical thresholding for the preprocessing steps. This will give more tolerance to the different light conditions, e.g. darkness or intensive artificial light. We will also work on the prediction of the eyes region position during the tracking process. This will be used to create smooth cursor movement on the screen and, in consequence, will



give the user more convenience during controlling the computer with his/her eyes.

References

- [1] Duchowski, Andrew T. *Eye Tracking Methodology: Theory and Practice*. Springer-Verlag, p. 251, 2003.
- [2] Nixon, Mark S., Aguado, Alberto S. *Feature Extraction and Image Processing*. Newnes, p. 350, 2002.
- [3] Leavers, V.F. *Shape Detection in Computer Vision Using the Hough Transform*. Springer-Verlag, p. 201, 1992.
- [4] Epstein, A., Paul, G.U., Vettermann, B., Boulin, C., Klefenz., F. A parallel systolic array ASIC for real time execution of the Hough-transform. E. S. Peris, A. F. Soria, V. G. Millan (Editors). *Proceedings of the 12th IEEE International Congress on Real Time for Nuclear and Plasma Sciences, Valencia*, pp. 68–72, 2001.
- [5] Hubel, D.H., Wiesel, T.N., Stryker, M.P. Anatomical demonstration of orientation columns in macaque monkey. *Journal of Comparative Neurology* 177, pp 361–380, 1978.
- [6] Brueckmann, A., Klefenz, F., Wuensche, A. A Neural Net for 2D-Slope and Sinusoidal Shape Detection, *International Scientific Journal of Computing*. Vol. 3, Issue 1, pp. 21 – 26, 2004.



Section 4

Natural materials engineering

This page intentionally left blank

Structural and torsional properties of the *Trachycarpus fortunei* palm petiole

A. G. Windsor-Collins¹, M. A. Atherton¹, M. W. Collins¹
& D. F. Cutler²

¹*School of Engineering and Design, Brunel University, UK*

²*Royal Botanic Gardens, Kew, UK*

Abstract

The *Trachycarpus fortunei* palm is a good example of a palm with a large leaf blade supported by a correspondingly large petiole. The way in which the material and functional properties of the petiole interact is analysed using engineering and botanical methods with a view to understanding how the petiole functions from a structural standpoint. Initially, the histological aspects of the petiole are analysed at a microscopic level from sections of the petiole taken at regular intervals along its axis, in order to determine the density and location of the *vascular bundles*. A modified *torsion* rig was used to measure the *torsion* and *shear stress* variation along petiole sample lengths. Knowledge of *vascular bundle* placement within the petiole sections and their torsional loading characteristics contribute to understanding the petiole function.

Keywords: palm petiole, vascular bundle, axial torque, geometry, rigidity modulus, composite, material properties, *Trachycarpus fortunei*, torsion, shear stress.

1 Introduction

The largest blades in the plant kingdom may be found in *Arecaceae* (the palm family) providing a reason for exploration into their structure and engineering properties. The palm *Trachycarpus fortunei* was chosen because of its overall large size (up to about 12m high), and its correspondingly large leaves of up to one metre in diameter [1]. This palm is native to China and the Himalayas, thriving in temperate regions and is one of the world's hardiest palms. A popular name for it is the Chinese windmill palm because its leaves are stiff and fan-



shaped. It has a slender single stem of about 250mm in diameter and is typically slightly narrower at the base than at the top. Environmental factors such as wind and rain acting on the blade generate bending and torsion loads on the petiole. How do the section properties of the petiole deal with this loading?

Work by Gibson *et al* [2] states that palms are among the most efficient materials available owing to their *composite* and cellular microstructures. The petiole of the palm *Chamaerops humilis* analysed in [2] was found to have a radially uniform distribution of *vascular bundles* within a parenchyma matrix. They modelled the petiole as a unidirectional fibre *composite*, with a uniform distribution of fibres in a honeycomb matrix of the same solid material. Such structures are common in many palms, ‘petioles’ and stems in other monocotyledonous species. By varying the volume fraction of fibres radially in a fibre *composite* of circular cross section they came to the conclusion that a non-uniform distribution leads to an increased flexural rigidity over a uniform distribution. They also found that further increases in rigidity were possible if the cross section is hollow like bamboo, whereas a thin walled tube gained little from a structural gradient.

Trachycarpus fortuneii however, has *vascular bundles* that are concentrated radially towards the outside of the petiole. The tensile modulus of palm *vascular bundles* is astonishing at 100GPa [3] compared to Kevlar which ranges from 83 to 186GPa (grades 29-149). *Sclerenchyma* (derived from the word ‘scleros’ in Greek meaning ‘hard’) is the lignified material that partially or entirely surrounds the *vascular bundles* which in effect forms tubes.

Ashby *et al* [4] found that wood, with its high value of $(E/\rho)^{1/2}$, is well suited to resist both bending and elastic buckling. In addition, palms, although having a simpler structure which is slightly less efficient than dicotyledonous or gymnospermous woods in bending resistance and buckling is nevertheless stronger in these regards than most engineering materials.

2 Torsion and botanical analysis

2.1 Petiole histology

In order to evaluate the internal structure of the petiole, cut sections were mounted in wax and scanned at a resolution of 1200dpi. This revealed the arrangement of *vascular bundles*. Three-centimetre samples were cut at six equal intervals (of 171mm) along the petiole axis ending at where the leaf blade joined the petiole (sample P6) as shown in fig. 1.

2.2 Section scanning

Fig. 2 shows that the remainder of each section embedded in the wax after removal of some slices with the microtome, was enough to use a scanner to analyse the placement and number of *vascular bundles*.

Each section was scanned at 1200dpi and a 0.25mm grid placed over them using Adobe Photoshop® software. Samples P1 and P6 are shown in fig. 3:



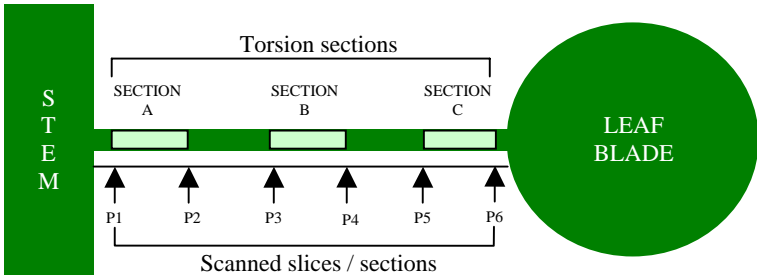


Figure 1: *Palm petiole* schematic showing the relative placement of samples for scanned slices P1 to P6 and sections A, B and C for the *torsion* experiments.

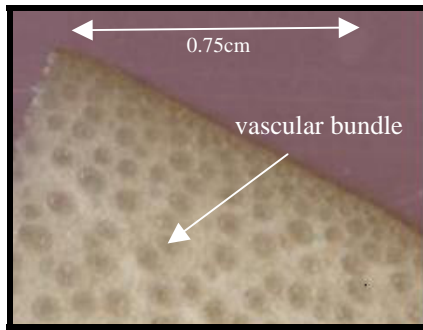


Figure 2: Part of sample P6 showing higher concentration of *vascular bundles* towards the petiole / air boundary.

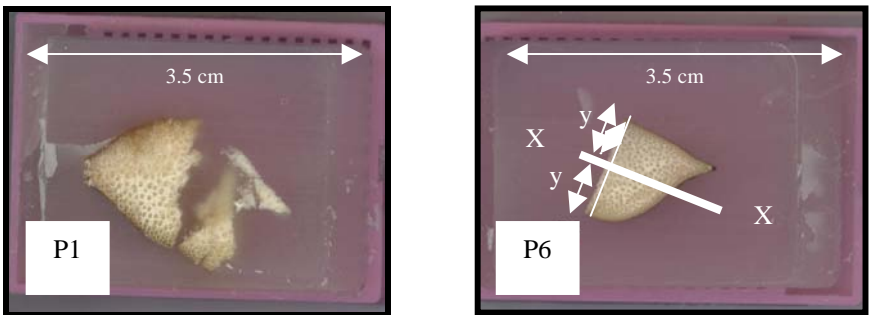


Figure 3: Sections P1 (nearest the palm stem) and P6 (nearest the blade) embedded in wax. Sample P1 was torn while cutting the hard sample using a scalpel. Line XX is a later reference when determining cross sectional area.

2.3 Vascular bundle distribution within petiole

The petiole acts as a compound cantilever and the number of *vascular bundles* in both the lower and upper halves of the petiole section P6 was counted using a graticule. The *vascular bundles* are like reinforcing rods in concrete from a structural point of view owing to the relatively high tensile strength of the *vascular bundles* within the comparatively weak surrounding parenchyma matrix. The white line shown in fig.3 sample P6 joins the adaxial and abaxial surfaces of petiole transverse section at its thickest part. Line XX also shown in the same figure bisects this line at right angles to it. It was found that there were 47% more *vascular bundles* to the adaxial side of Line XX shown on sample P6 than abaxial to it. Further to this, the 80% of the cross sectional area of the petiole in sample P6 was found to be adaxial to Line XX. The number of *vascular bundles* per 2.5mm² was counted using a graticule for the entire viewable area for all samples. The mean average was determined according to whether the *vascular bundles* were positioned internally or close to (within 1mm) the outer surface of the petiole. The results in fig. 4 show that the concentration of the peripheral and internal *vascular bundles* increases fairly steadily towards the leaf blade (which one would expect to some degree if number of bundles has to remain the same whilst the area of the cross section is decreasing). The gradients of the trend lines indicate that the concentration of the peripheral vascular bundles increases more per unit axial distance than that of the internal ones, correlating with the fact that the number of vascular bundles in the cross section increases distally. This is also proven as the number of vascular bundles in P4 is 330 and that in P6 is 375, an increase of 13% over a third of the petiole length.

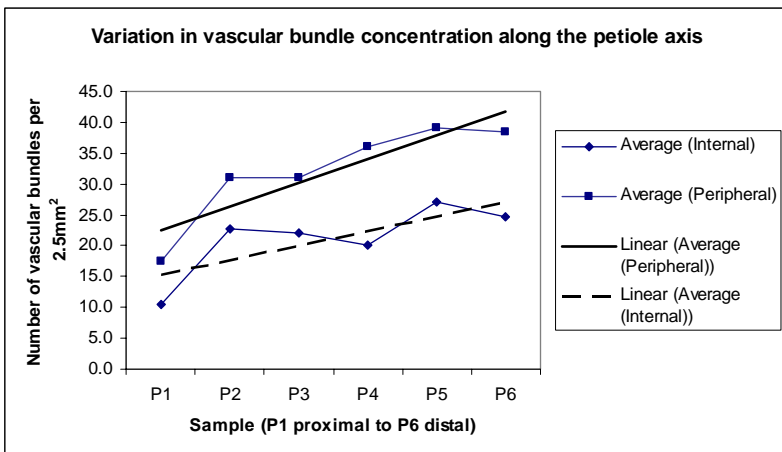


Figure 4: The variation of *vascular bundle* concentration along the petiole axis.



The external boundary (outline) of the petiole section is an irregular shape and as such is difficult to measure precisely. At the proximal end it encircles the trunk and may be an order of magnitude broader than the distal end of the petiole where it meets the leaf blade. For the purposes of the *torsion* test and aiming at straight samples as a first investigation, the most proximal part of the petiole was not tested (a distance of 100mm along the petiole axis from the trunk edge). The remainder of the petiole was tested in sections of similar cross-sectional area (not varying by more than $\pm 8\%$) to enhance the straightness of each section and to avoid the effect of clamp ends. During *torsion* it is the outer edge of the specimen that is expected to break first, being the furthest distance away from the neutral axis. Two tests were undertaken on each of the three samples in close succession in order to check the consistency of the data and observe any hysteresis present.

2.4 Torsion test preparation and acquisition

2.4.1 Petiole preparation

A disease-free petiole of 85cm in length was sawn and the cut end of each petiole section was immediately submerged in water in order to sustain freshness and transpiration. Each petiole was divided into five equal lengths of 211mm chosen to be the same intervals as the botanical section samples. Only the first (section A), third (section B) and fifth (section C) samples were used for this experiment. The specimen length was chosen as a balance between minimising the effect of the clamp ends and minimising section variation along the petiole. As 20mm of each sample end was to be embedded in epoxy, the tested length was a 171mm sample as in fig.5. The shape of each sample end was recorded by drawing around the profile with a sharp pencil. Cellulose film was wrapped around each cut end to inhibit transpiration, enhancing the freshness of the petiole.

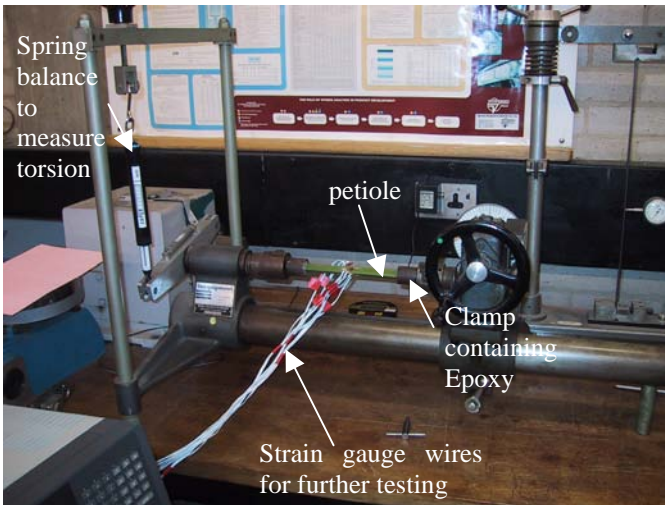


Figure 5: Torsion rig equipment showing petiole embedded in the clamps.



2.4.2 Torsion data acquisition

The sample was set up in the *torsion* rig after checking the alignment of the machine. Data for *axial torque* and angular twist was manually recorded every ten seconds after turning through one degree. This experiment was repeated to check the results albeit on already twisted sections and the time lapse noted. As the petiole is symmetrical about the central vertical plane, it was only necessary to apply torque in one sense of direction. From cutting the sample to taking the last reading, the first tests took less than two hours.

2.5 Torsion results

Fig. 6 shows that for both the first and second tests, the *torsion* values for section A are nearly twice those of the other two sections B and C when readings were taken every ten seconds and twisted through one degree. For each sample, the *torsion* values vary linearly with the angle of twist although this rate decreases slightly with increasing angles of twist (or data sample). The change in *torsion* readings per unit time would vary depending on time intervals between angular twisting increments (in this case ten seconds). The part of the petiole nearest the trunk is about twice as resistant to *torsion* as the middle and distal sections. For all of the sections, there was a time interval of ten minutes between the end of the first and the start of the second test. It can be seen from these results that section A nearest the trunk is the only one to display either strain hysteresis through plastic deformation or permanent damage.

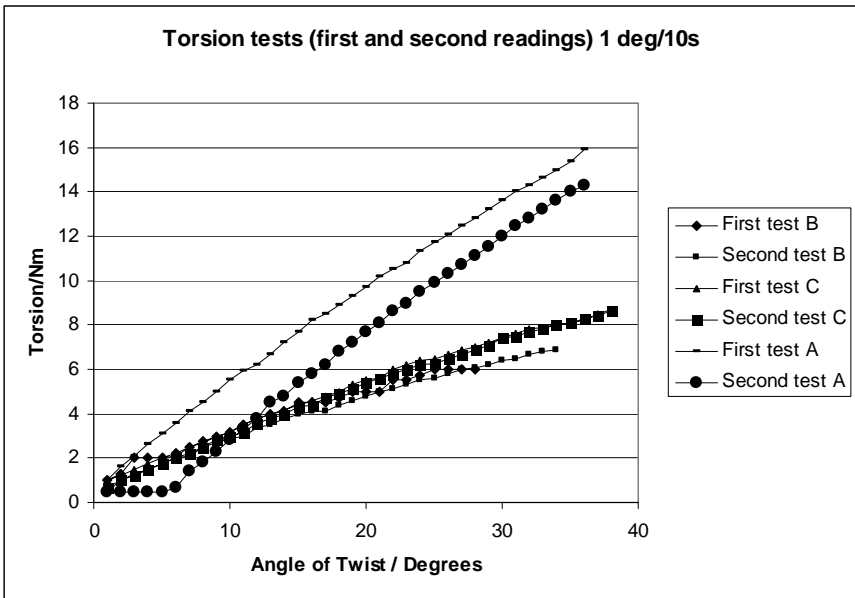


Figure 6: Results of both first and second torsion tests.



2.6 Analysis

The standard equations for *torsion* of a homogeneous section in eqn. (1) have been applied although it was found that the *vascular bundles* were not distributed evenly throughout the petiole cross section, the latter differing from the petiole analysed by Gibson et al. [2].

$$T/J = G\theta/L = \tau/r \tag{1}$$

where T is applied *axial torque*, J is polar second moment of area, G is the *rigidity modulus*, θ is angular twist, L is the specimen length, r is the section radius and τ the *shear stress*. The *rigidity modulus* was calculated for each section by taking the gradient of the graph of *torsion* versus angle of twist. The values for G were calculated from the graph gradients as J and L where known. As the petiole cross sections were not circular, J and r were derived from the average cross sectional area of the samples being then transformed into the equivalent circular cross section. The results are shown in fig. 7.

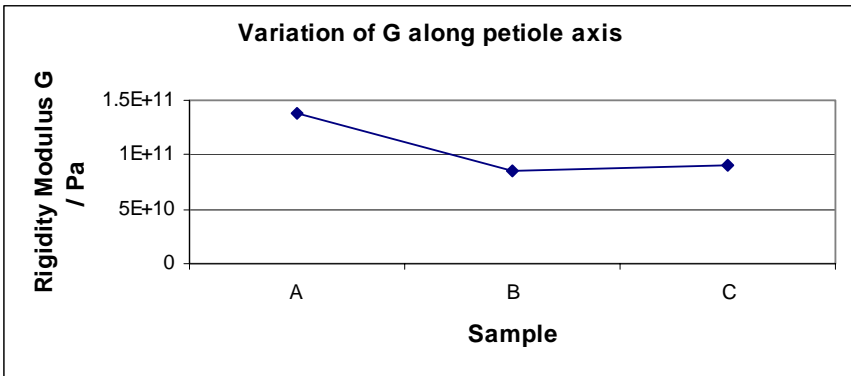


Figure 7: *Rigidity modulus* variation along the petiole axis.

J was calculated using eqn. (2) for solid cylinders using the equivalent cylindrical radius.

$$J = \pi r^4/2 \tag{2}$$

Even though the *palm petiole* was not a homogeneous material, eqn. 1 was used to calculate the *shear stress* (τ) during *torsion* for each of the three samples as shown in fig. 8. τ was observed to range linearly for each sample and the gradient of sample A when *shear stress* was plotted vs. increased angle of twist was approximately 150% greater than those of samples B & C.



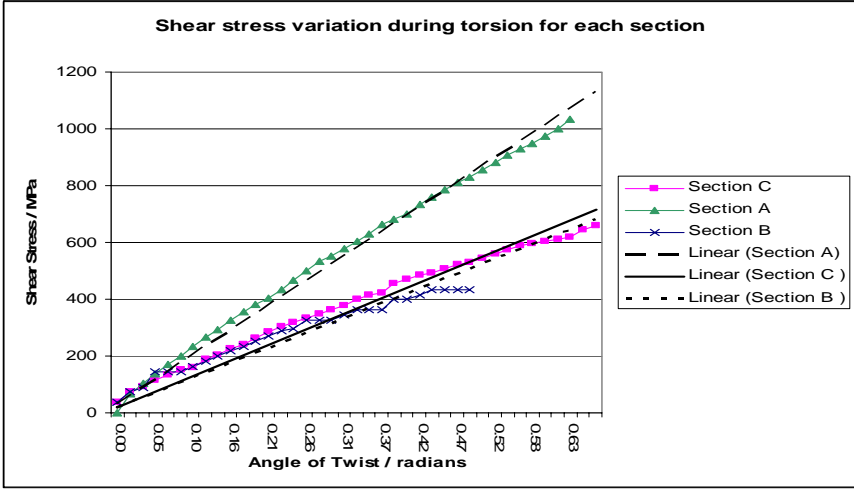


Figure 8: Shear stress variations during increased torsion derived from eqn. (1).

3 Discussion and conclusions

Using a scanner with a resolution of 1200dpi, the remainder of each sample embedded in the wax after removal of some slices with the microtome, enabled analysis of the location and number of *vascular bundles*. A higher concentration of *vascular bundles* was found towards the outer side of the petiole. In the tested sample (P6) there were 47% more *vascular bundles* in the top vertical half above line XX nearest the adaxial surface compared to the lower half nearest the abaxial surface of the petiole sample below line XX. Further to this, the area of P6 was found to be 80% more above line XX compared with below it. The concentration of both the internal and peripheral *vascular bundles* increases fairly steadily towards the leaf blade although the concentration of the peripheral *vascular bundles* increases more per unit axial distance than that of the internal ones. As the number of *vascular bundles* in P4 is 330 and that in P6 is 375, an increase of 13% over a third of the petiole length it may be the case that the *vascular bundles* branch distally. The increasing spatial density of *vascular bundles* towards the leaf blade should allow the petiole to twist about greater angles before any kind of overall fracture. It also shows that the *vascular bundles* have a higher bulk density than the matrix in which it is embedded – the parenchyma.

The maximum vertical distance (height) between the adaxial and abaxial surfaces of the sections decreased and the bulk density of the petiole increased towards the leaf blade end of the petiole. The cross sectional area of the petiole also decreases towards the distal end of the petiole apart from the middle Section B in our case, indicating that the *geometry* of the outer shape of the petiole



requires further investigation. This would be to determine if this is a typical result and to investigate, if so, why.

The first and second torsion test data match for both sections B and C, however these tests differ for section A indicating that the properties of this section have changed. For both the first and second tests, the *torsion* values for section A are nearly twice those of the other sections B and C when readings were taken every ten seconds each time being twisted through one degree. This results in section A being twice as resistant to twisting as the other two sections, partly being caused by the greater cross sectional area. The outcome of this is that the palm trunk is isolated from many of the dynamic forces on the blade. The *torsion* values vary almost linearly with the angle of twist although this rate decreases slightly with twisting. Perhaps a different relationship would be apparent if the rate of *torsion* changed. It may be partly due to creep and the small scale elastic adjustment of the petiole material. Much research on the plant response to mechanical and *forced convection* has identified mechanosensitive ion channels which regulate the amount of calcium ions entering the cell as a result of stress. Calcium ions probably regulate the first stage in the signal transduction pathway from the first perception of the mechanical stress to the activation of genes which synthesise proteins in response to the stress [5]. For all of the sections, a time interval of ten minutes between the end of the first and the beginning of the second test was set. It is interesting to see from the results that section A nearest the petiole is the only one to display stress hysteresis. Hysteresis in this part of the material where the cross sectional area of the petiole is largest, reduces damage to it. The repeated movements of the petiole caused by the forces of a prevailing wind (*forced convection*) are reduced as a result of hysteresis enabling the petiole to temporarily re-shape to the prevailing forces.

The shear stress, τ was observed to range linearly for each of the three samples on the graph plotting τ vs. increased angle of twist. The gradient of sample A was approximately 150% greater than those of samples B & C which were similar. This shows that the shear stress per unit *axial torque* did not decrease linearly but that a reduction in stress occurred in the middle petiole sample (B). This may be so that the distal end of the petiole is more able to support the blade locally. Bending stress experiments are required to investigate this anomaly.

From this small set of experiments, we have been given an insight into the mechanical behaviour of the *Trachycarpus fortunei palm petiole*. In the course of evolution the structure found in this, and petioles of other palm species, has become 'selected' by pressure from environmental and functional factors. It is shown to be an efficient structure, economical in materials, well suited to its function. These results have consequential design implications for manmade cantilevers.

Acknowledgement

The authors thank Dr. Ian Kill senior lecturer in Human Cell Biology Laboratory of Cellular Gerontology, Brunel University for his assistance with preparation of the petiole specimens.



References

- [1] Gibbons, M., A pocket guide to palms, Chartwell Books, Inc., New Jersey, 2003.
- [2] Gibson, L.J., Ashby, M.F., Karam, G.N., Wegst, U & Shercliff, H.R., The mechanical properties of natural materials. II. Microstructures for mechanical efficiency, The Royal Society, London, 1995.
- [3] Niklas, K.J., Plant Biomechanics: An Engineering Approach to Plant Form & Function, First Edition, The University of Chicago Press: Chicago, 1992.
- [4] Ashby, M.F., Gibson, L.J., Wegst, U & Olive, R., The mechanical properties of natural materials. I. Material property charts, The Royal Society, London, 1995.
- [5] Elliott, K.A. and Shirsat, A.H – Extensions and the plant response to tensile stress. Society for Experimental Biology Conference. J. Exp Bot Vol 49 p 16. 1988.



A model for adaptive design

T. Willey

*Department of 3D Design - Sustainable Practice,
University of Derby, UK*

Abstract

There is an ever-increasing global imperative to investigate and utilise sustainable natural materials. This paper proposes a sequential model of design and construction which contends directly with this material category and, which itself, is drawn from natural systems of organisation and the principles of adaptation. The suggested model deals with the unexpected properties of natural materials and adapts to new possibilities which are surfaced through the design sequence itself.

The paradigms offered by orthodox design are largely predicated on material consistency - materials which can be described through a representational design-language. However, it is proposed that the inconsistencies and variables that are found in unrefined natural materials are not easily integrated into this process, and a new model is needed. It is also argued that the high level of material specification, which is a prerequisite of reproductibility, has forced a dislocation between planning and doing - concept and activity. This is a bi-polar practice, which, although convenient for the mechanisms of industry, negates reflection and adaptation and denies the reiterative feedback loop, which is a salient feature of natural design systems.

Taking into account such models as reflective-practice and evolutionism, the proposed strategy is developed by incorporating the ecological concept of 'emergent properties', which, through its influential position within the schema, continually modifies both problem and solution.

Adaptive-design is described and as a cyclical sequence, which engages simultaneously with both the abstract and concrete domains of designing and constructing. The sequence is tested using case studies and finally, a visualisation tool is illustrated as a way of disseminating adaptive-design as model for practice.

Keywords: adaptive design, reflective practice, natural materials.



1 Introduction

Typically, design has been defined as a plan of action – a preliminary plan for making something Thomson [1]. David Pye [2] suggests that design is what can be conveyed ‘for practical purposes’ through words and drawings. In such accounts the practice of design is regarded as separate from the ‘making’ process, and to a large extent relies on theoretical assumptions. Three-dimensional design, when restricted to ‘two-dimensional planning’ is self-constraining.

Whether it employs the drawn line, the written word or the digital image, it is a process predicated on symbolic and iconic relationships. It might be regarded as an analogue process as it shares only similar or corresponding attributes with the reality it represents. This Analogue approach is also restrictive in the sense that it fails to deal with inconsistencies typically found in natural (unrefined) materials. For instance, un-machined, unseasoned coppice wood is a material with so many dimensional and dynamic variables it would be impossible to simulate its characteristics through the icon and symbol of conventional design tools.

David Pye [2] makes a distinction between the ‘workmanship of risk’ and the ‘workmanship of certainty’ and argues that only direct practical involvement can take on the risks of variables and inconsistencies. Design, he argues (and here he is referring to conventional design practice), deals with certainties, ‘In a designer’s drawing all joints fit perfectly’ [2, p.14]. It is this type of idealisation, and the associated pre-visualisation of ideal outcomes, that thwarts a flexible, adaptive response to design problems and as John Dewey suggests, analogue thinking is not an innate instinctive strategy: ‘Animals learn (when they learn at all) by a “cut and try” method; by doing at random first one thing and another thing and then preserving the things that happen to succeed. Action directed consciously by ideas – by suggesting meanings accepted for the sake of experimenting with them...’ Dewey [3]. This ‘cut and try’ approach when applied to design and construction would, by definition, bring together the processes of planning and doing. It would then be an undifferentiated and symbiotic activity, where actions would be directed by suggested understandings rather than idealised pre-visualisations. This is the basis for what will be called adaptive design, and upon which a new model of design practice is proposed.

2 Evolutionism

Magee [4] argues that in Karl Popper’s ‘evolutionism’, the concept of origination, whether related to life, theories, or works of art, is not susceptible to rational explanation, and that the evolutionary process can have a ‘rationale without there being...any overall plan or plot.’ [4]. Popper also offers a theory of continuous development embodied in the following formula:

‘where P1 is the initial problem TS is the trial solution, EE the process of error elimination applied to the trial solution and P2 the resulting situation, with new problems’. It is a feedback process where even ‘failure to solve a problem



teaches us something new about where its difficulties lie...and therefore alters the situation' [4, p.65]. Popper's formula demonstrates a continuous feedback loop between problem and acting on the problem, which has particular resonance for adaptive design; it is suggestive of an adaptive relationship between problem and solution; planning and doing; concept and activity.

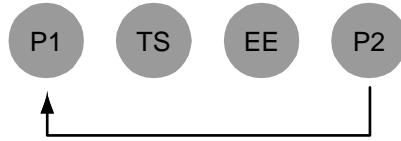


Figure 1: Popper's continuous development.

2.1 Perceptual cycle

In Neisser's perceptual cycle [5] a similar exchange relationship is expressed, where exploration samples information (object), modifies knowledge (the schema) and directs more exploration:

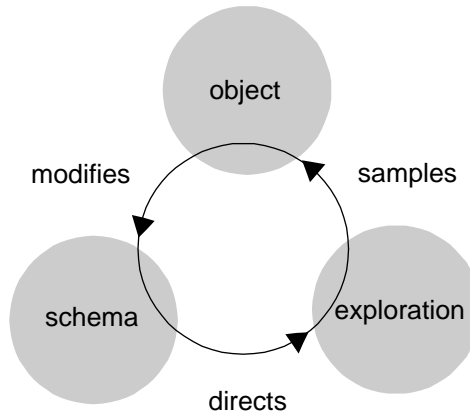


Figure 2: Neisser's perceptual cycle.

3 Reflective practice

Construction is essentially a practice-based activity and, like other practices, is susceptible to what Donald Schon describes as a 'dilemma' which is rooted in a particular epistemology of practice [6]. This dilemma – which Schon argues is endemic in academia and the professions – he describes as 'technical rationality' in which means are adjusted to ends through the application of science. It infers that *deciding* and *creating* (planning and execution) must be separated, as only *deciding* can be rationalised and approached with any degree of rigour. Schon argues [6] that the problem with this approach is that it cannot take into account what he calls the intermediate zones of practice such as:



- uncertain situations, where you do not have a clear problem
- uniqueness, where the situation you have has never been seen before and may never be seen again
- conflict, where you can't adapt means to ends because they don't fit

3.1 Reflection-in-action

Schon suggests that to answer these problems a reflective approach is necessary which he calls 'reflection-in-action' or 'reflective practice'. Yoong [7] describes this simply as 'thinking about the action while you are doing it', or as Schon describes it, ...'our knowing is in our action' [8].

Brown and Duguid [9] have argued that there is a 'breach between learning and use, which is captured by the folk categories "know what" and "know how"' [9] and that the meaningful acquisition of knowledge is at its best a process of 'situated cognition' – an activity contextualised and framed by 'authentic activity' [14]. They suggest that knowledge can be usefully regarded as a set of tools which are best understood through use: 'People who use tools actively rather than just acquire them,... build an increasingly rich implicit understanding of the world in which they use the tools and of the tools themselves. The understanding, both of the world and of the tool, continually changes as a result of their interaction'. Schon's reflection-in-action is a process which is predicated on situated cognition by acknowledging, describing and acting upon problematic situations as they develop through practice: 'As he tries to make sense of it, he also reflects on the understandings which have been implicit in his action, understandings which he surfaces, criticises, restructures, and embodies in further action'. Schon [8, p.50]

Schon introduces the concept of 'back talk' to describe something that is not anticipated but is revealed through practice. Scrivener [10] sees this as being central to the practice of the reflective practitioner who: 'will reflect-in-action on the situation's 'back talk', shifting stance as they do from "what if" to the recognition of implications, from involvement in the unit to consideration of the total and from exploration to commitment'. In forming the core of a design research methodology Scrivener suggests that reflection-in-action offers a 'paradigm of research within design' but acknowledges that we need to 'develop models for recording moments of reflection and the understandings implicit in the action...' [10].

What seems clear, is that 'understanding' and 'action' which are commonly regarded and interrogated as separate channels might, in relation to designing and constructing be best viewed (and practiced) as a simultaneous and symbiotic process.

In the transcription of the address to the Gulbenkian foundation, *Craft as a Reflective Conversation with Materials* [11] Schon relates his theory of reflective practice to the crafts. Referring to a particularly practical example (making a simple gate), Schon [11] applies a clearly defined sequence of reflection-in-action. This could be summarised as:



- image of intention (the image of what I want to do)
- acting on the Image (start making)
- talk back of material (not anticipated)
- reflection (consider the new situation)
- restructuring of ideas (take advantage of the new situation)

3.1.1 Reflective practice models

Yoong [7] develops a reflective model from a number of his own case studies which makes use of prior experience to provoke new adaptations:

- intuitive signal or feeling
- take notice of signal
- make connections with prior experience
- consider adaptations
- assess the risk
- make adaptation

The context of prior experience is expanded by Mark Smith in *Donald Schon: Learning Reflection and Change* [12], here, Smith regards prior experience as a portfolio of memories from which one can build theories and responses: ‘The ability to draw upon a repertoire of metaphors and images that allow for different ways of framing a situation is clearly important to creative practice and is a crucial insight.’

4 A generic model of reflective practice

A generic model of reflective practice was assembled and adopted for development through studio-based case studies. The model maintains the salient features common to reflective practice paradigms which are regarded as essential to the mechanism:

- problem
- frame problem
- reflection
- adaption

4.1 Developing the model

In developing the foundations of an adaptive design sequence, each key attribute of the generic model was rationalised and analysed in relation to both process and outcomes. This was achieved through practice-based case studies with undergraduate Sustainable-Design students tackling a wide range of design problems, but which particularly involve natural unrefined materials. Critically, the generic model was presented to practitioners as a cycle of practice with each stage transcribed in terms of workshop activity, thus:



problem: the design brief, scheme of work or project

frame problem: the problem is approached by the physical activity of acting on materials

reflection: new properties are considered and unexpected outcomes are evaluated

adaptation: the question is asked, ‘could this be new situation go some way in answering the problem?’

The process continues, with new discoveries (from acting on materials) being fed into the sequence, changing ideas about the problem and so suggesting further practical moves.

5 A two domain model of adaptive design

Following further case studies the adaptive design concept evolved. Critically, it was considered that the staging of the sequence (if only in the illustrated description) was not representative of the interrelationship of *planning* and *execution* (*ideas* and *activity*), which, as suggested at the beginning of this paper, was the driver towards a more adaptive model.

As these realisations began to emerge it became clear that a new two domain model (and a corresponding visualisation tool) should be considered, which would acknowledge the separation of the problem into two clear divisions the abstract ‘concept’ and the concrete ‘actions’ - parting *ideas* on solving the problem from the practical *activity* of working out the problem whilst clearly expressing the adaptive interrelationship.

The generic model of reflective practice provides the key for the new model but the formula is now predicated on four key components these being situated within two domains: (Concept) and (Actions/Materials/Properties):

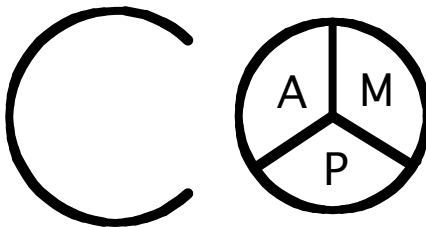


Figure 3: Two domain visualisation tool.

The concept can be regarded as the over-arching idea or as Schon puts it ‘the image of intention’ [11]. This is not an immutable constant in the sense of a fixed plan or visualisation, but rather a flexible open minded and reflective state, which responds to situations as they develop.

Actions are the catalyst for interaction and, as they react with materials, represent the principal activity in the reflective design-construction sequence. They involve mechanical, and sometimes chemical, alteration of materials. Actions can be drawn from material-associated technologies which are purposefully assembled through investigation, they can already be part of the practitioner’s repertoire, or they can be selected from any field of materially-based practice. It is important for actions to be regarded as the act itself, dissociated from any particular material; in this sense actions become readily transferable and can be applied to any material as the basis for exploration.

Materials can be arbitrarily employed (selected without a particular reason), prescribed (as part of a design brief), or more usually, associated with the problem itself (being part of the context of the problem).

Properties are derived from the notion of ‘emergent properties’ a term often associated with ecology and ecosystems. Marten [13] defines an emergent property as a ‘characteristic of a system as a whole that comes into existence from the organization of the system’s parts rather than from the characteristics of any of the parts themselves’. As it relates to adaptive design, properties could be considered in much the same way, where the characteristics of the new situation (the result of acting on materials) are revealed to the practitioner as a set of new conditions with a range of new possibilities. Properties are often not anticipated and it is the unpredictability of the interrelating system which calls for reflective consideration, and through which new discoveries and understandings are made.

The cycle is essentially symbiotic. Acting on materials creates new properties that are reflected on and influence the concept, then these new conceptual realisations suggest further practical moves; and so on:

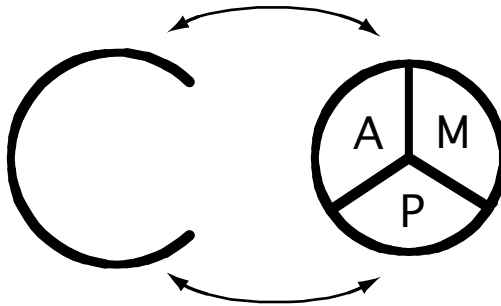


Figure 4: Symbiotic relationship of the two domains.

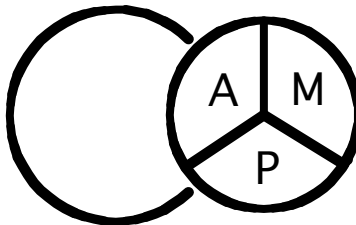


Figure 5: The cycle edges towards commitment.

As the process continues, the conceptual domain becomes increasingly informed by activity – concept and activity adapt, and the domains are brought closer together. As they merge the process edges towards commitment.

And finally, as the problem reaches solution, the two domains are brought into coincidence. Activity and concept are completely co-adapted.



Figure 6: Activity and concept co-adapted.

6 Conclusion

Adaptive design is not a conventional strategy but in many ways it does mimic natural design systems. At risk of over simplifying – in natural adaptation processes the mechanisms of growth and evolution are subordinate to the environment, a tree for instance might have a guiding concept of what it wants to be (a straight tall plant) but in reaction to the environment it may find it needs to put in a bend or two.

The case studies show, that this adaptive capability is particularly useful when approaching specific types of design-problem: problems where the details are perhaps unclear and where unexpected situations can arise. These are the typical characteristics encountered when working with unrefined natural materials.

The adaptive design model has proved to be, not only a tool for solving design-construction problems, but has also acted as a catalyst for rapid innovation, that is, creating a new way of doing something in reaction to an ‘on-the-spot’ problem.

With this in mind, adaptive design might well be called upon to achieve what Papanek [14] calls ‘optimum performance under marginal conditions’, that is, in critical conditions where design and construction become more allied to survival than convenience. Here, adaptive design could make a significant contribution as a highly reactive strategy, which could be used ‘out in the field’ and in situations where conventional design would languish.

References

- [1] Thomson, D; (ed). *The Oxford Compact English Dictionary*. Oxford University Press: Oxford, 1996.
- [2] Pye, D; *The Nature And Art Of Workmanship*. Cambridge University Press: Cambridge, 1968.



- [3] Dewey, J; *How We Think*. Prometheus Books: New York, 1910.
- [4] Magee, B; *Popper*. Fontana: London, 1973.
- [5] Neisser, U; *Cognition and Reality*. W. H. Freeman and Company: San Francisco, 1976.
- [6] Schon, D; *Craft As A Reflective Conversation With Materials*. Transcript of address: Gulbenkian Craft Initiative Furniture Forum, December 1986.
- [7] Yoong, P; Towards A Model Of 'Reflection-In-Action': an analysis of facilitators' intuitive behaviours in electronic meetings. (online). www.lupinworks.com/ar/papers.html.
- [8] Schon, D; *The Reflective Practitioner*. Arena: Aldershot, p.49, 1995.
- [9] Brown, J & Duguid, A; *Situated Cognition*; Columbia University. (online). <http://www.ilt.columbia.edu/ilt/papers/JohnBrown.html>.
- [10] Scrivener, S; *Design Research as Reflection On Action and Practice*. *Msc Research Methods in Design*. Design Research Centre, University of Derby: Derby, 1999.
- [11] Schon, D; *Craft As A Reflective Conversation With Materials*. Transcript of address: Gulbenkian Craft Initiative Furniture Forum, December 1986.
- [12] Smith, M; Donald Schon: Learning, Reflection, and Change; Infed, Informal Education Encyclopedia. (online). www.infed.org/thinkers/etschon.htm.
- [13] Marten, G; *Human Ecology*. Earthscan: London, pp. 43-45, 2001.
- [14] Papanek, V; *The Green Imperative*. Thames and Hudson: London, p. 234, 1995.



This page intentionally left blank

Reinforcement ropes against shear in leaves

C. Mattheck, A. Sauer & R. Kappel

Institute for Materials Research II,

Forschungszentrum Karlsruhe GmbH, Germany

Abstract

Biological structures consist of mechanical load carriers, which are highly optimized in terms of mechanical strength and minimum weight. Many parts of these structures act as tension ropes, even if this cannot always be identified immediately. The advantage of tension-loaded components is that they cannot fail by kinking or buckling like pressure-loaded ones if their aspect ratio is too high.

Special application ranges for tension ropes exist in structures, which are frequently exposed to shear loading. Examples are leaves in the wind or bird feathers during a flight. When looking at the supporting skeletons, there are tensile ropes releasing the structure from shear.

To verify this statement, the vein pattern of a leaf is studied for mechanical suitability using the Soft Kill Option (SKO) structure optimization program. It is found that the leaf is formed in a mechanically optimum manner. The structure is stiffened by tension ropes acting as shear killers. Subsequently, an SKO parameter study is performed to investigate and determine influencing parameters and their relevance to the formation of shear killers.

Keywords: leaf structure, shear killer, bionic, biomimetic, vein angle.

1 Introduction

When a storm shakes and bends a tree, enormous forces act on the leaves. The leaf surface with its side veins that branch off at about 45° resists these wind forces. Side veins transmit the tension induced by the wind from the leaf surface via the main vein into the branch and, hence, act like stiffening tension ropes. Their efficiency is reflected by the fact that in reality a storm will more likely tear the leaves off the stalks than rip off the leaf surface.



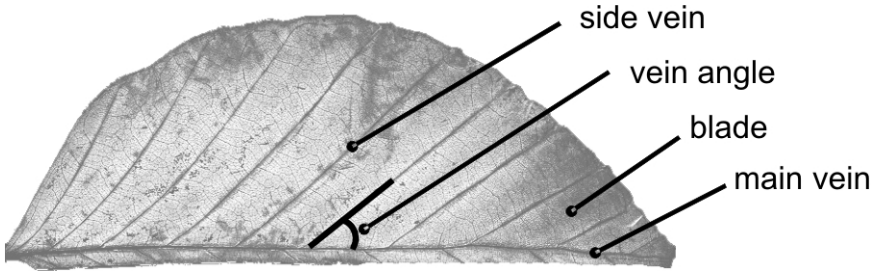


Figure 1: Leaf elements of a European Beech (*Fagus silvatica*).

Leaves wave like flags in the wind, which is why the wind force nearly always acts parallel to the main vein, Fig. 2. Longitudinal shear stresses prevent the leaf halves from shearing off the main vein. Symmetry of the stress tensor, see [2], requires equal lateral shear stresses that form the shear square together with the longitudinal shear stresses.

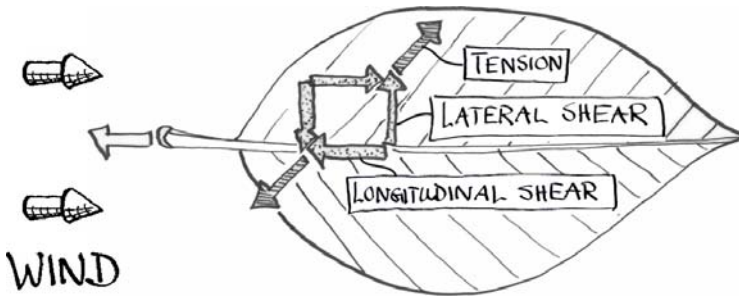


Figure 2: 45° side vein angle with the shear square.

The direction of the resulting tension force that is equivalent to the shear forces may be determined by vector addition of a longitudinal and a lateral shear arrow and, hence, is offset by 45°.

In [3], the 45° orientation of the leaves' side veins is explained theoretically with the help of the shear square. For verification, the SKO method (Soft Kill Option that simulates the osteoclasts in the living bone) will be used in this study.

2 FEM analogous model

To determine the loads of a leaf by means of FEM (finite-element method), a calculation model is needed, which is reduced to mechanically important properties. As the leaf is symmetrical to the center line, only half of a leaf is required by the model. As a result, calculation expenditure is also halved. The simplified setup of this leaf half, Fig. 3, resembles a layered cake and consists of a blade layer and a side vein layer on top. Both layers are firmly connected with

each other, each single layer being divided into numerous finite elements, which is shown schematically by the leaf cross section. The view from above additionally shows the homogeneous surface load caused by the wind and the leaf's fixation at the symmetry line (main vein).

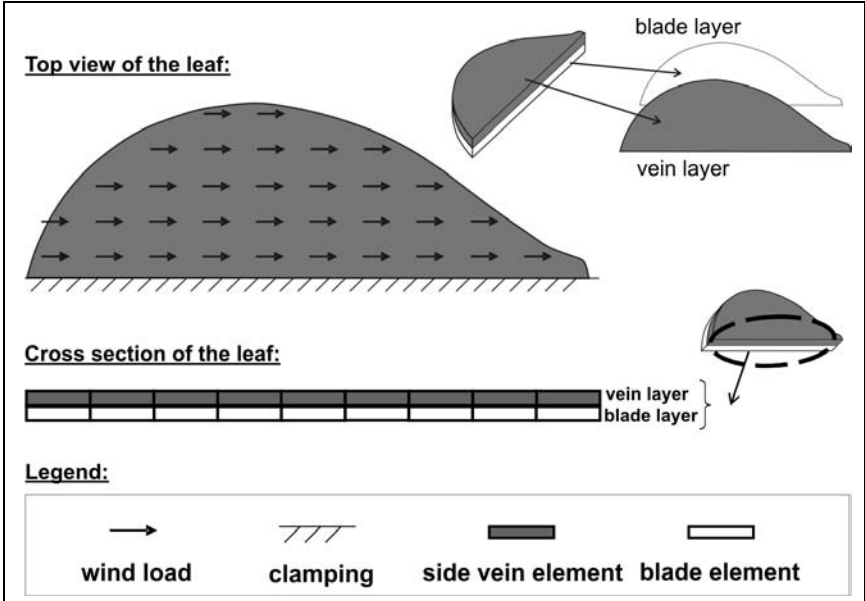


Figure 3: View from above and cross section of the finite-element analogous model.

3 SKO

The SKO method simulates adaptive mineralization processes in the living bone. Higher loaded areas are stiffened, less loaded areas are softened and eventually removed. In this way, the stability required is reached with a minimum use of material.

In this SKO optimization, the blade layer (light grey) is not changed. However, the load of the individual blade elements is determined. Depending on the element load, the following cases are distinguished and pictured in Fig. 4:

1. If the element load is smaller than a given reference stress, loadability of the blade is sufficient, nothing happens.
2. If the load of the blade element exceeds the reference stress, however, the leaf area is overloaded. In this case, the overloaded blade is reinforced by additional side vein elements and, hence, loadability is increased.

The result of a SKO calculation is displayed in Fig. 5. One can see how slender, triangle-shaped side veins develop from the center line towards the edge of the leaf in the formerly homogeneous side vein layer (dark grey). At the leaf edge and leaf tip, no side veins exist. In these areas, load remains below the



reference stress, as a result of which all side vein elements are removed by the SKO method and only the blade remains. This area is sufficient to take up the local forces.

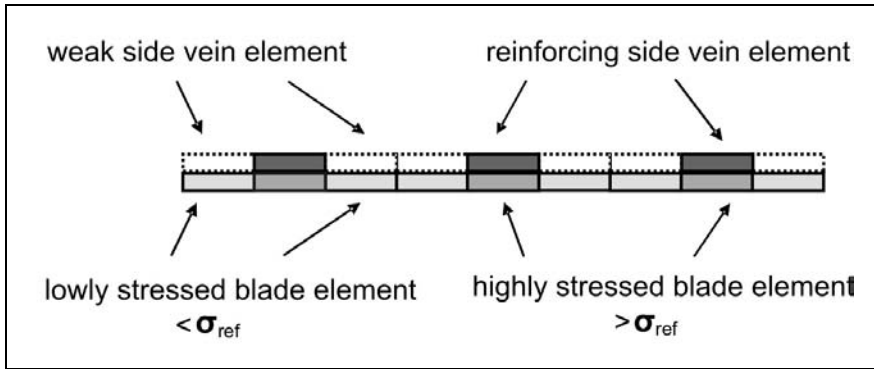


Figure 4: Principle of the SKO method.

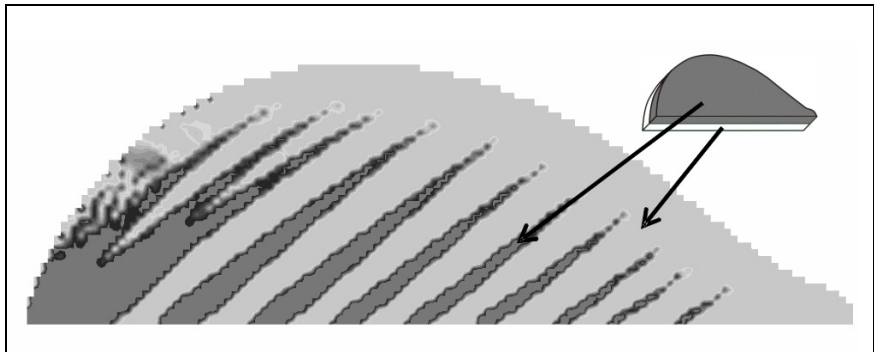


Figure 5: Principle representation of an SKO result.

4 Parameter study

In the following Figs. 6 and 7, the factors influencing side vein formation shall be studied in more details.

In Fig. 6, the reference stress of the blade layer is varied at the same surface load. The amount of this reference stress influences the development and number of side veins. In Fig. 7, the influence of the side “vein: blade” stiffness ratio on the side vein angle is plotted at constant load.

By changing the reference stress of the leaf blade, i.e. its permissible operation load, the number of side veins and their size are affected among others. A weak leaf blade (Fig. 6A) needs many side veins as helpers (shear killers) which are even connected to each other. A leaf blade with a higher loading



capacity transfers more forces and requires less stiffening side veins. Hence, the leaf with the highest loadable blade (Fig. 6D) has the least side veins.

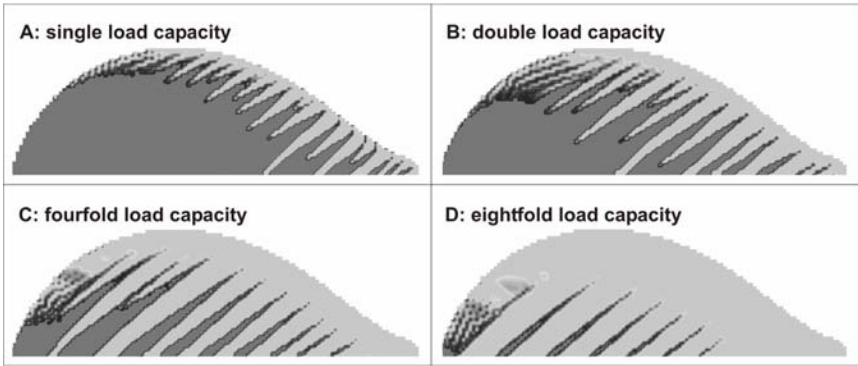


Figure 6: Influence of the reference stress on the formation of side veins.

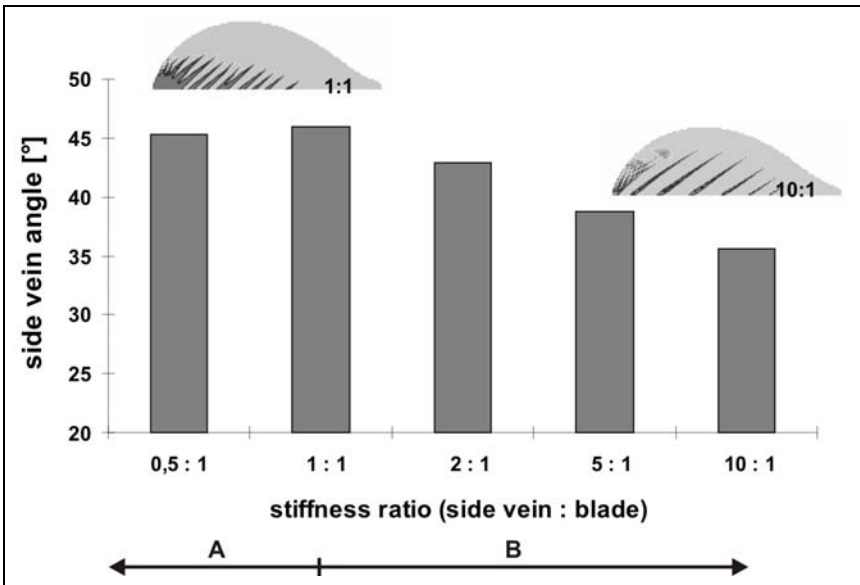


Figure 7: Influence of the stiffness ratio between side vein layer and leaf blade layer on the side vein angle.

When the stiffness of the side vein layer is increased in relation to the blade layer, the side vein angle is affected only slightly, but continuously. When changing the stiffness ratio by a factor of 20, the angle changes by just 10°.

The following two cases can be distinguished:

A. The side vein angle amounts to 45°



The blade is as stiff as or stiffer than the side vein.

B. The angle decreases

The side vein is stiffer than the blade. With increasing stiffness of the side vein, the optimum branching-off angle of 45° decreases slightly. In the extreme case (theoretical), the blade is so soft that it can no longer take up any pressure. In this case, the side veins will arrange along the main vein like brush hair.

5 Summary

With the help of the shear square, a side vein angle of approx. 45° is obtained for leaves with a homogeneous structure. Some natural leaves, however, exhibit an angle other than these 45° . This may be due to the fact that the side veins fulfil various functions at the same time, e.g. transport function and transpiration. This study is restricted to the mechanical property exclusively.

To study the mechanically optimum side vein angle, an FEM-supported parameter study is carried out. This study confirms that the optimum side vein angle is around 45° . It also becomes obvious that functions in certain areas are separated between tension- and pressure-transferring structural elements. The side vein transfers tension only, whereas the blade mainly transfers pressure.

Strength of the blade influences the side vein formation. A blade with a higher loadability needs less and smaller side veins than a weaker blade. The side vein angle is influenced by the stiffness ratio between side vein and blade. At the same stiffness ratio, the mechanically optimum angle amounts to 45° . If the side vein stiffness increases, however, the side vein angle decreases slightly, but continuously.

6 Conclusion

The SKO method that simulates bone growth may also be applied to leaves, as is shown here. Hence, the lightweight construction laws valid for bones are also valid for leaves. This means for the leaves that they reach the required structural stability with a minimum use of material and, hence, are optimized.

References

- [1] Mattheck, C., Kappel, R., Tesari, I. & Kraft, O., In Seilen denken. Konstruktionspraxis, 9, pp. 26-29, 2005.
- [2] Beitz, W. & Grote, K.-H., Dubbel – Taschenbuch für den Maschinenbau, Springer Verlag: Berlin Heidelberg New York, 20, 2001.
- [3] Mattheck, C. & Kappel, R., Festgekrallt – Verzweigung als Schubkiller. Konstruktionspraxis, 3, pp. 18-19, 2005.



Experimental investigation of moist-air transport through natural materials porous media

I. Conte & X. Peng

*Laboratory of Phase-Change and Interfacial Transport Phenomena,
Tsinghua University, China*

Abstract

Experimental investigations were conducted to characterize the moisture absorption of two different natural materials (coconut fibres and groundnut coquets). Two experimental samples were made: one with groundnut coquets (composed by void space and grain) and the other sample was made with coconut fibres (composed by void space and fibres). The samples were multi-layered sandwiches bounded on the top by ice while the bottom surface was exposed to the vapour with temperature close to 100°C. The percentage of water accumulation due to vapour absorption was calculated for each layer after a pre-set time of experiment (1h, 2h,...). The water content within both the coconut fibres and groundnut coquet increased with time. For the groundnut coquet sample the water was transferred mainly by diffusion through the solid; and in the coconut fibres sample with higher porosity, the water transferred by diffusion through void space was the most important. Since water is a better thermal medium, the thermal conductivity of the soaked insulation would increase and the insulating value of the material would be destroyed.

Keywords: natural material, air and moisture transport, porous media.

1 Introduction

Many natural materials (such as cork, coconut fibre...) are used in thermal insulation thanks to their relatively low thermal conductivity, low cost, harmless behaviour to the environment and human health. These materials are commonly used for insulation of low temperatures systems such as coldstore and living building because of their bad behaviour under high temperatures. However, one



main disadvantage of using most of natural materials in thermal insulation is the low resistance to moisture absorption. When heat transfer occurs through a separating wall because of the temperature difference, water vapour diffusion also occurs due to the pressure difference across the wall. As the temperature within the insulation decreases, the moisture already existing in the insulation may condense. Thermal insulation carrying cold fluids suffers thermal degradation due to condensation of water. The value of the water vapour transfer coefficient of the insulation materials is as important as that of the heat transfer coefficient. Many theoretical and experimental investigations of thermal conductivity and moisture absorption and condensation in porous media have been performed, with the aim of applying the results to thermal insulation and other industrial applications. Conte et al. [1] presented experimental investigations of the thermal conductivity of two natural low cost materials, coconut fiber and groundnut coquet. For the purpose of comparison, investigations were done for coconut fiber, groundnut coquet and aluminum silicate fiber as a standard insulation material. Their results showed that the thermal conductivities of both coconut fiber and groundnut coquet (with an average value of 0.08 W/m. k) increase with temperature as well as the thermal conductivity of the aluminum silicate fibers. The measured thermal conductivities showed that the coconut fibers and groundnut coquets may be used as thermal insulation for the tested temperature range. Fan et al. [2] reported an experimental investigation of the temperature and water content distribution within porous fibrous battings sandwiched by an inner and outer layer of thin covering fabrics using a novel sweating, guarded hot plate. They found that most of the change in temperature occurred within the first half hour and moisture absorption by the hygroscopic fibers affected the temperature distribution. They also found that the water content accumulated with time and higher water content was found in the outer region than that in inner regions of the battings. This paper presents experimental investigations of water absorption of two natural low cost materials, coconut fiber and groundnut coquet. The samples of testing materials were bounded on their top by ice and the bottom surface was exposed to vapor with temperature close to 100°C. The percentage of water accumulation due to vapor absorption was calculated for each layer.

2 Experiments

2.1 Testing materials

Coconut fibres and groundnut coquets, both natural low cost materials, are very abundant in nature. A coconut fibre is obtained by keeping the fruit envelope in water for 2 or 3 days. The fibres obtained can reach 30 cm in length with an average diameter of 0.3 mm, fig. 1. Coconut fibre is characterized by its high percentage of lignin (40 %), which accounts for its stiffness when used for carpet manufacturing. Coconut fibres may be used as panels, bulk or rolls for wall insulation. Since it is flammable, it should be treated with boric salt to improve its resistance.





Figure 1: Coconut fibres.



Figure 2: Groundnut coquettes.

Groundnut coquettes are the outer jacket or shells of peanuts. Groundnut coquette has low density and long durability but must be protected from attack of insects. Very similar to wood, groundnut coquet may be treated to different dimensions, fig. 2, treated industrially to get chips for making assemblies such as plywood. The thermal conductivity of plywood varies with timber species, however an average value of $k = 0.1154 \text{ W/(m } ^\circ\text{C)}$, (Edwin and William [3]) for softwood timbers is sufficiently accurate for determining the overall coefficient of heat transmission (U value) of a construction assembly. Thus, the decisive parameter for determining thermal conductivity of plywood is that of the wood species.

2.2 Experimental procedure

The experimental procedure was as follows, fig. 3:



- a) Produce an enclosure with 400x300x300 mm inside dimensions and 30 mm thick. The enclosure must be divided into two compartments by a metal plate (300x300 mm) which will support on its top surface a 90 mm thick wall made with polyester. The metal plate must have several little holes at the center where the samples will be placed to allow vapor to flow through the testing materials. Also, the 90 mm thick polyester wall has a rectangular gap of 100x80 mm at the center. Make a gap of 100x100 mm to the bottom wall of the enclosure for vapor recirculation and, a second gap on the top wall to remove and put the samples.
- b) Prepare the samples by making 3 layers with 100x80x30 mm dimensions, made with the materials to be tested. Cover the sample layers by wire mesh (wire diameter 0.071 cm, strands per meter 315). The testing materials should be carefully packed to get the greatest density and reduce the amount of air. Weight the samples on an electronic balance and install them on the plate through the gap of the 90 mm thick polyester wall at the center of the enclosure. Connect the thermocouples to the layers horizontal surfaces and measure the temperature of each layer before testing.

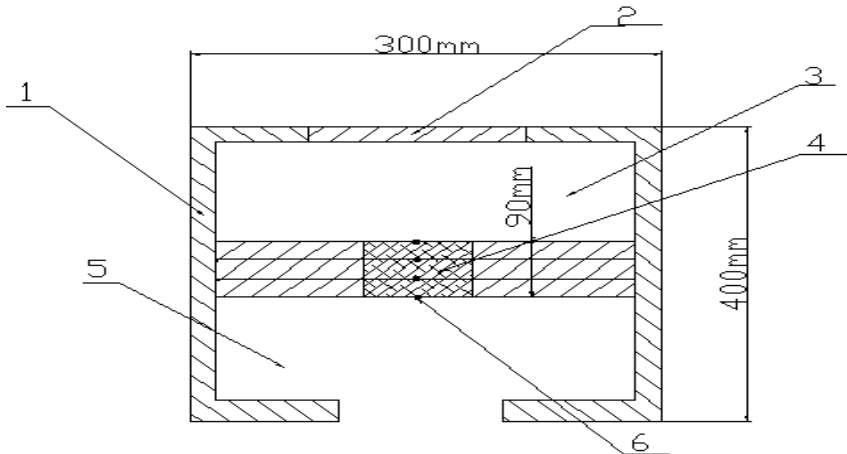


Figure 3: Experiment apparatus for water absorption analysis 1-Insulated box, 2-Gap to put and remove ice sack, 3- Space for ice, 4- Layers of testing materials, 5- Vapour recirculation, 6- Thermocouples connections.

- c) Put ice cube in the upper compartment of the enclosure and supply water vapor to the other compartment below; so that the sandwich multi-layer (100x80x30 mm dimensions of each layer) of testing materials is bounded on its top by ice and the bottom surface is exposed to vapor. After 1 hour of experiment, remove the sample layers and weight them immediately; then calculate the percentage of water accumulation due to the absorption of vapor using eqn (1). Repeat the same procedure for $t = 2h, 3h, 4h, \dots$

$$w_{ac} = \frac{w_i - w_o}{w_o} 100 \% \quad (1)$$

where w_i is the layer weight after testing, w_o the weight of the layer before testing, and w_{ac} the increase of water content (in %). The results are shown in fig. 5 and 6; x is the dimensionless distance from the layer one side of which is exposed to vapour.

$$x = \frac{x_i}{d} \quad (2)$$

where x_i is distance from the surface exposed to vapour ($x_i = 0$ at the bottom and $x_i = 90$ mm at the top) and d is the total thickness of the test sample.

The experimental uncertainty in weight is 0.1g; and thus, according to the procedure in Holman and Gajda [4] the uncertainty is about 6 % in water content.

2.3 Results and discussions

A sandwich multi-layer (100x80x30 mm dimensions of each layer) of testing materials was bounded on its top by ice and the bottom surface was exposed to vapour with temperature close to 100°C. Before testing, temperature at each location of thermocouple on the sample was about 20°C. After one hour of testing, the temperature at the bottom reached a maximum of 98°C and remained almost invariable. At the top surface cooled by ice, the temperature first decreased slightly and then increased to about 30°C after one hour and finally reached 35°C after 4 hours. The percentage of water accumulation due to vapour absorption was calculated for each layer. Figures 5 and 6 present the measurements of the water absorption. Very clearly, the water content within both the coconut fibres and groundnut coquet increased with time and, the water content for the groundnut coquets was higher than that of the coconut fibres.

For the groundnut coquet sample made with low porosity and high solid fraction, the water content considerably increased for the layer exposed to water vapour within two hours; but, the increase in the top layer water content was faster fig. 4. The bottom layer water content accumulation increased rapidly after being decreased between 2 and 3 hours, this may be explained by the fact that when the amount of condensate within the top layer exceeds a certain value, the water liquid is expected to fall down to the bottom and increase the two first layers weights. During the third and the fourth hours, two motions of species clearly occurred: the flow of vapour from the bottom to the top layer and the flow of condensate water by gravity and capillary action from the top to the bottom layer. However, during the first and second hours there was almost no motion of water from the top to the bottom. The water was transferred mainly by diffusion through the sample which explains why the top layer water content



increased respectively with time within 3 hours where a few amount of condensate flowed down to the bottom.

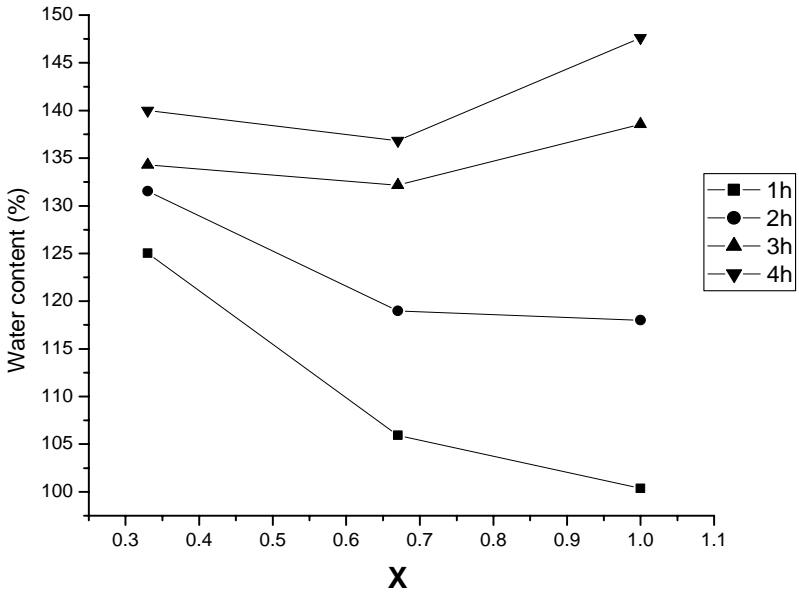


Figure 4: Water absorption for groundnut coquets.

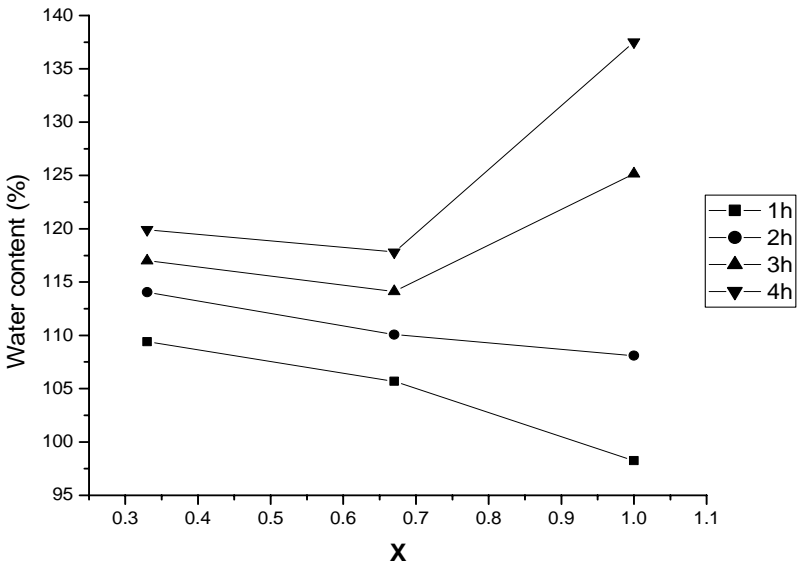


Figure 5: Water absorption for coconut fibres.



The saturated vapour flowed easily into the coconut fibres sample due to the higher porosity or larger spaces between fibres. Therefore, the two first layers (from the surface exposed to vapour) were wetted almost uniformly during the whole experiment with higher water content for the first layer, fig. 5. The difference in water content was very small for the all three layers after 2 hours. The fast increasing for the top layer is due to the water accumulation at the top thanks to the impermeable plastic placed on the top surface. After 4 hours, the main amount of water was accumulated near the top and a few amount of the condensate water from the top layer flowed by capillary and gravity toward the bottom layer during the whole experiment. In this case, moisture transferred through void space is very important. The water accumulation and distribution within the testing material were due to the transport of warm and moist air through the material towards the cold surface. At some location within the insulation in the cold region, the insulation temperature would be below the saturation temperature and moisture would condense and soak the material. The water content distribution is also affected by the liquid motion on the fibres surfaces. When the amount of liquid condensate reaches some threshold, the liquid water overcomes the surface tension effects and moves to regions with lower water content. Finally, both the coconut fibres and the groundnut coquet at low temperatures and high humidity may absorb water.

The following equation of thermal conductivity assumes that the liquid is distributed in continuous layers parallel to the direction of heat flow, Choudhary et al. [5].

$$k_{eff} = (1 - \varepsilon)k_s + \varepsilon(s_l k_l + s_g k_g) \quad (3)$$

where ε is porosity; k_s , k_l and k_g are thermal conductivity of solid matter, liquid and gas, respectively; s_l and s_g are phase saturation for liquid and solid (volumetric fraction of the void space occupied by a specific phase).

Eqn (3) shows that the thermal conductivity of moist insulations depends considerably on the amount of the liquid it contains. As a result, since water is a better thermal medium, the thermal conductivity of the soaked insulation would increase and the insulating value of the material would be destroyed.

3 Mathematical formulation

A porous media heat and mass transfer model and the coordinate used are presented in fig. 6 which represents a multilayered sandwich made of the testing materials. One side of the sample is exposed to saturated water vapour at $z = 0$, where the temperature and the vapour concentration are T_0 and w_0 , respectively. The opposite side is bounded by a plastic sheet and cooled by ice at $z = d$. When the saturated vapour flows through the porous media in the figure above, the following phenomenon may occur: diffusion of vapour through the pores in the materials (or fibres) toward the upper layer top surface; condensation on solid (cell) surface; diffusion of water within the cell wall; heat transfer due to



temperature difference existing in the sample and condensation (condensation is accompanied with the release of heat latent which acts as a heat source in the heat transfer process); transport of liquid (condensate water) by gravity and capillary action from the top surface of the upper layer toward the first layer. Thus, three phases are present in the sample: the solid matrix, the liquid water and the gaseous phase composed of water vapour and air.

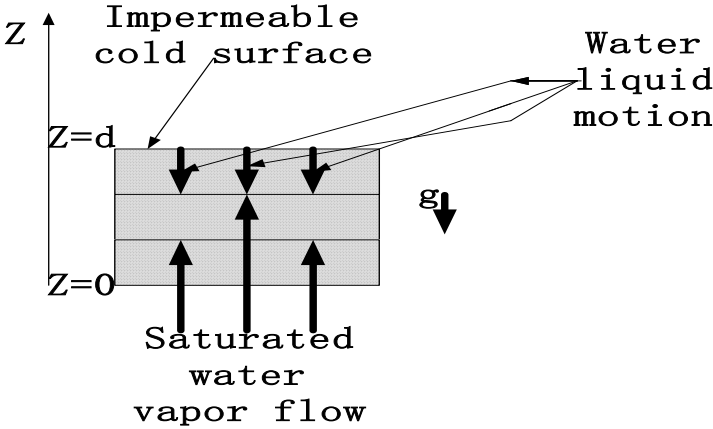


Figure 6: Analytical model and coordinate system for analysis.

The governing equations based on Whitaker’s work, (Choudhary et al. [5], Whitaker [6]) may be obtained by applying the local volume averaging to the mass, momentum, and energy equation for individual phase. Assuming that the process is one dimensional and the following assumptions: the samples made of testing materials are homogeneous; convection in the solid matrix is neglected; the total gas-phase pressure in the sample is constant; dry air is stagnated in the sample; however the water vapour is mobile.

Energy equation

$$\rho c_p \frac{\partial T}{\partial t} = \frac{\partial}{\partial z} \left(k_{eff} \frac{\partial T}{\partial z} \right) - \dot{m} h_{fg} \tag{4}$$

Water vapour diffusion equation

$$\frac{\partial}{\partial t} (\epsilon \rho_g s_g y_v) = \frac{\partial}{\partial z} (\epsilon \rho_g s_g D \frac{\partial y_v}{\partial z}) + \dot{m} \tag{5}$$

Water liquid transport equation

$$\frac{\partial}{\partial t}(\varepsilon \rho s_l) = \frac{\partial}{\partial z} \left(D_l \frac{\partial s_l}{\partial z} \right) - \frac{\partial}{\partial z} \left(\xi K \frac{k_{rl}}{v_l} \rho_l g \right) - \dot{m} \quad (6)$$

In Eqns (4), (5) and (6), the symbols s_g and s_l denote the phase saturation for gas and liquid, respectively. The phase saturation is defined as the volumetric fraction of the void space occupied by the corresponding phase. c_p is specific heat (J/kg K), D binary diffusion coefficient for transport of water vapour (m^2/s), D_l liquid diffusivity (m^2/s), g acceleration due to gravity (m/s^2), h_{fg} latent heat (J/kg), K absolute permeability (m^2), k_{eff} effective thermal conductivity (W/m K),

k_{rl} relative permeability, \dot{m} rate of phase change (negative for condensation) ($\text{kg}/\text{m}^3\text{s}$), t time (s), y_v mass fraction of water vapour in the gaseous mixture, ε the porosity, ρ the density (kg/m^3), ξ hindrance function. The hindrance function varies from 0 (in the region that are fully saturated with liquid) to 1 (in the region that contains no water). The solutions of the eqns (4), (5) and (6) require more theoretical and numerical investigations. Further studies are needed to find an appropriate solution procedure to describe and solve numerically the thermodynamic and physical phenomenon of the figure 5.

4 Conclusion

Experimental investigations are done to characterize the moisture absorption of two different natural materials (coconut fibres and groundnut coquets). A sandwich multi-layer (100x80x30 mm dimensions of each layer) of the testing materials was bounded on its top by ice and the bottom surface was exposed to vapour with temperature close to 100°C. The percentage of water accumulation due to vapour absorption was calculated for each layer after a pre-set time of experiment (1h, 2h,...). The water content of the groundnut coquet was lower than that of the coconut fibres but for all the materials the water content increased with time. For the groundnut coquet sample, the water was transferred mainly by diffusion through the porous media; but in the coconut fibres sample with higher porosity, the water transferred by diffusion through void space was the most important. Actually, moisture absorption may occur when the materials are used under very low temperatures and high humidity. The thermal conductivity of moist insulation depends considerably on the amount of the liquid it contains; as a result, since water is a better thermal medium, the thermal conductivity of the soaked insulation would increase and the insulating value of the material would be destroyed. A thin plastic vapour barrier should be placed over the insulation to prevent moisture from entering the insulation.

References

- [1] Conte, I., Peng, X., Christopher, D. M., Xie, J. & Xu, J., Transport Properties of Biomass Materials as Thermal Insulator. *Proc of the 7th Asian Thermophysical Properties Conf.*, eds. B. X. Wang, pp. 63, 2004.



- [2] Fan, J., Cheng, X. & Chen, Y.-S., An experimental investigation of moisture absorption and condensation in fibrous insulations under low temperature. *Experimental Thermal and Fluid Science*, **27**, pp. 723-729, 2002.
- [3] Edwin, F. S. & William C. T., *Thermal Insulation Building Guide*, Robert E. Krieger: Malabar, pp. 1-473, 1990.
- [4] Holman, J. P. & Gajda, W. J., *Experimental Methods for Engineers* 5th edition, McGraw-Hill: United States, pp. 37-379, 1989.
- [5] Choudhary, M. K., Karki, K. C. & Patankar, S. V. Mathematical modeling of heat transfer, condensation, and capillary flow in porous insulation on a cold pipe, *Int. Journal of Heat and Mass Transfer*, **47**, pp. 5629-5638, 2004.
- [6] Whitaker, S., *Theory and Applications of Transport in Porous Media: The Method of Volume Averaging*, Kluwer Academic: USA, pp. 1-180, 1999.



Simulation of perspiration in sweating fabric manikin-Walter

J. Fan

*Institute of Textiles and Clothing,
The Hong Kong Polytechnic University, Hong Kong*

Abstract

Thermal manikins are essential tools for the comfort evaluation of the thermal environment and clothing as well as research into the dynamics of heat and moisture transfer from the human body to the environment – a foundation for thermal physiology and environmental engineering.

Since the development of the first non-sweating, single segment copper thermal manikin by the US Army in 1940s, there have been numerous developments worldwide in thermal manikin technologies. Nevertheless, the simulation of perspiration has continued to be one of the major challenges. Inspired by the thermoregulation system of the human body, a novel sweating fabric manikin nicknamed “Walter” has been developed in Hong Kong Polytechnic University. The new sweating manikin achieved perspiration over the entire body and a very high measurement accuracy (viz. a CV of less 5%), yet with a cost of only a small fraction of other sweating manikins developed so far.

Keywords: sweating, perspiration, manikin, thermal comfort, clothing, environmental ergonomics.

1 Introduction

Comfortable clothes can be a matter of life or death in hazardous environments from wind-blasted mountain peaks and frozen Arctic wastes to space exploration. But thermal comfort also affects our everyday lives. Adequate insulation and good breathability are keys to comfort. In order to develop and optimize the functional design of clothing, it is essential to develop advanced



tools for the evaluation of clothing thermal comfort, and for the investigation of the dynamic thermal interaction between human body, clothing and environment.

Thermal comfort of clothing systems may be evaluated by subjective wearer trials or objective simulation tests. Subjective wearer trials can relate the results directly to the clothing in actual use, but tend to be inconsistent and costly and can sometimes expose the subjects to danger when testing under extreme conditions. Objective simulation tests include flat plate methods (e.g. Togmeter, KESF Thermolab), cylindrical methods (e.g. Cylindrical Togmeter) and thermal manikins. Flat plate and cylindrical methods are useful for evaluating the thermal properties of clothing materials and simple clothing assemblies, but have difficulties in applying the results to the actual clothing systems in use. Thermal manikins have therefore been considered as the most useful tools for evaluating the thermal comfort of clothing systems [1].

The development of thermal manikins started during the Second World War. It is estimated that there are over 100 thermal manikins in the world [2]. Some of the most advanced recent manikins are divided into many sections and the temperature of each section is controlled independently so as to achieve a distribution similar to that of the human skin. Sweating is simulated by supplying water through the tiny tubes to the holes distributed at the manikin surface. Such manikins are very costly due to the complicated control systems for heating and water supply. The development cost for the sweating manikin-“SAM” in Switzerland is said to be 10 million Swiss Franc [3]. Nevertheless, the simulation of sweating in the existing manikins is limited by the practically manageable number of water supplying tubes and holes, which are far less than the approximately six million sweating glands on human. Besides, they are not very accurate because of the difficulty in maintaining consistent sweating and in accurately determining the humidity at the skin surface [4]. They also have very different thermal properties from that of a human body.

The new invention-Walter is inspired by the thermoregulation system of human body. With the original use of a breathable fabric to simulate the skin and a water circulation system to simulate the blood circulation, the novel manikin achieved perspiration over the entire body and very high measurement accuracy (viz. a CV of less 5%), yet with a cost of only a small fraction of other sweating manikins developed so far.

2 Description of sweating manikin-Walter

The invention of “Walter” is based on a completely new concept. “Walter” is the first thermal manikin made of mainly water and high strength breathable fabric. Sweating is simulated by a waterproof, but moisture permeable, fabric ‘skin’ that holds the water, but allow moisture transmission from the manikin’s insides through the millions of tiny pores in the skin. Walter simulates human thermal physiology. The core of Walter’s body is controlled at 37°C and the body temperature regulation is achieved by regulating the rate of the pumps which supply warm water from the core region to the extremities. Simultaneous heat loss and evaporative water loss from the manikin are accurately measured, hence



it takes only one step to measure the two most important parameters - thermal insulation and moisture vapour resistance. The arms and legs of “Walter” can be motorized to simulate walking motion. The perspiration rate can be regulated by changing the skin temperature and having a fabric skin of different moisture permeability. Since it mainly consists of water, it has a similar weight and heat capacity to a human body, which is also composed of mainly water. Figure 1 shows the front view of “Walter”. The main dimension of “Walter” is listed in Table 1.

Table 1: Dimensions of Walter.

Height	172 cm
Neck Circumference	45 cm
Chest Circumference	95 cm
Waist Circumference	89 cm
Hip Circumference	100 cm
Surface Area	1.79 m ²



Figure 1: Front view of Walter.

“Walter” consists of the following sub-systems:

- Water circulation system.
- System for the simulation of “walking” motion
- Online water supply system.
- Control and measurement system

2.1 Breathable fabric skin

The “skin” of the manikin is very crucial to the success of this design. It should not only be able to produce the “perspiration”, but also to hold as much as 70 kg of water inside the body and allow flexing induced by the body movement. According to our requirements, a special waterproof and moisture permeable fabric was used. The fabric has a sandwich structure. Its face side is a strong nylon fabric, inner side a protective knitting fabric and the middle a patented microporous polytetrafluoroethene (PTFE) membrane. The membrane has billions of pores per square inch with the largest being less than 0.2 μm. The combination of the natural hydrophobicity of the PTFE polymer and the very small pore size and the great number of pores allows the membrane to discriminate between water as a gas and water as a liquid [5]. Since the water vapor molecular diameter is 2.72×10^{-8} cm, smaller than nitrogen gas molecular



(3.16×10^{-8} cm) and oxygen gas molecular (2.96×10^{-8} cm), and is about 700 times smaller than a pore in the membrane. Liquid water on the other hand has tens of thousands of these molecules bonded together because of free energy considerations. In its smallest configuration, liquid water as a macro droplet is many thousands of times larger than the pores in the membrane. The membrane takes advantage of the difference of water in the state of gas and liquid to discriminate between the two so as to keep water in the manikin body and to allow moisture transmission through the “skin” to generate gaseous “perspiration”.

2.2 Water circulation system

Just like human body’s blood circulation system, “Walter” has a water circulation system which distributes the heat produced in the core region to the head, arms and legs. Temperatures at extremities depend on the water flow rates into them. The water flow rates can be adjusted by altering the five valves connecting to the head, arms and legs regions and the four small valves at the ends of the legs and arms. The five valves connecting to the head, arms and legs regions should be pre-adjusted, but the four small valves at the ends of the legs and arms can be adjusted during operation. The skin temperature can be further regulated in real time by a control software, which adjusts the rate of the pumps through regulating the AC power supply to the pumps.

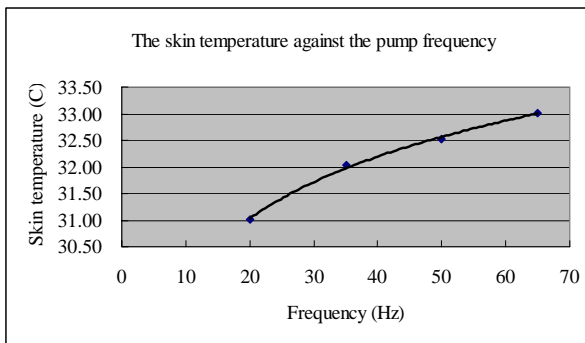


Figure 2: The relationship between the mean skin temperature and AC frequency of the pumps.

2.3 Simulation of “walking” motion

“Walter” has a soft body, the arms can be bent easily when pushed or pulled in a simulating “walking” motion. The legs are however more difficult to bend due to their large cross-section. Joints between the legs and the torso should therefore be designed. The design idea of the joints is to reduce the cross-section at the connection between the legs and the torso so that the legs can be bent more easily, when pushed and pulled in simulating “walking” motion, but not blocking the water flow into and out of the legs. To achieve this idea, two plastic ABS

rings are placed inside the body and one stainless steel ring is placed outside the skin on each leg. The inner plastic rings were used to keep the shape of the upper parts of the legs, whereas the external steel rings were used to limit the cross sectional area of the joints so as to facilitate bending. The diameter of the stainless steel ring is small than that of the ABS rings and it can be open and closed, so that the stainless steel ring could be inserted into the joint and used to reduce the cross-section of joint.

A quadric crank mechanism is used to create a forward and backward movement to push and pull the arms and legs to simulate “walk” motion. The “walking” pace can be adjusted by changing the position of the connection points of the cantilever. The pace size can be changed from 0.3 to 0.6 m. The “walking” speed can be automatically changed by changing the frequency of the AC power supply to the driving motor using a computer controlled AC frequency regulator. The “walking” speed can vary from 0 to 3.6 km/hr.

2.4 Online water supply system

The fully filled water in the body of Walter maintains the body shape, skin temperature and the water evaporation from the skin of “Walter”. Due to the large amount of water evaporated from “Walter” during its relatively long-time measurement cycle, an online automatic water supply system is necessary to compensate the water loss from “Walter”, and to keep “Walter” at consistent working condition. This system is also critical to achieving online measurement of “Walter” system.

The system consists of a small water container and a programmable electronic balance. The water container was connected to “Walter’s” body by a soft tube through siphon action. Figure 3 illustrates the online water supply system of “Walter”.

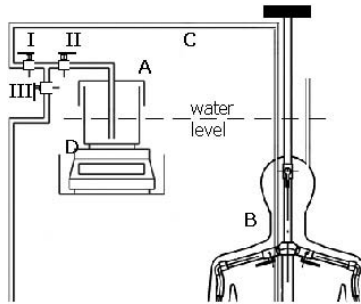


Figure 3: The automatic water supply system.

The water level in the water container is the same as that in the “Walter’s” body at any time because of siphon action. Therefore the water in the water container can automatically flow into “Walter” to compensate the water loss

from “Walter”. The amount of water compensated to “Walter” can be used to calculate the evaporative rate of water from the skin of “Walter”.

2.5 Control and measurement system

Figure 4 illustrates the control and measurement system of “Walter”.

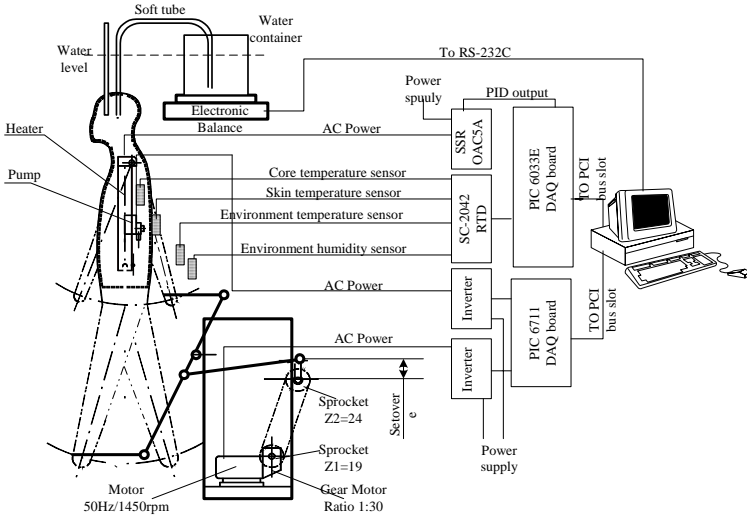


Figure 4: Control and measurement system of “Walter”.

With this sub-system, the core temperature or the mean skin temperature of the manikin can be controlled automatically to the precision of $\pm 0.05^{\circ}\text{C}$. The power supply (or heat loss), skin temperature at different positions and evaporative water loss can be measured in real time. Instead of weighing the entire manikin (about 70 kg) for measuring the evaporative water loss which would be less accurate, “Walter” measures the water loss from a container (less than 6 kg), which is connected to the manikin through a soft tube and the water level in the manikin is the same as that in the container as a result of siphon action. This greatly increased the measurement accuracy [6].

2.6 Measurement using Walter

By measuring the heat supply, evaporative water loss, skin temperatures at different locations, the two most important thermal comfort properties of clothing, viz. the thermal insulation (R_t) and moisture vapour resistance (R_{et}), can be calculated using the following formulae:

$$R_t = \frac{A_s(\bar{T}_s - T_a)}{H_s + H_p - H_e} \tag{1}$$



$$H_e = \lambda \cdot Q \quad (2)$$

$$R_{et} = \frac{A_s (P_s^* - RH_a P_a^*)}{H_e} - R_{es} \quad (3)$$

where, A_s is the total surface area of the manikin, $\overline{T_s}$ is the mean skin temperature, T_a is the mean temperature of the environment, H_s is the heat supplied to the manikin or the heat generated by the heaters, H_p is the heat generated by the pump ($H_p=12.6$ W), H_e is the evaporative heat loss from the water evaporation, λ is the heat of evaporation of water at the skin temperature. From the data-book of thermal physics, $\lambda = 0.67$ W.h/g at 34°C . Q is the “perspiration” rate or water loss per unit time, which is measured automatically through the electronic balance, P_s^* is the saturated water vapour pressure at the skin temperature, RH_a the relative humidity of the surrounding environment, P_a^* the saturated water vapour pressure at the surrounding environment, and R_{es} is the moisture vapour resistance of the “skin”. R_{es} is predetermined constant for each type of fabric skin. For a normal skin used in our experiment, R_{es} equals to 8.6 m²Pa/W [6].

From the thermal insulation (Rt) in m²°C/W and moisture vapour resistance (Ret) in m²Pa/W, one further derive the moisture permeability index Im by the following formula (Based on ISO9920) :

$$I_m = 60.6 \times \frac{R_t}{R_{et}} \quad (4)$$

The moisture permeability index Im is a dimensionless measure of the moisture permeability of the clothing system.

By weighing the garments before putting on “Walter” and after taking off from Walter after a specified period, one can also determine the percentage of moisture accumulation within clothing by the following formula:

$$M_a = \frac{W_a - W_b}{W_b} \times 100\% \quad (5)$$

The thermal insulation (Rt), vapour resistance (Ret), moisture permeability index (Im) and moisture accumulation (Ma) are important measures of clothing thermal comfort and can be interpreted in general as follows:

- The thermal insulation (Rt) should be as small as possible for summer clothing to keep cool;
- The thermal insulation (Rt) should be as high as possible for winter clothing to keep warm;
- The vapour resistance (Ret) of clothing should be as low as possible for any type of clothing to make the clothing permeable;
- The moisture permeability index (Im) should be as high as possible for any type of clothing to make the clothing permeable;
- The moisture accumulation Ma should be as low as possible for any type of clothing to keep the skin and clothing dry.



3 Results and discussion

3.1 The accuracy and reproducibility of Walter

The thermal insulation and moisture vapor resistance of the nude manikin were tested repeatedly for three times in different wind velocity under the 20°C and 50% RH. The mean values are listed in Table 2 and the standard deviation of each value is listed in Table 3.

Table 2: The mean values of Ioa and Roa vary with wind velocity.

Wind velocity (m/s)	Ts	Te	He	W	Q	Ioa	Roa
0.22	35.04	20.32	46.76	649.90	562.59	0.101	12.90
0.85	34.91	19.75	48.25	842.95	697.00	0.076	8.62
1.69	34.96	19.83	47.68	1046.46	833.76	0.058	5.86
2.48	34.82	19.89	53.87	1157.64	874.55	0.049	4.61
3.12	34.89	19.79	52.24	1271.96	916.97	0.043	4.19
4.04	34.94	19.84	49.33	1415.32	1004.19	0.038	3.29

Table 3: The standard deviation of Ioa and Roa measured on the manikin.

Wind velocity (m/s)	Ts	Te	He	W	Q	Ioa	Roa
0.22	0.02	0.01	0.50	4.71	6.63	0.003	0.32
0.85	0.01	0.02	0.10	1.88	5.43	0.001	0.13
1.69	0.01	0.17	0.35	0.01	6.18	0.001	0.11
2.48	0.05	0.03	0.02	18.28	3.48	0.001	0.01
3.12	0.02	0.01	0.41	10.32	5.67	0.000	0.01
4.04	0.01	0.01	0.51	1.56	6.87	0.000	0.01

The average thermal insulation of the nude manikin in the case of standing in still air was found to be 0.101 m²C/W with a standard deviation of 0.003 (viz. CV=3%), the average moisture vapor resistance of nude manikin is 12.90 m²Pa/W with a standard deviation of 0.32 (viz. CV=2.5%). These results show that the accuracy of "Walter" is very high.

A clothing ensembles include underwear and outerwear are used to valid the reproducibility. The experiment conducts three independent replications of thermal measurements. The independent replication means taking the all garments off and putting them back on for each replication of the test. The test



results are listed in Table 4. The CV of the repeated measurements of the clothing thermal insulation was 3.3% and that of the moisture vapour resistance is 2.2%, which are very good.

Table 4: The reproducibility of measurements on manikin.

	Ts	Te	He	W	Q	Rt	Re
Repeat1	35.14	20.31	49.22	314.5	279.7	0.218	34.06
Repeat2	35.01	20.38	49.25	318.5	277.9	0.206	33.89
Repeat3	35.13	20.31	49.43	315.3	271.2	0.206	35.32
mean	35.09	20.33	49.30	316.12	276.27	0.210	34.42
Stdev	0.07	0.04	0.12	2.14	4.50	0.007	0.78

3.2 Comparison with previously reported results

The results are generally comparable to those reported elsewhere. For example, the thermal insulation of the nude manikin standing in the almost still air was found to be $0.101 \text{ m}^2\text{C/W}$, which is within the range of the variations (from 0.051 to $0.104 \text{ m}^2\text{C/W}$) found in an inter-laboratory study [7]. The moisture vapour resistance of the nude manikin obtained in our experiments is $12.9 \text{ m}^2\text{Pa/W}$, which is at the lower end of the reported range of from 11.0 to $20.0 \text{ m}^2\text{Pa/W}$ [7]. The actual relative humidity at the skin surface of those sweating manikins reported in the previous the inter-laboratory study might be lower than the assumed value of 100%, which might make the values of the moisture vapour resistances greater than the actual ones.

4 Conclusions

Through the simulation of the human skin using a breathable fabric, the simulation of the human thermal regulation system using a water circulation and temperature control system and the simulation of human body using water, the new invention has demonstrated distinct advantages in terms of its physical characteristics and measurement accuracy. The invention is a breakthrough in manikin technology and has found important applications in comfort evaluation of functional clothing and research in thermal physiology and environmental engineering.

References

- [1] Fan, J. & Chen, Y. S. Measurement of Clothing Thermal Insulation and Moisture Vapour Permeability Using a Novel Perspiring Fabric Thermal Manikin, *Measurement Science and Technology*, 13, pp. 1115-1123, 2002.



- [2] Holmer, I. Thermal manikin history and application, *European Journal of Applied Physiology*, 92(6), pp. 614-618, 2004.
- [3] Richard, M. Private communication during the 4th international meeting on thermal manikins, September 2001, St. Gallen, Switzerland.
- [4] Richard M., Mattle N. & Becker C. Assessment of the protection and comfort of fire fighter's clothing using a sweating manikin, Proceedings of the 5th European Conference on Protective Clothing and NOKOBETEF7, May 2003, Montreux, Switzerland.
- [5] Tanner, J. C. Breathability, Comfort and GORE-TEX Laminates, *Journal of Coated Fabrics*, 8, pp. 312, 1979.
- [6] Fan, J. & Qian, X. New Functions and Applications of Walter, the Sweating Fabric Manikin, *European Journal of Applied Physiology*, 92, pp. 641-644, 2004.
- [7] McCullough, E. A., Interlaboratory Study of Sweating Manikins, Proceedings of the Fourth International Meeting on Thermal Manikins, EMPA, Switzerland, 27-28, September 2001.



Section 5

Bioengineering

This page intentionally left blank

State of the art of solid freeform fabrication for soft and hard tissue engineering

P. J. S. Bártolo

Department of Mechanical Engineering and Institute for Polymers and Composites, School of Technology and Management, Leiria Polytechnic Institute, Portugal

Abstract

Tissue engineering is an interdisciplinary field involving the combined efforts of cell biologists, engineers, material scientists, mathematicians and geneticists towards the development of biological substitutes to restore, maintain, or improve tissue functions. It has emerged as a rapidly expanding field to address the organ shortage problem.

Advanced solid freeform fabrication techniques are now being developed to fabricate scaffolds with controlled architecture for tissue engineering. These techniques combine computer-aided design (CAD) with computer-aided manufacturing (CAM) tools to produce three-dimensional structures layer-by-layer in a multitude of materials.

This paper introduces the concept of tissue engineering assisted by computer. Different solid freeform fabrication techniques for tissue engineering are described and their advantages and disadvantages discussed with great detail. Novel fabrication procedures, such as alginate rapid prototyping and cell printing, are also presented opening new and exciting possibilities within the tissue engineering field.

1 Introduction

In 1988, the concept of tissue engineering was presented for the first time as “the application of the principles and methods of engineering and life sciences toward fundamental understanding of structure-function relationship in normal and mammalian tissues and the development of biological substitutes for the repair or regeneration of tissues or organ functions” [1]. In 2003, 87 717 patients were



waiting for organ transplantation in USA alone [2]. This number has increased to 88 598 by May 2005, while 4 375 transplants were performed between January and February 2005[3]. Although clinics have tried to replace the function of failing organs mechanically or through implantation of synthetic replacements, these are often only temporary solutions, not allowing the patient to completely resume normal activities. Moreover, infection and device rejection are also serious concerns in such procedures.

Tissue engineering has emerged to address the organ shortage problem as cells might be able to organise into tissue and organ replacements when cultured in 3D under proper reactor conditions [4]. Scaffolds have been produced from either natural or synthetic materials to create the 3D environment for cellular attachment, migration, proliferation and differentiation [5]. These scaffolds must degrade slowly after implantation in a patient, being replaced by new tissue [6], so playing an important role as delivery vehicles for the sustained release of tissue growth factors, promoting natural wound healing and regeneration [7-8].

Several techniques were developed to produce 3D scaffolds for tissue engineering. The conventional techniques include fibre bonding, solvent casting, particulate leaching, membrane lamination, microwave baking and expansion, high pressure based methods and melt based technologies [9-12]. However, these techniques do not properly control pore size, pore geometry and spatial distribution of pores, besides being very difficult to construct internal channels within the scaffold. Beyond these limitations, these techniques involve the use of toxic organic solvents, long fabrication times on top of being labour-intensive processes.

Solid freeform fabrication (SFF) represents a new group of non-conventional techniques were recently introduced in the medical field. The main advantages of SFF are both the capacity to rapidly produce very complex 3D models and the ability to use various raw materials and surface finishing processes. In the medical field, SFF models have been mainly used for assisting diagnosis, planning treatment and manufacturing implants particularly in oral and maxillofacial surgery. Recently, SFF have been explored to produce scaffolds with customised external shape and predefined internal morphology [2,13]. In this case, SFF also allows one to control pore size and pore distribution [2,9].

Figure 1 provides a general overview of the necessary steps to produce SFF scaffolds for tissue engineering. The first step to produce a 3D scaffold through rapid prototyping is the generation of the corresponding computer solid model through one of the currently available techniques. These imaging methods produce continuous volumetric data (voxel-based data), which provide the input data for model generation. The model is then tessellated as an STL file, which is currently the standard file for faceted models. Finally, the STL model is mathematically sliced into thin layers (sliced model). The SFF systems use the slice data to replicate a physical object layer-by-layer.

Data acquisition techniques available for medical imaging and different SFF processes and its applications in the field of tissue engineering are described in the following sections of this paper.



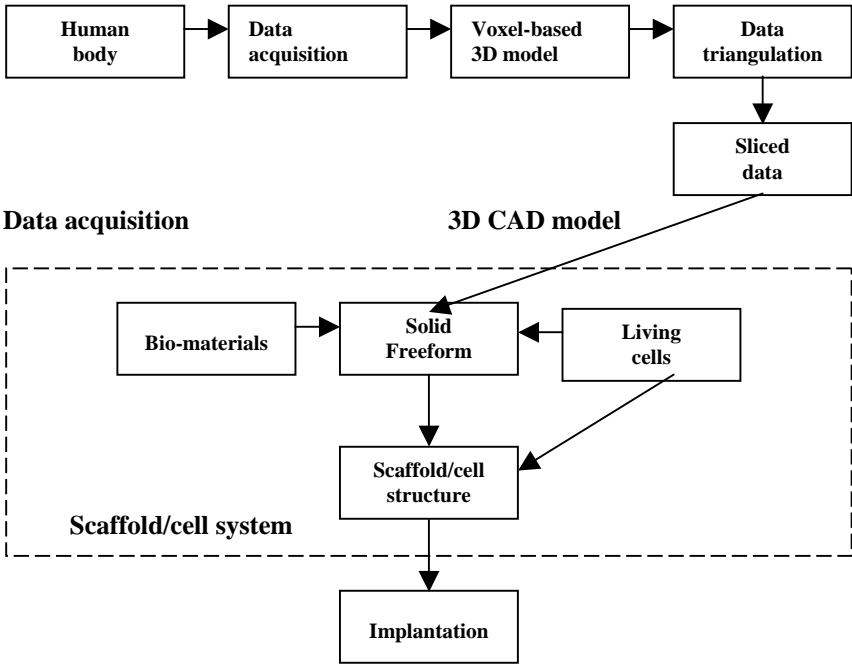


Figure 1: Steps for rapid prototyping scaffolds.

2 Data acquisition

Since the discovery of X-rays by Röntgen in 1895, medical imaging has made remarkable progress, playing a central role in medical care. The primary data acquisition techniques used in tissue engineering are:

- **Computer tomography (CT)** introduced in early 1970s as a neurological examination technique. It requires the exposure of a sample to small X-ray quantities, the absorption of which is detected and imaged. The result is a series of 2D images displaying a density map of the sample. The image contrast represents differences in X-ray attenuation. Stacking the images together create a 3D representation of the scanned data. Diverse software tools have been developed for 3D representation of the scanned data, like Velocity2 Plus (Javelin, USA), BioBuild (Anatomics, Australia), MIMICS (Materialise, Belgium) and InVesalius (CenPRA, Brazil) [14-17]. Recent developments comprise multislice CT, which uses multistage detectors for simultaneous collection of multislice data, as well a cone-beam CT using a flat panel detector providing highly precise 3D data [18,19].
- **Magnetic resonance imaging (MRI)** based on the magnetisation of water molecules, present in different concentrations for most types of tissues. MRI is more expensive and complex than CT, though it has an extensive application, due to its non-invasive and non-radiative nature [18]. An important disadvantage is the time a patient is required to be motionless during scanning.



Key current topics of research include both the improvement of image quality for fast imaging and the accuracy of functional MRI, as well the development of ultra-high magnetic field devices.

- **Nuclear medical imaging (NMI)** or molecular imaging is a process in which a radiochemical compound is injected and the information is obtained by both its distribution inside the body and density changes over time. In NMI, the main methods are single-photon emission CT (SPECT) using γ -emitting nuclei and positron emission tomography (PET), and positron-emitting nuclei.
- **3D ultrasound** is a promising medical imaging technique performed through modern scanners that are inexpensive, portable and safe [20]. Many different acquisition approaches have been developed for 3D ultrasound imaging. These approaches comprise 2D transducers arrays, mechanical scanners, and freehand methods [20]. Many features of modern scanners intend to improve both the overall usability of the devices and the automatic image optimisation. Important developments are expected for ultrasound imaging areas like mechanical properties of tissues, molecular imaging and gene therapy.

X-ray imaging is widely used to acquire morphological information, while magnetic resonance imaging is used to acquire both morphological and functional information [19]. Ultrasound imaging is better suited for acquiring functional information and nuclear medical imaging is used to obtain information on metabolism and molecular behaviour [19].

3 SFF in tissue engineering

The most important SFF processes for tissue engineering are:

- **Photo-polymerisation or stereolithographic processes:** use an ultraviolet (UV) laser beam to selectively solidify successive thin layers of photo-sensitive polymers, each built on top of the previous layer. The laser beam is guided onto the polymer surface in accordance to cross-sectional data. Support structures are required.

Levy *et al.* [21] used a direct irradiation stereolithographic process to produce hydroxyapatite (HA) ceramic scaffolds for orbital floor prosthesis. A suspension of fine HA powder into a UV-photocurable resin was formulated and used as building material. The photo-cured resin acts as a binder to hold the HA particles together. The resin is then burnt out and the HA powder assembly sintered for consolidation. A similar approach was used by Griffith and Halloran [22] that produced ceramic scaffolds using suspensions of alumina, silicon nitride and silica particles with a photo-curable resin. The binder was removed by pyrolysis and the ceramic structures sintered. Matsuda and Mizutani [23] developed a biodegradable, photocurable copolymer, acrylate-endcapped poly(ϵ -caprolactone-co-trimethylene carbonate) to produce scaffolds through stereolithographic processes. Very promising is also the research conducted by microTEC on the rapid micro product development (RMPD) concept [24].



- Laser sintering processes:** uses a high-power carbon dioxide laser emitting infrared radiation, to selectively heat powder material just beyond its melting point. The laser traces the shape of each cross-section of the model to be built, sintering powder in a thin layer. It also supplies energy that not only fuses neighbouring powder particles, but also bonds each new layer to those previously sintered. The sintering process takes place in a sealed heated chamber at a temperature near the powder melting point filled with nitrogen. Maintaining the hot environment in the build chamber also reduces both the power required from the laser and the thermal shrinkage of the model. After each layer is solidified, the piston over the model retracts to a new position and a new layer of powder is supplied using a mechanical roller. The powder that remains unaffected by the laser acts as a natural support for the model and remains in place until the model is complete.

Williams *et al.* [25] used selective laser sintering to produce porous PLC scaffolds, which were then seeded with bone morphogenetic protein-7 (BMP-7) transduced fibroblasts. In vivo results show that these scaffolds enhance tissue in-growth, on top of possessing mechanical properties within the lower range of trabecular bone. Lee *et al* [26] coated calcium phosphate powder with polymer by spray drying slurry of particulate and emulsion binder. The coated powder was then sintered to fabricate calcium phosphate bone implants. Afterwards, these structures were infiltrated with calcium phosphate solution or phosphoric acid-based inorganic cement.

- Extrusion processes:** uses filaments of material that are melted by heating and guided by a robotic device (extruder), controlled by a computer, to form the 3D object. The material leaves the extruder in a liquid form and hardens immediately. The previously formed layer, which is the substrate for the next layer, must be maintained at a temperature just below the solidification point to assure good interlayer adhesion.

Wang *et al.* [27] used a novel precision extruding deposition (PED) process to directly fabricate cellular poly- ϵ -caprolactone (PCL) with controlled pore size of 250 μm and designed structural orientations ($0^\circ/90^\circ$, $0^\circ/120^\circ$ or combined $0^\circ/120^\circ$ and $0^\circ/90^\circ$ patterns). Proliferation studies were performed using cardiomyoblasts, fibroblasts and smooth muscle cells. Additionally, mechanical tests were performed with the produced scaffolds showing compression modulus in the range between 150 MPa and 200 MPa. Hutmacher *et al.* [28] optimised the extrusion processing parameters for the production of PCL honeycomb-like scaffolds. Similar work was conducted by Zein *et al.* [29] that produced PCL scaffolds with a range of channel size 160-700 μm , filament diameter 260-370 μm , porosity 48-77% and regular honeycomb pores. The compressive stiffness ranged from 4 to 77 MPa, yield strength from 0.4 to 3.6 MPa, and yield strain from 4% to 28%. Other research studies carried out by Woodfield *et al.* [30], Chen *et al.* [31] and Widmer *et al.* [32] showed that extrusion processes can be used for tissue engineering.

- Ink-jet printing:** involves the bonding and the build up method. The bonding method deposits a stream of microparticles of a binder material over the surface of a powder bed, joining particles together to form the object. A



piston lowers the powder bed so that a new layer of powder can be spread over the surface of the previous layer and then selectively joined to it. The build-up method emits a stream of microparticles just above their solidification temperature until an exact co-ordinate where they solidify. The jet heads build the product from bottom up, spraying one layer at a time.

Kim *et al.* [33] employed this SFF technique with particulate leaching to create porous scaffolds, using polylactide-coglycolide (PLGA) powder mixed with salt particles and a suitable organic solvent. The salt particles were leached using distilled water. Cylindrical scaffolds were fabricated measuring 8 mm (diameter) by 7 mm (height) with pore sizes of 45-150 μm and 60% porosity. Hepatocytes were also successfully attached to the scaffolds.

The influence of pore size and porosity on cell adhesion and proliferation were investigated by Zeltinger *et al.* [34]. Disc shaped poly(L-lactic acid) (L-PLA) scaffolds measuring 10 mm (diameter) by 2 mm (height) were produced through both ink-jet printing and salt and leaching methods. The scaffolds were produced with two different porosities (75% and 90%) and four different pore size distributions (<38, 38-63, 63-106 and 106-150 μm), and tested with cell culture using canine dermal fibroblasts, vascular smooth muscle cells and microvascular epithelial cells. The cell culture results produced show the suitability of ink-jet printing to fabricate scaffolds for tissue engineering. Lam *et al.* [35] developed a blend of starch-based powder containing cornstarch (50%), dextran (30%) and gelatine (20%) that can be bound by printing distilled water. Cylindrical scaffolds were produced measuring 12.5 mm (diameter) by 12.5 mm (height) and infiltrated with different amounts of a copolymer solution consisting of 75% L-PLA and 25% polycaprolactone in dichloromethane to improve their mechanical properties. Sachlos *et al.* [36] uses an indirect approach to produce collagen scaffolds with complex internal morphology and macroscopic shape by using an ink-jet printing sacrificial mould. A dispersion of collagen was cast into the mould and frozen. The mould was then dissolved with ethanol and the collagen scaffold was critical point dried with liquid carbon dioxide. Other research works, like the ones of Taboas *et al.* [37], Limpanuphap and Derby [38] and Park *et al.* [39], have also exploited the capabilities of ink-jet printing for tissue engineering.

- **Bio-plotting:** is a novel dispersing technique developed at the Freiburg Materials Research Center, Germany, for soft tissue applications. The key feature of this process is the 3D dispersing of a viscous plotting material into a liquid medium with a matching density [40]. As a result of this buoyancy compensation, structures can be produced mostly without temporary support structures. A very large variety of materials can be processed including melts, pastes, reactive resins or hydrogels.

Ang *et al.* [41] developed a rapid prototyping robotic dispersing (RPBOD) using the same principle as the 3D bio-plotting system, which was used to produce chitosan-HA scaffolds. Solutions of chitosan-HA were extruded into a sodium hydroxide and ethanol medium to induce the precipitation of chitosan. The scaffolds were then hydrated, frozen and freeze-dried.



A similar process, called alginate-based rapid prototyping, has been developed at the Polytechnic Institute of Leiria. This process produces alginate solid structures (Figures 2 and 3), by extruding a previously prepared solution of sodium alginate in water, mixed with a solution of calcium chloride, providing a temporary support for the seeded cells in culture. Alginate is one of the most versatile biopolymers, with a wide range of pharmaceutical and biomedical applications, such as polymer films, cell encapsulation, wound dressings and surgical sponges [42]. Alginate also shows minimal cytotoxic effects and reduced hemolysis when in contact with blood [16]. In early 1970s, alginate was recognised as safe to be used in food and pharmaceutical ingredients by the US Food and Drug Administration (FDA). Similar procedures have been used by Mironov *et al.* [43], which developed the concept of cell printing. This process prints gels, single cells and cell aggregates offering a possible solution for organ printing. Organ printing involves three main steps: pre-processing or development of “blueprints” for organs, processing or organ printing and accelerated organ maturation.

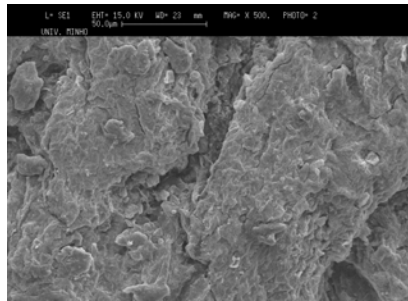


Figure 2: Surface morphology of an alginate solid tissue.

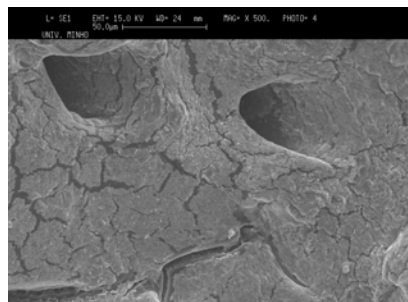


Figure 3: Cross section morphology of an alginate solid tissue.

Table 1 lists the main advantages and limitations of SFF for tissue engineering. Accuracy is an important issue to be addressed. Table 2 shows the main source of errors generated during the production of SFF structures for tissue engineering for each stage.



Table 1: Characteristics of rapid prototyping scaffolds for tissue engineering.

Rapid prototyping	Advantages	Limitations
Photo-polymerisation processes	Relative easy to achieve small feature	Limited by the development of photo-polymerisable, biocompatible and biodegradable materials; low geometrical complexity; limited to reactive and mostly toxic resins
Laser sintering	Relative higher scaffold strength; solvent free	Materials trapped in small inner holes is difficult to be removed; high temperatures in the chamber
Sheet lamination	Solvent free	Materials trapped in small inner holes is impossible to be removed
Extrusion	No materials trapped in the scaffold; solvent free	High heat effect on raw material; low geometrical complexity
Ink-jet technology	Low heat effect on raw powder; easy process; low cost	Materials trapped in small inner holes; lack of mechanical properties
Bio-plotting	Large variety of materials for both soft and hard tissues	Low geometrical complexity

Table 2: Source of errors generated during the production of SFF structures.

Stage	Source of errors
Digitisation	Pitch/gantry tilt Image construction algorithm Patient movements
3D modeller	Section thickness Threshold value Interpolation algorithm Smoothing algorithm Tesselation
Solid freeform fabrication	Laser or extrusion head diameter Scanning strategies Creation and removal of supporting structures Thickness of each layer Shrinkage and warping effects Surface finishing

4 Conclusions

SFF technologies have a great potential for tissue engineering. These technologies offer a high degree of freedom for tissue engineering either for the



design of scaffolds (pore size, pore geometry, orientation, interconnectivity, etc.) or for its fabrication. Several materials can also be used enabling the production of both soft and hard scaffolds. These characteristics can enhance the fabrication of biomimetic scaffolds and scaffolds for complex biomechanical applications. Future developments will allow establishing SFF as a key tool for tissue reconstruction and regeneration.

References

- [1] Chapekar, M.S., Tissue engineering: challenges and opportunities, *J. Biomed. Mater. Res.*, 53, pp. 617-620, 2000.
- [2] Mendes, A., Lagoa, R. and Bartolo, P.J., Rapid prototyping system for tissue engineering, *Proceedings of the International Conference on Advanced Research in Virtual and Physical Prototyping*, pp. 419-426, 2003.
- [3] United Network for Organ Sharing website: <http://www.unos.org>, 2005.
- [4] Lavik, E. and Langer, R., Tissue engineering: current state and perspectives, *Appl. Microbiol. Biotechnol.*, 65, pp. 1-8, 2004.
- [5] Langer, R. and Vacanti, J.P., Tissue Engineering, *Science*, 260, pp. 920-92, 1993.
- [6] Anseth, K.S. and Burdick, J.A., New directions in photopolymerizable biomaterials, *Mat Res Soc Bull*, 27, pp. 130-136, 2002.
- [7] Nguyen, K. and West, J.L., Photopolymerizable hydrogels for tissue engineering applications, *Biomaterials*, 23, pp. 4307-4314, 2002.
- [8] Kim, T.H., Browne, F., Upton, J., Vacanti, J.P. and Vacanti, C.A., Enhanced induction of engineered bone with basic FGF, *Tissue Eng*, 3, pp. 303-308, 1997.
- [9] Ho, M.-H, Kuo, P.-Y, Hsieh, H.-J., Hsien, T.-Y., Hou, L.-T., Lai, J.-Y. and Wang, D.-M., Preparation of porous scaffolds by using freeze-extraction and freeze-gelation methods, *Biomaterials*, 25, pp. 129-138, 2004.
- [10] Sachlos, E. and Czernuszka, J.T., Making tissue engineering scaffolds work. Review on the application of solid freeform fabrication technology to the production of tissue engineering scaffolds, *European Cells and Materials*, 5 pp. 29-40, 2003.
- [11] Hutmacher, D.W., Scaffold design and fabrication technologies for engineering tissues – state of the art and future perspectives, *J. Biomat Sci-Polym E*, 12, pp. 107-124, 2001.
- [12] Gomes, M.E. and Reis, R.L., Biodegradable polymers and composites in biomedical applications: from catgut to tissue engineering. Part2 Systems for temporary replacement and advanced tissue regeneration, *Int. Mat. Reviews*, 40, pp.274-285, 2004.
- [13] Freyman, T.M., Yannas, I.V. and Gibson, L.J., Cellular materials as porous scaffolds for tissue engineering”, *Prog. In Mat. Sci.*, 46, pp. 273-282, 2001.
- [14] Velocity2 Plus software from Javelin: www.javelin3d.com (accessed April 2005).



- [15] BioBuild from Anatomics: www.anatomics.net (accessed April 2005).
- [16] MIMICS from Materialise: www.materialise.com (accessed April 2005).
- [17] Meurer, M.I., Nobre, L.F.S., Meurer, E., Silva, J.V.L., Bárbara, A.S., Oliveira, M.G., Silva, D.N. and Santos, A.M.B., A critical review on acquisition and manipulation of CT images of the maxillofacial area for rapid prototyping, in *Advanced Research in Virtual and Rapid Prototyping*, Edited by Bártolo et al, Balkema, Leiden, 2005 (to appear).
- [18] Sakas, G., Trends in medical imaging: from 2D to 3D, *Computers & Graphics*, 26, pp. 577-587, 2002.
- [19] Endo, M., Recent Progress in Medical Imaging Technology, *Systems and Computers in Japan*, 36, pp. 1-17, 2005.
- [20] Huang, Q.H., Zheng, Y.P., Lu, M.H. and Chi, Z.R., Development of a portable 3D ultrasound imaging system for musculoskeletal tissues, *Ultrasonics*, 43, pp. 153-163, 2005.
- [21] Levy, R.A., Chu, T.G.M., Holloran, J.W., Feinberg, S.E. and Hollister, S., CT-generated porous hydroxyapatite orbital floor prosthesis as a prototype bioimplant, *Am J Neuroradiol*, 18, pp. 1522-1525, 1997.
- [22] Griffith, M.L. and Halloran, J.W., Freeform fabrication of ceramics via stereolithography, *J. Am Ceram Soc*, 79, pp. 2601-2608, 1996.
- [23] Matsuda, T. and Mizutani, M., Liquid acrylate-endcapped poly(ϵ -caprolactone-co-trimethylene carbonate). II. Computer-aided stereolithographic microarchitectural surface photoconstructs, *J Biomed Mater Res*, 62, pp. 395-403, 2002.
- [24] Rapid micro product development (RMPD) from microTEC: www.microtec-d.com (accessed May 2005).
- [25] Williams, J.M., Adewunmi, A., Schek, R.M., Flanagan, C.L., Krebsbach, P.H., Feinberg, S.E., Hollister, S.J. and Das, S., Bone tissue engineering using polycaprolactone scaffolds fabricated via selective laser sintering, *Biomaterials*, 26, pp. 4817-4827, 2005.
- [26] Lee, G. and Barlow, J.W., Selective laser sintering of bioceramic materials for implants, *Proceedings of the '96 SFF Symposium*, Austin, TX, August 12-14, 1996.
- [27] Wang, F., Shor, L., Darling, A., Khalil, S., Güçeri, S. and Lau, A., Precision deposition and characterization of cellular poly- ϵ -caprolactone tissue scaffolds, *Rapid Prototyping Journal*, 10, pp. 42-49, 2004.
- [28] Hutmacher, D.W., Schantz, T., Zein, I., Ng, K.W., Teoh, S.H. and Tan, K.C., Mechanical properties and cell cultural response of polycaprolactone scaffolds designed and fabricated via fused deposition modelling, *J Biomed Mater Res*, 55, pp. 203-216, 2001.
- [29] Zein, I., Hutmacher, D.W., Tan, K.C. and Teoh, S.H., Fused deposition modeling of novel scaffolds architectures for tissue engineering applications, *Biomaterials*, 23, pp. 1169-1185, 2002.
- [30] Woodfield, T.B.F., Malda, J., de Wijn, J., Péters, F., Riesle, J. and van Blitterswijk, C.A., Design of porous scaffolds for cartilage tissue engineering using a three-dimensional fiber-deposition technique, *Biomaterials*, 25, pp. 4149-4161, 2004.



- [31] Chen, Z., Li, D., Lu, B., Tang, Y., Sun, M. And Wang, Z., Fabrication of artificial bioactive bone using rapid prototyping, *Rapid Prototyping Journal*, 10, pp. 327-333, 2004.
- [32] Widmer, M.S., Gupta, P.K., Lu, L., Meszlenyi, R.K., Evans, G.R.D., Brandt, K., Savel, T., Gurlek, A., Patrick, C.W. and Mikos, A.G., Manufacture of porous biodegradable polymer conduits by an extrusion process for guided tissue regeneration, *Biomaterials*, 19, pp. 1945-1955, 1998.
- [33] Kim, S.S., Utsunomiya, H., Koski, J.A., Wu, B.M., Cima, M.J., Sohn, J., Mukai, K., Griffith, L.G. and Vacanti, J.P., Survival and function of hepatocytes o a novel three-dimensional synthetic biodegradable polymer scaffolds with an intrinsic network of channels, *Ann Surg*, 228, pp. 8-13, 1998.
- [34] Zeltinger, J., Sheerwood, J.K., Graham, D.M., Mueller, R. and Griffith, L.G., Effects of pore size and void fraction on cellular adhesion, proliferation, and matrix deposition, *Tissue Eng*, 7, pp. 557-572, 2001.
- [35] Lam, C.X.F., Mo, X.M., Teoh, S.H. and Hutmacher, D.W., Scaffold development using 3D printing with a starch-based polymer, *Mater Sci. Eng.*, 20, pp. 49-56, 2002.
- [36] Sachlos, E., Reis, N., Ainsley, C., Derby, B. and Czermuszka, J.T., Novel collagen scaffolds with predefined internal morphology made by solid freeform fabrication, *Biomaterials*, 24, pp. 1487-1497, 2003.
- [37] Taboas, J.M., Maddox, R.D., Krebsbach, P.H. and Hollister, S.J., Indirect solid free form fabrication of local and global porous biomimetic and composite 3D polymer-ceramic scaffolds, *Biomaterials*, 24 pp. 181-194, 2003.
- [38] Limpanuphap, S. and Derby, B., Manufacture of biomaterials by a novel printing process, *Journal of Materials Science: Materials in Medicine*, 13, pp. 1163-1166, 2002.
- [39] Park, A., Wu, B. and Griffith, L.G., Integration of surface modification and 3D fabrication techniques to prepare patterned poly(L-lactide) substrates allowing regionally selective cell adhesion, *J Biomater Sci-Polym E*, 9, pp. 89-110, 1998.
- [40] Pfister, A., Landers, R., Laib, A., Hübner, U., Schmelzeisen, R. and Mülhaupt, Biofunctional rapid prototyping for tissue-engineering applications : 3D bioplotting versus 3D printing, *Journal of Applied Polymer Science : Part A : Polymer Chemistry*, 42, pp. 624-638, 2004.
- [41] Ang, T.H., Sultana, F.S.A., Hutmacher, D.W., Wong, Y.S., Fuh, J.Y.H., Mo, X.M., Loh, H.T., Burdet, E. and Teoh, S.H., Fabrication of 3D chitosan-hydroxyapatite scaffolds using a robotic dispersing system, *Mater Sci Eng*, C20, pp. 35-42, 2002.
- [42] Bártolo, P.J., Mendes, A. and Jardini, A., Bio-prototyping, in Design and Nature II, Edited by M.W. Collins and C.A. Brebbia, WIT Press, Southampton, pp. 535-544, 2005.
- [43] Mironov, V., Boland, T., Trusk, T., Forgacs, G. and Markwald, R.R., Organ printing: computer-aided jet-based 3D tissue engineering, *Trends in Biotechnology*, 21, pp. 157-161, 2003.



This page intentionally left blank

Using Murray's law to design artificial vascular microfluidic networks

R. W. Barber¹, K. Cieřlicki² & D. R. Emerson¹

¹*Centre for Microfluidics and Microsystems Modelling, CCLRC Daresbury Laboratory, Warrington, UK*

²*Institute of Automatic Control and Robotics, Warsaw University of Technology, Poland*

Abstract

A generalised version of Murray's law has been derived for the design of microfluidic manifolds and hierarchical fluid distribution systems. Murray's law was originally obtained from a study of mammalian cardiovascular systems and describes the optimum conditions governing the ratio of diameters of the vessels in a branching vascular network. The optimum geometrical relationship, which is now known as Murray's law, states that the cube of the diameter of the parent vessel must equal the sum of the cubes of the daughter vessels. When the parent/daughter branches obey Murray's law, the system obeys the principle of minimum work. Furthermore, if the network consists of symmetric bifurcations, an important consequence of Murray's law is that the tangential shear stress at the wall remains constant throughout the vascular system. In the present paper, we generalise this important hydrodynamic principle and provide a biomimetic design rule for microfluidic systems composed of arbitrary cross-sections. In particular, the paper focuses on the design of constant-depth rectangular- and trapezoidal-sectioned microfluidic manifolds that are often used in lab-on-a-chip systems. To validate the biomimetic design principles, a comprehensive series of computational fluid dynamic simulations have been performed.

Keywords: biomimetic, microfluidic, vascular, manifold, lab-on-a-chip.

1 Introduction

It is evident that nature has perfected techniques and solutions that are often considered to be optimal. Understanding and extracting these "natural" design



strategies has opened up a whole new field of research known as *biomimetics*. Designs formulated using biomimetic principles range from novel surface treatments that mimic physiological processes to geometrical optimisation that improves the performance of a system.

One research area where biomimetic principles could play an important role is in the design of microfluidic and lab-on-a-chip systems. In recent years, microfluidic devices have been increasingly used in a range of chemical, biochemical and life-science applications. Miniaturisation offers many potential benefits including faster mixing and reaction times, increased chemical yields, and faster throughput rates for chemical assays. In addition, the small length scales of microfluidic systems offer the prospect of developing portable detection systems for point-of-care clinical diagnostics. However, little research is currently available concerning the optimisation of channel dimensions to ensure the most efficient flow through the device.

The present paper shows how biomimetic principles based on the laws that govern biological vascular trees could be used to design artificial microfluidic distribution systems. The study focuses specifically on microfluidic manifolds composed of constant-depth rectangular- or trapezoidal-sectioned channels that can readily be fabricated using standard micro-fabrication techniques such as photolithography and wet or dry etching. Furthermore, by carefully selecting a branching parameter governing each bifurcation, it is shown that it is possible to introduce a prescribed element of control into the flow behaviour in the system.

2 Theoretical basis of Murray's law

The geometrical configurations of vessels found in mammalian cardiovascular and respiratory systems have evolved, through natural selection, to an optimum arrangement that minimises the amount of biological work required to operate and maintain the system. The most distinctive feature of biological distribution systems is their hierarchical structure and the successive division of vessels which become smaller, both in length and diameter (as illustrated schematically in Fig. 1). The relationship between the diameter of the parent and daughter vessels was first derived by Murray [1] using the principle of minimum work. Murray found that the optimum relation between the diameter of the parent vessel (d_0) and the two daughter branches (d_{1a} and d_{1b}) can be written as

$$d_0^3 = d_{1a}^3 + d_{1b}^3. \quad (1)$$

This expression is nowadays known as *Murray's law* but it is sometimes referred to as "*the third power law*". For a symmetric bifurcation where $d_{1a} = d_{1b}$, eqn. (1) reduces to

$$d_0^3 = 2d_1^3. \quad (2)$$

By making the assumption that the flow is fully-developed and ignoring the energy losses at each bifurcation, it is possible to obtain relationships between vessel diameters, average velocity, wall shear stress, flow resistance, pressure, and residence time for each consecutive generation of the vascular system.



The work of Murray was overlooked for almost half a century, but recently biological scaling laws are beginning to receive more attention. However, with the exception of the brief study by Lim *et al.* [2], there appears to be little application of Murray’s law to the design of man-made structures and, in particular, to the design of microfluidic channels and manifolds.

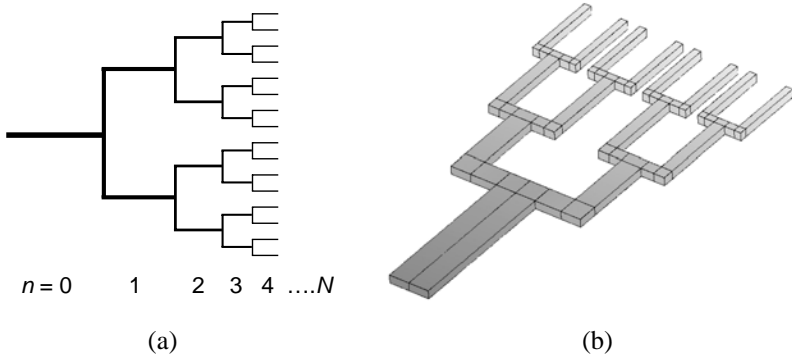


Figure 1: (a) Schematic representation of a symmetric bifurcating network of channels; (b) Layout of a typical constant-depth rectangular microfluidic manifold considered in the validation study.

2.1 Generalisation of Murray’s law

As demonstrated by Cieřlicki [3], Murray’s law can be generalised if the change in diameter of each consecutive generation can be represented by a *branching parameter*, X :

$$X = \frac{d_0^3}{2d_1^3} \tag{3}$$

For $X = 1$, the parent/daughter branches obey the principle of minimum work. However, the branching parameter does not have to be unity and the generalised case of $X \neq 1$ can be used to design microfluidic manifolds with specific properties e.g. shear stress distributions or residence times. Assuming that the branching parameter is held constant throughout the hierarchical network, then the segment diameter of the n^{th} generation can be written as

$$d_n = \frac{d_0}{(2X)^{n/3}} \tag{4}$$

Fig. 2(a) shows graphically how eqn. (4) behaves for a range of X values. It can be seen that the diameters systematically diminish when the branching parameter is greater than 0.5. For $X = 0.5$, the diameter at each generation is constant, whereas when $X < 0.5$, each diameter will systematically increase. For Murray’s law, ($X = 1$), the damping factor is equal to $2^{-1/3}$. This implies that the diameter of a segment will be halved after three successive generations.

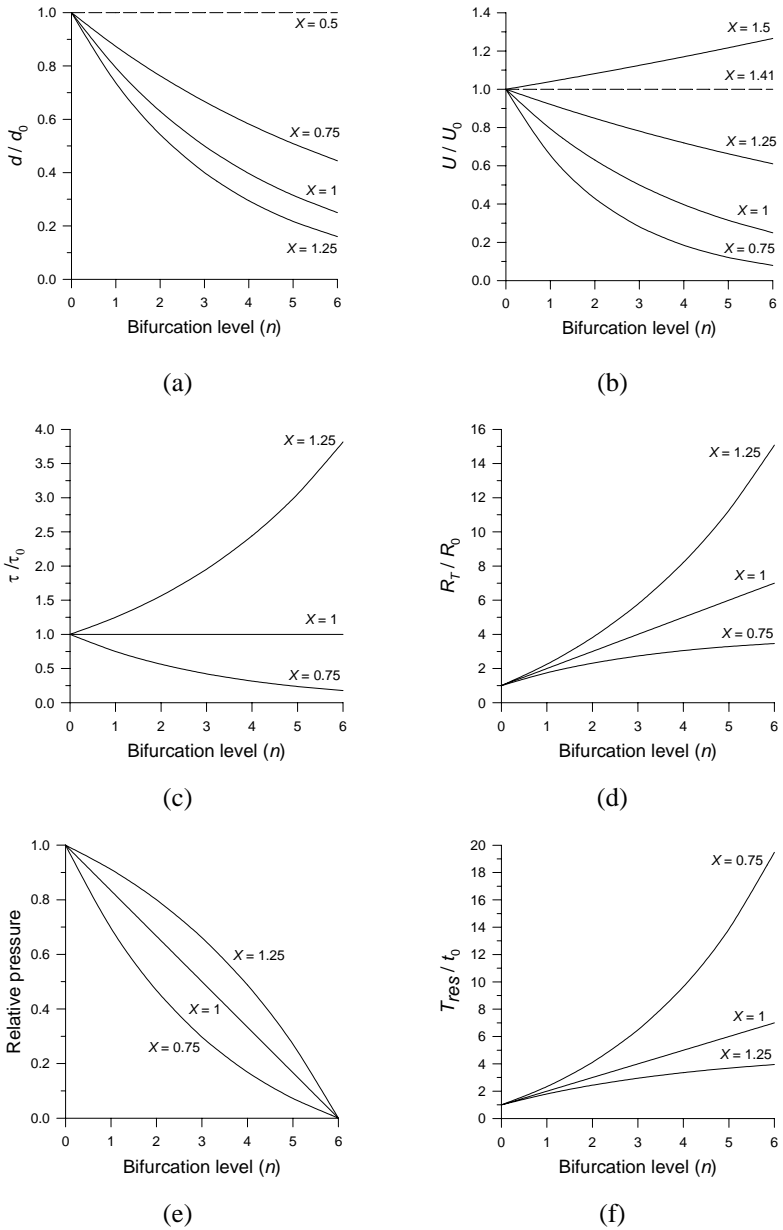


Figure 2: Normalised segment diameter (a), average flow velocity (b), wall shear stress (c), flow resistance (d), pressure distribution (e) and residence time (f) as a function of bifurcation level, n , in a vascular system that obeys the generalised form of Murray's law.



For a symmetric system, the volumetric flow rate halves at each bifurcation i.e. $Q_n = 2^{-n} Q_0$. Using eqn. (4), the mean flow velocity, \bar{U}_n , in each generation can be shown to be

$$\bar{U}_n = \bar{U}_0 \left(\frac{1}{2} X^2 \right)^{n/3} \tag{5}$$

Fig. 2(b) shows the predicted velocity behaviour throughout the manifold as the branching parameter X is varied. It can be seen that if $X < \sqrt{2}$, the average velocity will decrease in each generation.

The shear stress acting on the wall of a circular pipe in a fully-developed laminar flow can be written as follows:

$$\tau = \frac{8\mu\bar{U}}{d} \tag{6}$$

where μ is the fluid viscosity. Substituting eqns. (4) and (5) into (6) gives

$$\tau_n = \tau_0 X^n \tag{7}$$

where τ_0 is the wall shear stress in the inlet channel ($n = 0$). Eqn. (7) is plotted in Fig. 2(c) and clearly illustrates that if Murray’s law is obeyed ($X = 1$), the magnitude of the wall shear stress remains the same at every point in the branching hierarchy. However, by changing the value of X , it is possible to introduce an element of control into the shear stress distribution.

The hydraulic resistance of a single segment is defined as $\Delta P/Q$ and can be obtained from the Hagen-Poiseuille pipe friction formula. Furthermore, if the length of an individual segment is assumed to be proportional to its diameter ($L_n \propto d_n$), as frequently observed in biological systems [4], the resistance of a single segment in the n^{th} generation can be written as

$$R_n \propto d_n^{-3} \tag{8}$$

Using eqns. (4) and (8) allows the change of hydraulic resistance of consecutive generations to be related to the branching parameter X :

$$R_n = R_0 (2X)^n \tag{9}$$

The total resistance, R_T , of a bifurcating vascular tree can thus be written as

$$R_T = R_0 + \frac{R_1}{2} + \frac{R_2}{4} + \frac{R_3}{8} + \dots + \frac{R_n}{2^n} + \dots + \frac{R_N}{2^N} = R_0 \sum_{i=0}^N X^i = R_0 \frac{X^{N+1} - 1}{X - 1} \tag{10}$$

For Murray’s law ($X = 1$), eqn. (10) reduces to $R_T = (N + 1)R_0$. Examples of the total resistance of the network are shown in Fig. 2(d) for several values of X . When Murray’s law is obeyed, the resistance of each generation is identical, so the total resistance to the flow increases linearly with the number of generations. For $X > 1$ the resistance of subsequent generations increases rapidly. However, for $X < 1$, the resistance of subsequent generations decreases and the total resistance will tend to a constant value of $R_T = R_0 / (1 - X)$ as $N \rightarrow \infty$.



Using the analogy between pipe friction and electrical resistance allows the pressure to be determined throughout the network. It can be shown that

$$\frac{p_n - p_{out}}{p_{in} - p_{out}} = \frac{\sum_{i=n}^N X^i}{\sum_{i=0}^N X^i} = \left(\frac{X^{N+1} - X^n}{X^{N+1} - 1} \right), \tag{11}$$

where p_n is the pressure at the entrance to the n^{th} generation and p_{in} and p_{out} are the pressures at the inlet and outlet of a branching network with N bifurcation levels. Fig. 2(e) shows the normalised pressure distribution for a vascular system with 6 generations and several values of the branching parameter. For $X < 1$, the most significant loss of pressure occurs in the inlet channel ($n = 0$) with the pressure drop gradually diminishing at each successive generation, leading to a concave distribution. Conversely, for $X > 1$, the pressure drop becomes most significant at the outlet of the hierarchical tree, giving a convex profile. When $X = 1$, the pressure loss along each successive generation is constant, leading to a linear pressure distribution along the vascular structure.

If the length of an individual segment is again considered to be proportional to its diameter (i.e. $L_n = kd_n$ where k is a constant), then the average residence time for a single segment in the n^{th} generation, t_n , can be written as

$$t_n = \frac{L_n}{\bar{U}_n} = \frac{kd_n}{\bar{U}_n} = \frac{kd_0}{\bar{U}_0 X^n} = \frac{L_0}{\bar{U}_0 X^n} = \frac{t_0}{X^n}. \tag{12}$$

The total residence time, T_{res} , for the entire vascular tree with N bifurcation levels will then be

$$T_{res} = t_0 \sum_{i=0}^N \frac{1}{X^i} = t_0 \frac{X^{N+1} - 1}{X^{N+1} - X^N}. \tag{13}$$

Typical residence time profiles are shown in Fig. 2(f) for different values of the branching parameter X . For $X < 1$, the time to flow through each successive generation increases with the number of generations. Conversely, for $X > 1$, the residence time decreases at each successive generation and the total residence time converges to a normalised value of $X / (X - 1)$.

2.2 Extension of Murray’s law to non-circular ducts

The extension of biomimetic principles to non-circular ducts has recently been demonstrated by Emerson *et al.* [5] who proposed that the design rule should be defined using an analogous expression to eqn. (7) but based on the *mean* value of the tangential shear stress in each segment, i.e.

$$\bar{\tau}_n = \bar{\tau}_0 X^n. \tag{14}$$



The mean wall shear stress can be related to the Fanning friction factor, f , which in turn can be expressed in terms of the Poiseuille and Reynolds numbers [6]:

$$\bar{\tau} = \frac{1}{2} \rho \bar{U}^2 f = \frac{1}{2} \rho \bar{U}^2 \frac{Po}{Re} = \frac{\mu \bar{U} Po}{2D_h}, \tag{15}$$

where $D_h = 4 \times \text{area/wetted perimeter}$ is the *hydraulic diameter* of the cross-section and \bar{U} is the mean flow velocity. Substituting eqn. (15) into (14) gives a generalised biomimetic principle that can be applied to all channel shapes irrespective of the cross-sectional geometry:

$$\frac{\bar{U}_n Po_n}{D_{hn}} = \frac{\bar{U}_0 Po_0}{D_{h0}} X^n. \tag{16}$$

The only practical limitation on the use of eqn. (16) as a biomimetic design rule is the requirement to know the hydraulic diameter and the Poiseuille number of the cross-section. As an aside, for vascular systems composed of circular pipes, the Poiseuille number is identical in each generation ($Po = 16$) and the hydraulic diameter, D_h , is equal to the diameter of the section, d . Under these conditions, eqn. (16) reduces to eqn. (5).

2.3 Application to constant-depth biomimetic networks

The present study focuses on microfluidic manifolds composed of constant-depth rectangular- or trapezoidal-sectioned channels since these geometries can readily be fabricated using conventional micro-fabrication techniques such as photolithography and wet or dry etching.

For a system composed of constant-depth rectangular channels, as typically encountered in dry etching techniques, the aspect ratio of the n^{th} generation can be defined as $\alpha_n = d / w_n$ where d is the depth and w_n is the width of the channel. After some algebraic manipulation, it can be shown that the biomimetic design rule defined in eqn. (16) can be written as a function of the aspect ratio:

$$\alpha_n (1 + \alpha_n) Po(\alpha_n^*) = (2X)^n \alpha_0 (1 + \alpha_0) Po(\alpha_0^*). \tag{17}$$

The Poiseuille number for a rectangular cross-section can be determined analytically [6] as follows:

$$Po(\alpha_n^*) = 24 \left[1 - \frac{192}{\pi^5} \frac{1}{\alpha_n^*} \sum_{i=1,3,5,\dots}^{\infty} \frac{1}{i^5} \tanh\left(\frac{i\pi\alpha_n^*}{2}\right) \right]^{-1} \left(1 + \frac{1}{\alpha_n^*} \right)^{-2}. \tag{18}$$

Eqn. (18) is valid when $\alpha_n^* \leq 1$, which requires the width to be greater than the depth. To obtain the value of the Poiseuille number when the width is less than the depth ($\alpha_n > 1$), it is necessary to set $\alpha_n^* = w_n / d$ but it is important to note that α_n in eqn. (17) remains as previously defined (i.e. $\alpha_n = d / w_n$). Any appropriate method for finding the root, α_n , can be used and in the present study a simple bisection method has been found to be reliable.



Another important fabrication technique for constructing microfluidic channels involves anisotropically etching [100] silicon wafers using KOH. This results in a trapezoidal section with an angle of $\tan^{-1}(\sqrt{2}) = 54.74^\circ$. It can be shown that the biomimetic design rule for KOH etched silicon channels can be written as

$$\frac{\sqrt{2}\gamma_n + (\sqrt{3}-1)\gamma_n^2}{(\sqrt{2}-\gamma_n)^2} \text{Po}(\gamma_n) = (2X)^n \frac{\sqrt{2}\gamma_0 + (\sqrt{3}-1)\gamma_0^2}{(\sqrt{2}-\gamma_0)^2} \text{Po}(\gamma_0), \quad (19)$$

where $\gamma = d/a$ is the aspect ratio of the channel, defined in terms of the upper width, a . For many practical channel geometries, including trapezoidal channels, the Poiseuille number cannot be obtained analytically. However, Morini [7] has shown that the Poiseuille number for KOH-etched [100] silicon channels can be determined from a 5th order polynomial as follows:

$$\text{Po}(\gamma_n) = 24 \left[1 - b_1\gamma_n + b_2\gamma_n^2 - b_3\gamma_n^3 + b_4\gamma_n^4 - b_5\gamma_n^5 \right], \quad (20)$$

where the coefficients have the values of $b_1=1.7611$, $b_2=2.6780$, $b_3=4.9342$, $b_4=10.0883$, and $b_5=7.4496$, respectively.

3 Numerical validation

The generalised biomimetic design rules for constant-depth channels have been validated by conducting a comprehensive series of computational fluid dynamic simulations on a range of rectangular- and trapezoidal-sectioned manifolds. The networks were restricted to four generations ($n = 0, 1, 2, 3$) and the channels were assumed to be 125 μm deep. For the rectangular channels, the initial aspect ratio was assumed to be either 2:1 ($\alpha_0 = 0.5$) or 5:1 ($\alpha_0 = 0.2$), while the initial aspect ratio for the trapezoidal section was taken to be 8:1 ($\gamma_0 = 0.125$). Table 1 presents the dimensions of the channels used in the numerical study. The channel widths were obtained by solving either eqn. (17) for α_n or eqn. (19) for γ_n .

Table 1: Channel dimensions employed in the numerical study.

Bifurcation level, n	Channel widths (μm)				
	Rectangular				Trapezoidal
	$X = 0.75$	$X = 1.0$	$X = 1.25$	$X = 1.0$	$X = 1.0$
0	250.0	250.0	250.0	625.0	1000.0
1	177.7	143.3	123.0	312.9	536.7
2	132.0	91.8	71.4	171.5	323.9
3	101.7	62.5	44.2	106.3	230.1



The numerical simulations were conducted using the commercial computational fluid dynamics software package, CFD-ACE+ (ESI CFD, Huntsville, USA [8]). Fig. 3 shows the predicted normalised wall shear stress distribution in a rectangular microfluidic manifold and illustrates the progressive decrease in shear stress through the vascular system when $X < 1$. The effect of varying the branching parameter is further demonstrated in Fig. 4 which shows the normalised shear stress distribution and flow resistance for a range of channel aspect ratios and branching parameters. The theoretical and numerical predictions are in very good agreement, demonstrating the applicability of the proposed biomimetic design principle.

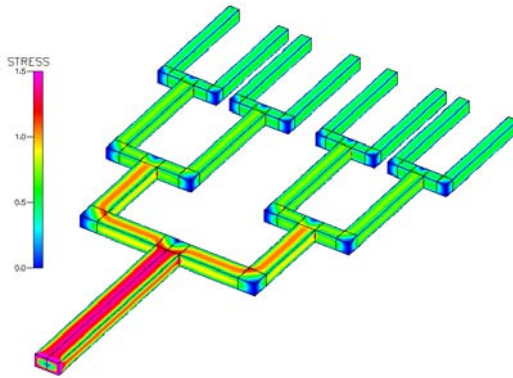


Figure 3: Predicted normalised wall shear stress distribution ($\bar{\tau}_n / \bar{\tau}_0$) in a rectangular microfluidic manifold with a branching parameter of $X=0.75$ and an initial aspect ratio of $\alpha_0 = 0.5$.

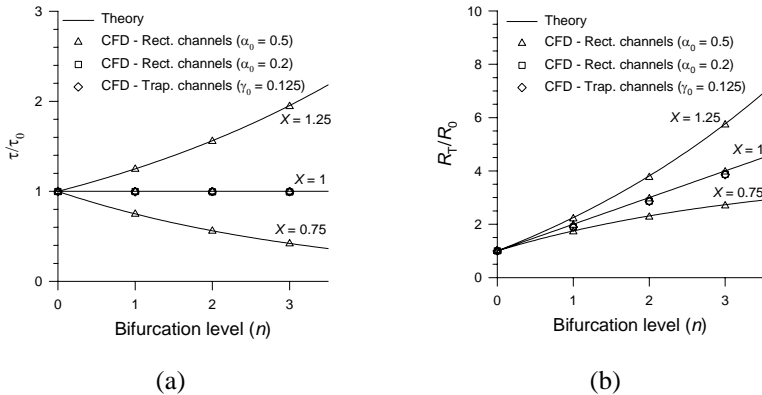


Figure 4: Normalised wall shear stress distribution (a) and flow resistance (b) in constant-depth rectangular and trapezoidal vascular systems that obey the generalised form of Murray’s law. Comparison between theoretical predictions (lines) and CFD results (symbols).



4 Conclusions

Murray's law was originally developed for cardiovascular systems composed of multi-diameter circular pipes. For symmetric bifurcating systems, an important consequence of Murray's law is that the tangential shear stress at the wall remains constant throughout the vascular network. In the present paper, this important biomimetic principle has been generalised so that it is applicable to microfluidic networks composed of channels of arbitrary cross-section. The paper focuses specifically on the design of constant-depth rectangular- and trapezoidal-sectioned microfluidic manifolds that are often used in lab-on-a-chip systems. By carefully selecting a branching parameter governing the change in channel dimension at each bifurcation, it is shown that it is possible to introduce an element of flow control into the artificial vascular network.

Acknowledgements

The authors would like to acknowledge partial support from the Framework VI PATENT DfMM Network of Excellence (contract no. 507255). Additional support was provided by the UK Engineering and Physical Sciences Research Council (EPSRC) under the auspices of Collaborative Computational Project 12.

References

- [1] Murray, C.D., The physiological principle of minimum work: I. The vascular system and the cost of blood volume, *Proc. Natl. Acad. Sci. USA*, **12**, pp. 207-214, 1926.
- [2] Lim, D., Kamotani, Y., Cho, B., Mazumder, J. & Takayama, S., Fabrication of microfluidic mixers and artificial vasculatures using a high-brightness diode-pumped Nd:YAG laser direct write method, *Lab Chip*, **3**, pp. 318-323, 2003.
- [3] Cieřlicki, K., Resistance to the blood flow of a vascular tree – a model study, *Polish Journal of Medical Physics and Engineering*, **5**, pp. 161-172, 1999.
- [4] West, B.J., *Fractal Physiology and Chaos in Medicine*, World Scientific: Singapore, 1990.
- [5] Emerson, D.R., Cieřlicki, K., Gu, X.J. & Barber, R.W., Biomimetic design of microfluidic manifolds based on a generalised Murray's law, *Lab Chip*, **6**, 447-454, 2006.
- [6] Shah, R.K. & London, A.L., *Laminar Flow Forced Convection in Ducts*, Academic Press: New York, 1978.
- [7] Morini, G.L., Laminar liquid flow through silicon microchannels, *J. Fluids Eng.*, **126**, pp. 485-489, 2004.
- [8] *CFD-ACE+ User Manual: Version 2004*, ESI CFD, Huntsville, USA.



Biomimetic robots for robust operation in unstructured environments

S. R. Gajjar

*Department of Mechanical Engineering,
Dr. Babasaheb Ambedkar Marathawada University, India
MIT-Aurangabad, India*

Abstract

Animal models are used as the inspiration for many different types of robots by closely studying the mechanics of various animals and then applying these observations to robot design. The goal is to develop a new class of biologically-inspired robots with greater performance in unstructured environments, able to respond to changing environmental factors such as irregular terrain. Unlike traditional science fiction views of robots that closely resemble animals in outward appearance, this has used biomimicry of the cockroach, one of nature's most successful species. Insects are studied to understand the role of passive impedance (structure and control), humans are studied to understand adaptation and learning. Novel layered prototyping methods are used to create compliant biomimetic structures with embedded sensors and actuators. Biomimetic actuation and control schemes are developed that exploit "preflexes" and reflexes for robust locomotion and manipulation. Preliminary experiments are carried out to determine insect leg properties. The first prototypes of embedded sensors and actuators are illustrated. Locomotion focus: rough terrain traversal, inspired by the cockroach running over blocks surface.

Keywords: hexapedal, tripod, legged locomotion, mobile robot motion and path planning, modelling.

1 Introduction

Design guidelines for small and fast robots capable of fault-tolerant action in known and unstructured environments are very demanding. Many of these robots



are legged, leading to the control problem associated with balance and locomotion. With many legs, postural stability can be attained. On the other hand, stable locomotion cannot be solved only by body design. It requires a reconfigurable controller that can handle locomotion with variation in ground slope, payload mass, speed, etc. In this paper, I described tools to build a controller for such a running robot, using only experimental data without precise knowledge of robot dynamics and running behavior of arthropods. Although it is clear how a biomimetic legged robot should react with its environment while running, the design of such systems remains a challenge. Available power sources and actuators are less efficient than what is observed in nature. The size-to-payload ratio of actuators, their drives, and energy storage are high, compared with muscles. One approach is to make a Functional copy of the anima. Designing controllers that deliver some of the versatility inherent in the animal motor-control system, especially regarding motor learning, adaptation, and motion planning, might be a useful first step. The biomimetic principles in the design of a running insect-like robot and its controller have already proven to be a promising design guideline. An insect of choice for building fast biomimetic robots is the cockroach. It has a relatively simple motor-control system and yet it displays extraordinary speed and dexterity, even over rough terrain. In fast runs, it maintains its center of gravity low to support dynamic stability. The oscillations of the pitch yaw and roll rotational movements of the body are modest, thus saving energy. For a robust run, each leg of the tripod in the cockroach firm contact with ground. Instead, it uses kinetic energy to bridge from one firm contact to another. The controller design of a cockroach-like robot might be based on the observation that in walking and running, a cockroach uses a tripod gait with one middle leg on one side acting as virtual legs in an equivalent biped run. Even when negotiating a curve, the stable tripod gait may be a proper walking policy. General parameters that described the tripod gait are stride period, which is the time interval between two activations of one tripod, and duty factor, which is the percentage of time, with respect to half of the stride period that the legs are actively producing force. The robot has six independently actuated legs that rotate with one degree of freedom. The sticks that make up the legs are compliant. The three by three legs rotate in a clock-driven fashion producing alternate tripod gait. The existence of the tripod ensures static mobility. Presently it is capable of achieving five bodies' lengths per second. Its size of nearly half a meter makes it capable of running difficult terrain, even climbing stairs. It control their velocity by the rotation frequency of legs or whigs, and, perhaps, by the physic relationship between the legs.

My effort was a project to build biologically inspired robots that are cheap, fast, smart, compliant and fault-tolerant using mostly off the shelf technology. My approach was to make efficient models of robot-environment interaction for model-based control and locomotion planning under external disturbances such as sloped ground and added payload mass. Controlling of robots made of plastic with poor tolerances is challenging. A way proceed is to mimic a cockroach motor control system. Its locomotion is usually explained by reflexive, spring



and damper-like behavior of the leg, responsible for rapid stabilization augmented in certain direction by its motor control system.

2 Design of a hexapedal robot

We used the legs except that the flexures (the compliant area at each joint) were interchangeable, allowing us to examine the role of compliance in stable locomotion. Our robot has a compact aluminum body, different from *Sprawl* in size, shape, material and weight. It also has six small DC servomotors that act like hips, i.e., they control orientation of each leg in an offline fashion. The DC motors have their own servo controllers that accept serial communication for setting up the posture before the start of the run. Each leg has a one-way air-piston with a reverse spring action, and a passive flexure functioning like a knee. The robot runs by alternate tripod gait. Three out of six legs make one tripod. Two tripods are controlled by two valves. Therefore, we have two control inputs. The valves are powered by a custom design interface logic connected to a parallel PC port. A PC controls the robot by commanding locomotion sequences. The air pressure comes from off board. The tripod activation is defined by Stride Period and Duty Factor (DF) the percentage of time that the valves are kept open during half of the stride period. The motors are used only to fix the orientation of the tethered part of the legs throughout the run. We had two reasons for this: First, from a practical point of view, with the motors we had it would be impossible to position them so quickly within the stride. Second, proper leg orientations are based on measurement of the actual body pitch angle and ground slope. Both of them had to be measured while the robot is still, and it would take a second or two to get reliable readings from the tilt sensors. Hence, by changing the tripod gait between completion of a run and the start of another run, it is possible to download commands from the operator that steers the robot allowing one to achieve a piecewise constant velocity. The result is a robot that runs straight ahead, pauses to change its orientation, and then continues to run. In the next three subsections, we will explain the mechanical design of the robot, and the procedure of modeling posture.

2.1 Mechanical considerations and optimal posture

The backbone of the robot was a thin aluminum bar. Six rectangular aluminum tubes were glued on two sides of the bar. Each held a DC motor that tethered a leg. The leg design is given in Fig. 1. Two air valves were placed on the back of the robot. The 3-way solenoid valves were normally closed. Along with the flexures, they produced a force-moment couple that was transmitted to the body, producing gait. The compliance of the flexure was chosen according to the mechanical properties of the body and ground. The idea was to choose a compliance that would allow the leg to bend back and return the energy while the piston was still in contact with the ground. Otherwise the energy would be returned too soon or too late, interfering with stride rhythm.



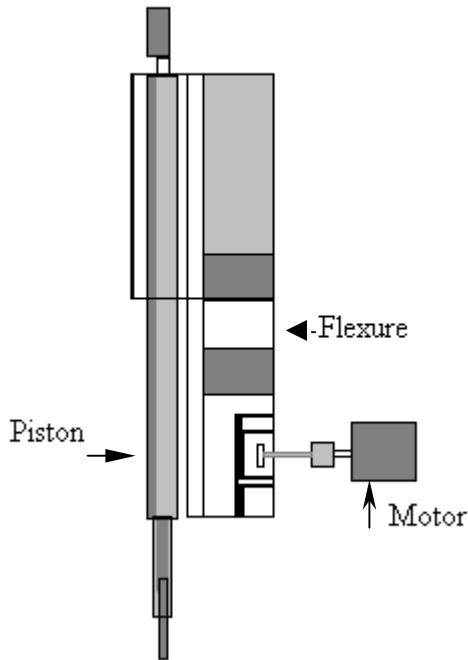


Figure 1: Two views of leg with piston and interchangeable flexure. Lower part of the leg is tethered to the DC motor located beneath body. Legs are modular with a flexure connecting the part with a gear and the part with the piston. Flexures are made in four thicknesses, denoted Types I, II, III, and IV, ranging from 2-3 mm.

Results from bipedal walking as well as studies on hexapod insects suggest that the moment around the center of mass of the body should be as low as possible in order to achieve transfer of impact energy into kinetic energy. Studies on animal walking and running suggest that during locomotion, the point around which there is zero moment is kept within the footprint most of the time. That point is known as the Zero Moment Point. In a tripod gait, the footprint triangle ensures stable stance but not necessarily stable locomotion. Without an exact model of the geometry and masses, and without appropriate sensors, it is impossible to compute the location of the ZMP. Instead, we hypothesized that smooth locomotion would take place if ground reaction forces (in the static case) intersected at one point to form a resultant force that passed through the Center-of-Mass (COM) of the robot. In order to achieve this, let us briefly consider the mechanics of the robot in the static case.

Each leg in the tripod produces a Ground Reaction Force (GRF) that forms a resultant force-moment couple. It is assumed that the GRFs reside in a plane parallel to the sagittal plane. Although the legs are compliant at the knee, the

lateral compliance of the leg is negligible compared to the forward/ backward compliance; this is due to the shape of the flexure element (Fig.1). Forces **F1** and **F5** are acting from one side of the body while force **F4** is acting from the other side. We have plotted the projections of the GRF in the lateral plane in Fig. 2A, and in the body plane in Fig. 2B, whereas Fig. 4 shows projections of the GRF in the sagittal plane.

The robot posture is pictured in Figs.2 and 3. Consider one tripod, formed by legs 1, 4, and 5 in contact with the ground. The coordinate system is located at the CoM (Figs. 2 and 3). Note that the CoM is not located in the middle of the robot; rather it is closer to its tail. A non-zero resultant moment gives rise to the yaw angle. Since tripods are symmetric and act alternatively it is reasonable to expect that a non-zero resultant moment will produce a change of yaw angle that would be cancelled by the opposing tripod. However, due to the flexures in the legs, this cancellation is never perfect, making the robot veer from a straight path, as was experimentally observed. Similarly, the net moment around the O_x axis is the result of the vertical component of the GRFs. Moments are denoted by **T15x** and **T4x** (Fig. 2.A). The resultant moment changes the roll angle during a run. This produces a wobbling from left to right. In order to keep wobbling as low as possible, it is desirable to push middle legs further away from robot's longitudinal axis because it is the middle leg that produces the thrust against the two legs on the other side. This also helps reduce yaw oscillations.

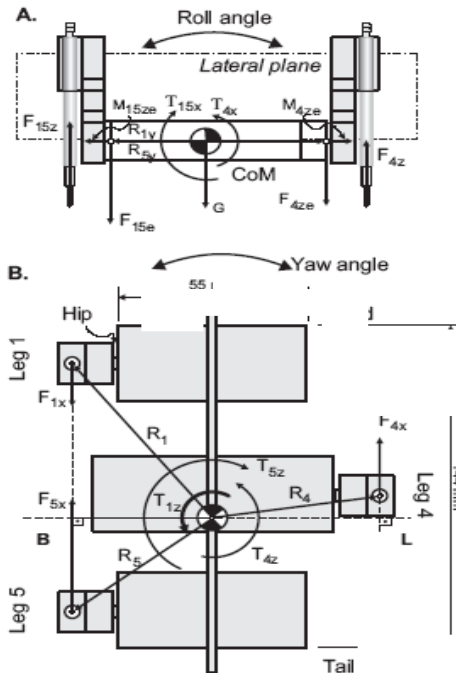


Figure 2: Views of one tripod. Rear view (A) and top view (B) of the robot with one tripod (legs 1, 4, and 5).

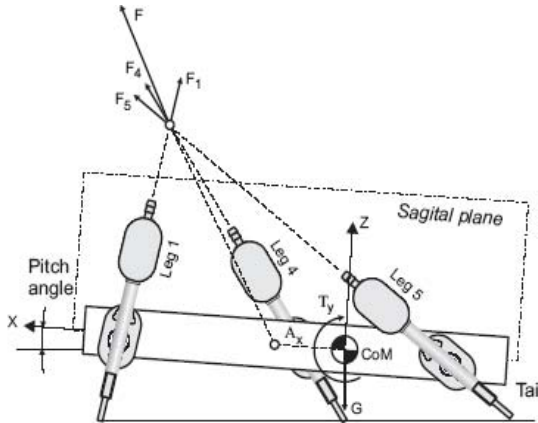


Figure 3: Side view of the robot standing on one tripod. The angle of the resultant force determines locomotion velocity.

2.1.1 Modeling the pitch angle of the robot

The relationship between leg orientation and body pitch angle under gravity load is a non-linear map, mostly due to flexures in the legs. In general, six legs will produce six controllable degrees of freedom of the robot's body. This problem is augmented by engaging synergies. First, we have three by three legs forming tripods and, second, they have symmetrical orientation. We simplified the search for a pitch angle model by keeping the front legs in the fixed position (10° from vertical, tilting backwards). While varying the middle and rear legs, due to compliant legs, we ensured that two constraints were satisfied: (a) all six legs were on the ground and (b) the legs were orientated in such a way that the resultant torque around O_y axis at CoM was near zero. The flexures used in determining the pitch angle model were chosen among available types III-I-II, III-II-I, and III-II-II, for front-middle-rear legs, respectively. The experimental procedure was as follows: First, middle legs were positioned randomly, and then rear legs were positioned in accordance to constraints. Next, body pitch angle was measured by a tilt sensor. Front legs, left and right, were at fixed position and were not included in modeling. Resulting model can be used in two ways. First, for a desired pitch we can determine legs orientations. Body pitch angles between 3.5° and 7.0° were used in modeling. Data for cross validation included pitch angles ranging from 3° to 7.75° .

2.1.1.1 Key areas in robotics Path planning – given a start location, a goal location and a map, find a (perhaps optimal) path from start to goal. Replanting is often necessary if information about the environment change. Perfect path planning is based on mapping just like 1) Topological mapping – which include distinctive places, connection graph, lessened for accurate location; 2) Geometric mapping in which spatial relationships maintained, uncertainties multiply.



Stereo vision- two cameras at a fixed distance (base line) form each other. Different perspectives of two cameras (right and left) lead to relative difference between the location of the same object in two images, which varies by distance.

Colors vision- composed of red, green and blue (rgb) components. By knowing the color characteristics of an object (and normalizing for light) specific object can be recognized. Solid colors are easy, as shown in fig. 4.

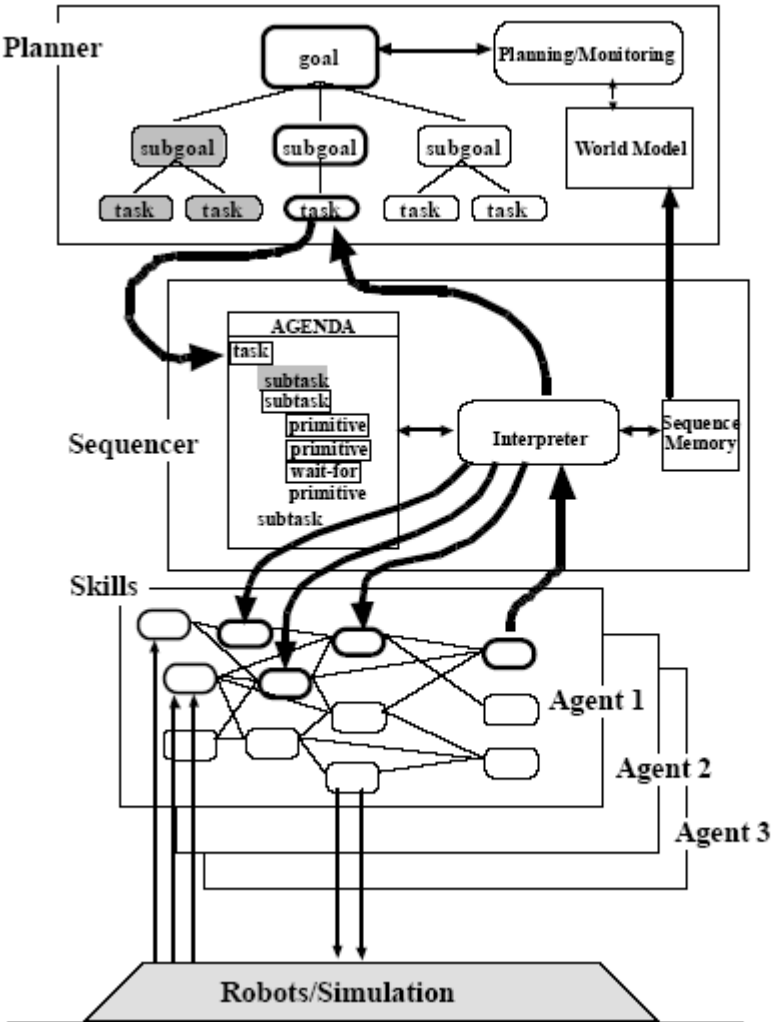


Figure 4: Architectures of path planning, sequencing, control.

3 Conclusion

I presented an approach to the design of a small 6-legged robot. This air-powered robot had six pistons, one per leg, three per tripod with two valves, and one per



tripod. Each leg had interchangeable passive flexures connecting tethered parts of the leg with the part that embodied the piston. Small DC motors beneath the body orient the legs in an off-line fashion. The robot moved by hopping from one tripod to another. Our design of robot's body differs from its Sprawl predecessors in two major aspects. All six legs had the same type of flexure. In addition, leg orientations did not follow a specific procedure that might lead to successful running. In my robot, middle legs were pushed backwards, closer to the rear legs, shifting the COM backwards. Several combinations of flexures were tested, leading to conclusion that front legs require higher stiffness, whereas middle and rear legs require softer flexures. I chose leg orientations based on the static analysis, supported by experiments later on, following the constraint that all ground reaction forces of one tripod should intersect in a single point. In this way, ground reaction forces from the tripods did not produce resultant moment at the COM of the robot. I also hypothesized that locomotion velocity may be controlled by changing the angle of the remaining resultant forces. My goal was to apply parametric modeling tools to build a feed-forward locomotion velocity model with typical task parameters: ground slope and payload mass. The only parameter in the model that I used to control the robot's performance was body pitch angle. Body pitch angle is set up by leg orientation at the beginning of the run. My kinematic model used polynomials to approximate experimental data. Once formed, the model allowed us to compute how the legs should be oriented in order to achieve desired body pitch and consequently locomotion velocity. The pitch angle model embodies information on flexures in each leg. My modeling used a modified version of the Successive Approximations algorithm. It also enables refinement of the model as interaction with the environment changes over time and through experience. My experience with this robot suggested that the robot design was robust. Neither the robot nor sensors suffered a failure. Indeed, not a single screw fell off. The legs and body remained in excellent condition. This robustness suggested that the technology applied in the design can produce robots that are genuinely durable. Altered environment conditions, minor changes in robot design parameters may also benefit of the proposed parametric modeling procedure.

References

- [1] M. Ahmadi, and M. Buehler, "Stable control of a simulated one-legged running robot with hip and leg compliance," in Proc. IEEE Transactions on Robotics and Automation, vol. 13, no. 1, pp. 96–104, 1997.
- [2] R. McN. Alexander, "Three uses for springs in legged locomotion," *The International Journal of Robotics Research*, vol. 9, no. 2, pp. 53–61, 1990.
- [3] J. J. Abbas, and R. J. Full, "Neuromechanical interaction in cyclic movements," In *Biomechanics and Neural Control of Posture and Movement*, (eds. Winter & Crago). Springer Verlag-New York, 2000.
- [4] S. A. Bailey, J.G. Cham, M. R. Cutkosky, and R.J. Full, "Biomimetic robotic mechanisms via shape deposition manufacturing," *Robotics*



- Research: 9th International Symposium*, J. Hollerbach and D. Koditschek (Eds), Springer-Verlag, London, 2000.
- [5] S. A. Bailey, J. G. Cham, M. R. Cutkosky, and R.J. Full, "Comparing the locomotion dynamics of the cockroach and a shape deposition manufactured biomimetic hexapod," in *Proc. ISER 2000*, Honolulu, HI, December 10–13, 2000, pp. 239–248.
 - [6] R. Blickhan, and R. J. Full, "Similarity in multilegged locomotion: bouncing like a monopode." *Journal of Comp. Physiology*, 173, pp. 509–517, 1993
 - [7] N. Bhushan, and R. Shadmehr, "Computational nature of human adaptive control during learning of reaching movements in force fields," *Biological Cybernetics*, Vol. 81, Issue 1, pp 39–60, 1999.
 - [8] C. Bartling, and J. Schmitz, "Reaction to disturbances of a walking leg during stance," *Journal of Experimental Biology*, vol. 203, pp. 1211–1233. 2000.



This page intentionally left blank

Section 6

Solutions from nature

This page intentionally left blank

Animal analogies for developing design thinking

C. Dowlen

London South Bank University

Abstract

The paper covers the development of a project aimed at first year design students starting out at university. This consists of a series of creative design techniques wrapped up in a managed project to design an animal. These techniques range from conventional processes such as specification writing and model making through to more off-the-wall techniques such as forced serendipity and genetic breeding processes. Students are also introduced to developmental processes such as structural design and systems design through the project. It is hoped to develop the project into an interactive tool for the development of creativity using the animal design project as an illustrative vehicle for the techniques.

Keywords: creativity, animals, design methods, design projects, natural analogies, design education.

1 Introduction

This project started out as a method of getting students on product design courses to think creatively from the start of their courses. The premise was that students need to be able not just to understand how the business of creativity works, but also need to put it into practice. This needed a vehicle for creative development skills; what was developed was the *Design an Animal* project. It was first used a decade ago and has been refined and developed, but the essential features have not changed significantly. It was recorded in a paper presented at ICED'05 . This paper looks in more detail at the specific exercises involved in the project and the connections between animals, creativity and methods.



2 Invented animals

God... invented the giraffe, the elephant, the cat... He has no real style. He just goes on trying things.

Pablo Picasso

Invented animals are all around us. Not in the theological sense, perhaps, but those invented by humans. They may have started with strange noises round a campfire with werewolves, leviathan, behemoth and the rest of the gang. Or with the Minotaur, centaurs, phoenix, unicorns, griffins, dragons and the like. They have continued with other fictional creatures such as hobbits, orcs, Gollum, trolls: moomins, hemulens, hattifatteners, and fillyjonks: gruffaloes, wombles, and clangers. Even when we make furry, cuddly toy models or write stories about of what animals they seldom resemble their natural counterparts. Winnie the Pooh – of course, such a lovable bear – has little resemblance to a real bear other than liking honey and being approximately the same shape. Real bears don't have that sort of relationship with rabbits and piglets. Stuffed toys of elephants, elks and echidnas are different from the real thing!



Figure 1: A toy echidna and a real Beagle.

And if you invent stories about them, their characters would be totally different from the real thing. Snoopy – well known as a beagle – is not a real beagle (although this one might still sit on the top of her doghouse).

3 Creativity

Dempsey has a view of creativity that it is inherent in some people – and seemingly not in others:

Creativity is a magical thing that you are born with. It presents itself early and like a virus is unstoppable.

It inhabits the kids who daydream and are good at drawing, but not much else. If I knew where it came from, I would bottle it up and make a fortune.

Michael Dempsey

Robinson reckons that it is something that needs to be developed in schools and universities (but isn't) and is a general skill that should be developed:

Employers are complaining that academic programmes from schools to universities simply don't teach what people now need to know and be able to do. They want people who can think intuitively, who are imaginative and innovative, who can communicate well, work in teams and are flexible, adaptable and self-confident

Robinson

Sternberg collected essays that explored the nature of creativity. These investigated the role of the environment, the role of the individual, and the role of the individual-environment reaction. Creativity, he concludes, has many natures, and these are distinctive. He uses a food analogy to describe the variations, calling some milk, meat, bagels and so on (the final page of the summing up at the end).

3.1 Developing creativity

More practically, Petty has a useful little book on creativity – *How to be better at... creativity*. He doesn't try to define creativity. He describes rather than defines it. He investigates different aspects of the process by which the creative initiative becomes embodied in an output. He outlines a combination of six processes that take place, in any order, during this process. These phases are remembered using the ICEDIP mnemonic: Inspiration, Clarification, Evaluation, Distillation, Incubation and Perspiration. Other books take a similar line. Alex Osborn's *Applied Imagination* was perhaps one of the first to take this approach, but that has been followed up with books such as Roger von Oech's *A Whack on the Side of the Head*, full of a set of special, illogical methods for the generation of creative ideas. Other texts just provide inspiration for illogicality, such as Alan Fletcher's *The Art of Looking Sideways*, full of quotations, some of which make sense and others which are totally off the wall.

3.2 When to develop creativity

In university design courses creativity should be developed from the day the students appear, and its development should carry on to the end of the course.



4 The specific exercise

This exercise was part of the students' initial design project experience on Product Design degrees.

Students carried out a range of techniques to develop creativity around the topic of designing an animal. How the idea of creating animals arrived is hidden somewhere in the mists of time, although it has proved a worthy vehicle for the exercise. Some of the techniques work particularly well with that as a topic, whilst some work as well with animals as with other topics. Some techniques are group ones: others are individual. Some are designed to generate ideas; others to develop them and to put flesh onto them to arrive at functional solutions. Some are conventional processes written in texts: others those that seem to fit with the topic at hand but could be utilised on many other design tasks. Using animals as the project provided a useful metaphor so that purposeful but slightly off-the-wall techniques could be integrated, tried and tested in a manner that might have seemed irrelevant otherwise. The managed project approach guided students to carry out specific procedures rather than leaving them to develop their own thinking processes.

4.1 Particular techniques

These were as follows: animal consequences (or a modification of potpourri), brainstorming, forced serendipity, emotional responses, forced serendipity, use of existing ideas, selection of wild ideas, morphological charts, affinity diagrams, combinatory processes, NAF, criteria selection, systems diagrams, genetic processes, imaginative composition, personal analogy, SWOT, three-dimensionality, structural design, embodiment design, specification writing, revision of drafts, model making, packaging / display.

Firstly, students are put into groups. Whilst this can be done in many ways, a simplistic approach is taken using each student's favourite animal as an indicator. When this was done first the groups were mixed ones so that cats, dogs, chimpanzees and creepy-crawlies were spread around the class. Later, better results were obtained all round by making groups with similar animals.

4.2 Ideation techniques

4.2.1 Animal consequences

An introductory game to get the students thinking laterally and to develop group interaction. The process is a children's game played in a group. Each person starts with a sheet of paper. Eventually a complete animal will be drawn by each person drawing bits of the animal in turn. The results are not predictable: students find the group design effort greater than the individual one – they see that interactions between the design team lead to mixed output and see something of the need to look for serendipity within the creative process.



4.2.2 Brainstorming

Once these initial drawings have been produced, the next task, still in groups, is to have a formal brainstorming session. The term has been developed from its coining by Osborn and some formality of the framework has been lost so it simply means getting ideas. It needs to be recaptured and the structure put back in. It is a group process to generate as many ideas as possible in the least possible time. The use of the animal project allows students to be a little removed from reality and so the process can build on the improbability of the possible outcomes.

4.2.3 Forced serendipity

Otherwise known Random Input. The process is carried out using a dictionary to find a random word and students are told to find twenty animal ideas connected with that word. For instance, the random word may be hexavalent. This is not easy to connect with animals – although an immediate connection is that the animals have to connect in groups of six. Or do they have six legs? Or six ways of having sex? Or that they need to have a relationship with six of their kind in order to be happy? And so on. That was only four ideas. Idea generation moves into a different plane as the input has come from outside the group. The character is different from tutor input which focuses more on how students were thinking instead of coming from an unexpected and perverse angle.

4.2.4 Selection of wild ideas

The group selects the craziest ideas and uses these to build on to get several others. It is a standard addition to a brainstorming session and one that is particularly useful in the context of developing novelty.

	<u>SLIME</u>	<u>FUR</u>	<u>FEATHER</u>	<u>LEATHER</u>
SKY	BALLOON FROG "PUMPS ITSELF TO" FLOAT A	PARACHUTE CAT "GLIDE" B	BUTTERFLY PENGUIN C	BOOMERANG MONKEY ROTATES 360° D
LAND	SPAGUETTI BOY "CAN STRETCH LONG" E	NOT SO SMALL FLEA "GIANT FLEA" F	CHICK EGG MIX CHICKEN + EGG G	GIRAFF TREE "LEAFS ON HEAD" H
WATER	INTELLI JELLYFISH "SEE THROUGH" "BRAINS" I	SEA HORSE UNICORN "HORN ON HEAD" J	BUBBLE HONEYBIRD "FLIES INSIDE" BUBBLE K	UNDERWATER PIGASS "TRAVELS THROUGH" FART L

Figure 2: A modification of a morphological chart.



4.2.5 Morphological charts

A standard technique that design students need to be able to use is the morphological chart. Students are asked to produce one of these individually after the group session and to bring the results to the group. The process is explained in Otto and Wood's book *Product Design*, and in Jones' *Design Methods*, who refers back to Zwicky. This method is one of the quickest at producing huge quantities of ideas in a limited amount of time: typically there will be millions from a single chart, although the example in Jones only produces 160 ideas and that in Otto and Wood only 65,536 (but note that this is on a single page in the book). Students sometimes misinterpret the concept and produce variations on the morphological chart such as figure 2.

4.2.6 Use of existing ideas

In practice, design projects utilise existing ideas to a great extent. This part of the exercise is given as homework. Students find pictures of animals that they respond to emotionally. This can be positive or one of revulsion. It's a useful tool for students to discover the limits of what they will or won't work on. These existing animals are allowed to come into the mix of animals.

4.2.7 Review of ideas

It is important that during the gaps between classes students keep a review process going. Students transfer the animal ideas that they have to sheets of A5 paper, one to a sheet, ready for the next part of the process.



Figure 3: A selection of animal ideas.



4.2.8 Affinity diagrams

Students come with a pile of sheets, each with a different animal idea. They pin them onto a notice board. Then they look at the arrangement of sheets and restructure it, silently, so that it makes sense. Once no further movements take place categories are invented for each cluster.

4.2.9 The unethical process of stealing ideas

Students raid the other groups' boards for ideas. Sharing ideas increases the overall quality and builds on the good ones. Students gain judgement by selecting as many useful ideas as possible, and see the currency and worth of their own ideas compared with those of others.

4.3 Selection techniques

4.3.1 NAF

At this point students are overwhelmed with the quantity of ideas. This is deliberate: it is well known that the more ideas there are, the better the quality of those ideas. Quantity breeds quality. Or, as Petty reports:

Many people wonder where creative people find their good ideas. The answer is, in among a huge pile of bad ones. , p15.

NAF is a quick process for sorting out ideas. It uses three categories: N, A and F. Or Novelty, Attractiveness and Functional. Each group selects ten ideas; five novel, three attractive and two functional ones.

4.3.2 Selection criteria

After students have used NAF, general selection criteria are introduced, explaining how product designers would typically use them. It is difficult to determine what criteria might be used to select suitable animals– there don't appear to be customers in the accepted sense of the word.

4.3.3 Genetic processes

These are taken loosely in this project. No attempt is made to describe genetic algorithms. Students are introduced to the crazy idea that mixed, confusing animals can breed with each other. Students have to select animals from as large a gene pool as possible and breed them promiscuously. This is a powerful design method – and very effective when using animals. Once a student had been deciding that he was going to use a vampire – only he couldn't spell, so it came out *vampire*. This neatly threw a mutation into the system.

4.4 Developmental techniques

Then students revisit the selection processes and to continue the development with a single animal idea each. Processes become developmental and there is more energy tied up in the individual creature.



4.4.1 Imaginative composition

Literary processes are used to develop aspects of the animal's lives. Students describe a day in the life of the animal. How does it sleep? Where does it find food? How does it eat it? What does it breathe? When does it contact others of the species? What do they do together? How social are they? How do they mate? What makes a good day? And so on.

4.4.2 Personal analogy

This takes imaginative composition further, asking students to describe how it actually feels to become that animal. What sort of emotions does it have? What are its senses like? How does it know about its surroundings? How does it think? Sometimes it's about students putting forward fantasies, but more often they become more involved in improving the development of the creature.

4.4.3 Three-dimensionality

The scene shifts from ill-defined ideas to adding flesh onto the bones. They work out how the physical animal goes together and how to present the results of their thinking. The animal has to be three dimensional, and they model it.

4.4.4 Embodiment design

This is about putting flesh onto the model. In this phase students are expected to work out physical sizes, loads, weights and so on.

4.4.5 Structural design

Firstly, they need to work out what sort of structure takes loads. Natural structures have several forms: chassis-type structures like skeletons, exoskeletons from insects or system structures like plants. There are also structures such as those that are largely supported by the buoyant sea – like jellyfish – and land animals like slugs and worms. How does the animal move? How many legs are on the ground at any one time in order to support the weight?

4.4.6 Systems design

How does the animal system work? What happens to food? Where do waste products go? Does it have a circulatory system such as blood? Does it breathe? What happens to matter and energy in the animal? What about controls and feedback systems for nerves? Where do the commands come from? Is there a single command position such as a brain or is there a distributed system?

4.5 Techniques involved with the deliverable – the model etc

Students are now told they need to produce a model and associated scenery to demonstrate their animal design.

4.5.1 Specification writing

They have to write a specification for the model they are going to make – not for the animal itself, but for it as if the representative model or animal toy.



Is it full-size or larger or smaller? What facilities have to be used to manufacture it? What toy regulations need to be satisfied? And so on.

4.5.2 Revision of drafts

A continuing process but one that students have difficulty with. Getting them to finish a project early to revise it is fraught with difficulty. Revisiting drafts, making multiple prototypes and modifying final drafts is an important design processes.

4.5.3 Model making and Scene setting

The embodiment becomes more concrete. Although the project is not covering these areas substantially, it is incomplete without producing some sort of realisation. The scene setting was a small environmental scenario illustrating the animal in its habitat or forming packaging and advertising.

4.6 Project results

Figure 4 shows a selection of animals produced over the years.

It can be seen that students build ideas on what they have known before and skills on the skill base they have. But some animals are totally different from anything students have known before – such as the String Glob that had more in common with spaghetti than with a vertebrate.



Figure 4: A selection of animal designs created over the years.

Do students show evidence of developing creativity? Students on the London South Bank courses are creative and obtain employment where creativity is important. Whether this project provides them with creativity tools is harder to quantify. It is clear is that students do not associate the project with a series of creative methods. It seems to be part of the ‘mush’ of projects that they carry out when they started rather than a discernable toolkit of techniques.

5 The way forward

The project has moved on to the next stage. Whilst providing a hands-on toolkit of techniques for first year students is still deemed to be a Good Thing, their forgetting how to use them in the later parts of their courses is not so good. The approach is to embed the processes in a software package for any level of the course to guide them through techniques, applying them to the design of animals as illustrative of how they might be used.

References

- [1] Dowlen, C., Design an animal. Analogies for the development of creativity, *International Conference on Engineering Design*, The Design Society: Melbourne, 2005.
- [2] Dempsey, M., Creative Accounts. In Creative Survey, *Design Week*, November 2002
- [3] Robinson, K., *Out of our minds*, Capstone: Oxford, 2001.
- [4] Sternberg, R. J., *The Nature of Creativity: Contemporary Psychological Perspectives*, Cambridge University Press: Cambridge, 1988.
- [5] Petty, G., *How to be Better at ... Creativity*, Kogan Page: London, 1997.
- [6] Osborn, A. F., *Applied Imagination*, Scribner: New York, 1953.
- [7] Von Oech, R., *A Whack on the Side of the Head*, Thorsons: London, 1990.
- [8] Fletcher, A., *The Art of Looking Sideways*, Phaidon: London, 2001.
- [9] Belbin, R. M., *Management Teams: how they succeed or fail*,
- [10] Levin, P., *Successful Teamwork!*, Open University Press: Maidenhead, 2005.
- [11] Otto, K. and Wood, K., *Product Design: Techniques in Reverse Engineering and New Product Development*, Prentice Hall: 2001.
- [12] Jones, J. C., *Design Methods: Seeds of Human Futures*, Van Nostrand Reinhold: 1992.
- [13] Zwicky, F., The Morphological Method of Analysis and Construction, *Courant*, Anniversary Volume, 1948



Development of a novel flapping mechanism with adjustable wing kinematics for micro air vehicles

A. T. Conn, S. C. Burgess & R. A. Hyde

Department of Mechanical Engineering, University of Bristol, Bristol, UK

Abstract

There is currently significant interest in developing micro air vehicles (MAVs). Insects provide a natural blueprint for such vehicles and can outperform current man-made miniature flyers through the exploitation of low Reynolds number aerodynamics. However, designing a flapping mechanism that replicates the complex wing kinematics of insects is a demanding task, due to limitations in current actuation technology and the miniature scale of MAVs. The majority of current MAV flapping mechanisms produce constrained wing kinematics and therefore have little capacity for replicating insect flight manoeuvres and hence controlled flight. This paper presents a novel mechanism that produces partially constrained insect inspired wing motion with adjustable kinematic parameters. The parallel crank-rocker mechanism can modulate the phase difference between the rocker links to achieve this and hence produce controllable flight. Its overall development is described and the wing kinematics it produces are compared with those of a hawkmoth.

Keywords: micro air vehicles, insect flight, wing kinematics, flapping wing mechanism, biomimetic, bio-inspired, unsteady aerodynamics.

1 Introduction

1.1 A Brief History of MAVs

Micro air vehicles (MAVs) are miniature flying craft that are distinguishable from the current smallest flying vehicles such as military unmanned air vehicles and hobby-enthusiast model airplanes and helicopters by their scale, which in



terms of mass and volume is at least an order of magnitude less. The concept of a MAV was initiated by military strategists, inspired by rapidly advancing technologies such as micro-electromechanical systems (MEMS) and miniature digital cameras [1]. They envisioned low cost, highly miniaturised autonomous robots capable of unheralded levels of reconnaissance, surveillance and hazardous substance detection. A miniature, autonomous flying vehicle also has many civil and commercial applications such as search and rescue, traffic monitoring and air quality sampling.

MAVs are commonly defined by a 15 cm dimensional limit, instigated by the U.S.A.'s Defense Advanced Research Projects Agency (DARPA), that founded the first MAV research program. There are likely to have been two primary reasons behind this limit. The first is simply due to anthropometrics, since 15 cm approximately conforms to being "hand-held" and is also suitable for personal storage [2]. The second and more profound reason was based on aerodynamic principles. Having a maximum characteristic length of under 15 cm coupled with a relatively low flight speed means MAVs are certain to operate in a laminar flow regime with a Reynolds number below 5×10^5 , the value commonly attributed to the transition between laminar and turbulent flow for a flat plate [3].

1.2 Insect inspired flapping MAVs

A MAV can have any type of propulsion system, but currently the three most viable platforms are fixed wing, rotorcraft and flapping wing. Flight performance varies between them but can be characterised as fixed wing MAVs being better suited to outdoor operations while rotorcraft and flapping wing MAVs' abilities to hover and vertically take-off and land (VTOL) allow them to manoeuvre through cluttered indoor environments. If the desire is to create a MAV capable of flying indoors, at first it appears the basic flight performance (flight speed, hover capabilities etc.) of rotorcraft and flapping wing MAVs are similar. Flapping wing MAVs, however, have a much greater potential for extreme manoeuvrability and high payload capacity. This potential is apparent in a tangible sense by the fact that millions of natural flapping wing "MAVs" already exist in the form of insects and small birds, who regularly exhibit exceptional flight agility.

Insects, in particular, achieve this outstanding flight performance by exploiting unsteady aerodynamic mechanisms that exist at the low Reynolds number flow regime they share with MAVs. This has led to great interest in mimicking the complex wing kinematics of insects with the explicit aim of replicating the same unsteady aerodynamic phenomena. This paper details research into the development of an insect inspired flapping mechanism for application to a highly manoeuvrable, hover-enabled MAV. It should be noted that flapping MAVs that have not copied wing kinematics found in nature have been successfully flown but with limited hovering ability e.g. Jones and Platzer [4].



2 Insect inspired biomimetic design

2.1 Unsteady aerodynamics

The understanding of the theory behind the unsteady aerodynamic mechanisms employed by insects has significantly improved over the last two decades, but is still subject to some uncertainty and contradiction. Also, not all insects utilise the same mechanisms, in part due to differing morphologies, wing kinematics and Reynolds numbers. While both the smallest and largest insects fly in a laminar flow regime, they span the transition from viscosity dominated flow ($Re = 10^0-10^2$) to inertia dominated flow ($Re = 10^2-10^4$) respectively [5, 6]. It is likely a flapping MAV will operate in inertia dominated flow and so the unsteady aerodynamic mechanisms of interest are those thought to be employed by larger insects:

- Leading edge vortex (LEV) and dynamic stall
- Wing rotation force - Kramer effect
- Wake recapture
- Virtual mass

A full description of how these mechanisms augment lift from insect wings will not be given, as they have been subject to numerous review studies (e.g. Lehmann [7]; Sane [8]). The two most important unsteady mechanisms in terms of lift are the LEV and the timing-dependent rotational force thought to be produced through the Kramer effect [8]. It has been shown with a mechanical hawkmoth model that a LEV may account for lift equal to two thirds of a hawkmoth's body weight [9]. Dickinson *et al.* [10] found that the rotational force contributed 35% of the lift produced by a similar flapping mechanical model and that this value was extremely sensitive to the timing of the rotation.

2.2 Mimicry of insect flight

From the perspective of designing a flapping MAV, replicating the unsteady aerodynamic mechanisms utilised by insects appears to be a difficult task. It is simply not feasible to reverse engineer an insect's thorax, which contains its flight muscles and wing joint, so the best approach is to mimic just the insect's wing kinematics and not its thorax morphology. However, there is great variation of wing kinematics amongst insects (even for the same species), suggesting they are altered to suit specific aerodynamic demand [11]. This has caused a gap in knowledge over what the optimal wing kinematics are for a particular wing and hence uncertainty over which kinematical features each unsteady aerodynamic mechanism is dependent on. Therefore mimicking insect wing kinematics is likely only to provide the starting point for flapping MAV design, with aerodynamic experimentation leading to wing kinematics optimisation currently a necessity for optimal performance.

Apart from their wing kinematics, insects possess other features pertinent to biomimicry. Insect wings are complex, lightweight structures that possess several common features to maximise the production of lift and thrust. The form



and orientation of wing veins in particular create regions of high stiffness and of high compliance to ensure the wing reacts favourably to local airflows throughout the entire wing stroke. Another optimal design feature is insects' use of resonance and elastic storage. The insect's thorax is a mechanically resonant system that incorporates highly elastic elements, composed of resilin, which store kinetic energy at the end of each upstroke and downstroke and release it during the half-stroke. Creating a material that matches resilin's elastic properties is not currently feasible, yet the principle of elastic storage remains a hugely beneficial method of minimising power expenditure.

2.3 Insect wing kinematics

It was outlined in the previous section that there is great variation of wing kinematics amongst insects and therefore it is necessary to generalise them for application to a flapping MAV mechanism. Wing strokes involve two translatory stages (downstroke and upstroke) interspersed by two short rotational stages (supination and pronation), at which point the wing reverses direction. The motion of the wing through these stages is described using a set of *kinematic parameters*, of which typical values are given in Table 1. Producing a flapping mechanism that matches the kinematic parameters of insects should produce the desired unsteady aerodynamic mechanisms. However, if these parameters cannot be dynamically adjusted then the MAV will have no capacity for flight stability or manoeuvring and will have no chance of staying airborne. Detailed knowledge of insect flight control is currently lacking, but it is possible to classify which kinematic parameters need to be adjusted to perform certain manoeuvres (as shown in Table 2). It should be noted that a MAV might not need to adjust all its kinematic parameters for controlled flight, and it may be beneficial for the design of the flapping mechanism to constrain certain parameters.

Table 1: Typical values of kinematic parameters for insects.

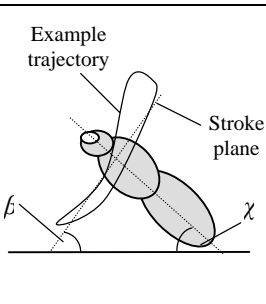
Side View of Insect	Kinematic Parameter	Typical Value
	Wingtip trajectory	(shown on diagram)
	Angle of attack, α	30° [6]
	Stroke amplitude, Φ	120° [12]
	Wing beat frequency, n	20 – 40 Hz for large insects [12] ($n \propto m^{-1/4}$) [5]
	Stroke timing, d/u	1.0 – 1.1 [13]
	Stroke plane angle, β	10° → 50° [6] (flight speed: 0 → max.)
	Body angle, χ	50° → 10° (flight speed: 0 → max.)



Table 2: Kinematic parameter modulation required for performing manoeuvres.

Manoeuvre	Roll	Pitch	Yaw	Kinematic Parameter	Wing Balance
Forward acceleration		(X)		Stroke plane angle [6]	Symmetric
		(X)		Stroke amplitude [6]	Symmetric
		(X)		Wing beat frequency [14]	Symmetric
Nose up/nose down		X		Stroke timing [14]	Symmetric
Vertical acceleration				Stroke amplitude	Symmetric
				Wing beat frequency	Symmetric
Lateral acceleration	X			Stroke amplitude [6]	Asymmetric
	X			Angle of attack [6]	Asymmetric
Flat Turn			X	Angle of attack [10]	Asymmetric
			X	Stroke timing [14]	Asymmetric
Banked turn	X		X	Stroke amplitude [6]	Asymmetric
	X	X	X	Stroke plane angle [6]	Asymmetric

3 Selection of flapping mechanism

3.1 Actuation system

The extreme mass and volume constraints on-board MAVs, as well as a limited power supply, require them to be highly integrated systems, much like their natural inspiration. As a result, even when considering just the flapping mechanism it is critical to include the actuation devices at an early stage of the design process. Assessing the actuation technologies currently available, it is clear there are no currently available products that come close to matching muscle's extremely high strain output (likely to be essential for a compact mechanism to produce a large enough stroke amplitude). Piezoelectric ceramic benders possess excellent power densities and frequency ranges, but require very high activation voltages to achieve a large enough strain. This is major issue since a MAV's on-board power supply will be extremely limited. A new class of similar smart materials called electro-active polymers (EAPs) may bridge the gap and provide high strain at low voltages but their development is still in its infancy. Brushed DC motors provide a rotary alternative and have a high power density since they do not need bulky driver electronics.

3.2 Mechanism classification

As well as the previously stated kinematic parameters, the limitations of available actuation devices add further design specifications to the flapping mechanism. This can be generalised to a linear input mechanism needing high amplification ratios (maximise the input displacement) while a rotary input mechanism requires linkages that can convert rotary motion into controlled



flapping. Also, since linear actuators can usually modulate their output displacement, they can drive under-constrained mechanisms. Rotary actuators, however, need to continuously perform full revolutions so the corresponding wing motion is likely to be constrained to a single path. The general effect the level of constraint has on a mechanism's performance is described in Figure 1.

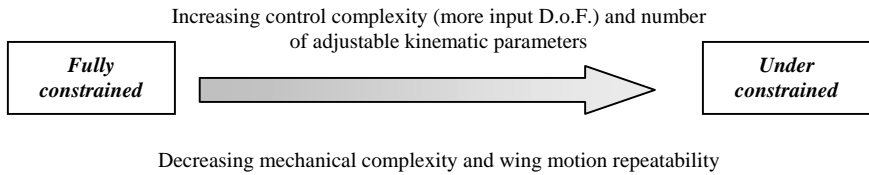


Figure 1: Relationship between level of constraint and performance/complexity.


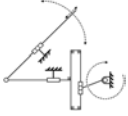
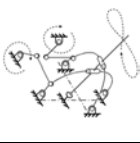
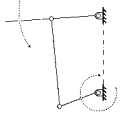

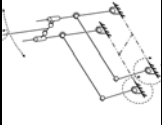
Since increasing mechanical complexity generally adds more weight while greater control complexity does not, an under-constrained mechanism appears to be the optimum solution. Yet when the limited strain output of available linear actuators is considered, the mechanical realisation of such a mechanism becomes less viable. This is reflected by the flapping mechanisms that have thus far been developed for application to an insect inspired MAV, a selection of which are listed in Table 3. The table summarises each mechanism's kinematical properties in terms of its mechanical complexity (i.e. number of links and joints) and capability for controlling wing kinematics. Note that none of the mechanisms in Table 3 can adjust the stroke plane angle and it is assumed that all can modulate the wing beat frequency, which is an actuation issue.

The parallel four-bar mechanism has the greatest potential for controlled flight as it can dynamically adjust its wing kinematics [15]. Correspondingly, it also has the highest number of input D.o.F and thus control complexity. The other existing mechanisms developed all produce constrained wing kinematics from a single rotary input. All the mechanisms can approximately replicate the kinematic parameters listed in Table 1, although some have simplified the flapping trajectory to a single plane. However, only mechanisms with freely adjustable kinematic parameters can enact the manoeuvres described in Table 2, which are essential for controllable flight.

An alternative solution has been developed to the current flapping mechanisms that uses parallel crank-rockers and is shown in Table 3 in bold. It utilises a rotary input for the main drive and two subsidiary inputs that may be linear or rotary. Since the main drive is rotary, a low voltage DC motor can be used. It requires a comparatively high number of links and joints, but because the links are orientated in the same plane as the wing's stroke plane it is extremely compact. Its main advantage, however, is the ability to adjust each wing's angle of attack asymmetrically. This is achieved by reciprocating two phased rockers per wing. When the phase difference between each rocker is modulated, the angle of attack is altered. This allows it to accelerate laterally and perform flat turns as well as maximising the timing-dependent wing rotation force produced via the Kramer effect.



Table 3: Kinematical properties of MAV flapping mechanisms.

Mechanism	Four-bar coupler and Geneva wheel [17]	Scotch yoke [18]	Double scotch yoke and Geneva wheel [19]	Crank-rocker [20]	Non-planar crank-rocker [21]	Parallel crank-rockers
Kinematic Diagram						
No. of links	12	8	15	5	9	18
No. of joints	18	14	29	7	13	22
Input Type	Rotary	Rotary	Rotary	Rotary	Rotary	Rotary
Input D.o.F.	1	1	1	1	1	3
Wing trajectory	Fixed 2 D.o.F.	Fixed 1 D.o.F.	Fixed 2 D.o.F.	Fixed 1 D.o.F.	Fixed 1 D.o.F.	Fixed 1 D.o.F.
Angle of attack, α	Fixed	Fixed	Fixed	N/A	Fixed	Adjustable
Stroke amplitude, Φ	Fixed	Fixed	Fixed	Fixed	Fixed	Fixed
Timing, d/u	Fixed	Fixed	Fixed	Fixed	Fixed	Fixed



4 Design of parallel crank-rocker mechanism

The parallel crank-rocker mechanism forms the basis of an experimental test-rig that produces adjustable wing kinematics that is being manufactured at the University of Bristol. The test-rig has been designed to be fabricated at near-MAV scale and will be used to test both the chosen mechanism's feasibility and for wing kinematics optimisation. The optimisation should help eliminate gaps in knowledge linking wing kinematics and unsteady aerodynamic lift production. The mechanism's link ratios were selected after kinematic analysis, with a final ratio of 1:3.8:1.3:4. This ratio produces a stroke amplitude of 102° and a stroke timing (d/u ratio) of 1, which match the general kinematic parameter values given in Table 2 and suggests the unsteady aerodynamic mechanisms should be produced. A comparison of the wing kinematics produced by the mechanism with those of a hawkmoth is shown in Figure 2a. The mechanism's wing kinematics are similar to the hawkmoth's, although the stroke amplitude and d/u ratio are less and the wing motion is restricted to a single plane. The adjustable phase difference between each wing's rockers directly controls the wing angle of attack, and can be adjusted by slowing one crank relative to the other.

Dynamic analysis was undertaken using a combined physical and electrical model created in the Simulink® SimMechanics environment. The results show that mimicking insects' use of elastic storage by attaching springs to the rockers can lower the work done per wing stroke by over 50% as shown in figure 2b, even when operating outside of the system's resonant frequency. A geared Maxon RE10 miniature brushed DC motor (7 g mass) was selected and is expected to drive the 75 mm long wings at a wing beat frequency of 31.7 Hz. Figure 3 shows an annotated CAD view of the final assembly, which has an estimated weight of 62.6 g with major dimensions of 25×29×62.75 mm. The parts are predominantly composed of aluminium, although certain parts were fabricated using brass due to its availability in lengths of miniature cross-section.

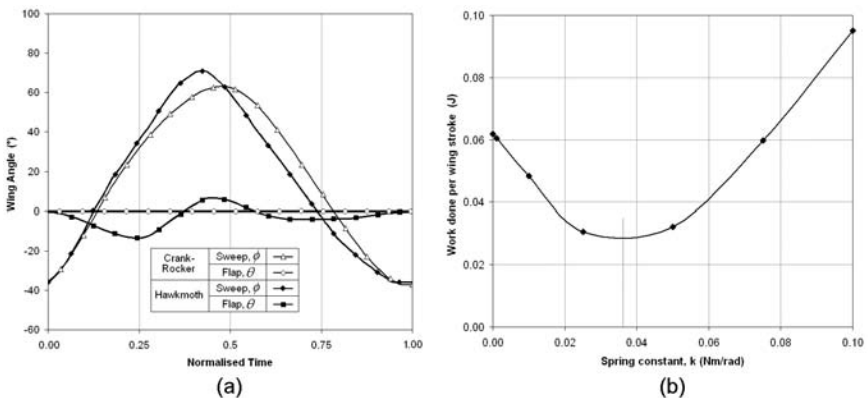


Figure 2: (a) Comparison of wing kinematics where the sweep and flap angles describe the wing trajectory relative to the stroke plane [11]; (b) Effect of elastic storage on wing stroke work (optimum spring constant indicated by broken line).



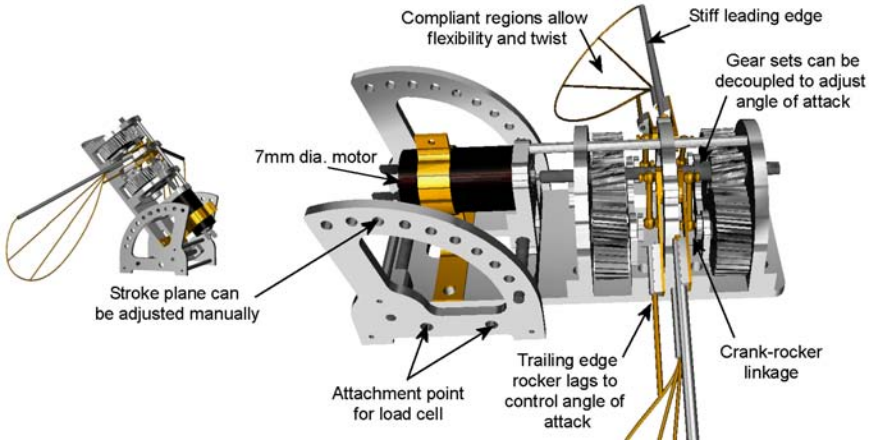


Figure 3: CAD view of mechanism test-rig assembly with key features labelled.

5 Conclusions

Insect inspired MAV flapping mechanisms are required to produce complex wing trajectories while possessing compact and lightweight components. A key performance factor in insect flight is the adjustability of wing kinematics, as it is a necessity for controlled flight. Selection of a flapping mechanism should take into account the potential degree of adjustability. The parallel crank-rocker mechanism presented in this paper produces planar wing strokes with a fully adjustable angle of attack, a key kinematic parameter. When integrated with a separate stroke adjustment mechanism this should allow for flight stability and manoeuvring capabilities sufficient for controlled flapping flight.

References

- [1] McMichael, J.M. & Francis, M.S., *Micro Air Vehicles – Toward a New Dimension in Flight*, DARPA Document, Online. http://www.fas.org/irp/program/collect/docs/mav_auvsi.htm
- [2] Defense Advanced Research Projects Agency, News Release, Online. www.fas.org/irp/news/1997/b12121997_bt676-97.html
- [3] Anderson Jr., J.D., *Fundamentals of Aerodynamics*, second edition, McGraw-Hill: New York, 1991.
- [4] Jones, K.D. & Platzer, M.F., On the design of micro air vehicles. *Design and Nature*, eds: C.A. Brebbia, L.J. Sucharov and P. Pascolo, WIT Press: Southampton, pp. 67-76, 2002.
- [5] Dudley, R., *The Biomechanics of Insect Flight: Form, Function, Evolution*, Princeton University Press: Princeton, New Jersey, 2000.
- [6] Ellington, C.P., The novel aerodynamics of insect flight: applications to micro-air vehicles. *Journal of Experimental Biology*, **202**, pp. 3439-3448, 1999.



- [7] Lehmann, F.-O., The mechanisms of lift enhancement in insect flight. *Naturwissenschaften*, **91(3)**, pp. 101-122, 2004.
- [8] Sane, S.P., The aerodynamics of insect flight. *Journal of Experimental Biology*, **206**, pp. 4191-4208, 2003.
- [9] Van den Berg, C. & Ellington, C.P., The three-dimensional leading-edge vortex of a 'hovering' model hawkmoth. *Philosophical Transactions of the Royal Society of London, Series B: Biology*, **352**, pp. 329-340, 1997.
- [10] Dickinson, M.H., Lehmann, F.-O. & Sane, S.P., Wing rotation and the aerodynamic basis of insect flight. *Science*, **284**, pp. 1954-1960, 1999.
- [11] Willmott, A.P. & Ellington, C.P., The mechanics of flight in the hawkmoth, *Manduca Sexta*. I. Kinematics of hovering and forward flight. *Journal of Experimental Biology*, **200**, pp. 2705-2722, 1997.
- [12] Brodsky, A.K., *The Evolution of Insect Flight*, Oxford University Press, Oxford, 1994.
- [13] Ellington, C.P., The aerodynamics of hovering insect flight. III. Kinematics. *Philosophical Transactions of the Royal Society of London, Series B: Biology*, **305**, pp. 79-113, 1984.
- [14] Taylor, G.K., Mechanics and aerodynamics of insect flight control. *Biological Reviews of the Cambridge Philosophical Society*, **76(4)**, pp. 449-471, 2001.
- [15] Avadhanula, S., Wood, R.J., Steltz, E., Yan, J. & Fearing, R.S., Lift force improvements for the micromechanical flying insect. IEEE Int. Conference on Intelligent Robots and Systems, Las Vegas, Nevada, October, 2003.
- [16] Banala, S.K., Karakaya, Y., McIntosh, S., Khan, Z. & Agrawal, S.K., Design and optimization of a mechanism for out of plane insect wing motion with twist. *Proc. of DETC, ASME Design Engineering Technical Conferences*, Salt Lake City, Utah, September, 2004.
- [17] Żbikowski, R., Galiński, C. & Pedersen, C.B., A four-bar linkage mechanism for insect-like flapping wings in hover: Concept and an outline of its realisation. *Transactions of the ASME: Journal of Mechanical Design*, **127**, pp. 817-824, 2005.
- [18] Tarascio, M.J., Ramasamy, M., Chopra, I. & Leishman, J.G., Flow visualization of micro air vehicle scaled insect-based flapping wings. *Journal of Aircraft*, **42(2)**, pp. 385-390, 2005.
- [19] Galiński, C. & Żbikowski, R., Insect-like flapping wing mechanism based on a double spherical Scotch yoke. *Journal of the Royal Society: Interface*, **2(3)**, pp. 223-235, 2005.
- [20] Pornsin-Sirirak, N., Tai, Y.-C., Nassef, H. & Ho, C.-M., Titanium-alloy MEMS wing technology for micro aerial vehicle application. *Sensors and Actuators A: Physical*, **89**, pp. 95-103, 2001.
- [21] Burgess, S.C., Alemzadeh, K. & Zhang, L., The development of a miniature mechanism for producing insect wing motion. *Design and Nature II*, eds. M.W. Collins & C.A. Brebbia, WIT Press: Southampton, pp. 237-244, 2004.



Section 7

Sustainability studies

This page intentionally left blank

Bionics vs. biomimicry: from control *of* nature to sustainable participation *in* nature

D. C. Wahl

Centre for the Study of Natural Design, University of Dundee, UK

Abstract

Quantum theory, complexity theory, and ecosystems theory, along with anthropogenic climate change and ecosystem collapses are confronting humanity with insights that will crucially inform the re-design of products, processes, services and institutions in order to catalyse the transition towards a sustainable human civilization. In a fundamentally interconnected and unpredictable world, where local actions have global consequences, the intentionality behind science and design needs to shift from aiming to increase prediction, control and manipulation *of* nature as a resource, to a transdisciplinary cooperation in the process of learning how to participate appropriately and sustainably *in* Nature.

A participatory conception of nature–culture relationships acknowledges the dependence of humanity on healthy ecosystems and a healthy biosphere. It implies the need for a salutogenic design approach that increases human, societal and ecological health synergistically. In order to create sustainable designs that are sensitive to the unique social, cultural and ecological conditions of a particular place and facilitate the emergence of health as a system-wide and scale linking property, designers will have to move from a detached perspective of culture as *apart from* nature and learning *about* nature, to a more holistic and participatory perspective of culture as *a part of* Nature and learning *from* Nature.

This paper suggests that bionics and biomimicry represent two distinct approaches to ‘design and nature’ based on different conceptions of the relationship between nature and culture. An effective transition towards sustainability, mediated by design, will have to be informed by a holistic and participatory conception of nature and culture within a fundamentally interconnected and unpredictable complex dynamic system.

Keywords: sustainability, complexity, bionics, biomimicry, transdisciplinary, design, health, scale-linking, salutogenic, ecology.



1 Introduction

Five hundred years ago Leonardo da Vinci [1] warned: “Those who take for their standard any one but nature – the mistress of all masters – weary themselves in vain” (p.xxx). Did da Vinci foresee that the Scientific Revolution would set humanity on a path predominantly driven by the aim to increase our ability to predict, control, and manipulate nature, rather than to learn from and integrate into nature?

Galileo Galilei called for a focus on the measurable, quantitative aspects of nature and regarded qualitative aspects to be of secondary importance. Francis Bacon described the vision of humanity as ‘master of nature.’ Rene Descartes created the conceptual separation of mind and body, humanity and nature, and subject and object into dualistic, mutually exclusive categories; he also offered the mechanistic clockwork metaphor. Together, they created the basis for a reductionistic science of detached objectivism.

This approach to science separated human beings, as objective observers, from their biological nature as participants in a fundamentally interconnected natural process. The root cause of the utter unsustainability of modern civilization lies in the dualistic separation of nature and culture. It is in nature, that all peoples and all species unite into a community of life. Yet culture is commonly conceived of as *apart* from nature, rather than *a part of* nature. Since the Industrial Revolution, reductionist science has enabled us to design a whole host of powerfully manipulative technologies, which have transformed the planet.

These technological inventions have undeniably improved the standard of living of many people, but for centuries, the hidden connections [2] linking human activities to ecosystems and the biosphere, have been ignored. Many modern technologies of comfort (e.g. jet travel, the use of internal combustion engines, air conditioning, industrialized agriculture and food systems) are actually creating more problems than benefits, when such designs are considered in an ecological and planetary context. Their effects on the quality of life of this and future generations will not be beneficial in the long-term.

The unbridled use of fossil fuels and other natural resources along with the unrestrained disruption of ecosystems have, within only two centuries, altered the planet’s atmospheric composition and climate patterns [3] and decreased the resilience [4] and health of many of the world’s ecosystems [5].

The avant-garde sciences, represented by quantum physics [6], cognitive biology and consciousness studies [7], chaos theory [8], ecosystem science [9], human ecology [10], and the theory of complex dynamic systems [11], have long moved beyond the anachronistic paradigm of prediction and control of nature. These sciences acknowledge that we are living in a complex, interconnected, constantly changing, and - beyond a very limited spatial and temporal scale – fundamentally unpredictable and uncontrollable world. Local actions can have far-reaching global consequences. Cause and effect relationships in complex dynamic systems are non-linear, multi-causal, and often time-delayed and spatially removed [12].



Modern science has begun to transcend and include the detached, quantitative and reductionist approach of Cartesian science and now seeks to integrate it into a more participatory, qualitative and holistic conception of humanity's relationship to the natural world. The aim of science is shifting towards informing appropriate participation in natural process, rather than the enabling of new technologies of prediction, manipulation and control [13].

The transition towards sustainability will require a new approach to design and technology that is based on a participatory and holistic worldview informed by science, ethics and the transdisciplinary integration of multiple perspectives [14]. It is a biophysical and ecological fact that culture is *never* truly separate from nature. Quality of life and the spectrum of consciousness have a psychological, spiritual, inner dimension that cannot be described solely scientifically.

All human design and technology interacts with the natural cycles that maintain the health of ecosystems and the planetary life-support system. Humanity depends on ecosystems services for its survival [15]. Sustainability depends on healthy individuals in healthy communities and societies [15, 17] just as much as these depend on healthy ecosystems and planetary health [18–20].

Hawken [21] identified design as an integrative concept for the prevention of environmental damage. Design also implies a need for decision-making based on multiple perspectives and disciplines. When design is informed by ecological literacy [22] it offers an integrative framework for meeting human needs within the limits set by natural process at a local, regional and global scale [23–26].

Orr [27] describes ecological design as “a large concept that joins science and the practical arts with ethics, politics and economics” (p.4) and emphasizes that such a design approach “is not so much about how to make things as about how to make things that fit gracefully over long periods of time in a particular ecological, social, and cultural context” (p.27). David Orr writes: “The problem is simply how a species pleased to call itself *Homo sapiens* fits on a planet with a biosphere. This is a design problem and requires a design philosophy. The very idea that we need to build a sustainable civilization needs to be invented or rediscovered, then widely disseminated, and put into practice quickly” (p.50).

2 Learning from nature as model, measure, and mentor

In the 1960s and 70s, McHarg [28] and the founders of the ‘New Alchemy Institute’ - Todd, Jack-Todd and McLarney [29] - were among the pioneers of a new approach to design, aiming to integrate into natural process and apply nature's design lessons to the creation of more sustainable human infrastructures, products and processes.

John Todd [30] describes his vision for design in the 21st century: “The Earth's ecologies are embedded with a set of instructions that we urgently need to decode and employ in the design of human systems” (p.1). After forty years of research at the nexus of biology, ecology and design, Todd emphasizes: “it is possible to design with Nature ... through ecological design, it is possible to



have a high civilization using only one tenth of the world’s resources that industrial society uses today” (p.3).

2.1 Bionics: A prediction and control approach to learning from nature

In parallel with the emergence of ecological design and its strategy of biomimicry, a more technologically oriented approach to applying nature’s design lessons has also evolved since the 1960s, when the US Air Force engineer, Major J.E. Steele coined the term ‘bionics.’ While it has, at points, been predominantly identified with the creation of artificial human body parts – bionic ears, limbs, and eyes [31], the field of bionics is currently gaining in scope and popularity.

Since the 1970s, particularly through the pioneering work of the German zoologist Werner Nachtigall, bionics has developed into an increasingly influential support discipline for engineers and technologists. According to Nachtigall [32] bionics is the process of “learning from nature as an inspiration for independent technical design” (p.1). Nachtigall formulated a series of principles of bionic design, a translation of which is provided in table 1.

Table 1: Principles of bionic design.

<ol style="list-style-type: none"> 1. Integrated instead of additive construction 2. Optimisation of the whole, rather than maximization of individual elements 3. Multifunctionality instead of monofunctionality 4. Fine-tuning adapted to particular environments 5. Energy saving instead of energy squandering 6. Direct and indirect use of solar energy 7. Temporal limitation instead of unnecessary durability 8. Total recycling instead of waste accumulation 9. Networks instead of linearity 10. Development through the process of trial and error
--

Source: Nachtigall [32], pp.21-34

As a scientific discipline, bionics takes a systems approach to the technical realization and application of construction processes and developmental principles observed in biological systems. It has contributed to technological innovations in aero- and fluid-dynamics, echolocation and sonar, lightweight construction, ventilation, packaging, adhesion, propulsion, pumping, locomotion, material composition, volume optimisation and other fields [32]. However, the technical rigor and engineering mindset of bionics has merits and limitations.

Germany is currently taking a leading role in the field of bionics research. There is a ‘Society for Technical Biology and Bionics’, as well as an established ‘Bionics Competency Network.’ The University of the Applied Sciences in Bremen offers the first ‘BSc. in Bionics’, and organized a conference in



November 2004, which united a vibrant community of researchers. Unfortunately the focus was so exclusively on technological innovation that it almost actively tried to discourage ecological concerns and the issue of sustainability.

Without acknowledging the complex context of sustainability and ecological and social interactions, bionics, planning, design, engineering, and resource management, all run the risk of staying trapped in a prediction and control mindset. This will ultimately perpetuate unsustainable practices, as it ignores the complex interplay of diverse social, cultural, economic *and* ecological factors that have to be brought into synergy in order to create sustainable solutions and design.

2.2 Biomimicry: ecologically informed design for sustainability

The first researchers to offer a list of principles for ecologically or biologically informed design were John Todd and his wife Nancy Jack-Todd [24, 33]. During the 1970s, research at the 'New Alchemy Institute' began to explore how ecology, biology, and a bio-cybernetic systems approach, could inform more sustainable solutions to meeting fundamental human needs. Table 2, below reproduces the initially proposed nine precepts, augmented by a tenth precept that was added more recently [34] to stress the centrality of design as an expression of intentionality in all human interactions and relationships.

Table 2: Precepts of biological design.

<ol style="list-style-type: none"> 1. The living world is the matrix for all design. 2. Design should follow, not oppose the laws of life. 3. Biological equity must determine design. 4. Design must reflect bioregionality. 5. Projects should be based on renewable energy sources. 6. Design should be sustainable through the integration of living systems. 7. Design should be co-evolutionary with the natural world. 8. Building and design should help heal the planet. 9. Design should follow a sacred ecology. 10. Everyone is a designer! <p style="text-align: right;">Source: Jack-Todd & Todd, [33] p.19-79, [34]</p>
--

This list of biological design precepts clearly reflects the holistic and participatory worldview that informs integrated sustainable design. The diverse and transdisciplinary movement that has grown out of this participatory, and ethically responsible approach to ecological design has been described as the 'Bioneers' [35, 36], as natural design [37], or the natural design movement [38].

After investigating a wide range of research initiatives aimed at creating new and more sustainable technologies, materials, and products based on insights



gained through the detailed investigation of biological and ecological processes, Janine Benyus [39] documented and integrated her findings in *Biomimicry – Innovation Inspired by Nature*. Her definition of the biomimicry approach is reproduced in table 3, below.

Table 3: The biomimicry approach.

<ol style="list-style-type: none"> 1. <i>Nature as model.</i> Biomimicry is a new science that studies nature's models and then imitates or takes inspiration from these designs and processes to solve human problems. 2. <i>Nature as a measure.</i> Biomimicry uses an ecological standard to judge the "rightness" of our innovations. After 3.8 billion years of evolution, nature has learned: What works. What is appropriate. What lasts. 3. <i>Nature as a mentor.</i> Biomimicry is a new way of viewing and valuing nature. It introduces an era based not on what we can <i>extract</i> from the natural world, but on what we can <i>learn</i> from it. 	<p>Source: Benyus, [40] p.iii</p>
---	-----------------------------------

Johnson and Hill [40] recently edited an informative compendium on how ecological insights can profoundly shape the way we design. They argue: "To ignore [the] reciprocal relationship of human culture and ecosystems is to turn away from a fundamental reality of the landscapes we share with other people and other species" and suggest: "As a basic principle for collaboration among design disciplines and the new fields of applied ecology, we propose that all landscape design, planning, and management should be evaluated through a thorough accounting of its consequences for ecological health, biotic integrity, and cultural well-being - human, social, and economic" (p.12).

3 Sustainability: *the* 'wicked problem' of design

First Horst Rittel and later Richard Buchanan [41] described design problems that involve complex, interrelated issues and diverse stakeholders, and are fuzzy and ill defined as 'wicked problems.' Recently, Wahl [38] suggests that sustainability is *the* wicked problem of design in the 21st century. From now on, all problem solving, decision and policy-making, and all aspects of design have to consider their impact on the health of individuals, communities, societies, ecosystems and the planetary life-support system in order to be sustainable.

Sustainable solutions require transdisciplinary integration of multiple knowledge bases. Design can play the role of integrator and facilitator in this process [14]. The complexity of the interrelated social, economic, cultural and ecological problems that are facing humanity not only call for collaboration between diverse disciplines but also for political and civic cooperation on a local, regional, national, and global scale. The creation of a sustainable civilization is a design challenge of unprecedented magnitude and generational importance.



Batram [42] explains: “Complex adaptive systems are constantly revising and rearranging their components in response to feedback from the environment” (p.36). He emphasizes that such systems are continuously changing and transforming. Participating agents are never able to optimise their fitness or utility, since there are too many possibilities.

Vester [12] points out: “Since complex systems require a constant dynamism in the way we think about them and therefore a heuristic structure” our approach to problem-solving has “to include the entire range of ways in which humans can reach insights” (p.38). Vester describes a study by the German systems-psychologist Dietrich Dörner that investigated the way transdisciplinary teams engage in the process of solving complex, unpredictable and interrelated problems. Table 4 lists six common mistakes in dealing with complex systems.

Table 4: Common mistakes in dealing with complex systems.

- | |
|--|
| <ol style="list-style-type: none"> 1. Inadequate definition of goals (vision) 2. Lack of a joined-up systems analysis 3. The creation of irreversible emphasis 4. Lack of attention to side-effects 5. The tendency to over-steer or over-react 6. The tendency to act in an authoritarian (controlling) way |
|--|

Source: after D. Dörner, in Vester, [12], pp.36-37

The complex dynamic systems that join nature and culture into a mutually dependent whole require us to create flexible and adaptable solutions that can respond to dynamic system changes. Nature constantly changes! Anthropogenic climate change and ecosystem degradation only accelerate systemic change. Sustainability is not an achievable steady state! Rather, it is a continuous process of community-based learning of how to participate appropriately in natural process.

Design for sustainability is materially expressed through sustainable products and infrastructures, but more profoundly, through sustainable communities, lifestyles, and societies. Increasing sustainability is about creating flexible and dynamically networked structures of self-sustaining, autopoietic [7] wholes within wholes. This requires the creation and empowerment of sustainable communities of responsible, eco-literate citizens adapted to the challenges and opportunities of a particular, local ecology and culture [22,27], cooperatively linked into mutual support networks that span from local to regional to global scale [38].

Such design requires sensitivity to the various scales of ecological design as proposed by Janis Birkeland [43]: product design, eco-architecture, construction ecology, community design, industrial ecology, urban ecology, and bioregional planning. The restoration of ecological and cultural health and well-being requires scale sensitive design – the creation of healthy, resilient, flexible and adaptive ‘holarchies’ [38], ‘holonocracies’ [19], or ‘panarchies’ [4]. The future



is unpredictable and uncertain. Adaptive complex dynamic networks are nature's way of responding effectively to change. Sustainable design that reintegrates culture and nature has to emulate nature's way of dealing with unpredictability, fundamental interconnectedness and dynamic transformation.

Nature is fundamentally scale linking. Events at the molecular scale of photosynthesis and digestion affect the bio-productivity of ecosystems, as well as atmospheric composition and climate patterns. Design has to integrate into natural processes at the appropriate scale [23–26]. In general, sustainable design has to be scale linking, synergistic, symbiotic, sacred and salutogenic (health-promoting) [38]. These are nature's lessons for natural design!

4 Conclusion

It is of limited use to draw a sharp line between the approaches of bionics and biomimicry, based on the relative importance these approaches give to achieving greater sustainability. Much of the British research in biomimetics is done in a bionics mindset of aiming for increased prediction, manipulation and control. Both fields, if they are indeed distinct, can contribute greatly to more sustainable solutions. The intention of this paper is not a discussion of semantic definition, nor the creation of dualistic categories; rather it aims to highlight the crucial role of intentionality in the design of more sustainable products, processes and services. Nature can teach us how to be life sustaining and health promoting.

As the postmodern world is taking shape amidst globalisation, climate change, economic instability, global and local inequality, resource wars and rapid species loss, an ecologically and socially literate worldview is emerging. It not only acknowledges the complex interactions and relationships between social, cultural, economic, and ecological systems, but also integrates multiple perspectives and considers material, ethical, psychological, and spiritual issues.

Most broadly defined, design is the expression of intentionality through interactions and relationships. This intention changes significantly when design is approached from within a perspective of culture as separate from nature and aiming to control and manipulate nature more effectively, or from within a more holistic and eco-literate perspective that regards culture as a co-dependent participant in natural process. Such changes in intention are changes in meta-design that affect all human activity. Changing the intentions behind design – changing mind set – is design at the paradigm level and life style level. The creation of a sustainable civilization is primarily about such fundamental changes in dominant worldviews, value systems, intentions, and life styles.

References

- [1] Schneider, M.S., *A Beginner's Guide to Constructing the Universe: The Mathematical Archetypes of Nature, Art, and Science*, HarperCollins: New York, 1995
- [2] Capra, F., *The Hidden Connections: A Science for Sustainable Living*, HarperCollins: New York, 2002



- [3] Intergovernmental Panel on Climate Change (IPCC), *Climate Change 1995*, Cambridge University Press, Cambridge, 1995
- [4] Gunderson, L.H. & Holling, C.S., *Panarchy: Understanding Change in Human and Natural Systems*, Island Press: Washington D.C., Covelo, London, 2002
- [5] Millennium Ecosystem Assessment, *Living Beyond Our Means: Natural Assets and Human Well-Being*, www.millenniumassessment.org
- [6] Capra, F., *The Tao of Physics: An Exploration of the Parallels Between Modern Physics and Eastern Mysticism*, third edition, Shambhala Publications, Boston, 1991
- [7] Maturana, H.R. & Varela, F.J., *The Tree of Knowledge: The Biological Roots of Human Understanding*, Shambhala Publications, Boston, 1988
- [8] Briggs, J. & Peat, D.F., *Seven Life Lessons of Chaos: Timeless Wisdom from the science of change*, HarperCollins, New York, 1999
- [9] Botkin, D., Quammen, D., McPhee, J., Gould, S.J., Margulis, L. *et al.*, *Forces of Change: A New View of Nature*, Smithsonian National Museum of Natural History & The National Geographic Society, Washington, 2000
- [10] Marten, G.G., *Human Ecology: Basic Concepts For Sustainable Development*, Earthscan Publications: London, Sterling VA, 2001
- [11] Goodwin, B.C., *How the Leopard Changed its Spots: The Evolution of Complexity*, Weidenfeld & Nicolson: London, 1994
- [12] Vester, F., *Die Kunst vernetzt zu Denken: Ideen und Werkzeuge für einen neuen Umgang mit Komplexität*, Der neue Bericht an den Club of Rome, Deutscher Taschenbuch Verlag: München, 2004
- [13] Goodwin, B.C., From Control to Participation via a Science of Qualities. *Revision: A Journal of Consciousness & Transformation*, **21(4)**, pp. 2-10, 1999
- [14] Wahl, D.C., Ecoliteracy, Ethics and Aesthetics in Natural Design: The Artificial as an Expression of Natural Process, *Design System Evolution*, European Academy of Design Conference, Bremen, 2005
- [15] Daily, G.C., (ed). *Nature's Services: Societal Dependence on Natural Ecosystems*, Island Press: Washington, D.C., Covelo, California, 1997
- [16] Wilkinson, R.G., *Unhealthy Societies: The Afflictions of Inequality*, Routledge: London, 1996
- [17] Wilkinson, R.G., *The Impact of Inequality: How to Make Sick Societies Healthier*, Routledge: London, 2005
- [18] Todd, J., Human Health/Planetary Healing: A Necessary Unity. *Annals of Earth*, **21(1)**, pp. 16-17, 2003
- [19] Waltner-Toews, D., *Ecosystem Sustainability and Health: A Practical Approach*, Cambridge University Press: Cambridge, 2004
- [20] Brown, V.A., Grootjans, J., Ritchie, J., Townsend, M. & Verrinder, G., *Sustainability and Health: Supporting Global Ecological Integrity in Public Health*, Earthscan Publications: London, 2005
- [21] Wann, D., *Deep Design: Pathways to a Livable Future*, (foreword by Hawken, P.), Island Press: Washington, D.C., Covelo, California, 1996



- [22] Orr, D.W., *Ecological Literacy: Education and the Transition to a Postmodern World*, State University of New York Press: New York, 1992
- [23] McHarg, I.L., *Design with Nature*, The American Museum of Natural History & Doubleday: New York, 1969
- [24] Jack-Todd, N. & Todd, J., *Bioshelters, Ocean Arks, City Farming: Ecology as the Basis of Design*, Sierra Book Club: San Francisco, 1984
- [25] Lyle, J.T., *Design for Human Ecosystems: Landscape, Land Use, and Natural Resources*, Van Nostrand Reinhold Company: New York, 1985
- [26] Van der Ryn, S. & Cowan, S., *Ecological Design*, Island Press: Washington, D.C., Covelo, California, 1996
- [27] Orr, D.W., *The Nature of Design: Ecology, Culture, and Human Intention*, Oxford University Press: Oxford, 2002
- [28] McHarg, I.L. & Steiner, F.R., *To Heal the Earth – Selected Writings of Ian L. McHarg*, Island Press: Washington D.C., Covelo, California, 1998
- [29] Jack-Todd, N., *A Safe and Sustainable World: The Promise of Ecological Design*, Island Press: Washington D.C., Covelo, California, 2005
- [30] Todd, J., Ecological Design in the 21st Century. Annual Schumacher Lecture, Schumacher Society, Bristol, www.oceanarks.org, pp. 1-3, 2000
- [31] Rosaler, M., *Science on the Edge: Bionics*, Blackbirch Press: USA, 2003
- [32] Nachtigall, W., *Vorbild Natur: Bionik-Design für funktionelles Gestalten*, Springer Verlag: Berlin, Heidelberg, New York, 1997
- [33] Jack-Todd, N. & Todd, J., *From Eco-Cities to Living Machines: Principles of Ecological Design*, North Atlantic Books: Berkeley, 1993
- [34] Todd, J & Jack-Todd, N., Personal communication, Course in *Ecological Design* at Schumacher College, Devon, May 2004
- [35] Ausubel, K., *Restoring the Earth – Visionary Solutions from the Bioneers*, HJ Kramer: Tiburon, California, 1997
- [36] Ausubel, K., (ed.) *Nature's Operating Instructions: The True Biotechnologies*, Bioneers Series, Sierra Book Club: San Francisco, 2004
- [37] Baxter, S., Deep Design and the Engineers Conscience: A Global Primer for Design Education. *Crossing Design Boundaries*, eds. P. Rodgers, L. Brodhurst & D. Hepburn, Taylor & Francis: London, pp.283-287, 2005
- [38] Wahl, D.C., *Design for Human and Planetary Health: A Holistic/Integral Approach to Complexity and Sustainability*, PhD. thesis submitted at the Centre for the Study of Natural Design, University of Dundee, Scotland
- [39] Benyus, J.M., *Biomimicry: Innovation Inspired by Nature*, 2nd edition, HarperCollins: New York, 2002 (first publ. in 1997)
- [40] Johnson, B.R. & Hill, K., (eds.) *Ecology and Design – Frameworks for Learning*, Island Press: Washington D.C., Covelo, London, 2002
- [41] Buchanan, R., Wicked Problems in Design Thinking. *The Idea of Design*, eds. V. Margolin & R. Buchanan, MIT Press: Cambridge, pp. 3-20, 1995
- [42] Battram, A., *Navigating Complexity – The essential Guide to Complexity theory in Business and Management*, Stylus Publishing: Sterling, VA, 1998
- [43] Birkeland, J., (ed.) *Design for Sustainability: A Sourcebook of Integrated Eco-logical Design*, Earthscan Publications: London, 2002



Active and adaptive sustainable environments for children's outdoor space

M. Winkler & S. Macaulay

*Department of Architectural Science, Faculty of Engineering,
Architecture and Science, Ryerson University, Canada*

Abstract

The slow and often cantankerous momentum of transforming children's school grounds and public open space areas in to stimulating environments for learning has grown steadily over the past decades. In North American, Europe and Asia partnerships have been formed between school communities, school boards, politicians, big business, and NGO's (non-government organization), to develop, design, and convert often bleak landscapes in to rich and diverse natural environments with plentiful curriculum, play and environmental connections. This process primarily focuses on the initial and immediate physical outcome of the capital venture. There is generally limited consideration for the long term sustainability and integrity of the site. Multi-disciplinary professionals often neglect understanding that a completed landscaped site is dynamic, not static, in terms of natural processes, physical forms, social needs and practical functions. Issues include the selection of natural and manufactured materials for short and long term durability, disposability and sensitivity to the environment; visual enjoyment and inherent appreciation of material weathering; foreseen and unforeseen maintenance costs. These matters need to be addressed upfront in the design process and not be relegated as an afterthought. Only then can we attempt to ensure that material selection, installation techniques and monitoring of the site can effectively and economically support an active and adaptive sustainable environment for children's current and future outdoor spaces.

Keywords: design, natural, open space, children, plant materials, sustainability, environment, communities, school grounds, hard landscape materials.

1 Introduction

The design process for the creation of children's outdoor urban space has evolved over many decades. In the 1950's North American school yards and



children's designed open spaces consisted primarily of patchy grass areas, black asphalt paving and cold steel playground equipment. In the 1970's New York City's landscape architect M. Paul Friedberg [1] and other professionals introduced a new generation of children to modern play areas made of tactile wooden structures and rubber tires often built above the softer and more pliable wood chipped surfaces. By the 1980's brightly coloured, complex plastic structures dotted children's landscapes. Through all these decades' active physical play and socialization remained the primary focus of children's outdoor designed spaces.

2 Shift in paradigms

In 1980 The Brundtland Report, commissioned by the United Nations entitle, "Our Common Future. World Commission on Environment and Development", was released to the public. The report spoke about responsible growth in first and third world countries and coined the term "Sustainable Development" [2]. It was also during this period that books such as architect Michael Hough's, "City Form and Natural Processes", brought the concept of appreciating and understanding one's local "Sense of Place". [3] New programs and courses were introduced to universities such as environmental studies, environmental engineering, landscape ecology, naturalization of highway corridors, native planting design. This information was disseminated to many, as well as those in charge of and interested in children's open space. The movement towards developing play spaces that directly related to the site's bioregion or natural environment had begun.

2.1 Transformation of ideas

In 1990's school grounds and open space design began to embrace the idea of local nature as the outdoor classroom. Designers, educators and communities began developing principles toward the transformation of school grounds [4] and public open spaces as part of an active holistic system. New designs began to emerge encouraging a strong sense of place and understanding that diverse learning environments need to be rich in curriculum, environmental, health and safety issues and their intertwining connections. Now, like never before master plans for new, rejuvenated and restored sites are increasingly and consciously including areas high in biodiversity of plant materials and wildlife. With this increasing commitment to the environment, comes a need to revisit phases of the design process. Designing, building, managing and maintaining an area rich in biodiversity is more complex. Sites are no longer composed of a monoculture landscape filled with asphalt, grass and ornamental trees. A comparison can be made in architecture when buildings have a single function, for instance a storage warehouse versus a science centre. The former requires arguably less understanding of material selection, application and user need. While a science centre is much richer and diverse in its functions, forms and user activities.



2.1.1 “How to” books

User friendly books, pamphlets, papers, conferences, workshops and lectures discuss the need for environmentally friendly school grounds promoting the use of native planting and naturalization [5], understanding of ecozones and embracing the importance of designing for shade [6]. “How to”, literature for organizing and recruiting the community, [7] seeking funding and providing the necessary tools to guide the design process continue to flourish and be embraced by designers and communities.

2.1.1.1 Beyond the ribbon cutting ceremonies Initiatives used to generate funds for these capital projects require enormous effort, particularly on the part of the community. The excitement of the inclusive design process and resulting new environment is generally heralded by all. However, after the ribbon cutting ceremony, the on going support of the site is often over looked and generates little interest by the initial partnerships.

3 Greater responsibility

Along with the new paradigm shift comes a greater responsibility on the part of designers to be more actively engaged in understanding the benefits of sustainability both pre and post design selection, installation and maintenance. In Ontario, services of Landscape Architects are demarcated into categories. Categories include; consulting & advising, pre-conceptual planning and pre-design, design & contract documents, services before & during construction and responsibilities of Landscape Architect and client (payment & copyright) [8] Within these guidelines there are few clearly defined guidelines for long term maintenance for an active and adaptive landscape design.

Sustainable designed environments require forward thinking designers who are actively mindful and aware of the site and users present and long term needs. The designer should evaluate the project’s layout, material selection and installation applications in terms of local sourcing of materials, life cycle assessment of materials, sustainable installation techniques, costs, aesthetics and user requirements of site. Life cycle assessment for buildings and construction are available for the architectural and engineering profession and industry with LCA software programs such as Environment Australia’s [9] and Athena’s Sustainable Materials Institute in Ottawa, Canada [10]. Software of this kind is presently unavailable to outdoor, landscape sites. [11] It is time for monitoring and maintenance plans and budgets, which are often ignored, be placed up front and centre in the design process and not relegated as an afterthought.

3.1 Monitoring and managing change

A young school ground and children’s open space landscape design is not unlike the young family that uses it. The needs of the whole family and each individual member evolve over time. The excitement of forming a family is quickly tempered by the responsibilities and necessary changes required for this new life



style. There is also tremendous excitement when designing a school ground and children's open space. The family in this context consists of children, caregivers, staff, volunteers, community, policy makers, designers and politicians. Over time, demands on and responsibilities toward the site change, yet the basic need for a safe, healthy and sustainable environment remains core. Adaptive sustainable environments monitor and manage predictable and unforeseen changes that occur post construction and beyond. This is achieved through developing a workable and adaptable monitoring and managing maintenance plan and budget.

3.1.1 Abiotic paving materials and biotic materials

School grounds and children's open space are generally composed of commonly used paving and vegetative materials. Each material is both multi-purpose in function, aesthetics and physical form. Understanding the components of these materials and their design connections assist in the promotion of sustainable design.

Paving Materials /Abiotic	Vegetation Groupings/Biotic
Asphalt	Trees
Concrete Pavers, Interlocking Concrete Pavers (ICP)	Shrubs
Natural Stone Pavers	Vines
Limestone Screening/Aggregates	Perennials
Pea Gravel	Grasses
Wood Boardwalk	Bulbs and Tubers
Wood Chips	Annuals
Sand	Vegetable/Herbs
Poured in Place Concrete	Grass
Brick	
Rubber	

Figure 1: Commonly used paving materials and vegetation groupings.

4 Active and sustainable design solutions

The following information contains examples of typical design problems that can be resolved prior to completion of design work and suggestions of adaptable landscape applications.

4.1 Design problem 1: outdoor seating

Timber logs are often used in school grounds and open space landscapes for seating. Logs are usually inexpensive to attain or donated to projects. Transportation to the site is easily accomplished. When numerous logs are arranged in a circle it is referred to as a "Council Ring". This term was originally coined in the first half of 1900's by Danish landscape architect Jens Jensen. In



the school yards, council rings are wonderful multi purpose seating areas, serving as outdoor lunchrooms, outdoor classroom and play areas. Over time these logs begin to decompose and decay, resulting in a weakened structure along with growth of unwanted mushrooms. It will be the principal’s responsibility to request removal of these logs by the school board’s maintenance staff. The cost of removal and disposal of the logs can be high and generally comes from the principal’s own school budget. In essence, six free wood logs, could cost a school \$600 to remove and dispose from the grounds [12].


Landscape Design Intent		
Design Outcome	Adaptive Management Solutions	Graphic Sample
Wooden logs weather and deteriorate, requiring removal using scarce monetary budgets.	Selection of quarried stones or large rocks will provide similar function to site. Material has longer life cycle.	Decomposing wood 

Figure 2: Landscape design intent: outdoors seating space [13].

Active and Adaptive Sustainable Design Solution: Use small boulders from nearby excavated residential or commercial construction sites. Contact local developers who access boulders on a regular basis. Boulders are often donated to school projects and have a long life cycle. Another material with long life cycle is ledge rock. Ledge rock is pre-cut and pre-sized for site specific design intent. This hard landscape material can be purchased at local quarries.

4.2 Design problem 2: staking young caliper trees

Small caliper trees are often given to school grounds through grants and community partnerships. These young trees and whips require tender care if they are not only to survive but thrive. Small caliper trees and children can be a receipt for disaster unless supportive maintenance and monitoring safe guards are installed. For a small caliper trees, proper mechanical staking, guying, or bracing is required for support against harsh winds, snow deposition, animals and people [14].

Active and Adaptive Sustainable Design Solution: There are a variety of biodegradable staking materials and suitable techniques to select from. Tree staking can create tripping hazards, so each area must be assessed on an individual basis. Tree staking requires proper identification in both design specifications and detail drawings. The first two growth years are the most critical for the plant’s survival. Stakes are typically removed after two years, but this policy should be re-evaluated on school grounds.



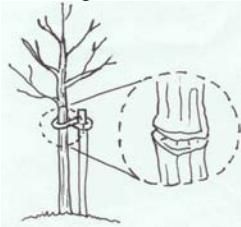
Design Outcome	Adaptive Management Solutions	Graphic Sample
<p>Trees often require staking at new sites. If the staking is not monitored, the bark can be restricted and girdling can begin in just one year. Girdling can restrict proper plant growth and create a haven for disease and decay.</p>	<p>Trees must be monitored for height, caliper, habit and general well being. Staking material type, length and location will change based on continuous plant growth.</p>	<p>Choking of Tree Trunk</p> 

Figure 3: Landscape design intent: planting small caliper trees [15].


Design Outcome	Adaptive Management Solutions	Graphic Sample
<p>Natural stone has advantages and disadvantages depending on material selection, site stresses and location. [10]</p>	<p>Place natural stone on sharply pointed and well compacted aggregates. These sharp edges provide greater opening between aggregates allowing for more water infiltration.</p>	<p>Tripping Hazards/Screening Material</p> 

Figure 4: Landscape design intent: material selection for paths [16].

4.3 Design problem 3: material selection for path

Natural stone has a long life cycle on pathways. Natural stones is found in a beautiful range of colours and can be purchased from local supplier either square cut or irregular shape. Hard landscape materials such as shale weather and flake over a relatively short time period. Others such as Owen Sound are much stronger. In cold climates, the natural freezing and thawing action cause the stone to lift and shift from the installed location. This creates serious tripping hazards for individuals, particularly individuals with physical handicaps.

Limestone screenings is often used for pathways due to low cost, aesthetically pleasing colour, ease of installation and sourcing. Limestone screening is a powdery like sustain when dry. The small partials collect on the outer soles of shoes in school yards. This often creates a maintenance problem as children re-enter the school building after recess and lunch. The small and numerous limestone screening footprints of students can be seen up and down the hallways and classrooms of the school building.



Heavy rains turn this soft powdery material into compacted areas where water is prevented from infiltrating back into the groundwater and puddles appear.

Active and Adaptive Sustainable Design Solution: Removing excessive amounts of paving material will assist in returning more water back to the subgrade [17]. When walking paths are required, install 3” (7.6cm) – 4” (10cm) of well compact angular aggregates. Recycled plastic grids are also commercially available to stabilize aggregates. [18] If plant roots are near the path, reduce the amount of excavation to a minimum. Examine slope and drainage pattern of surrounding area and place mulch bark.

4.4 Design problem 4: autumn foliage

Large open space areas are often bordered with large deciduous trees. Trees are randomly located in the open space areas. In the autumn, leaves drop and are collected with both hand held leaf blowing machines and leaf blowing service vehicles. They are neatly piled up high, lifted by a bobcat into a dump truck and transported off site. There is a tremendous waste of energy and people power to remove this natural material.


Design Outcome	Adaptive Management Solutions	Graphic Sample
Autumn foliage is usually removed from the site with costly manpower and large consumption of energy. Land is compacted and oxygen is reduced through the use of heavy equipment.	Lawn mowers over fallen leaves provide natural mulch for the grass.	

Figure 5: Landscape design intent: autumn foliage [19].

Active and Adaptive Sustainable Design Solution: A sustainable method would be to mow the leaves, (as you would grass) and place this new mulch on planting areas through out the site. This mulch would create a natural blanket for perennials and grasses during the upcoming winter season.

4.5 Design problem 5: aboveground concrete planters

The average life span of a tree in an above ground container is seven years. Plant roots have extremely limited space to move and grow in this unnatural and hostile environment. Maintenance and monitoring of plant growth is rarely done and poorly executed. Actual watering of above grade containers is almost negligible thereby threatening survival [20] [21].

Active and Adaptive Sustainable Design Solution: Plant trees in large above ground container islands. This allows for shared root space and more soil



volume. Larger trees have better long term survival in this environment. Although PVC pipes are not recyclable, they can assist in plant survival. Placed in the aboveground container, they collect rainwater and direct it to the root system.

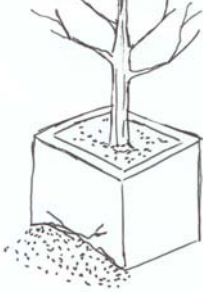
Design Outcome	Adaptive Management Solutions	Graphic Sample
In cold climates, the freezing and thawing action of the soil and root ball places pressure on the aboveground planters, eventually forming cracks at grade level.	Plants thrive in larger aboveground planters, especially in cold climates. The entire plastic container for root ball should be removed from tree.	

Figure 6: Landscape design intent: aboveground concrete planters [22].

5 Toward active and adaptable design

Designers need to take a more active role in obtaining relevant information towards the pursuit of sustainability in children’s open spaces. There are many organizations such as Interlocking Concrete Paving Institute, (ICPI), American Nursery Landscape Association (ANLA) and Canadian Nursery Landscape Association (CNLA) which offer the latest scientific research information on these products. Equally important is sustaining a healthy site through monitoring, maintenance and recording of landscape components. Review of the original design in terms of adequate layout, solid technical applications, material life cycles, existing functions, safety, natural processes and human use are to be noted. Based on this information monies can be allocated to adapted the site for current and future needs and/or requirements.

5.1 Planning for maintenance in the design

It is time to insist on a proactive approach to the funding of children’s open space designs. Abiotic and biotic material selection and intended usage require evaluation during the design decision making process and post construction review. Allocation of money for monitoring, managing and maintaining the site needs to be incorporated into the capital budget. This will assist in ensuring children’s school grounds and open space areas will not return to the monoculture of grass and asphalt.

6 Conclusion

Sustainable and diverse open space children area’s that recognize and integrate existing systems and contextual areas can be a long term a source of enjoyment



and enrichment for children and as they make the journey through the education system.

At the same time, it would be incorrect to believe these sites will remain permanent fixtures on the land. Natural weathering, decay of materials, cultural shifts, economic realities, and time itself will eventually have the greatest impact on a site. Because this is inevitable, projects need to be archived for future generations.

References

- [1] Friedberg, M. Paul. *Play and Interplay: A Manifesto for New Design in Urban Recreational Environment*. London: The Macmillan Company, 1970.
- [2] Bruntland, G. (ed.) *Our Common Future: World Commission on Environment and Development*. Oxford University Press: Oxford. 1987.
- [3] Hough, Michael. *City Form and Natural Processes*. Routledge, London: 1984.
- [4] Toronto District School Board, *Transforming the Schoolyard*, Toronto District School Board, pp. 8-9. 2000.
- [5] Aboud S. & Kock H., *A Life Zone Approach to School Yard Naturalization*, The Arboretum University of Guelph. pp. 44-55, 1996.
- [6] Evergreen, *Hand For Nature: A Volunteer Management Handbook*, Evergreen: Toronto, pp. 3-19, 2003.
- [7] Schaefer, Joseph M. et al., *Schoolyard Ecosystems for Northeast Florida*, University of Florida, pp 13-23 year.
- [8] Ontario Association of Landscape Architects. <http://www.oala.on.ca/articles>.
- [9] *Greening the Building Life Cycle*. Life Cycle Assessment Tool in Building and construction. <http://buildlca.rmit.edu.au/>.
- [10] *Life- Cycle Assessment for Building Buildings: Seeking the Holy Grail*. <http://www.buildinggreen.com/auth/article.cfm?fileName=110301a.xml>.
- [11] Athena Sustainable Materials Institute. Personal Phone Call. 2005.
- [12] Day, Bruce. Personal Conversation. 09 Oct. 2002. Head of Grounds Maintenance. Toronto District School Board. Toronto, Canada.
- [13] Winkler, Alexandra. Illustration 2006.
- [14] Harris, R.W., A.T. Leiser, and W.B. Davis. *Staking landscape trees*. University of California, Davis, Division of Agricultural Sciences Leaflet No. #2576. pp.13 1978.
- [15] Winkler, Alexandra. Illustration 2006.
- [16] Winkler, Alexandra. Illustration 2006.
- [17] J. William Thompson and Kim Sorvig, *Sustainable Landscape Construction A Guide to Green Building Outdoors*. Island Press: Calif., pp.73-74. 2000.
- [18] J. William Thompson and Kim Sorvig, *Sustainable Landscape Construction A Guide to Green Building Outdoors*. Island Press: Calif., pp. 187. 2000.



- [19] Winkler, Alexandra. Illustration 2006.
- [20] Peter J. Trowbridge and Nina L. Bassuk, *Trees in the Urban Landscape*, John Wiley & Sons: N.J. pp 82-89, 2004.
- [21] Gary W. Watson and E.B. Himelick, *Planting Trees and Shrubs*. International Society of Arboriculture. United Graphics: Il. pp. 43-47. 1997.
- [22] Winkler, Alexandra. Illustration 2006.



The creation of an eco-tourism site: a case study of Pulau Singa Besar

A. Abdullah, A. M. Abdul Rahman, A. Bahauddin & B. Mohamed
*School of Housing, Building and Planning, Universiti Sains Malaysia,
Malaysia*

Abstract

Ecotourism is the fastest growing form of tourism in Malaysia. It currently makes up about 10% of the country's tourism revenue. The Malaysian Government, specifically the Minister of Culture, Arts and Tourism has adopted a National Tourism Policy and National Ecotourism Plan (1996–2005) to encourage visitation to rural areas in order to enhance economic development as well as to meet the demands of what was perceived to be increased interest in the natural heritage of the country by the international tourism market. The development of Pulau Singa Besar, a small island off the legendary and more famous Langkawi Island in Malaysia is among one of the many efforts. The importance of sustainable planning, design and management is critical if an ecotourism site is to continue in generations to come. This paper addresses fundamental issues in the planning, design and implementation of various projects on the island of Pulau Singa Besar. It focuses on the lessons learned for future development.

Keywords: ecotourism, sustainability, development, design.

1 Introduction

In 1987, the concept of sustainable development was first introduced in a report entitled *Our Common Future* by the World Commission on Environment and Development of the United Nation [1]. According to the Commission, sustainable development is defined as “...*development that meets the need of the present without compromising the ability of future generations to meet their own needs.*”



Sustainable development has been proposed as a model that can have utility in creating the impetus for structural change within society. It consists of the following four interrelated goals:

- Meeting both present and future needs
- Meeting the needs which define the goal for development
- Maintaining consistency between population size and ecosystem productivity capacity
- Implementing change which acknowledges that the definition of needs and requirements for achieving sustainability will change over condition and time.

Strategies on tourism and sustainability were then discussed during the Globe '90 [2] conference in Canada where representatives from the tourism industry, government, non-government agencies (NGO's) and academics suggested that the goals of sustainable tourism include:

- To develop a greater awareness and understanding of the significant contributions that tourism can make to environment and the economy.
- To promote equity and development.
- To improve the quality of life of the host community.
- To provide a high quality of experience for visitors.
- To maintain the quality of the environment on which the foregoing objectives depend.

In the early 90's, promoting tourism that is sustainable became fashionable. A lot of individuals and organizations have joined the bandwagon. It gave the opportunity for nature lovers to promote and conserve nature while tour operators do it mainly for economic benefits. Terms such as "ecotourism" became a buzzword. However, the definition of the term became rather confusing. Orams [3] suggested that the term can be traced back to the late 1980s although Higgins [4] argued that Miller's work on eco-development actually dates back to the late 1970s. According to Boo [5], the first person to coin the term was Ceballos-Lascurain, who defined ecotourism as:

"traveling to relatively undisturbed or uncontaminated natural areas with the specific objective of studying, enjoying the scenery and its wild plants and animals, as well as any existing cultural manifestations found in these areas"

According to Goodwin [6], ecotourism should contribute significantly in the preservation of species and habitats either directly through conservation efforts or indirectly, by providing revenue to the local community sufficient for them to protect the wildlife heritage area as a source of income. Laarman and Durst [7] stressed that the visit should combine both, recreation and education. Wallace and Pierce [8] emphasized that true ecotourism addresses six principles:

- It contributes to the conservation and management of legally protected and other natural areas.
- It should generate economic and other benefits
- It should minimize negative impacts to the environment and to local people.



- It should increase the awareness and understanding of an area's natural and cultural systems and the subsequent involvement of visitors in issues affecting those systems.
- It should increase participation of local people in the decision-making process that determines the kind and amount of tourism that should occur.

2 Ecotourism in Malaysia

Since the mid 1990s, ecotourism became the fastest growing form of tourism in Malaysia. At present, it contributes about 10% of the country's tourism revenue. The Malaysian Government, specifically the Minister of Culture, Arts and Tourism Malaysia has adopted a National Tourism Policy and National Ecotourism Plan (1996–2005) to encourage visitation to rural areas in order to enhance economic development as well as to meet the demands of what was perceived to be increased interest in the natural heritage of the country by the international tourism market. The development of Pulau Singa Besar, a small island off the legendary and more famous Langkawi Island in Malaysia is among one of the many efforts. This paper addresses fundamental issues in the planning, design and implementation of various projects on the island of Pulau Singa Besar. It focuses on the lessons learned for future development.

3 Pulau Singa Besar

Located on the North-East of Penang Island, Malaysia, Pulau Singa Besar is one of the four major islands that collectively formed the Island of Langkawi. The island belongs to the Kedah State Government, which presented it to the Ministry of Science & Technology (MOSTE) to be developed as an ecotourism spot. It was planned to be a showcase of science & technology. The island was previously designated as a Wildlife Sanctuary. However, the concept has not been successfully implemented and the park was neglected despite abundant natural resources.

USAINS Holding Sdn. Bhd which is wholly owned by the Universiti Sains Malaysia was given the task to materialise the concept. A Project Management Team was formed amongst the three entities viz., USAINS Holding Sdn Bhd., the Department of Wildlife and Kedah State Development Board. USAINS Holding Sdn Bhd. was given an initial implementation budget of RM5 million to carry out several projects. The identified stakeholders are then committed to preserving 636 hectares of Pulau Singa Besar and its surrounding marine environment as a Science & Technology Park. The mission statement states that the island is:

“... to be managed in a manner that is consistent with the socio-economic aspirations of the people of Langkawi through the innovative and artful applications of science and technology in conserving the rich natural resources, both terrestrial and marine, for the promotion of ecotourism and sustainable development.”



3.1 Approach to the island

As an island, Pulau Singa Besar can be accessed from all sides but the main entry point is at the bay. The main jetty is known as the Pulau Singa Besar Jetty where one would normally embark. The most convenient way to visit Pulau Singa Besar from mainland Langkawi would be from the Teluk Baru Jetty or the Awana Porto Malai Jetty.

3.2 The Infocenter

The first place that greets the visitors is the Infocenter. Information at the centre gives an overview of what is available on the island. A huge resource of information is available for the visitors in various forms (posters, leaflets, interactive CCTV). This is the first marker (information about the nucleus) as suggested by Leiper [9]. From there the visitors can decide to choose where they would like to go for further observation

3.3 The Herbs Garden

A herbs garden is located just in front of the Infocenter. It is an open space planted with selected tropical herbs annotated for public viewing and education.

3.4 Mangrove Walk

Along the beach next to the Infocenter and the Botanical Garden, one can view the mangrove in its natural state by walking along the timber boardwalk. Information and signages are located at specific intervals along the walkway explaining the fauna that can be spotted regularly.

3.5 Fossil Point

Archeologists from Universiti Sains Malaysia discovered a promontory off Pulau Singa Besar. It was a significant finding because the fossils were believed to have been formed more than 350 million years ago. Some of the fossils were noted to have originated from the Australian continent. They have identified as many as ten fossil exhibits that were worthy for public viewing. During high tide, this promontory submerges and looks like an independent island detached from Pulau Singa Besar. An isthmus would also appear during low tide.

3.6 Night activities

Pulau Singa Besar offers a good spot for star gazing. The Genting Promontory has been identified as the best location for the purpose. A dormitory is provided for the enthusiasts to rest before getting up early in the morning to view the stars.

In addition, a night tour operation is planned where tour guides take visitors into the forest to see the night fauna along the Perdana Trail and other minor trails. Among the animals they can expect to see include: mousedeers, bats, big spiders, wild boars, monkeys etc.



3.7 Biodiversity on the island

There are several species of plants, birds, fishes, insects and animals on the island and that makes it a good real life-size laboratory for research, education and public awareness on what a typical tropical island has to offer. A snake indigenous only to the island and not found anywhere else in peninsula Malaysia has also been identified. A Frog Pond was designed and built to accommodate at least ten different species of frogs found on the island. The frogs are located in a reasonable sized cage with lights at night to attract flying insects as fodder for the frogs. They are contained in the cage for viewing for the public so that they are easily identified.

A Worm House is also located on the island. The worms convert organic materials into manure for recycling as fodder for plants. Fallen leaves which are abundant at Pualau Singa Besar are churned into manure and the process can be observed at the Worm House. In addition, there are various locations where boatmen would feed eagles by throwing remains of chicken to the surface of the sea. The eagles would appear from all directions in the vicinity and descend rapidly to grab the food, thus creating an interesting show for tourists.

4 The passive approach

Wallace and Pearce [8] suggested that an ecotourism site should minimize the negative impact to the environment. Passive systems do not generate thermal pollution because they do not require external energy input and produce no by-products or waste [10]. Interest in the passive approach is strong because it is simple in concept, requires only few moving parts and needs little or no maintenance. Pulau Singa Besar relies solely on a passive solar system for its electricity supply.

4.1 Passive solar system in Pulau Singa Besar

The Infocentre is powered by a set of eighty-six amorphous solar panels located along the walkway from the Jetty. This photovoltaic system is designed to supply 4 kW of energy although the actual amount of supply generated will depend greatly on the weather. The supply of electricity obtained via the panels is stored in batteries located at the Infocentre. This system provides solar electricity for the liquid emission diodes, emergency lighting, electric ceiling fans, computer system and electric extractor fans used in the Infocentre.

For comparison, a typical house would use 3 kW of energy per day. It is the first of its kind and probably the largest installation of amorphous solar panels in the region of South-East Asia. This system of using the sun's energy as a renewable energy is clean, low maintenance and operates at minimum running cost. It is also a very appropriate solution for Pulau Singa Besar as the conventional way of providing electricity generated by burning fossil fuel would be expensive because the conventional method requires getting electrical supply from mainland Langkawi via cable underneath the sea.



4.2 Solar electric boat

A solar electric boat was introduced to carry a maximum of six passengers from the PSB Jetty to either the Fossil Point or to the mangrove swamp. It is powered by batteries (the power comes from the solar panels). A solar electric boat is a most appropriate vehicle to take tourists to the mangrove swamps to observe the flora and fauna because it is silent and therefore would not scare the fauna away from its habitat unlike the noisy diesel engine boats which are presently being used.

4.3 Passive design approach for the Infocentre

During the upgrading of the island, the existing Infocentre has been renovated to provide more exhibition space for the public. Existing walls were demolished and extended to the outer perimeter of the corridor. During the renovation, passive solar design elements were introduced to increase comfort. The passive approach prevents heat build up without having to depend heavily on mechanical aids.

During the renovation, the original stilted design was maintained as cool breeze flowing underneath the building helps to cool the floor. Door height window leafs are introduced to capture any wind velocity into the building during daytime to cool the interior. Fixed timber louvered openings were located right above the door height windows. This is to cool the roof space. Timber material is preferred in order to maintain harmony with the natural setting. Powered by solar, two turbine ventilators help release hot air from the building. However, during the dry season, these elements may not be effective enough to provide reasonable comfort. Therefore, the help of mechanical aids such as electric fans and extractors are required. In addition, as much green area is maintained around the area and that hard landscaping is reserved for pathways and for the area under the Infocentre, which is mainly used for storing the batteries for the solar panels and to avoid the area becoming muddy during extreme high tides.

5 Issues and problems

5.1 Unclear vision and direction

The management team faces several issues and challenges in turning Pulau Singa Besar into an ecotourism spot. The balance between development and preservation, though often discussed, was not easy to practice. One of the reasons for this was due to differences in views between the stakeholders. On one end, there are those who view that the island should be sufficiently developed to attract enough tourists for it to be economically sustainable. On the other end, there are those who perceive that the island should be minimally developed and that it was irrelevant whether the island could sustain itself based on the income generated from tourist arrivals. These differences in view had affected the planning and implementation of projects on the island.



5.2 Illegal removal of fossilised rocks

Another problem faced by the management team was the loss of valuable fossilized rocks from the Fossil Point due to illegal collection by irresponsible parties. The area affected by this problem was mainly the southern part where large amounts of fossilised rocks are available. These rocks were mainly taken for use in the construction industry. It was a great concern because these parties were destroying invaluable national heritage.

This was an ongoing issue despite numerous warnings and attempts taken to eradicate the problem. It was almost impossible to monitor these activities because of the size of the area and the lack of manpower and financial resources to do so.

5.3 Litter

The abundant amount of rubbish around and on the island was also a major problem for Pulau Singa Besar. There are two different issues relating to this matter. The litter on the island were mainly due to the rubbish thrown by visitors despite the warning and penalty imposed on offenders. The lack of implementation was again partly to blame.

The huge amount of rubbish on the shores of Pulau Singa Besar was also providing a setback for the management team. Despite numerous attempts to clean the rubbish, a lot of rubbish from mainland Langkawi and from foreign vessels has been washed ashore by waves towards the beaches of the island. Floating sediments are difficult to curb as it comes from multi-direction as dictated by the wind forces that determine the direction of the waves.

In a research project funded by UNEP, high levels of suspended sediments, low dissolved oxygen and high biochemical oxygen demand have been identified as the main concerns for the coastal regions around Langkawi Island [11]. These environmentally poor conditions may be hazardous to public health and have harmed some coral ecosystems. Unless this issue is addressed seriously, the coral ecosystem of Pulau Singa Besar will suffer significantly.

6 Conclusion

Pulau Singa Besar has a lot to offer to the ecotourists. From nature trail to fossilized rocks, the island has abundant natural resources. However, the attempt to develop the island into a Science and Technology showcase in line with the principles of ecotourism had its fare share of success as well as failure. The use of passive solar energy to run the island was a brilliant accomplishment as it gave various ecological benefits. It was clean, easy and cheap to maintain despite costing a huge amount of money to install. In fact, in the long run, it would prove to be more economical. In addition, the solar powered boat used to bring visitors to the site contributed minimal pollution and intrusion to the wildlife.

However, different views on how to develop the island among the stakeholders resulted in various poor projects being implemented. Some projects



on the island were mainly set up to attract tourists although not in line with the concept of ecotourism. The lack of public awareness on the importance of preserving natural heritage is a major concern in developing countries like Malaysia. More effort in educating the public should be emphasised. Focus should also be on the values of preserving nature.

References

- [1] World Commission on Environment and Development, *Our Common Future*, Oxford: Oxford University Press, 1987.
- [2] Globe 90', *An Action Strategy for Sustainable Tourism Development*, Ottawa: Tourism Canada, 1990.
- [3] Orams, M.B., Towards a more desirable form of ecotourism, *Tourism Management* 16(1), pp. 3-8, 1995.
- [4] Higgins, B. R., The global structure of the nature tourism industry: ecotourists, tour operators and local businesses, *Journal of Travel Research* 35(2), p.p 11-18, 1996.
- [5] Boo, E., *Ecotourism: The Potentials and Pitfalls*, Washington D.C: World Wildlife Fund, 1990.
- [6] Goodwin, H., In pursuit of ecotourism, *Biodiversity and Conservation* 5(3), pp. 129-133, 1996.
- [7] Laarman, J.G & Durst, P.B., *Nature travel and tropical forests, FPEI Working Paper Series*, Southeastern Centre for Forest Economic Research, Northern Carolina State University, Raleigh, 1987.
- [8] Wallace, G.N. & Pierce, S.M., An evaluation of ecotourism in Amazonas, Brazil, *Annals of Tourism Research* 23(4), pp. 843-873, 1996.
- [9] Leiper, N., Tourist attraction systems, *Annals of Tourism Research* 17(3), pp. 367-384, 1990.
- [10] Mazria, E., *The Passive Solar Handbook*, Pa: Rodale Press, 1979.
- [11] Koh H.L. Din, Z. & Lee, H.L., *Modeling Water Quality in Selat Kuah, Langkawi, Malaysia*. Final Report. Penang: Universiti Sains Malaysia, 1995.



Section 8

Education and training

This page intentionally left blank

Development and experience with a technical elective course “fluid flows in nature”

J. A. Schetz

*Department of Aerospace and Ocean Engineering,
Virginia Polytechnic Institute and State University,
Blacksburg, Virginia, USA*

Abstract

This course was designed to build upon and broaden a basic, traditional engineering knowledge of fluid flows into new and stimulating areas concerning a wide variety of natural occurrences and phenomena that involve fluid motions in important ways. Topics covered include: drag of sessile systems and motile animals; gliding and soaring; flying and swimming; internal flows in organisms; low Reynolds number flows; fluid-fluid interfaces; unsteady flows in nature; atmospheric flows and wind engineering; and environmental fluid mechanics. The course is intended for upper-level students in engineering and science and presumes a background in the fundamentals of fluid flows at the level of a first engineering course in fluid mechanics. It has proven popular with students majoring in mechanical, civil, aerospace and ocean engineering, with occasional students from mathematics and sciences. An unexpected, but welcome and powerful, benefit occurs in the form of reinforcing and deepening student understanding of traditional topics in engineering fluid mechanics by contrast with the often very different situations encountered in nature. An online version of the course was introduced for the Spring Semester of 2006.

Keywords: fluid flows in nature, flying and swimming, environmental fluid mechanics, wind engineering.

1 Introduction

In 1998, a new course was designed to build upon and broaden a basic, traditional engineering knowledge of fluid flows into new and stimulating areas concerning a wide variety of natural occurrences and phenomena that involve



fluid motions in important ways. Topics covered included: continuity, pressure and momentum and applications in nature; drag of sessile systems and motile animals; gliding and soaring; flying and swimming; internal flows in organisms; low Reynolds number flows; fluid-fluid interfaces; unsteady flows in nature; atmospheric flows and wind engineering; and environmental fluid mechanics. The course involved classroom lectures using an interesting, but only partially suitable, text supplemented by handouts and lecture notes, an extensive internet website, complementary films and videos and four laboratory experiments.

The laboratory experiments were intended to demonstrate important concepts and also to familiarize the students with specialized facilities outside of their major fields of study. The experiments covered drag measurement of a trout model in a towing tank, pressure distributions and surface flow visualization on an airfoil in a wind tunnel, flow visualization of stall in a smoke tunnel, and flow in flooded, wooded areas in a river flume.

Useful materials for the website and handouts have been found in newspapers and magazines and also in scientific magazines such as *American Scientist* and *Mechanical Engineering*.

The course was and is intended for upper-level undergraduate and beginning graduate students in engineering and science and presumes at least a background in the fundamentals of fluid flows at the level of a first engineering course in fluid mechanics. It has proven popular with students majoring in mechanical, civil, aerospace and ocean engineering, with occasional students from mathematics and sciences. Typical enrollments averaged about 60 students every Spring Semester through 2005. Anonymous student evaluations are very supportive.

An unexpected, but welcome and powerful, benefit occurs in the form of reinforcing and deepening student understanding of traditional topics in engineering fluid mechanics by contrast with the often very different situations encountered in nature. One example is the better understanding of high Reynolds flows resulting from a detailed study of low Reynolds flows in nature.

In 2005, a decision was reached to prepare an Online version of this course. This decision was prompted by a number of factors. First, there is a desire to offer the course more frequently and to a wider group of potential students. The Online course can be offered in both the Fall and Spring Semesters. Also, our university has an extensive Distance Learning program with many off-campus engineering graduate students who can now access the course. Second, the textbook originally required of all students, *Life in Moving Fluids* by Steven Vogel, lacked coverage of some important topics desired here, such as environmental flows. And, it is devoid of photographs which are deemed critical in this subject area. The use of Handouts is severely limited by the cost of color copies. In principle, these issues can be handled on a website, and that was tried. But, this contributed to the next issue. The third and last matter of concern was the disorganized arrangement of the instructional material. The students were dealing with a textbook, handouts, a website, videos shown in class and four laboratory experiments. This proved less than optimal. The hope is that the



Online course can bring all of the instructional material together in one easily accessible place.

2 Online course format

The basic format of the new online course centers on the use of a large number of *PowerPoint* slides with a voice-over narration implemented with *Breeze* plug-in software for *PowerPoint*. All of the instructional material, except for the videos, was incorporated into these slides as a single source for the students. Two sample slides are included here at the end of the paper. These slides are only accessible to students registered for the course because of copyright issues. A *Blackboard* website hosts this material as well as: Announcements, Course Documents, a Week-by-week study plan, Assignments, Exams, and Grades.

The main sources of instructional materials for the narrated slides were the books (in alphabetical order), multimedia sources, scientific magazines, and newspapers listed here:

Anderson, J.D., *Introduction to Flight*, Third Edition, McGraw Hill: New York, 1989.

Azuma, A., *Biokinetics of Flying and Swimming*, Springer: Tokyo, 1993.

Hertel, H., *Structure-Form-Movement*, Reinhold: New York, 1966.

Hoerner, S.F., *Fluid-Dynamic Drag*, Hoerner Fluid Dynamics: Vancouver, 1965.

Munson, B.R., Young, D.F. and Okiishi, T.H., *Fundamentals of Fluid Mechanics*, Second Edition, John Wiley & Sons: New York, 1994.

Potter, M.C. and Wiggert, D.C., *Mechanics of Fluids*, Third Edition, Brooks/Cole: Pacific Grove, 2001.

Schetz, J.A., *Boundary Layer Analysis*, Prentice Hall: Englewood Cliffs, 1993.

Tennekes, H., *The Simple Science of Flight*, The MIT Press: Cambridge, 1997.

Tricker, R.A.R. and Tricker, B.J.K., *The Science of Movement*, American Elsevier: New York, 1967.

Vogel, S., *Life in Moving Fluids*, Second Edition, Princeton University Press: Princeton, 1994.

Multimedia Fluid Mechanics, Cambridge University Press, 2000.

American Scientist, *Mechanical Engineering*, *USA Today*, *Wall Street Journal*, and *New York Times*

The slide presentations are complemented by a number of excellent videos that are critical in a course such as this one. In particular, it is simply not workable to discuss topics such as flying and swimming or tornadoes with static materials alone. First, a selection of the excellent films produced in the 1950's by the National Committee for Fluid Mechanics are employed: *Pressure Fields and Fluid Acceleration*, *Fluid Dynamic Drag*, *Fundamentals of Boundary Layers*, *Turbulence*, *Vorticity*, *Low Reynolds Number Flows*, *Waves in Fluids* (first 20 minutes), and *Stratified Flows*. These are now conveniently available online at:



<http://web.mit.edu/fluids/www/Shapiro/ncfmf.html>. Students are also referred to *Form Drag, Lift and Propulsion* at: www.iuhr.uiowa.edu/products/pubvid/RouseMovies/pgm5.mpg and the videos on the Project Ornithopter website at: www.ornithopter.net/index_e.html. In addition, abridged versions of *Secrets of the Tornado* by The Tornado Project (www.tornadoproject.com) and *Flying High* by Scientific American Frontiers on PBS Home Video have been posted on a website at our university accessible only to students registered for this course. A few other very short film clips are also posted.

The slide presentations and the videos and films listed above now form the body of instructional materials used in the online version of the course. We have not found a workable way to include the laboratory experiments developed for the classroom version. We are considering making professional videos of the labs conducted at our university for inclusion in the online course at a later date.

The next important issue in any course is homework assignments. It has proven possible to find quite suitable problems and their solutions mostly in the Vogel; Munson, Young and Okiishi; Schetz; and Potter and Wiggert books, as well as in *Theory and Problems of Fluid Mechanics and Hydraulics* in Schaum's Outline Series published by McGraw Hill and miscellaneous other sources. A sample homework problem taken from the Munson, Young and Okiishi book is reproduced below.

Some animals have learned to take advantage of the Bernoulli effect without having read a fluid mechanics book. For example, a typical prairie dog burrow contains two entrances—a flat front door, and a mounded back door as shown in Fig. P3.13. When the wind blows with velocity V_0 across the front door, the average velocity across the back door is greater than V_0 because of the mound. Assume the air velocity across the back door is $1.07V_0$. For a wind velocity of 6 m/s, what pressure differences, $p_1 - p_2$, is generated to provide a fresh air flow within the burrow?



FIGURE P3.13

Figure 1: Homework problem used in the Fluid Flows in Nature course taken from Munson, Young and Okiishi, 1994.

Students turn in their homework for each week via e-mail to a temporary e-mail address, and the grades are posted on the *Blackboard* site.

Finally, all exams are given as a combination of Multiple-Choice and True/False questions. Perhaps surprisingly, the students are generally comfortable with that format. The writer has also found that format effective in probing student understanding. Further, that format has the great virtue of at least minimizing student complaints over “partial credit” in grading. With that format, the answers are simply either right or wrong. Students turn in their exam solutions via e-mail to a temporary e-mail address, and the grades are posted on the *Blackboard* site.



Homework and exams are covered by our university Honor Code to insure integrity.

With all of this, the week-by-week semester (15 week) course outline is shown in Table 1 below.

Table 1: Fluid flows in nature online course schedule.


Week	Slide Presentations	Supplements
1	Introduction (15 slides) Continuity and in Nature (7) Pressure and Momentum (18)	<i>Pressure Fields and Fluid Acceleration, Fluid Dynamic Drag I</i>
2	Drag, Part A (29)	<i>Fluid Dynamic Drag II,III</i>
3	Drag, Part B (30)	<i>Fluid Dynamic Drag IV, Fund. of Bound. Layers</i>
4	Boundary Layers in Nature (25)	<i>Turbulence, Vorticity I</i>
5	Vortices in Nature (39)	<i>Vorticity II, Tornado video</i>
6	Lift, Gliding and Soaring A (29)	<i>Form Drag, Lift and Propulsion video</i>
7	MIDTERM EXAM	
8	Lift, Gliding and Soaring B (34)	X-Ray Flying Filmclip
9	Thrust, Flying and Swimming (65)	<i>Flying High video</i>
10	Internal Flows (53)	Bronchial CFD Filmclip
11	Low Reynolds Number Flows (40)	<i>Low Re Flows</i>
12	Unsteady and Interfacial Flows (56)	<i>Waves in Fluids (20 min.) Stratified Flow</i>
13	Environmental Fluid Mech. (62)	
14	Wind Engineering (55)	<i>Flow Over Buildings</i>
15	FINAL EXAM	



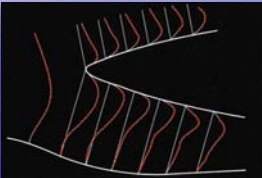
3 Current status

At the time this paper is being written, students are just beginning the course for the first time in the online format. One possible indicator of success is that more than 130 students have registered for the course in this format. That is more than double the average enrolment for the course taught in a classroom format for the first eight times. At the conference, the results of anonymous student evaluations and instructor impressions will be presented.

Examples of Fluid Flows in Nature




Internal wall shear
External wall shear



Laboratory Simulation

Flow behavior in arteries has been shown to affect the health of the artery. For example, a low wall shear causes a decrease in the health of the artery wall. Local separation causes low wall shear.

From American Scientist



Boundary Layer Fundamentals (7)

Turbulent boundary layer on a flat plate

$C_f = 0.0456(Re_x)^{-1/4}$ (7-13)

This equation is valid up to approximately $Re_x = 10^7$. Many people use the famous Schoenherr (1932) formula:

$$\frac{1}{\sqrt{C_f}} = 4.15 \log(Re_x C_f) + 1.7$$
 (7-14)

$$\frac{\delta}{x} = \frac{0.375}{Re_x^{1/4}}; \delta' = \frac{1}{8}; \frac{\theta}{\delta} = \frac{7}{72}$$

For the total frictional resistance coefficient C_D for turbulent flow over a flat plate of length L , these same two researchers proposed

$$C_D = \frac{0.427}{(\log(Re_L) - 0.407)^{2.58}}$$
 (7-13a)

and

$$\frac{1}{\sqrt{C_D}} = 4.13 \log(Re_L C_D)$$
 (7-14a)

Friction velocity $u_* = \sqrt{\tau_w / \rho}$ is a useful scaling quantity

 $u_* / U_\infty = \sqrt{C_f} / 2$

From Schetz, 1993

Figure 2: Sample sides.



New educational tools and curriculum enhancements for motivating engineering students to design and realize bio-inspired products

H. A. Bruck, A. L. Gershon, I. Golden, S. K. Gupta,
L. S. Gyger Jr., E. B. Magrab & B. W. Spranklin
*Department of Mechanical Engineering, University of Maryland,
College Park, MD, USA*

Abstract

The use of bio-inspiration to create new products and devices requires the development of new design tools and manufacturing technologies, as well as the education of students capable of using them. At the University of Maryland, we have developed new educational tools that emphasize bio-inspired product realization. These tools include the development of a bio-inspired design repository, a concurrent fabrication and assembly technology that focuses on the use of multi-piece, multi-stage molds to affordably manufacture large numbers of bio-inspired products, and a series of undergraduate curriculum enhancements. This paper provides an overview of these two technologies and describes how these technologies are integrated into the Mechanical Engineering curriculum. The new educational tools provide students with the fundamental design and manufacturing principles needed in bio-inspired product and device development. The curriculum changes culminate in an elective course undertaken in their senior year.

Keywords: bio-inspired design and manufacturing, design repository, concurrent fabrication and assembly, multi-piece multi-stage molding, mechanical engineering curriculum.

1 Introduction

For millions of years, nature has been creating materials, plants, insects, and animals that are optimized in many regards. These materials and creatures have



evolved in ways that enable them to sustain their existence in variety of ways. One example is the common housefly, shown below in *Figure 1*. It has wings that are extremely thin, with minimal reinforcement, allowing for high speed oscillations, resulting in high efficiency and speed. Another example of a creature that nature has optimized is the eye of the golden eagle, which has a shape and size that enables it to detect prey from high places. Some creatures, such as the chameleon, optimize their survivability by changing color to camouflage them from predators in a variety of environments.

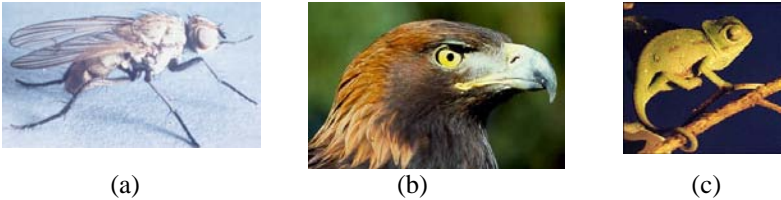


Figure 1: Natural Designs: (a) house fly; (b) golden eagle; (c) chameleon.

Engineers are frequently asked to design new materials, structures, mechanisms, and processes. To design these new products and artifacts often requires a search for new ideas. One source for new ideas can be found in nature. By learning about the way plants and animals have been created and function in nature through millions of years of evolution, engineers gain new inspiration to develop new products, which has been termed “bio-inspired” or “biologically-inspired” products. Many existing design tasks can also be re-examined to find new solutions using nature as a tool for inspiration. Unfortunately, many engineers may not think to use nature as a source of inspiration because most undergraduate engineering curriculums do not adequately emphasize its importance. It is our belief that if engineers are educated on the ways nature handles certain tasks, they will in turn be able to apply new concepts to future designs.

Bio-inspired design has recently been explored by many researchers, and this has had very positive outcomes for robotics, aerodynamic systems, biomedical devices, materials, and computational systems. The materials community has gained much knowledge from nature to develop better microstructures for materials, and several books have been published dealing with the natural materials themselves as well as synthetic replicas, or biomimetic materials ([1], [2], and [3]). The robotics community has also turned to nature for inspiration and published books ([4] and [5]) that have helped designers develop robots that use animal-like gaits rather than wheels for better functionality and efficiency to meet special requirements. Structural engineering researchers have also been studying nature for new ideas on how geometry affects load handling ability and how it can be sensed ([6], [7], and [8]) to create stronger and more adaptive structures. Success has already been realized using bio-inspired concepts, and it is our aim to educate undergraduate students on these recent advances in bio-inspired design so that they may be able to use ideas taken from nature and apply them to future designs.



Slowly, bio-inspired concepts have been implemented into a variety of products. The reason for this slow growth has been two challenges that need to be overcome for students to learn about and discover the full potential of nature's designs. The first challenge is to make students more aware of biological concepts and bio-inspired products. Currently, many engineers overlook solutions found in nature simply because they do not know how to look there and there is no repository of bio-inspired solutions that they can explore. To address this challenge, we are developing a searchable and expandable bio-inspired design repository that complements another approach being developed at The Center for Biomimetic and Natural Technologies at the University of Bath that focuses on integrating biology into an indexing method for design retrieval, known as TRIZ, by introducing biomimetic design concepts [9]. The second major challenge comes from the fact that most biological systems are geometrically complex and are highly heterogeneous and use variation in the material properties to achieve improved material-function compatibility. Furthermore, to achieve high degree of fault tolerance and adaptive behavior, they make use of sensors and actuators distributed throughout the system. Traditional manufacturing processes are not able to easily manufacture bio-inspired designs based on these characteristics. To address this challenge, we have developed a new multi-piece multi-stage molding processes that is part of a new class of manufacturing technologies that permit concurrent fabrication and assembly for realizing bio-inspired designs.

While the design repository and concurrent fabrication and assembly manufacturing technology are needed in order for students to learn about designing and realizing bio-inspired products, it will be difficult for them to properly utilize these tools without introducing the appropriate design, manufacturing, and materials subjects into the curriculum. These teaching materials must provide students with an understanding of the motivation behind bio-inspired products, an understanding of what has already been achieved, and a knowledge of the core mathematical and scientific principles behind the realization of bio-inspired products that have been achieved through design and manufacturing.

This paper will now describe educational activities being pursued in the Department of Mechanical Engineering at the University of Maryland to meet these challenges through new educational tools and curriculum. The next section will introduce the approach and techniques that were used to create a new repository of bio-inspired products and concepts, a new multi-piece multi-stage molding technology for manufacturing of bio-inspired products with no assembly, and a new undergraduate mechanical engineering curriculum for bio-inspired product realization.

2 Development of new bio-inspired design repository

In developing a repository of bio-inspired products and concepts, it is important to include information about the biological systems, as seen in the biological effects database, while also presenting information on product development that



will aid engineers. When creating a functional language to access this information, a functional basis has proven to aid in archiving and retrieving the information. However, it is also important to allow the user freedom to express the functions in terms of language and sentence structure. Whatever terms are used should be common language terms and not arranged in an arbitrary hierarchy. The natural language analysis has also shown that by searching for many alternatives to a single function term, many useful results may be found. Lastly, easy to use and flexible search tools are required to locate meaningful results.

The complete system has three parts: (a) Repository of bio-inspired products and concepts, (b) Functional Description Template, and (c) Search tools. The interaction of these three elements is shown in *Figure 2*. In order to add a product or concept into the repository, the user must fill out the data entry form. The entry may often be made by a biologist adding concepts from biological research or by an engineer archiving a bio-inspired product. In either case, the Functional Description Template is used to record the functions of the product or biological system. Following this process, the entry is stored. A user may then use a search form to locate information on bio-inspired work. The products or concepts that are returned can then be applied to the design to create a new bio-inspired design. This design can then be added into the repository as a new bio-inspired product.

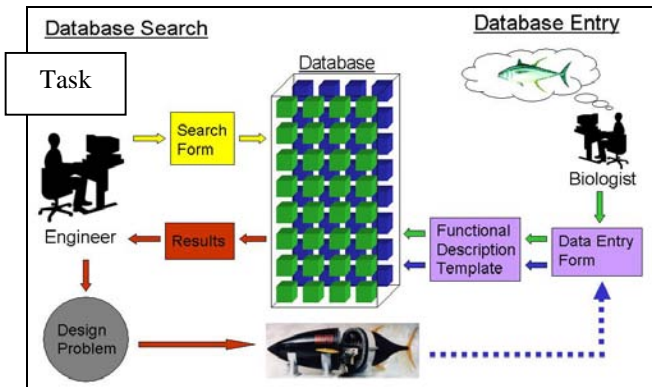


Figure 2: System overview.

2.1 Contents of repository

The repository being developed archives bio-inspired products and concepts. Bio-inspired products refer to products in any stage of development that have taken their inspiration from nature. These products may be anything from a new material substance to a complex mechanical device; they do not necessarily have to be consumer products. A bio-inspired concept refers to an observation of some function being met in nature. This concept need not be implemented into a product yet. Such concepts may be archived into the repository and any potential

applications may be recorded. Currently, the repository contains 85 records of bio-inspired products. These products were identified and researched through a search of journal papers, conference papers, magazine articles, and websites that discuss current bio-inspired research. The searches that were conducted explored bio-inspired actuators, sensors, materials, robots, and various other mechanical devices and consumer products that were inspired by nature. All of the products that were located were then recorded into the repository. For a bio-inspired product, all of the above fields may be populated. If a bio-inspired concept is being archived, the product information fields will remain empty, except possibly the applications field. The product function, or in the case of a concept the function of the biological system, requires many fields that are populated by using the Functional Description Template.

2.2 Functional Description Template

In order to develop an easy to use and expressive method for recording functions, it was necessary to first understand how people naturally express a functional statement. To accomplish this, an informal study was done asking people to write down the functions of common products. From these results, it was clear that there was no uniform way to represent a function. Some functions were very brief statements, while others were lengthy descriptions. However, all the functional statements used the same elements to form a sentence (verbs, nouns, etc.) Therefore, if common arrangements of these terms could be identified, then standardized templates could be provided for users and the desired terms could be entered. This concept is the basis for the Functional Description Template, a new method for recording product functions in our design repository that provides a predetermined sentence structure as a template to allow the user to form more complete functional descriptions. The methods of data entry used to fill in the template are a combination of freeform text entry and menu selection, which allow the recorded information to be efficiently archived and retrieved while ensuring that the system is easy to use by both engineers and biologists. In our design repository, the template makes use of the following three primary terms: (a) *Action*, (b) *Entity*, and (c) *Property*. Prepositions and conjunctions are also available. Adjectives and adverbs, however, are currently not used in the Functional Description Template. This omission is due to the fact that such terms were found to be non-essential to describing a function and merely offer additional information. However, the addition of these terms to the template could be completed at a later time.

2.3 Performing search on the repository

It is essential that the information stored in the repository be easily accessible to users in a straightforward manner and must provide meaningful results. To accomplish this, we have made the following three search tools available: (a) keyword search, (b) category filter, and (c) function search. In the keyword search a user enters the desired search terms using freeform text entry. fields will be searched. The search for our bio-inspired design repository is conducted by using a string matching algorithm that is a combination of two other string



matching algorithms; namely, equivalence method and similarity method. For the category filter, results are filtered based upon the fields that are recorded using menu selection. These fields include: (a) *Product Type*, (b) *Biological Type*, and (c) *Development Stage*. The final search tool is the function search, which is used to specifically search for products or concepts that meet a particular function or set of functions. While the keyword search may be used to search the functions of the products and concepts in the repository, the function search is specifically designed to search by function. This search tool aids the user in creating the functional statements for which to search and conducts a more flexible search that returns more useful results.

Product Information

Product Name: VCUUV

Product Type: Mechanism: Robot

Product Description: An unmanned underwater vehicle with a low drag body and flexible hull. Uses vorticity control for both propulsion and maneuvering, and caudal and pectoral fins for steering.

Development Stage: Product development

Applications: Mine reconnaissance, surveying, cable laying

Functions

- Propel robot through water
- Detect position of mines
- Measure volume of mines
- Regulate linear velocity of robot
- Regulate angular velocity of robot



Biological Inspiration

Biological Name: Yellow fin Tuna

Biological Type: Animal: Fish

Biological Description: The tuna has a very streamlined body and is highly maneuverable. It can accelerate and decelerate rapidly and maneuver in tight space

Resources

Primary Source: J.M. Anderson and P.A. Kerrebrock, “The Vorticity Control Unmanned Undersea Vehicle (VCUUV): Performance Results,” *11th International Symposium on Unmanned Untethered Submersible Technology*, Draper Report No. P-3747, Durham, NH, August 1999.

Additional References: <http://www.draper.com>

Figure 3: Example of record from search of bio-inspired design repository.

2.4 Example

Consider a scenario in which a student is designing an automated vehicle that can be used for underwater surveillance. The student, familiar with the recent advances in bio-inspired engineering, decides to search the repository of bio-



inspired products and concepts. The student may search for ideas using a combination of the search tools described above. In this case, a search is conducted for the keywords “underwater reconnaissance”, as well as the function “move device in liquid”. From this search, many results are returned, some of which contain only the keyword “underwater” and some of which contain a variation of the function “move device in liquid”. However, the top result is one that describes an unmanned underwater vehicle that was inspired by the tuna [10]. This entry in the repository contains the keyword “underwater” in the product description and contains the keyword “reconnaissance” in the applications. Furthermore, one of the product’s functions, “propel robot through water”, closely matched the search function. The student may then view the complete record, as shown in *Figure 3*.

3 Multi-piece multi-stage molding for bio-inspired product

For students to implement designs such as the one described in the case study, a new *Concurrent Fabrication and Assembly* technology based on *Multi-Piece Multi-Stage Molding* process was developed at the University of Maryland to affordably manufacture large quantities of bio-inspired products. This technology is focused around the design and manufacturing of the molds. Designing the mold for bio-inspired products is a very challenging task, because the complexity of the material distributions and geometries are not conducive to generating the single parting direction required for a standard two-piece mold. In addition, complex molds often require very complex undercuts to realize the entire structure. Multi-piece molds overcome these restrictions by having many parting directions. These molds have more than one primary parting surface, and consist of more than two mold pieces or sub-assemblies. Each of these mold pieces will have a different parting direction. The freedom to remove the mold pieces from many different directions eliminates the undercuts produced by two-piece molds. A multi-piece mold can be visualized as a 3D jigsaw puzzle, where all the mold pieces fit together to form a cavity and then can be disassembled to eject the molded part. Moreover, since there are no actuated side cores in multi-piece molds, the tooling cost is significantly lower. This makes multi-piece molding technology an ideal candidate for making geometrically complex objects. The multi-piece mold can be enhanced through multi-stage molding, where different material sections are injected in sequence into a mold or set of molds. This enables fully assembled components to be fabricated ‘in-mold’, resulting in concurrent fabrication and assembly.

The concurrent fabrication and assembly of components using the multi-piece multi-stage molding process allows one to fabricate heterogeneous structures with material interfaces that are geometrically complex and exhibit superior fracture and fatigue behavior, as well as improved functional performance [11, 12]. Specifically, multi-piece multi-stage molds can create multi-material objects to improve material-function compatibility for the overall object, and to embed prefabricated sensors/actuators during the molding process to eliminate the need for post-molding assembly and to significantly improve reliability. It is also



more scalable, simpler, faster, and cheaper than conventional manufacturing processes.

An example of a bio-inspired design that was manufactured using this technology is a snake robot module. A solid model of the module is shown in *Figure 4*. The mechanical structure of the module was assembled entirely in-mold, and consists of a universal joint, along with docking connectors. The male and female connectors are located at opposite ends of the structure, and are geometrically correct, although a more flexible material must be used in order for them to be functional (something that can easily be done with a different grade of polyurethane). The module was assembled via a two-stage transfer molding process, where a second material was used to make the universal joint. The entire module consisted of only three parts, the two on either side of the joint, and the cross-shaped piece making the joint; consequently, no additional fasteners or shafts are required. The concave interior feature of the female side of the docking mechanism was created using a split-core technique. An assembled snake robot can be seen in *Figure 5*.

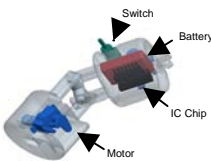


Figure 4: Solid model of snake robot module.



Figure 5: Assembled snake robot.

4 Curriculum for bio-inspired product realization

To realize bio-inspired products using the new design tool and manufacturing technology, a new undergraduate curriculum for mechanical engineers was developed and implemented at the University of Maryland [13]. This curriculum involves several single-lecture modules that cover a broad range of topics in bio-inspired design, manufacturing, and materials that are implemented in several core courses, as well as some senior electives. The courses and modules developed for these courses are as follows:

Introduction to Design – Introduction to bio-inspired design

Controls and Robotics – Bio-inspired design of mobile robots

Controls and Robotics – Bio-inspired artificial muscles

Measurement and Instrumentation – Bio-inspired sensors

Manufacturing Processes – Bio-inspired concurrent fabrication and assembly

Manufacturing Processes – Bio-inspired self-assembly

Introduction to Materials – Bio-inspired functionally graded materials

Descriptions of these modules can be found at www.bioinspired.umd.edu, and are available in PDF format by emailing a request to the authors. In addition to



these modules, a new senior elective was developed for Bio-inspired Product Realization to provide more content to these modules, as well as a design project resulting in bio-inspired products as the Snake Robot in Figure 6. An assessment of one of the manufacturing modules and the materials module were also undertaken to determine the efficacy of the curriculum. These assessment results indicated that a large majority of the students had very little prior knowledge of bio-inspired products and expressed strong interest in the subject. In addition, they indicated that they were able to acquire introductory knowledge from the modules.

5 Conclusions

The work presented in this paper describes three distinct contributions to motivate engineering students to use bio-inspiration to design and realize products. (1) A *design repository* of bio-inspired products and concepts based on a *Functional Description Template* was developed which contains detailed information about existing products in various stages of development and biological systems that provides new design concepts to students. (2) A *concurrent fabrication and assembly* technique for manufacturing products from the bio-inspired designs using a new *multi-stage multi-piece molding* technology for manufacturing products from bio-inspired designs that solves many of the mold design issues for complex material distributions and geometries. (3) A new *curriculum for bio-inspired product realization* to educate and train undergraduate mechanical engineering students to include bio-inspired ideas in their products using the new design tool and the new manufacturing technology.

Our new developed tools should also provide benefits to the engineering community at large. The repository, when populated with more and more products and concepts, will make knowledge of bio-inspired ideas more accessible to engineers. This information can lead to the development of new and innovative products that may provide improved product performance and lower cost devices. Additionally, the repository and functional description template are not limited to archiving bio-inspired products and concepts. In time, the repository could be used to archive any product or design concept and offer a more complete knowledge base for engineers seeking candidate design concepts.

Acknowledgement

This worked was supported by NSF grant EEC0315425. Opinions expressed in this paper are those of the authors and do not necessarily reflect opinions of the sponsors.

References

- [1] S. Mann, ed. *Biomimetic materials chemistry*. New York: VCH, 1996.



- [2] M. Sarikaya and I.A. Aksay, eds. *Biomimetics: design and processing of materials*. Woodbury, N.Y.: AIP Press, 1995.
- [3] R.P. Wool and X.S. Sun. *Bio-based polymers and composites*. Boston: Elsevier Academic Press, 2005.
- [4] R.J. Duro, J. Santos, and M. Graña, eds. *Biologically inspired robot behavior engineering*. New York: Physica-Verlag, 2003.
- [5] S. Hirose. *Biologically inspired robots: snake-like locomotors and manipulators*. New York: Oxford University Press, 1993.
- [6] A. Bejan. *Shape and structure, from engineering to nature*. New York: Cambridge University Press, 2000.
- [7] C. Mattheck. *Design in nature: learning from trees*. New York: Springer-Verlag, 1998.
- [8] A. Skordos, P.H. Chan, J.F.V. Vincent, and G. Jeronimidis. "A Novel Strain Sensor Based on the Campaniform Sensillum of Insects". *Phil. Trans. of the Royal Society London A*, Vol 360, pp 239 – 253, 2002.
- [9] J.F.V. Vincent and D.L. Mann. "Systematic Technology Transfer from Biology to Engineering". *Philosophical Transactions of the Royal Society: Physical Sciences*, Vol 360, pp 159-173, 2002.
- [10] J.M. Anderson and P.A. Kerrebrock "The Vorticity Control Unmanned Undersea Vehicle (VCUUV): Performance Results". *11th International Symposium on Unmanned Untethered Submersible Technology*, Draper Report No. P-3747, Durham, NH, August, 1999.
- [11] H.A. Bruck, G. Fowler, S.K. Gupta, and T.M. Valentine. "Towards bio-inspired interfaces: Using geometric complexity to enhance the interfacial strengths of heterogeneous structures fabricated in a multi-stage multi-piece molding process". *Experimental Mechanics*, Vol 44, pp 261-271, 2004.
- [12] R.M. Gouker, S.K. Gupta, H.A. Bruck, and T. Holzchuh. "Manufacturing Of Multi-Material Compliant Mechanisms Using Multi-Material Molding". to appear in *International Journal of Advanced Manufacturing Technology*, 2006.
- [13] H.A. Bruck, A.L. Gershon, and S.K. Gupta. "Enhancement of Mechanical Engineering Curriculum to Introduce Manufacturing Techniques and Principles for Bio-inspired Product Development". *Proceedings of the ASME International Mechanical Engineering Congress and Exposition*, pp 1-6, 2004.



Author Index

Abdul Rahman A. M.....	309	Kappel R.	205
Abdullah A.	309	Klefenz F.	175
Atherton M. A.....	185		
		Lin Y.....	81
Bahauddin A.	309	Liskiewicz T.	157
Barber R. W.....	245	Liu Y.....	137, 167
Bártolo P. J. S.	233	Luchsinger R.	105
Benjamin E. L.....	23		
Bethge K.....	13	Macaulay S.	299
Bruck H. A.....	325	Magrab E. B.....	325
Burgess S. C.	277	Mattheck C.	13, 205
Busch S.....	105	McIntosh A. C.	115
		McL. Roberts D.....	23
Cieśllicki K.	245	Mirjalili V.....	35
Collins M. W.	23, 185	Mohamed B.	309
Conn A. T.	277	Morina A.	157
Conte I.	211		
Cutler D. F.	185	Neville A.	157
Dawson M. A.....	145	Pasini D.	35
De Kooning E.	49	Peng X.	211
De Luca G.....	127	Platzer M. F.	3
De Meyer R.	49		
Despang M.....	71	Ren L. Q.	137, 167
Dowlen C.....	267	Rey A. D.....	127
		Rüggeberg M.....	105
Emerson D. R.	245		
		Sassi P.....	91
Fan J.....	221	Sauer A.	205
		Schetz J. A.....	319
Gajjar S. R.	255	Schikowski P.	175
Gershon A. L.	325	Sörensen J.....	13
Gibson L. J.....	145	Speck O.	105
Golden I.	325	Speck T.....	105
Gupta S. K.	325	Spranklin B. W.	325
Gyger Jr. L. S.	325		
		Taerwe L.....	49
Han Z. W.....	137, 167	Van de Voorde S.....	49
Hardzeyeu V.	175	Van De Walle R.	49
Hu H. X.....	167		
Hyde R. A.	277	Wahl D. C.....	289
		Willey T.....	195
Jones K. D.....	3	Windsor-Collins A. G.....	185

Winkler M..... 299

Yıldız P..... 61

Yu S. R. 137, 167

Zmeureanu R. 81



WITPRESS

Compliant Structures in Nature and Engineering

Edited by: C. H. M. JENKINS, Montana State University, USA

Nature is the grand designer and human engineers have taken great motivation from it since the earliest of times.

This book celebrates structural compliance in nature and human technology. Examples of compliant structures in nature abound, from the walls of the smallest cell, to the wings of the condor, to the tail of the gray whale. The subject of compliant structures in nature and engineering is timely and important, albeit quite broad and challenging. A concise summary of the important features of these interesting structures, this volume demonstrates, wherever possible, a mapping between naturally compliant structures and the promise and opportunity commensurate in human engineering.

Series: Design and Nature Vol 5

**ISBN: 1-85312-941-0 2005 296pp
£97.00/US\$175.00/€145.50**

Harmonisation between Architecture and Nature

Edited by: S. BAN, Shigeru Ban Architects, Japan, G. BROADBENT, University of Portsmouth, UK,

C. A. BREBBIA, Wessex Institute of Technology, UK, J. WINES, SITE Environmental Design, USA

Unlike the mechanistic buildings it replaces, Eco-Architecture is in harmony with nature, including its immediate environs. Eco-Architecture makes every effort to minimise the use of energy at each stage of the building's life cycle, including that

embodied in the extraction and transportation of materials, their fabrication, their assembly into the building and ultimately the ease and value of their recycling when the building's life is over. Featuring papers from the First International Conference on Harmonisation between Architecture and Nature, the text brings together papers of an inter-disciplinary nature, and will be of interest to engineers, planners, physicists, psychologists, sociologists, economists, and other specialists, in addition to architects. Featured topics include: Historical and Philosophical aspects; Ecological and Cultural Sensitivity; Human Comfort and Sick Building Syndrome; Energy Crisis and Building Technologies; Carbon Neutral Design; Alternative Sources of Energy (wind, solar, wave, geothermal etc); Design with Nature; Design with Climate; Siting and Orientation; Re-use of Brownfield Sites; Material Selection; Minimal Transportation Approaches and use of Indigenous Materials; Life Cycle Assessment of Materials; Design by Passive Systems; Conservation and Re-use of Water; Building Operation and Management; Applications in Different Building Types; Regulations and Contracts.

**ISBN: 1-84564-171-X 2006 apx 450pp
apx £165.00/US\$295.00/€247.50**

WIT eLibrary

Home of the Transactions of the Wessex Institute, the WIT electronic-library provides the international scientific community with immediate and permanent access to individual papers presented at WIT conferences. Visitors to the WIT eLibrary can freely browse and search abstracts of all papers in the collection before progressing to download their full text.

Visit the WIT eLibrary at
<http://library.witpress.com>



WITPRESS

Flow Phenomena in Nature

A Challenge to Engineering Design

Edited by: R. LIEBE, SIEMENS Power Generation, Germany

Do we have an adequate understanding of fluid dynamics phenomena in nature and evolution, and what physical models do we need? What can we learn from nature to stimulate innovations in thinking as well as in engineering applications?

Concentrating on flight and propulsion, this unique and accessible book compares fluid dynamics solutions in nature with those in engineering. The respected international contributors present up-to-date research in an easy to understand manner, giving common viewpoints from fields such as zoology, engineering, biology, fluid mechanics and physics. This transdisciplinary approach eliminates barriers and opens wider perspectives to both of the challenging questions above.

Contents: Introduction to Fluid Dynamics; Swimming and Flying in Nature; Generation of Forces in Fluids - Current Understanding; The Finite, Natural Vortex in Steady and Unsteady Fluid Dynamics - New Modelling; Applications in Engineering with Inspirations From Nature; Modern Experimental and Numerical Methods in Fluid Dynamics.

ISBN: 1-84564-001-2 2006 apx 800pp
apx £195.00/US\$312.00/€292.50

We are now able to supply you with details of new WIT Press titles via

E-Mail. To subscribe to this free service, or for information on any of our titles, please contact the Marketing Department, WIT Press, Ashurst Lodge, Ashurst, Southampton, SO40 7AA, UK

Tel: +44 (0) 238 029 3223

Fax: +44 (0) 238 029 2853

E-mail: marketing@witpress.com

Optimisation Mechanics in Nature

Editors: M.W. COLLINS, D.G. HUNT and M.A. ATHERTON, London South Bank University, UK

This book comprises a study of the two great organic solids in Nature, namely wood and bone. The common scientific laws which act in parallel for both natural and man-made materials are detailed as wood and bone are studied in their natural structural environment as well as in the fields of engineering structural analysis and medical analysis. The relationship between them enables wood to be used in engineering structures and man-made materials to be used as scaffolding for tissue restoration in the human environment. The 'two-way traffic' relationship explored in this volume is termed biomimesis, a modern development of the ancient Greek concept of mimesis - the man-made imitation of nature.

Contents: Preface; Wood as an Engineering Material; Uniform Stress - A Design Rule For Biological Load Carriers; Nature and Shipbuilding; The Structural Efficiency of Trees; Application of the Homeostasis Principle to Expand Gaudi's Funicular Technique; Bones - The Need For Intrinsic Material and Architectural Design; Restoration of Biological and Mechanical Function in Orthopaedics - A Role For Biomimesis in Tissue Engineering; Design in Nature.

Series: Design & Nature, Vol 4

ISBN: 1-85312-946-1 2004 176pp
£70.00/US\$112.00/€105.00

Find us at

<http://www.witpress.com>

Save 10% when you order from our encrypted ordering service on the web using your credit card.



WITPRESS

Nature and Design

Editors: M.W. COLLINS, London South Bank University, UK, M.A. ATHERTON, London South Bank University, UK and J.A. BRYANT, University of Exeter, UK

Combining authority, inspiration and state-of-the-art knowledge, this volume provides a comprehensive study of the fundamental laws of nature and design.

Partial Contents: Optical Reflectors and Antireflectors in Animals; Adaptive Growth; Robustness and Complexity; A Medical Engineering Project in the Field of Cardiac Assistance; Creativity and Nature; Design in Plants; The Tree as an Engineering Structure.

Series: Design & Nature, Vol 1

ISBN: 1-85312-852-X 2005 360pp
£133.00/US\$213.00/€199.50

Design and Nature

Comparing Design in Nature with Science and Engineering

Editors: C.A. BREBBIA and L.J. SUCHAROV, Wessex Institute of Technology, UK and P. PASCOLO, Università degli Studi di Udine, Italy

Providing researchers in this subject with fresh impetus and inspiration, this book consists of papers presented at the first international conference on this subject. The contributions reflect the rich variety of work taking place and cover topics within shape and form in engineering and nature, solutions from nature, design and sustainability studies, nature and architectural design, mechanics and thermodynamics in nature, biomimetics and materials, and vision in science and nature.

Series: Design & Nature, Vol 3

ISBN: 1-85312-901-1 2002 460pp
£149.00/US\$223.00/€223.50

Design and Nature II

Comparing Design in Nature with Science and Engineering

Editors: M.W. COLLINS, London South Bank University, UK and C.A. BREBBIA, Wessex Institute of Technology, UK

Containing the proceedings of the Second International Conference on Design and Nature, this book brings together contributions from researchers working around the world on a variety of studies involving nature and its significance for modern scientific thought and design.

Over 55 papers are featured and these span the following broad range of topics: Architectural Design and Structures; Architecture and Sustainability; Acoustics; Biology; Biomimetics; Design Philosophy and Methods; Human Biology and Medicine; Materials; Nature and Architectural Design; Space.

Series: Design & Nature, Vol 6

ISBN: 1-85312-721-3 2004 648pp
£186.00/US\$298.00/€279.00

All prices correct at time of going to press but subject to change.

WIT Press books are available through your bookseller or direct from the publisher.

WITPress

Ashurst Lodge, Ashurst, Southampton, SO40 7AA, UK.

Tel: 44 (0) 238 029 3223

Fax: 44 (0) 238 029 2853

E-Mail: marketing@witpress.com



This page intentionally left blank

This page intentionally left blank

This page intentionally left blank

This page intentionally left blank

This page intentionally left blank

This page intentionally left blank

This page intentionally left blank

This page intentionally left blank

This page intentionally left blank

This page intentionally left blank

This page intentionally left blank